

# Doctorate Program in Molecular Oncology and Endocrinology

XVIII cycle - 2002–2006  
Coordinator: Prof. Giancarlo Vecchio

## **Novel genes involved in the pathogenesis of Insulin-resistance: new targets for the treatment of Type 2 Diabetes Mellitus**

Angela Cassese

University of Naples Federico II  
Dipartimento di Biologia e Patologia Cellulare e Molecolare  
“L. Califano”

## **Administrative Location**

Dipartimento di Biologia e Patologia Cellulare e Molecolare “L. Califano”  
Università degli Studi di Napoli Federico II

### **Partner Institutions**

#### **Italian Institutions**

Università di Napoli “Federico II”, Naples, Italy

Istituto di Endocrinologia ed Oncologia Sperimentale “G. Salvatore”, CNR, Naples, Italy

Seconda Università di Napoli, Naples, Italy

Università del Sannio, Benevento, Italy

Università di Genova, Genoa, Italy

Università di Padova, Padova, Italy

#### **Foreign Institutions**

Johns Hopkins University, Baltimore, MD, USA

National Institutes of Health, Bethesda, MD, USA

Ohio State University, Columbus, OH, USA

Université Paris Sud XI, Paris, Francia

#### **Supporting Institutions**

Università di Napoli “Federico II”, Naples, Italy

Ministero dell’Istruzione, dell’Università e della Ricerca

Istituto Superiore di Oncologia (ISO)

Polo delle Scienze e delle Tecnologie per la Vita, Università di Napoli “Federico II”

Polo delle Scienze e delle Tecnologie, Università di Napoli “Federico II”

Terry Fox Foundation

Istituto di Endocrinologia ed Oncologia Sperimentale “G. Salvatore”, CNR, Naples, Italy

Centro Regionale di Competenza in Genomica (GEAR)

## Faculty

### Italian Faculty

Giancarlo Vecchio, MD, Co-ordinator  
Francesco Beguinot, MD  
Angelo Raffaele Bianco, MD  
Francesca Carlomagno, MD  
Gabriella Castoria, MD  
Angela Celetti, MD  
Fortunato Ciardiello, MD  
Sabino De Placido, MD  
Pietro Formisano, MD  
Massimo Imbriaco, MD  
Paolo Laccetti, MD  
Antonio Leonardi, MD  
Barbara Majello, PhD  
Rosa Marina Melillo, MD  
Claudia Miele, PhD  
Pacelli Roberto, MD  
Giuseppe Palumbo, PhD  
Silvio Parodi, MD  
Renata Piccoli, PhD  
Giuseppe Portella, MD  
Antonio Rosato, MD  
Massimo Santoro, MD  
Giampaolo Tortora, MD  
Donatella Tramontano, PhD  
Giancarlo Troncone, MD  
Bianca Maria Veneziani, MD

### Foreign Faculty

#### *National Institutes of Health (USA)*

Michael M. Gottesman, MD  
Silvio Gutkind, PhD  
Derek LeRoith, MD  
Stephen Marx, MD  
Ira Pastan, MD

#### *Johns Hopkins University (USA)*

Vincenzo Casolaro, MD  
Pierre Coulombe, PhD  
James G. Herman MD  
Robert Schleimer, PhD

#### *Ohio State University, Columbus (USA)*

Carlo M. Croce, MD

#### *Université Paris Sud XI, Paris, Francia*

Martin Schlumberger, MD

**Novel genes involved in the  
pathogenesis of Insulin-resistance:  
new targets for the treatment of  
Type 2 Diabetes Mellitus**

# TABLE OF CONTENTS

<b>ABSTRACT.....</b>	<b>5</b>
<b>BACKGROUND.....</b>	<b>6</b>
1. Diabetes Mellitus.....	6
2. Pathophysiology of type 2 diabetes mellitus.....	6
3. Insulin signaling and pathways in insulin action.....	7
3.1 The insulin receptor.....	8
3.2 Insulin-receptor substrates.....	8
3.3 The PI-3 kinase pathway and Akt/PKB signaling.....	9
3.4 The MAPK pathway.....	10
3.5 The protein kinase C superfamily.....	11
3.6 Glucose transport.....	12
4. Defects in insulin action.....	13
4.1 Insulin resistance.....	14
4.2 Mechanisms of insulin resistance.....	14
5. PED/PEA-15 protein.....	15
5.1 PED/PEA-15 and its antiapoptotic function.....	16
5.2 PED/PEA-15 and its role in insulin resistance.....	17
6. Phospholipase D protein.....	19
6.1 PLD1 isoform: expression and regulation.....	21
7. PED/PLD1 interaction: D4 domain.....	22
<b>AIM OF THE STUDY.....</b>	<b>23</b>
<b>MATERIALS AND METHODS.....</b>	<b>24</b>
Plasmids construction.....	24
Cell culture and Transfections.....	24
Western Blot Analysis and Immunoblotting.....	24
PLD assay in intact cells.....	25
Co-immunoprecipitation.....	25
Immunofluorescence microscopy.....	26
PLD assay in vitro.....	26
Flow cytometry.....	26
Intramuscular injection and Tissue collection.....	27
$\beta$ -Galactosidase assay and X-Gal staining.....	27
Adenovirus construction.....	27

2-deoxy-D-glucose (2-DG) uptake. . . . .	28
Densitometry and statistical analysis. . . . .	28
<b>RESULTS AND DISCUSSION . . . . .</b>	<b>29</b>
PED/PEA-15 proteins binds PLD1 and enhances PLD1 activity in HEK293 and L6 cells . . . . .	29
The role of PED/PEA-15 phosphorylation. . . . .	32
Generation of D4 fragment: its effects <i>in vitro</i> . . . . .	32
Generation of PED/PEA-15 derived peptides. . . . .	35
The interaction between PED/PEA-15 and PLD1 <i>in vivo</i> . . . . .	37
<i>In vitro</i> and <i>in vivo</i> modulation of adenovirus. . . . .	38
Generation of an adenovirus containing D4 fragment. . . . .	41
<b>CONCLUSIONS. . . . .</b>	<b>43</b>
<b>ACKNOWLEDGEMENTS. . . . .</b>	<b>44</b>
<b>REFERENCES. . . . .</b>	<b>45</b>

# LIST OF PUBLICATIONS

This dissertation is based upon the following publications:

1. Condorelli G, Trecia A, Vigliotta G, Perfetti A, Goglia U, Cassese A, Musti AM, Miele C, Santopietro S, Formisano P, Beguinot F. Multiple members of the mitogen-activated protein kinase family are necessary for PED/PEA-15 anti-apoptotic function. *J Biol Chem* 2002; 277(13):11013-8.
2. Trecia A, Perfetti A, Cassese A, Vigliotta G, Miele C, Oriente F, Santopietro S, Giacco F, Condorelli G, Formisano P, Beguinot F. Proteine Kinase B/Akt binds and phosphorylates PED/PEA-15 stabilizing its anti-apoptotic action. *Mol Cell Biol* 2003; 23(13):4511-21.
3. Vigliotta G, Miele C, Santopietro S, Portella G, Perfetti A, Maitan M.A, Cassese A, Oriente F, Trecia A, Fiory F, Romano C, Tiveron C, Tatangelo L, Troncone G, Formisano F, Beguinot F. Overexpression of the ped/pea-15 Gene Causes Diabetes by Impairing Glucose-Stimulated Insulin Secretion in Addition to Insulin Action. *Mol Cell Biol* 2004; 24(11):5005-5015.
4. Miele C, Raciti GA, Cassese A, Romano C, Giacco F, Oriente F, Paturzo F, Andreozzi F, Zabatta A, Troncone G, Bosch F, Pujol A, Chneiweiss H, Formisano P, Beguinot F. Ped/pea-15 regulates glucose-induced insulin secretion by restraining potassium channel expression in pancreatic beta-cells. *Diabetes. In press.*

# ABSTRACT

PED/PEA-15 is a cytosolic protein whose overexpression is a common feature of type 2 diabetes. It has been involved in generating insulin resistance by blocking insulin-stimulated glucose transport in differentiated L6 skeletal muscle cells and 3T3-L1 adipocytes.

Transgenic mice ubiquitously overexpressing PED/PEA-15 exhibit mildly elevated random-fed blood glucose levels and decreased glucose tolerance compared to their non transgenic littermates. Furthermore, these mice were hyperinsulinemic in the basal state and showed elevated free fatty acids (FFAs) and triglyceride blood levels. Consistent with these results, insulin-stimulated glucose uptake was decreased in fat and muscle tissues of the PED/PEA-15 transgenic mice, accompanied by protein kinase C (PKC) alpha activation and blockage of insulin-dependent PKC zeta activation. In addition, PED/PEA-15 transgenic mice featured whole body insulin resistance and a reduction in insulin response to glucose loading. Finally, the treatment with a 60% fat diet led PED/PEA-15 transgenic mice to develop diabetes.

Thus, *in vivo*, overexpression of PED/PEA-15 may lead to diabetes by impairing insulin action and insulin secretion. Studies to elucidate the molecular mechanism responsible for PED/PEA-15-induced insulin-resistance were also performed. Previous investigations evidenced that PED/PEA-15 binds to phospholipase D (PLD), an enzyme responsible for diacylglycerol production, which then mediates activation of classical PKC isoforms including PKC $\alpha$ .

In this work, I sought to test the hypothesis that blocking PED/PEA-15/PLD1 interaction may improve insulin-sensitivity both in cellular models and *in vivo*. To this aim, I identified a molecule (PLDi peptide) that is able to inhibit PED/PEA-15/PLD1 interaction, PLDi corresponds to aminoacids 712-1074 of PLD1 protein. Therefore, I verified whether the expression of this inhibitory peptide rescues normal insulin sensitivity and insulin-stimulated glucose transport in HEK293 and L6 cell lines overexpressing PED/PEA-15. Based on results obtained from these experiments, I tested the possibility to reduce PED/PEA-15-PLD1 interaction by adenoviral-mediated expression of D4 *in vivo*.

The outcome of these experiments may provide the rationale for setting-up high-throughput screening systems to identify additional molecules antagonizing PED/PEA-15 action. Such molecules may include novel agents to improve beta-cell function and to correct deranged metabolism in fat and muscle tissues in type 2 diabetes.

# BACKGROUND

## 1. Diabetes mellitus

Diabetes is one of the most common metabolic disorders. There are 200 million diabetic individuals in the world; this creates a need to understand the etiology of the disease and the genetic and environmental factors influencing its pathogenesis. Diabetes mellitus is a chronic metabolic syndrome caused by insulin deficiency and characterized by elevated glucose level; often it may be associated with microvascular, neurological, and macrovascular complications including retinopathy, nephropathy, neuropathy, and increased risk of cardiovascular disease (Malecki and Klupa 2005).

According to the classification recommended by the American Diabetes Association (2004), diabetes mellitus can be classified as type 1, type 2, other specific types, and gestational diabetes mellitus.

Type 1 diabetes mellitus (T1DM) always occurs in childhood and adolescence with an absolute insulin insufficiency caused by autoimmune or idiopathic destruction of insulin-producing  $\beta$ -cells in the pancreas by CD4 and CD8 T cells and macrophages infiltrating the islets. Insulin injection is always necessary for survival in T1DM because of the complete lack of endogenous insulin (Gillespie 2006).

Type 2 diabetes mellitus (T2DM) is more complex in etiology and is characterized by a relative insulin deficiency, reduced insulin action, and insulin resistance of glucose transport in skeletal muscle and adipose tissue. The manifestation of type 2 diabetes is a continuum of insulin resistance culminating in the failure of insulin secretion to compensate for insulin resistance, and the progression to full diabetes ensues when pancreatic  $\beta$ -cell hypersecretion of insulin fails to compensate for insulin resistance (Del Guerra et al. 2005).

## 2. Pathophysiology of type 2 diabetes mellitus

The susceptibility to the development of T2DM is determined by two factors: genetics and environment. The pathophysiology of T2DM is very complex and has not been completely understood. Any gene mutation or metabolic disturbance leading to a defect in insulin secretion, insulin transport, insulin action, glucose transport, or enzymes associated with glucose metabolism can theoretically result in hyperglycemia or clinical diabetes. Most patients with T2DM exhibit two different defects: the impairment of insulin secretion and decreased insulin sensitivity (Tseng 2004).

The substantial contribution of genetic factors to the development of diabetes has been known for many years. An example for genetic subtypes of

T2DM involves mutations in glucokinase, which phosphorylates glucose to glucose-6-phosphate, leading to impaired glycolysis, showing higher concordance rate for T2DM among monozygotic twins (between 41% and 55%) in comparison to dizygotic twins (between 10% and 15%). There are populations with extremely high prevalence of T2DM, for example Pima Indians that can not be explained solely by environmental factors, but also by familial clustering of diabetes-related traits.

However, it is well known that the incidence of T2DM is also associated with environmental factors. The differences in the prevalence of T2DM in relative populations living in different geographical and cultural regions (for example Asians in Japan and USA) also support the role of non-genetic factors (Malecki and Klupa 2005). The relations between genetic and environmental factors in the development of T2DM may be complex. Environmental factors may be responsible for the initiation of  $\beta$ -cell damage or other metabolic abnormalities, while genes may regulate the rate of progression to overt diabetes. On the other hand, in some cases genetic factors may be necessary for environmental factors even to start processes leading to the development of the disease (Zimmet et al. 2001).

### **3. Insulin signaling and pathways in insulin action**

Insulin is the most potent anabolic hormone known and is essential for appropriate tissue development, growth, and maintenance of whole-body glucose homeostasis. The molecule contains two peptide chains called A chain and B chain linked together by two disulfide bonds. This hormone is secreted by the  $\beta$  cells of the pancreatic islets of Langerhans in response to increased circulating levels of glucose and amino acids after a meal.

Insulin regulates glucose homeostasis at many sites by reducing hepatic glucose output (gluconeogenesis and glycogenolysis) and by increasing the rate of glucose uptake in skeletal muscle and fat to regulate blood glucose concentration (Figure 1). In liver and fat cells, insulin also promotes the synthesis and storage of carbohydrates, lipids, and proteins, inhibits their degradation and release into the circulation, and attenuating fatty acid release from triglycerides in fat and muscle (Pessin and Saltiel 2000).

The first step by which insulin increases energy storage or utilization involves the regulated transport of glucose into the cell, mediated by the glucose transporter GLUT4. Insulin stimulates the translocation of a pool of GLUT4 to the plasma membrane, through a process of regulated recycling, in which endocytosis, sorting into specialized vesicles, exocytosis, tethering, docking, and fusion of the protein are tightly regulated (Chang et al. 2004).

The precise intracellular events that mediate insulin action are initiated through the binding to and activation of its cell-surface receptor, the insulin receptor substrates, and the molecules that interact with these substrates.

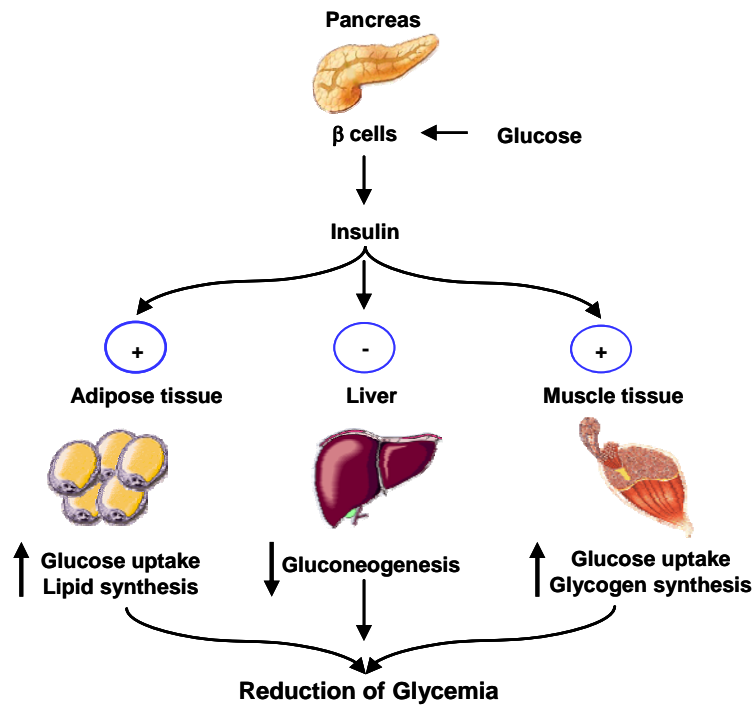


**Figure 1: Glucose homeostasis.** The balance among gluconeogenesis by liver, insulin-dependent utilization of glucose by adipose and muscle tissues is regulated by insulin production from β cells.

### 3.1 The insulin receptor

The insulin receptor is an heterotetrameric bifunctional transmembrane glycoprotein composed of two extracellular  $\alpha$  subunits and two transmembrane  $\beta$  subunits linked by disulfide bonds. The  $\alpha$  subunits contain the insulin-binding domain while the transmembrane  $\beta$  subunits function as a tyrosine-specific protein kinase (IRK), resulting in the increased catalytic activity of the kinase (Paz et al. 1997). Binding of insulin triggers oligomerization and receptor autophosphorylation on tyrosine residues and tyrosine phosphorylation of insulin receptor substrates that include the insulin receptor substrate family (IRS1 through 4), IRS5, IRS-6, Gab-1, Cbl, APS and Shc isoforms, and signal regulatory protein (SIRP) family members (Bandyopadhyay et al. 1997).

### 3.2 Insulin-receptor substrates

The finding that insulin stimulates tyrosine phosphorylation of a 185 kDa protein in all cell types and tissues led to the hypothesis that substrate phosphorylation mediates insulin signal transduction. Four related proteins have recently expanded this family, including IRS-2, IRS-3, Gab-1 and p62<sup>dok</sup>. These docking proteins are not related by extensive amino acid sequence identities, but are related functionally as insulin receptor substrates.

They amplify receptor signals by recruiting SH2-proteins to their autophosphorylation sites and dissociate the intracellular signaling complex from endocytic pathways of the activated receptor, important for insulin-stimulated biological effects such as glucose uptake. The IRS family members vary in molecular weight between 60 KDa and 180 KDa. Each contains several common structures: an NH<sub>2</sub>-terminal PH and/or PTB domain that mediates protein-lipid or protein-protein interactions; multiple COOH-terminal tyrosine residues that create SH2-protein binding site; proline rich regions to engage SH3 domain; serine/threonine-rich regions which may regulate overall function through other protein-protein interactions (White 1998).

Recent data from knockout mice and cell lines suggest that IRS proteins are differentially expressed, may engage different signaling molecules and mediate distinct responses (Saltiel and Kahn 2001). One of the major mechanisms used by IRS-proteins to generate downstream signals is the direct binding to the SH2 domains of various signaling proteins. One pathway proceeds through the insulin receptor substrates IRS-1 and IRS-2 and depends on the activation of the enzyme phosphatidylinositol-3-kinase (PI-3 kinase). PI-3 triggers a series of downstream events involving protein kinase C (PKC), leading to insulin-stimulated translocation of glucose transporters (GLUTs) to the plasma membrane and glucose transport via the transporters (Chang et al. 2004). Another pathway proceeds through Grb2/Sos and Ras, leading to the activation of the MAP kinase isoforms ERK1 and ERK2, that are involved in proliferation and differentiation processes. However, in most cases, a specific effect of insulin requires the participation of both the pathways in a complex interplay which could explain the pleiotropy and the specificity of the insulin signal (Cusi et al. 2000).

### **3.3 The PI-3 kinase pathway and Akt/PKB signaling**

PI-3 kinase is the best studied signaling molecule activated by IRS-1. It plays an important role in the regulation of biological responses by various hormones, growth factors and cytokines, including mitogenesis, differentiation, chemotaxis, membrane ruffling, and insulin-stimulated glucose transport. Moreover, PI-3 kinase dependent pathway has a pivotal role in many insulin-regulated metabolic processes, including glucose uptake, GLUT4 translocation, general and growth-specific protein synthesis and glycogen synthesis. PI-3 kinase was originally identified as a dimer composed of a 110 KDa catalytic subunit (p110 $\alpha$  or p110 $\beta$ ) associated with an 85 KDa regulatory subunit (p85 $\alpha$  or p85 $\beta$ ). The latter one possesses two SH2 domains that interact with tyrosine-phosphorylated pYMXM and pYXXM motifs in IRS proteins, thereby activating the associated catalytic domain. This effect is maximal when both the SH2 domains are occupied (Le Roith and Zick 2001).

Following its activation by insulin, PI-3K catalyses the phosphorylation of phosphatidylinositol-4,5-diphosphate (PIP<sub>2</sub>) to produce phosphatidylinositol 3,4,5 triphosphate (PIP<sub>3</sub>). It binds to the pleckstrin homology (PH) domains of

phosphoinositide-dependent kinase (PDK1), which further phosphorylates Protein kinase B (PKB/Akt) and atypical Protein Kinase Cs (aPKCs) propagating the PI3K signal (Lietzke et al., 2000; Klarlund et al., 1997). Moreover, PI-3-kinase possesses serine kinase activity by interacting with other signaling proteins involved in insulin action independently from PIP3 generation (Kessler et al. 2001).

Akt is a 57 KDa serine/threonine kinase characterized by a pleckstrin homology domain (PH) located in its NH<sub>2</sub> terminal region and a catalytic domain related to protein kinase C (PKC) and protein kinase A (PKA) family members. The three Akt isoforms show a broad tissue distribution and can be activated by a wide variety of growth stimuli such as growth factors and cytokines (Vanhaesebroeck and Alessi 2000). Akt is an important mediator of biological functions of insulin, involving membrane translocation and phosphorylation

Several studies recognized that Akt promotes insulin-stimulated glucose uptake, mediating translocation of vesicles containing GLUT4 from intracellular stores to the plasma membrane. Furthermore, in response to insulin, Akt promotes glycogen synthesis through phosphorylation of both alpha and beta isoforms glycogen-synthase kinase-3 (GSK-3), resulting in the inactivation of the catalytic activity of the enzyme and therefore, activating pathways that are normally repressed by GSK3 (Cantley 2002).

### **3.4 The MAPK pathway**

Another pathway for insulin signaling is the MAPK cascade. This pathway is initiated by tyrosine phosphorylation of IRS1 or Shc proteins by the receptor kinase, inducing their association with the SH2 domain of the adapter protein Grb2 (Figure 2). This association with phosphorylated Shc induces Grb2 to target the nucleotide exchange factor SOS, which in turn associates with and activates the GTP-binding protein p21<sup>ras</sup> (Skolnik et al. 1993). The activation of p21<sup>ras</sup> leads to the stimulation of Raf and other kinases that can phosphorylate MAPK kinase or MEK, a dual specificity kinase that catalyzes the phosphorylation of MAPK on threonine and tyrosine residues, causing its activation (Crews et al. 1992). Activated ERKs mediate the growth promoting effects of insulin; they can translocate into the nucleus, where they catalyze the phosphorylation of transcription factors, phospholipase A<sub>2</sub> and other kinases, such as Elk-1, p62<sup>TCF</sup> etc., initiating a transcriptional programme that leads to cellular proliferation or differentiation. Increased basal Erk1/2 MAPK activity seems to contribute to the development of insulin resistance, on the contrary, the p38 MAPK has been proposed as a positive regulator of insulin action for its capability to increase the uptake of glucose by plasma membrane- localized GLUT4 transporter (Pirola et al. 2004).

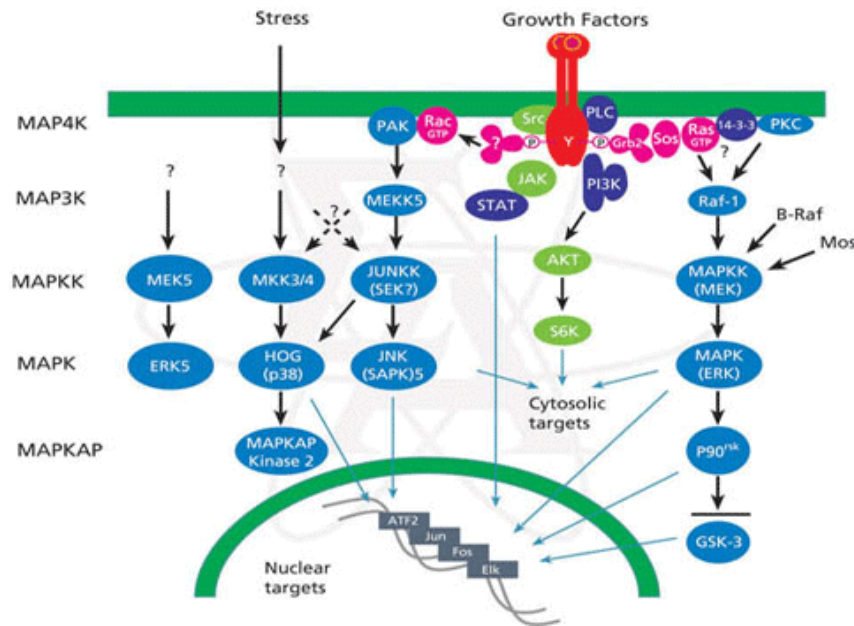


**Figure 2: MAPK pathway.** Extracellular stimuli lead to activation of MAP kinase via a signaling cascade (MAPK cascade) composed of MAP kinase, MAP kinase kinase (MKK or MAP2K), and MAP kinase kinase kinase (MKKK or MAP3K). A MAP3K that is activated by extracellular stimuli phosphorylates a MAP2K on its serine and threonine residues, and then this MAP2K activates a MAP kinase through phosphorylation on its serine and tyrosine residues. This MAP kinase signaling cascade has been evolutionarily well-conserved from yeast to mammals.

### 3.5 The protein kinase C superfamily

Other signaling proteins that have been proposed to function in parallel with Akt include members of the mammalian protein kinase C (PKC) superfamily, which are heterogeneous members of phospholipids-dependent kinases that can be divided into three categories on the basis of cofactor requirements and structure.

The isoenzymes have been classified into three subclasses as follows: the *classical* isoenzymes (PKC- $\alpha$ , - $\beta$ , - $\gamma$ ) which are activated by phorbol esters and calcium; the *novel* (PKC- $\delta$ , - $\epsilon$ , - $\eta$ ), calcium-independent isoenzymes, which can be stimulated by phorbol esters; the *atypical* isoenzymes (PKC- $\zeta$ , - $\lambda$ ), which do not respond to either phorbol esters or calcium (Jaken 1996). The human genes coding for the different PKC isoenzymes have been localized on different chromosomes and show different tissue distributions (Farese 1994).

The isoenzymes consist of a single polypeptide chain that contains similarly to other kinases, an amino-terminal regulatory region (of 20-70 KDa) and a carboxy-terminal kinase domain (of 45 KDa). The regulatory region maintains the catalytic domain in an inactive state because it contains an autoinhibitory domain, or pseudosubstrate, and one or two different membrane-targeting motifs, called C1 domain, which is present in all isoenzymes, and the C2 domain, which is present in conventional and novel protein kinase Cs. The

C1 domain is a cysteine-rich sequence that binds diacylglycerol and phorbol esters, functional analogs of diacylglycerol; the C2 domain binds acidic phospholipids and different regulators that participate in protein activation. The catalytic domain, instead, is responsible for transferring a phosphate group from ATP to appropriate serine or threonine residues in the PKC substrates (Newton 1997; Cortright et al. 2000).

Protein kinase C transduces a myriad of signals and appear to be important their role in insulin action. It has been shown that PKCs mediate insulin effects in muscle and adipose cells, by phorbol esters activation, an analog of DAG (Farese et al. 2005). Nevertheless, PKC $\alpha$  and  $\beta$  have also been shown to inhibit insulin signaling. In particular, overexpression of PKC $\alpha$  determines an increased serine/threonine phosphorylation of IR and IRS1 with a subsequent reduction of IR tyrosine kinase activity and signaling (Chin et al. 1993). Much more accepted, instead, is the concept that PKC $\zeta$  and  $\lambda$  are relevant molecules in mediating insulin effect on glucose transporters translocation and glucose uptake in different cell systems.

### **3.6 Glucose transport**

Glucose transport in mammalian cells and tissues occurs by facilitated diffusion mediated by a family of glucose transporters. Six different transporter proteins, encoded by distinct genes, have been characterized in mammalian tissues, denoted GLUT1 through GLUT5 and GLUT7, according to their chronological identification by molecular cloning. The GLUT1 gene product is most abundant in red blood cells and brain microvessels but is present in almost every tissue. GLUT2 is found predominantly in liver, enterocyte basolateral membranes and pancreatic  $\beta$  cells. GLUT3 is expressed almost exclusively in brain neurons and fetal muscle. GLUT4 expression is restricted to tissues where glucose transport is insulin sensitive, i.e., skeletal and cardiac muscles, brown and white fat. GLUT5 is present in human enterocyte luminal membranes, sperm, skeletal muscle and adipocytes. GLUT6 is pseudogene with no protein product and GLUT7 is the intracellular glucose transporter of liver microsomes (Klip et al. 1994).

The major GLUT isoforms involved in glucose uptake by cells and tissues in response to insulin stimulation are GLUT1 and GLUT4. GLUT1 contributes to basal glucose uptake because it is localized mostly at the plasma membrane in the basal state, whereas GLUT4 is sequestered in intracellular organelles and translocates to the cell surface only after insulin stimulation. Several studies from L6 muscle cells and 3T3-L1 adipocytes demonstrated the mechanism involved in GLUT4 translocation (Condorelli et al. 1998). In particular, activation of the insulin receptor induces tyrosine phosphorylation of the IRS family of protein substrates that, in turn, engages the SH2 domains of the p85 subunit of PI 3-kinase (Figure 3). This activation generates the formation of PIP3 that stimulates the kinase activity of PDK, interacts with PKB and activates the atypical PKC family members (zeta and lambda), responsible for insulin-stimulated glucose transport (Watson and Pessin 2006).

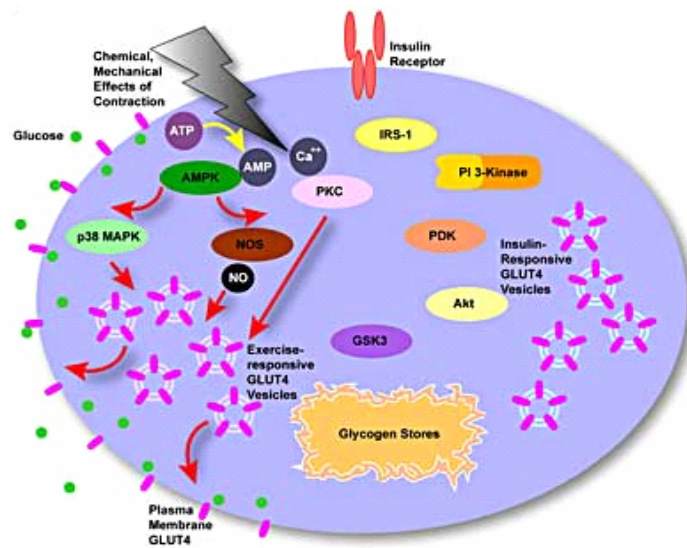


**Figure 3: Insulin signal transduction.** A schematic model for insulin-stimulated glucose transport depicting the involvement of the classic PI 3K-dependent pathway and the proposed PI-3K-independent, alternative pathway. The activated insulin receptor catalyzes IRS tyrosine phosphorylation, leading to recruitment of downstream effectors, the most crucial for glucose transport being PI-3K. Akt and the atypical PKC isoforms have both been implicated as PtdIns(3,4,5)P3 effectors involved in GLUT4 translocation, although it has been proposed that these two Ser/Thr kinases target separate GLUT4 compartments.

Moreover, recent observations indicate that high insulin levels and not insulin deficiency cause a reduction in GLUT4 mRNA by inhibiting GLUT4 transcription. This may provide an explanation for the reduction in GLUT4 mRNA levels observed in adipose cells and skeletal muscle of some animal models of non-insulin-dependent diabetes (Flores-Riveros et al. 1993).

#### 4. Defects in insulin action

Many mutations in the insulin receptor gene are known to lead to impaired insulin receptor biosynthesis, while others can affect post-translational modification of the proteins and thus, reduce the transport of the receptor to the cell surface and in turn, the ability to phosphorylate substrate proteins. Other mutations can impair the binding of insulin to its receptor or the activation of the receptor tyrosine kinase. These mutations typically behave in recessive manner and can be associated with severe insulin resistance and rare syndromes (Stern 2000).

Several studies have been conducted to investigate this topic, including studying rare monogenic forms of insulin resistance, assessing insulin resistance in the relatives of diabetic individuals, comparing the differential concordance of insulin resistance between monozygotic and dizygotic twins and studying nuclear families. The major negative control results from

phosphorylation of serine/threonine residues on the receptor and/or IRS proteins. A deleterious role for molecules released from the adipose tissue is postulated in the insulin-resistance of the liver and muscles present in type 2 diabetes, obesity and metabolic syndrome.

#### **4.1 Insulin resistance**

Insulin resistance (IR) has emerged as an impaired biological response to insulin caused by reduced insulin-stimulated glucose uptake in skeletal muscle and by impaired suppression of endogenous glucose production, which are critical for maintaining normal glucose homeostasis. Initially, is present a compensatory increase in insulin secretion to maintain normal blood glucose levels and, if this is insufficient, blood glucose concentration increases in both the fasting (impaired fasting glucose) and postprandial (impaired glucose tolerance) states. The coexistence of insulin resistance and hyperinsulinaemia appears to contribute directly or indirectly to many other disorders, such as typical forms of type 2 diabetes mellitus, dyslipidaemia, hypertension, atherosclerosis and a pro-coagulant state (Samaras et al. 2006).

#### **4.2 Mechanisms of insulin resistance**

Numerous studies focused on dysregulation of insulin post-receptor signaling have established associations between molecular events and insulin resistance, with deregulated concentrations of cytokines (TNF- $\alpha$ , IL-6), metabolites (glucose, glucosamine, fatty acids) and glycated proteins, which often contribute to IR by increasing Ser/Thr phosphorylation of IRS-1 (Figure 4). TNF- $\alpha$  and IL-6 decrease insulin signaling by impairing the insulin-stimulated tyrosine phosphorylation of IRS molecules and by inducing the suppressors of cytokine signaling, SOCS-1 and -3, which have at least three different mechanisms of action: they compete with IRS-1 for association with insulin receptor, they inhibit Janus kinase, involved in insulin signaling, and they augment proteosomal IRS-1 degradation (Mlinar et al. 2006).

Hyperglycaemia also has adverse consequences on the efficacy of insulin action because severely decreases Akt/PKB activity. Besides glucosamine produced from glucose and being the main substrate for cellular glycosylation, enhances glycosylation of IRS-1, thereby decreasing its activity and glycosylation of glycogen-synthase, which reduces its insulin responsiveness. High concentrations of circulating fatty acids contribute to the induction of insulin resistance by decreasing insulin-induced PI3K activation and inhibit insulin-mediated glucose metabolism by affecting a number of protein kinases in rats. Finally, glycated proteins, emerging as a consequence of hyperglycaemia, were shown to diminish intracellular PI3K, PKB and GSK-3 activity, thus possibly contributing to IR (Pirola et al. 2004).

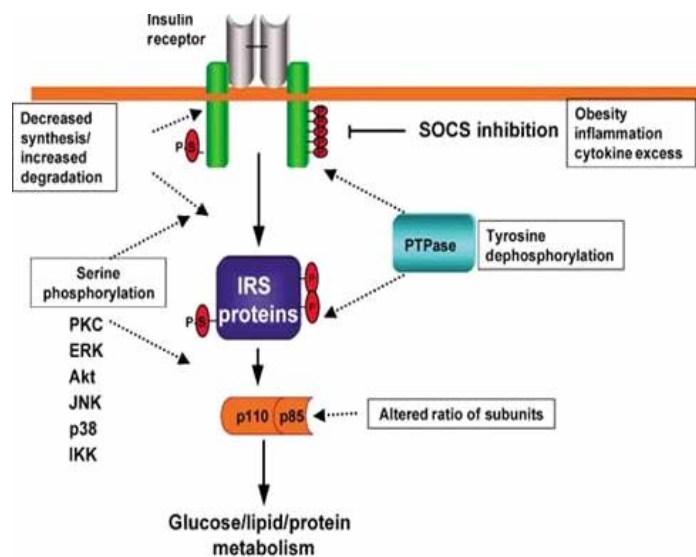


**Figure 4: Mechanisms that can produce insulin resistance.** Multiple mechanisms exist for down regulation insulin signaling, such as decreased synthesis, increased degradation, inhibitory serine phosphorylation, interaction with inhibitory proteins, and alteration of the ratios of different molecules.

## 5. PED/PEA-15 protein

The Phosphoprotein Enriched in Diabetes/ Phosphoprotein Enriched in Astrocytes-15 (PED/PEA-15) is a 15 kDa cytosolic protein widely expressed in different tissues and highly conserved among mammals, whose gene maps on human chromosome 1q21-22 (Estelles et al. 1996).

The structure of PED/PEA-15 includes a canonical N-terminal Death Effector Domain (DED) of 80 aminoacids that regulate apoptotic signaling pathways (Figure 5). Within the N-terminus there is a nuclear export sequence (NES) that mediate its cytoplasmic localization. In particular, PED/PEA-15 regulates the actions of ERK-MAP kinase cascade by binding to ERK in the nucleus, exporting it into the cytoplasm and preventing the entrance into the cell cycle caused by sustained phospho-ERK nuclear accumulation (Formstecher et al. 2001; Brunet et al. 1999).

In the C-terminal domain, PED/PEA-15 protein can be phosphorylated on two different residues: the Ser104, identified as a site of regulation for protein kinase C (PKC) (Araujo et al. 1993; Estelles et al. 1996), and the Ser116 regulated by calcium-calmodulin kinase 2 (CaMKII) (Kubes et al. 1998) and PKB/Akt (Trencia et al. 2003; see below attached publications).

PED/PEA-15 can interact with a number of proteins: FADD and FLICE through its DED domain; ERKs, whose bindings requires distinct regions in both the DED and C-terminal region (Hill et al. 2002); OMI/HtrA2, whose binding requires the DED (Trencia et al. 2004); PLD, whose interacting site consists of part of the DED plus additional C-terminal flanking sequences (Zhang et al. 2000).

It has been recently demonstrated that PED/PEA-15 plays an important role both as antiapoptotic and as inducer insulin-resistance.

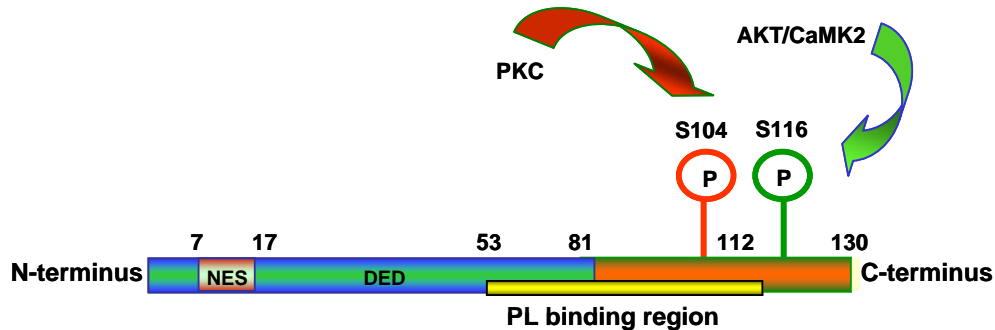


Figure 5: Structure of PED/PEA-15 protein.

### 5.1 PED/PEA-15 and its antiapoptotic function

Several lines of evidence showed that PED/PEA-15 exerts its antiapoptotic action through at least three distinct mechanisms. Firstly, the DED of PED/PEA-15 binds the DED of both Fas Associated Death Domain (FADD) and caspase 8 (FLICE), thereby inhibiting FLICE activation by tumor necrosis factor- $\alpha$  and Fas-L, preventing DISC assembly and blocking the apoptotic effects of these cytokines (Condorelli et al. 1999). Interestingly, PED/PEA-15, also plays a crucial role in the negative regulation of TRAIL, a member of the TNF family that triggers rapid apoptosis in different types of tumor cells, included malignant glioma cells. This study has demonstrated that PED/PEA-15 plays an important role in tumor sensitivity to anti neoplastic agents (Hao et. al. 2001). Increased levels of protein confer, indeed greater susceptibility to skin carcinogenesis *in vivo* and may enhance cutaneous tumor progression toward malignancy (Formisano et al. 2005).

Secondly, PED/PEA-15 prevents stress-activated protein kinase (SAPK) activation triggered by growth factor deprivation, oxidative stress (exposure to  $H_2O_2$ ) and anisomycin treatment. The inhibition of apoptosis induced by these stimuli is exerted by blocking JNK1/2 and p38 phosphorylations, and inhibits stress-induced Cdc-42, MKK4 and MKK6 activation by requiring also the interaction of PED/PEA-15 with ERK1/2 (Condorelli et al. 2002; see below attached publications).

Thirdly, it has also been recently shown that PED/PEA-15 also binds to Omi/HtrA2, a serine protease and a mitochondrial protein, inhibiting apoptosis triggered by stress and physical agents. After UV exposure, Omi/HtrA2 released into the cytosol binds and displaces the mammalian caspase inhibitor XIAP releasing their suppressive effect on caspases activity. Interestingly, this mechanism was accompanied by a significant decrease in cellular PED/PEA-15 levels, due to an increased PED/PEA-15 degradation upon OMI/HtrA2 release into the cytoplasm (Trencia et al. 2004).

## 5.2 PED/PEA-15 and its role in insulin resistance

Overexpression of the PED/PEA-15 gene is a common defect in type 2 diabetes. During a study using a differential display technique to identify genes whose expression was altered in type 2 diabetes, it has been demonstrated that both PED/PEA-15 mRNA and protein levels were overexpressed in fibroblasts from type 2 diabetics compared with non-diabetic individuals (Figure 6). Also skeletal muscle and adipose tissues, two major sites of insulin resistance in type 2 diabetes, showed the same behaviour (Condorelli et al. 1998).

Furthermore, a recent study showed that PED/PEA-15 overexpression represents a common abnormality in both T2DM and their First Degree Relatives (FDR) and can be easily detected in peripheral blood leukocytes. In susceptible individuals, this defect associates with the presence of T2DM-affected subjects in the pedigrees and not with other major T2DM risk factors. In euglycemic FDR of T2DM, high PED/PEA-15 levels strongly correlate with resistance to insulin action in the lean mass, suggesting that PED/PEA-15 contributes to early appearance of insulin-resistance in these individuals (Valentino et al. 2006).

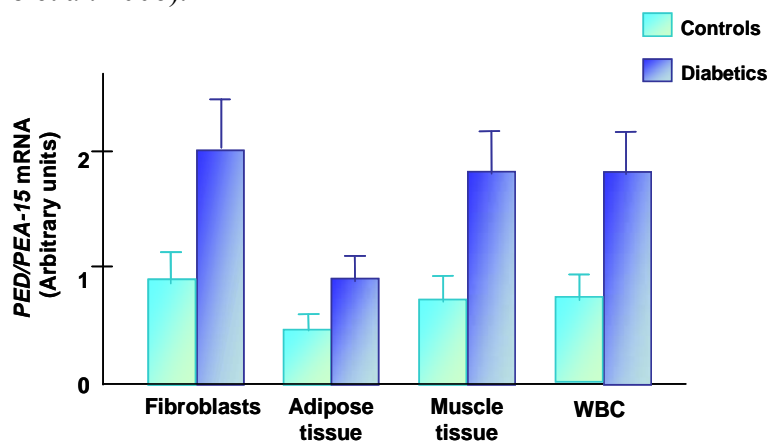


**Figure 6: PED/PEA-15 mRNA levels.** RNA was extracted from fibroblasts, skeletal muscle, adipose tissues and white blood cells from type 2 diabetics and their controls. The quantification by real-time PCR showed that PED/PEA-15 mRNA was overexpressed both in tissues and in blood cells.

To investigate the role of ped/pea-15 gene in the insulin resistance, several studies have been performed *in vitro* and *in vivo*.

*In vitro*, Ped/Pea-15 cDNA has been stably transfected in L6 skeletal muscle and 3T3-L1 adipose cells to levels comparable to those occurring in type 2 diabetes. These cells overexpressing PED/PEA-15 showed an impaired glucose uptake with a lack of further insulin-dependent uptake and the use of an antisense oligonucleotide to inhibit endogenous PED/PEA-15 expression in muscle cells and adipocytes significantly expanded insulin sensitivity of glucose uptake. Thus, PED/PEA-15 may represent a physiological regulator of glucose transporter trafficking and glucose transport in the major insulin-

responsive skeletal muscle and adipose tissues (Condorelli et al. 1998). A following study has shown that in L6 skeletal muscle cells overexpressing PED/PEA-15 (L6<sub>PED</sub>), PKC $\alpha$  and  $\beta$  are also constitutively activated, while PKC $\zeta$  features no basal change but completely loses insulin sensitivity in L6<sub>PED</sub>. In these cells, blockage of PKC $\alpha$  and  $\beta$ , additively rescues glucose uptake to the levels of cells expressing only endogenous PED/PEA-15 (L6), restoring most of the defect in both basal and insulin-stimulated glucose uptake. Blockage of PKC $\alpha$  and  $\beta$  also restores insulin activation of PKC $\zeta$  in L6<sub>PED</sub> cells. Similar rescue of normal glucose uptake and PKC $\zeta$  activation were also achieved by overexpression of PKC $\zeta$  in L6<sub>PED</sub> cells. Thus, chronic activation of PKC $\alpha$  and  $\beta$  caused by the overexpression of PED/PEA-15 appears to downregulate insulin induction of PKC $\zeta$  activity (Condorelli et al. 2001).

*In vivo*, we reported that transgenic mice overexpressing PED/PEA-15 to levels comparable to those occurring in human type 2 diabetes exhibit mildly elevated random-fed blood glucose levels and become hyperglycemic after glucose loading, indicating that increased expression of this gene is sufficient to impair glucose tolerance. Moreover, transgenic mice become diabetic after administration of high-fat diets, indicating that, *in vivo*, the overexpression of PED/PEA-15 in conjunction with environmental modifiers may lead to diabetes. Based on the insulin tolerance tests, ped/pea-15 transgenic mice were less sensitive to insulin as compared with their nontransgenic littermates. Furthermore, transgenic mice were markedly hyperinsulinemic in the basal state and exhibited increased free fatty acid levels in blood: these findings indicate the presence of insulin resistance in PED/PEA-15 mice. This abnormality has been associated with a decrease in insulin stimulated glucose uptake. GLUT4 membrane translocation in response to insulin was also significantly decreased in tibialis muscles and perigonadal adipose tissues from PED/PEA-15 transgenic mice, without a significant change in the total GLUT4 levels in transgenic muscle or adipose tissues.

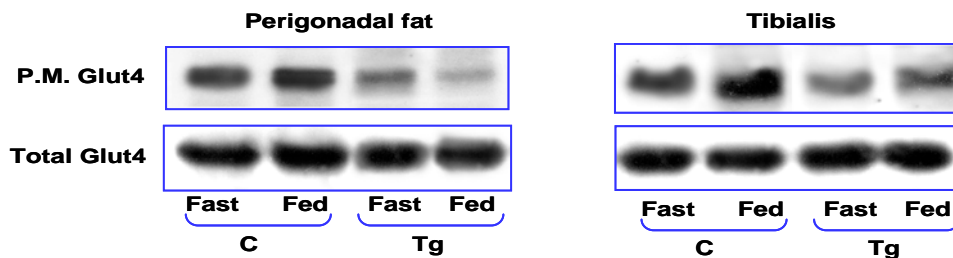


**Figure 7: GLUT4 membrane translocation.** Tissues from insulin-injected animals were frozen in liquid nitrogen and harvested for plasma membrane preparation. Total homogenates and plasma membrane lysates were then analyzed by Western blotting with GLUT4 antibody. Blots were revealed by enhanced chemiluminescence and autoradiography. The autoradiographs shown are representative of four independent experiments ( see below attached publications).

This defect was accompanied by dysregulation of protein kinase C signaling, independently of the phosphatidylinositol 3-kinase/Akt/PKB pathway. Indeed, transgenic mice showed an increased PKC $\alpha$  activation and a block of insulin induction of protein kinase C $\zeta$ . Furthermore, the transgenic mice showed reduced insulin response to a glucose challenge, indicating that the overexpression of PED/PEA-15 impairs insulin secretion in addition to insulin action (Vigliotta et al. 2004; see below attached publications).

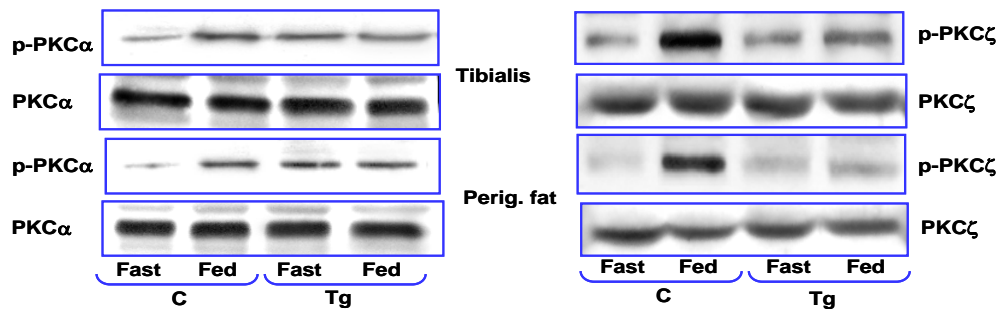


**Figure 8: PKC signaling in ped/pea-15 transgenic mice.** The mice were fasted overnight or fed ad libitum, followed by intraperitoneal insulin injection ( $0.75 \text{ mU g}^{-1}$  body weight). The animals were killed, and tibialis or perigonadal fat tissue was collected, homogenized, and solubilized. The lysates were Western blotted with phospho-PKC $\alpha$  (P-PKC $\alpha$ ) and PKC $\alpha$  antibodies (left panel) to analyzing PKC $\alpha$  activation, while with phospho-PKC $\zeta$  (P-PKC $\zeta$ ) and PKC $\zeta$  antibodies to evaluate PKC $\zeta$  activation (see below attached publications).

Thus, these findings identify PED/PEA-15 as a novel gene controlling insulin action and insulin secretion contributing, under appropriate environmental conditions, to genetic susceptibility to type 2 diabetes in humans.

## 6. Phospholipase D protein

As noted above, PED/PEA-15 interaction with PLD may represent an initial major event in dysregulating insulin action (Vigliotta et al. 2003; see below attached publications). Classical phospholipase D (PLD) enzymes hydrolyze the principal membrane lipid phosphatidylcholine (PC) to generate phosphatidic acid (PA) and free choline (Cho) and performs a transphosphatidylation reaction using water or primary alcohols (ethanol or 1-butanol) as the nucleophile to generate PA, phosphatidylethanol or phosphatidylbutanol (PBut), respectively (Figure 9) (Jenkins and Frohman 2005). PLD is a member of a superfamily, which includes phosphoinositide-specific phospholipase C, phospholipase A<sub>2</sub> and sphingomyelinase; all are phospholipids-degrading enzymes that generate biologically active products which are assumed to play important functions in cell regulation. In the context of these specific roles, PLD has been proposed to function in regulated secretion, cytoskeletal reorganization, membrane trafficking, transcriptional

regulation and cell-cycle control (Liscovitch et al. 2000).

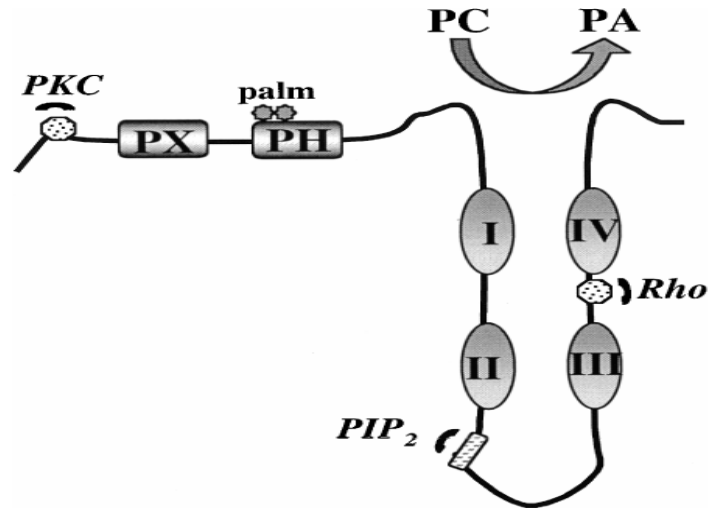


**Figure 9: Structure of PLD1 with some notable structural features.** Catalysis requires the four conserved regions (I - IV), which can even be co-expressed separately. Sites of interaction of two activators (PKC and Rho) are indicated. Near the N-terminus of the protein, three potential membrane-targeting signals are evident, a PX domain, a PH domain and a dual palmitoylation site (palm; cysteine residues 240 and 241) within the PH domain.

PLD superfamily members are found in organisms ranging from viruses to bacteria, yeast, plants and animals, where PLD activity is present in a wide variety of cell types including blood platelets, hepatocytes, lymphocytes, fibroblasts, neuronal cells, muscle cells and endothelial cells. Cloning of the plant and yeast PLDs led ultimately to the cloning of two mammalian isoforms: PLD1 and PLD2, each of which is expressed as two splice variants and localized the first, on the Golgi or perinuclear vesicular structures, whereas the second, appears to be associated with the plasma membrane (Exton et al. 2002). The defining feature of PLD enzymes is the catalytic motif designated HKD, denoting the HxxxxKxD sequence, where the aminoacids are histidine (H), any amino acid (x), lysine (K) and aspartic acid (D), which are critical for enzymatic catalysis both *in vitro* and *in vivo*, as evidenced by the observation that point mutations in the motif disrupt PLD activity (Sung et al. 1997). Other highly conserved regions the PLD genes are the phox consensus sequence (PX), the pleckstrin homology (PH) domain and the PI<sub>4</sub>,5P<sub>2</sub> binding site at their N-terminal which are implicated in phospholipids and protein binding (Figure 10) (Exton 2002). Further, only in PLD1 is present a conserved loop region proposed to function as a possible negative regulatory element (Sung et al. 1999). The C-terminal four amino acids of mammalian PLDs are completely conserved and any change of these residues causes loss of catalytic activity (Xie et al. 2000).

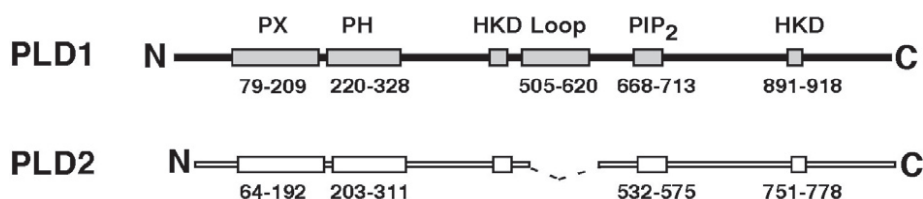


**Figure 10: Basic Structure of PLD1 and PLD2.** Structure showing amino (N) and carboxy (C) terminals. Conserved domains are shown as boxes: the catalytic HKD motif, phox consensus sequence (PX), pleckstrin homology (PH), phosphatidylinositol bisphosphate (PIP<sub>2</sub>) and PLD1 loop region.

Mammalian PLD activity is regulated by many factors, including phosphoinositides, Protein kinase C- $\alpha$  (PKC $\alpha$ ), ADP ribosylation factor (ARF), Rho GTPases such as RhoA, Cdc42, Rac1 and non-PKC protein phosphorylation. In comparison with PLD1, recombinant PLD2 exhibits high basal activity *in vitro*, so it can be activated mildly by ARF, exhibiting 1,5-2 fold activation (Sarri et al. 2003).

### 6.1 PLD1 isoform: expression and regulation

The mammalian PLD1 cDNA was cloned from HeLa cell library and found to encode a 1074-amino-acid protein. PLD1 has been renamed PLD1a after another splice variant has been identified, PLD1b, that lacks a 38-amino-acid region. The domain structure contains the four core domains I-IV, a putative PX domain, a C-terminal motif which is conserved in all eukaryotic PLDs and a 116-amino-acid loop between domains I and II (Sung et al. 1997). The phospholipase D1 is highly expressed in kidney and lung, but detectable levels were also observed in small intestine, colon, liver, heart and spleen, but very low levels were seen in the testis, thymus and muscle (Katayama et al. 1998). Several studies have showed that PLD activity correlated with metabolic regulation, hormone response, mitogenesis, cardiac and brain function, immune response, senescence and neoplasia, and is regulated by various small GTPases such as Arf1 and its isoforms, RhoA, other Rho family members, and RalA (Colley et al. 1997). The members of Rho family G proteins activate PLD1 *in vitro* and *in vivo* (Chong et al. 1994); all Arf family G proteins activate PLD1 *in vitro*, whereas the evidence for an *in vivo* role is strongest for Arf 6, which is principally localized to the plasma membrane (Cavenagh et al. 1996). Ras and Ral appear to play a role in the regulation of PLD by tyrosine kinases even if the mechanisms involved are not clear (Jiang et al. 1995). Studies with inhibitors of tyrosine kinases suggest a role for tyrosine phosphorylation in the activation of PLD by many agonists whose receptors couple to heterotrimeric G proteins (Exton 2002). In addition, Protein kinase C- $\alpha$  is a major regulator of PLD activity both *in vivo* and *in vitro*, through a direct non-phosphorylating mechanism (Kim et al. 2000).

## 7. PED/PLD1 interaction: D4 domain

Recent studies showed that PLD1 associated with GLUT4-containing membranes acted in a constitutive manner to promote the mechanisms of GLUT4 translocation by insulin (Emoto et al. 2000). Given the proposed roles for PLD1 in regulation of GLUT4 translocation, in signal transduction, apoptosis and its regulation by PKC, PED/PEA-15 appeared to be an interacting partner of potential biological significance.

Interestingly, observations suggested that PED/PEA-15/PLD1 binding resulted in increased PLD1 levels, thus increasing PLD activity both *in vitro* and *in vivo*. The PLD1 interaction domain of PED/PEA-15 was identified based on multiple overlapping clones obtained using a two hybrid screening approach. The amplification by polymerase chain reaction to obtain shortest overlapping region identified the D4 domain as the minimum interacting domain (Figure 11). Then, pull-down experiments using GST-fused proteins demonstrated that PED/PEA-15 binds PLD1 and the D4 domain was detected using Western blotting visualization. Finally, the interaction PED/PEA-15/PLD1 has been also examined in extracts from different eukaryotic cells, using antibodies anti-PED/PEA-15. The D4 fragment of PLD1 co-immunoprecipitated efficiently with PED/PEA-15 and vice-versa, demonstrating that the interaction was specific (Zhang et al. 2000).

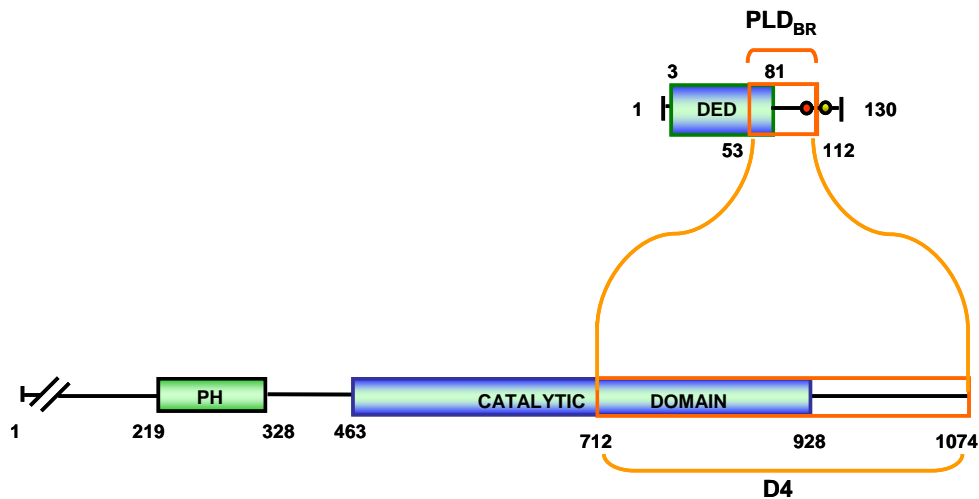


Figure 11: Schematic representation of PED/PEA-15/PLD1 minimal interaction domain.

## AIM OF THE STUDY

Ped/Pea-15 gene is overexpressed in peripheral tissues from type 2 diabetics. In cultured cells and in transgenic mice, PED/PEA-15 overexpression impairs insulin-resistance and insulin secretion.

Recent findings from our own as well as other groups indicated that PED/PEA-15 is a phospholipase binding protein. Increased interaction of PED/PEA-15 with PLD1 could be a key event in mediating abnormalities in insulin action *in vitro* and *in vivo*.

The aim of this work has been to prove the concept that limiting PED/PEA-15/PLD1 interaction may improve insulin-sensitivity *in vitro* and *in vivo* and ameliorate glucose tolerance in PED/PEA-15 overexpressing mice and in other animal models of type 2 diabetes.

# MATERIALS AND METHODS

## **Plasmids construction**

The cloning of PED/PEA-15 cDNA in pcDNA3 vector containing the Myc-tagged has been previously described (Condorelli et al. 2002; see below attached publications). The D4 cDNA fragment has been amplified by PCR by HeLa cells in a reaction mixture with Taq-Long Expand PCR System (Roche Diagnostics, Mannheim, Germany) and with the following primers: Hind III-D4 5'-CGATCAAGCTTCGCTGGAACCTCACAAAAAT-3' and Xba I-D4 5'-CGATCTCTAGAGGATACGAGAATGCGTCAGG-3' for cloning in pcDNA3-HA vector and with the following primers: Hind III-D4-F 5'-GCTAGGGTACCGGATACGAGAATGCGTCAGG-3' and Kpn I-D4-R 3'-CGATCAAGCTTCCGCTGGAACCTCACAAAAAT-5' for cloning in pEGFP-C2 vector. The fragment D4 in both vectors has been amplified with following program: 1 cycle (94°C for 2'), 10 cycles (94°C for 10'', 58°C for 30'', 68°C for 3'), 25 cycles (95°C for 30'', 58°C for 30'', 68°C for 3'and 20'') plus an increase of 20'' to each cycle for elongation time, 1 cycle (68°C for 7'), stop 4°C. The PCR-derived fragment was sequenced to confirm its predicted composition (Primm San Raffaele Biomedical Science Park, Milan Italy). The D4 fragment (1,1 kb) has been cloned into pcDNA3-HA vector carrying Hind III-XbaI restriction sites and in pEGFP-C2 vector carrying Hind III-Kpn I restriction sites. The presence of D4 fragment has been confirmed by DNA sequencing (PRIMM).

## **Cell culture and Transfections**

The 293 human kidney embryonic cells and L6 rat skeletal muscle cells were grown in Dulbecco's Modified Eagle's Medium supplemented with 10% fetal calf serum, 10,000 U/ml penicillin, 10 mg/ml streptomycin and 2% L-Glutamine in a 5% humidified CO<sub>2</sub> incubator. Transient transfections have been performed using the Lipofectamine Plus as according to the manufacturer's instructions (Invitrogen Corporation, Carlsbad, CA) and total of 4-6 µg plasmid DNA for dish. Stable transfections have been performed by selecting positive clones with G418 (Calbiochem, Darmstad, Germany) at the effective dose of 0,8 mg/ml. Cellular loading of PED/PEA-15 peptides (1-53, 53-79, 79-112) has been performed with cationic lipid mixture ProVectin<sup>TM</sup> Protein Delivery Reagent (Imgenex Corporation, San Diego, CA).

## **Western Blot Analysis and Immunoblotting**

Cells grown in a subconfluent culture were lysed in lysis buffer (50 mM HEPES, pH 7.5, 150 mM NaCl, 10 mM EDTA, 10 mM Na<sub>4</sub>P<sub>2</sub>O<sub>7</sub>, 2 mM Na<sub>3</sub>VO<sub>4</sub>, 100 mM NaF, 10% glycerol, 1% Triton X-100, 1 mM PMSF, 10 mg/ml aprotinin) for 2 h at 4°C and lysates were centrifuged at 14,000 x g for 15 minutes to remove cellular debris. Protein concentrations were determined by Biorad Dc Protein Assay kit and equal amounts of the protein from each sample were separated by sodium dodecyl sulfate-polyacrylamide gel electrophoresis (SDS-PAGE) with 12% gels, as described by Laemmli, 1997.

Proteins separated on the gels were electroblotted onto nitrocellulose filters and probed with antibodies to PED/PEA-15 antiserum (1:2000), anti-PLD (1:1000 Cell Signalling Technology, Beverly, MA), p-PKC $\alpha$  and HA (1:2000 Upstate Biotechnology, Lake Placid, N.Y.), p-PKC $\zeta$ , and Tubulin (1:2000 Santa Cruz Biotech Inc., CA), GFP-peptide living colors (BD Transduction Laboratories, USA). Immunoreactive bands were visualized by enhanced chemiluminescence (ECL kit, Amersham Pharmacia Biotech, Piscataway, NJ, USA).

#### **PLD assay in intact cells**

*In vivo* PLD activity was performed measuring phosphatidic acid and phosphatidyl-butanol. For experiments involving insulin and TPA stimulation, the cells were transfected with 6  $\mu$ g of PED/PEA-15 cDNA. The cells were labelled with 5  $\mu$ Ci of [ $^{14}$ C] palmitic acid for 60-min dish, added to the starvation medium (DMEM + 0,25%BSA) and incubated over night at 37°C in a 5% CO $_2$ -enriched, humidified atmosphere. The cells were washed twice in HHBG buffer (10 mM HEPES pH 7.4, 1,26 mM CaCl $_2$ , 0,5 mM MgCl $_2$ , 0,4 mM MgSO $_4$ , 5,37 mM KCl, 137 mM NaCl, 4,2 NaH $_2$ PO $_4$ , 1% (w/v) BSA, 10 mM glucose) and incubated in 0,5% butan-1-ol in HHBG buffer for 20 minutes at 37°C. Subsequently, the cells were treated with or without insulin (160 ng/ml) for 30 minutes. After incubation the buffer was aspirated and 0,5 ml of ice-cold methanol was added to each dish. The cell debris was scraped as described by B. and Dyer into a glass vial and kept on ice. Chloroform and 2 N HCl were added to give a final chloroform/methanol/HCl ratio of 1:1:0,04 (by vol.). After vortex-mixing the vials were centrifuged at 1200 g for 5 minutes and the lower phase containing lipids was prelevated and incubated with 500  $\mu$ l of chloroform and 50  $\mu$ l of 2 N NaCl in other vials. After vortex-mixing the vials were centrifuged at 1200 g for 5 minutes and the lower phase was prelevated to unite it to previous phase. The organic phase was dried with N $_2$  e the lipids were resuspended in 20  $\mu$ l of chloroform. Then, they were spotted on to Wathmann TLC plates. The labelled products were separated by TLC using the upper phase of a mixture of ethylacetate/2,2,4-trimethylpentane/acetic acid/water ratio of 13:2:3:10 (by vol.). The positions of the spots corresponding to [ $^{14}$ C] phosphatidyl-butanol were determined by autoradiography. The area containing phosphatidylbutanol was scraped and the radioactivity was counted.

#### **Co-immunoprecipitation**

Lysates from HEK293 and L6 transfected and untransfected cells and tissues (i.e. brain and skeletal muscle) from Ped/Pea-15 transgenic mice were precleared with 20  $\mu$ l of pre-immune serum at 4°C for 30 minutes. For each condition, 2  $\mu$ g of PED/PEA-15 or PLD 1 antibodies were added to 500  $\mu$ g of cleared lysates and incubate at 4°C for 16 h. After incubation, the mixture was incubated with 20  $\mu$ l of protein A Sepharose resin pre-equilibrated (Sigma-Alderich Chemie Steinheim, Germany) with HNT buffer (50 mM HEPES, pH 7.5, 150 mM NaCl, 0,1% Triton X-100) for 2 h at 4°C with vibrant shaking. The protein A Sepharose resin were precipitated by centrifugation at 10,000 rpm for 2 minutes and washed with 500  $\mu$ l of washing buffer for five times.

The bound antibody-antigen complexes were eluted in sample buffer and total elute was separated by 12% SDS-PAGE, transferred to nitrocellulose membranes and blotted with PLD1 or PED/PEA-15 antibodies. The enhanced chemiluminescence was performed as previously described.

#### **Immunofluorescence microscopy**

Cells were grown onto glass coverslips in six-well multidishes and allowed to adhere for 24 hours. Cells were fixed with methanol for 5 minutes at  $-20^{\circ}\text{C}$  and blocked with PBS containing 3% normal goat serum for 1 hour at room temperature. The primary antibody was made in blocking solution and incubated for 1 hour at room temperature. The cells were incubated in a 1:1000 dilution of the appropriate secondary antibody conjugated to fluorescein isothiocyanate for 30 minutes at room temperature for GFP detection. After washes with TBS-0,1% Tween 20, the coverslips were stained with 4,6-Diamidino-2-phenylindole (DAPI) to identify the nucleus. Immunostaining and DAPI staining were mounted with 50% glycerol in PBS and were examined under a fluorescence microscopy (Leica, Exton, PA).

#### **PLD assay *in vitro***

For PLD1 activity assay, brain and muscle tissue from Ped/Pea-15 transgenic mice were homogenized in T-PER<sup>TM</sup> extraction reagent (Pierce, Rockford, IL). Each homogenate was centrifuged at 10,000 rpm for 5 minutes: the pellet was discarded, while the supernatant was designated as crude membranes. PLD1 activity was determined under the assay condition by measuring the transphosphatidylolation activity in the presence of butan-1-ol. The standard assay mixture, containing 50 mM HEPES/NaOH, pH 7.5, 200 mM NaCl, 3 mM MgCl<sub>2</sub>, 2 mM CaCl<sub>2</sub>, 3 mM EGTA, 1 mM dithiothreitol, 400 mM butan-1-ol, 140  $\mu\text{M}$  phosphatidylethanolamine (PE), 12  $\mu\text{M}$  PIP<sub>2</sub> and 8,6  $\mu\text{M}$  1-palmitoyl-2-[1-<sup>14</sup>C] palmitoyl-PC (Amersham International) in a total volume of 100  $\mu\text{l}$ , was incubated for 60 minutes at  $37^{\circ}\text{C}$ . 1  $\mu\text{M}$  of PC, 1,4  $\mu\text{M}$  of PIP<sub>2</sub> and 16  $\mu\text{M}$  of PE were added as a mixed micelles. Recombinant 1  $\mu\text{M}$  of ARF1 and 0,05  $\mu\text{M}$  of RhoA were added to the mixture and were activated using 10  $\mu\text{M}$  of Guanosine 5'-[ $\gamma$ -thio]-triphosphate (GTP[S]). The reaction was stopped with 100  $\mu\text{l}$  of 1 M HCl and the lipid product was extracted with 1 ml of chloroform/methanol (2:1 by vol.) and washed with 0,5 ml of 170 mM NaCl. The lower phase was isolated, concentrated in a centrifugal vaporizer and separated on a Silica Gel 60 TLC plate with chloroform/methanol/acetic acid (13:3:1 by vol.) as the developing solvent. The positions of the spots corresponding to [<sup>14</sup>C] phosphatidyl-butanol were determined by autoradiography. The area containing phosphatidyl-butanol was scraped and the radioactivity was counted.

#### **Flow cytometry**

Six-well multidishes containing  $2,5 \times 10^5$  L6 and L6<sub>PED</sub> cells were incubated for 24 hours at  $37^{\circ}\text{C}$  in 2 mL complete medium and were infected with AdGFP adenovirus for 16 hours. Cells were then detached from the dishes by trypsinization, centrifuged, washed twice with 1 mL PBS, and resuspended in 500  $\mu\text{l}$  PBS containing 0,25% BSA. Samples were stored in ice-cold before

final readings. The cellular green fluorescent protein was detected in a linear scale using flow cytometer (Dako Cytomation CyAn<sub>ADP</sub>). About 20,000 events were recorded for each sample and data were analyzed with Software Dako associated.

#### **Intramuscular injection and Tissue collection**

Three-months old transgenic and control mice (25-30 g) were anaesthetized intramuscularly with 2,2,2-tribromoethanol (Sigma-Aldrich Chemie Steinheim, Germany). The legs were shaved and moistened with 70% ethanol. AdGFP and Ad $\beta$ Gal adenoviruses were injected into tibialis anterior muscle with a U-100 insulin syringe in a proximal to distal direction. The concentration injected was  $2 \times 10^7$  pfu in a volume of 200  $\mu$ l. Mice were fed *ad libitum* and maintained under a 12-h light/dark cycle. Animal procedures were performed in accordance with recommendations for the proper care and use of laboratory animals. After infection times, tissue samples (brain, tibialis and soleus muscles, perigonadal adipose tissues) were collected rapidly after transgenic mice were sacrificed by 2,2,2-tribromoethanol overdose. Tissue samples were homogenized in a Polytron (Brinkman Instruments, N.Y.) in T-PER<sup>TM</sup> extraction reagent (25 mM Bicine, 150 mM Sodium Chloride, pH 7.6) with a ratio of 1 g of tissue to 20 ml according to manufacture's instruction (Pierce, Rockford, IL). After centrifugation at 10,000 rpm for 5 minutes, the supernatants were performed as cellular lysates.

#### **$\beta$ -Galactosidase assay and X-Gal staining**

To analyze total  $\beta$ -Galactosidase expression activity the muscles from Ped/Pea-15 transgenic mice and their controls were homogenized in 2 ml of a 1x reporter lysis buffer from a  $\beta$ -Galactosidase enzyme assay System (Promega Corporation, Madison, WI, USA). Following 15 minutes of incubation at room temperature, the samples were centrifuged at 14,000 rpm for 5 minutes at 4°C. Supernatants were collected and 10  $\mu$ l were placed into the 96-well plate containing assay buffer (50  $\mu$ l of Galacton and 25  $\mu$ l of Emerald). All samples have been mixed by pipetting the well contents. The absorbance of the samples was measured at 420 nm in a luminometer (Centro LB960 Berthold Technologies). To perform X-Gal staining with In Situ  $\beta$ -Galactosidase Staining Kit (Stratagene, La Jolla, CA) L6 cells were fixed in 20% formaldehyde and 2% glutaraldehyde in PBS pH7,4 for 10 minutes at room temperature and then washed in PBS. Cells were incubated for 16 hours at 37°C in staining buffer (5 mM K<sub>4</sub>Fe(CN)<sub>6</sub>, 5 mM K<sub>3</sub>Fe(CN)<sub>6</sub>, 2 mM MgCl<sub>2</sub>, 10% dimethyl sulfoxide (DMSO) in PBS with X-Gal staining solution (100 mg/ml 5-Bromo-4-chloro-3-indoyl- $\beta$ -D-galactopyranoside). Staining solution was removed and cells were washed two times with PBS. Quantification of blue cells to determine the infection efficiency was performed by the manual tagging in the total population.

#### **Adenovirus construction**

The D4 cDNA was excised from the pEGFP-D4 expression construct by digestion with Hind III and Kpn I restriction enzymes. The fragment was gel-purified and ligated into the Hind III-Kpn I sites of pAdTrack-CMV shuttle

vector (containing CMV promoter, a polyadenylation site and GFP fusion protein) using a cloning system described in He et al. 1998). The resulting plasmid was linearized with Pme I and transformed together with a supercoiled adenoviral vector (pAdEasy-E1) into electrocompetent *E. coli* strain BJ5183. Recombinants were selected with kanamycin and screened by restriction endonuclease digestion. The positive transformants were linearized with Pac I digestion. The resulting recombinant pAdTrack-CMV containing D4 sequences were linearized with Pac I digestion and transfected in  $1.5 \times 10^6$  packaging cell lines (HEK293) plated in 25 cm<sup>2</sup> flasks using Lipofectamine Plus (Invitrogen Corporation, Carlsbad, CA). After 24 hours of transfection, the cells were overlaid with agarose to permit isolation of individual virus plaques; visible plaques were selected 7-10 days following transfection and expanded. Virus was purified from 293 cells by three freeze/thaw cycles using, alternately, liquid nitrogen and a 37°C water bath. After three freeze/thaw cycles, the cell lysates were centrifuged on cesium chloride step gradients at 60,000 x g for 2 hours at 20°C to separate viruses from defective particles and empty capsids. The purified viral stocks were subjected to dialysis against 1 x TE (10 mM Tris-HCl + 1 mM EDTA pH 8.0) containing 17% glycerol for 24 hours at 4°C with fresh buffer being added every 12 hours. Aliquots of purified recombinant virus were frozen and stored at -80°C until used.

#### **2-deoxy-D-glucose (2-DG) uptake**

Briefly, confluent cells were infected with AdTrack-CMV-D4 adenovirus for 16 hours. Following, the cells were incubated in DMEM supplemented with 0.25% albumin for 18 h at 37°C. The medium was aspirated and cells were further incubated for 30 min in glucose-free HEPES buffer (5 mmol/l KCl, 120 mmol/l NaCl, 1.2 mmol/l MgSO<sub>4</sub>, 10 mmol/l NaHCO<sub>3</sub>, 1.2 mmol/l KHPO<sub>4</sub>, and 20 mmol/l HEPES, pH 7.8, 2% albumin). The cells were incubated with 100 nmol/l insulin for 30 min, supplemented during the final 10 min with 0.2 mmol/l [<sup>14</sup>C]2-DG. Cells were then solubilized and the 2-DG uptake was quantitated by liquid scintillation counting.

#### **Densitometry and statistical analysis**

Densitometric analysis was performed using a Scion Image Analyzer. All the data were expressed as mean ± SD. Significance was assessed by Student's *t* test for comparison between two means. Data were analyzed with Statview software (Abacusconcepts) by one-factor analysis of variance. P values of less than 0.05 were considered statistically significant.

## RESULTS AND DISCUSSION

### **PED/PEA-15 protein binds PLD1 and enhances PLD1 activity in HEK293 and L6 cells**

Several studies *in vitro* have been performed to elucidate the molecular mechanisms responsible for insulin-resistance induced by PED/PEA-15 overexpression. Investigations from our own as well as other groups evidenced that PED/PEA-15 is a phospholipase binding protein (Zhang et al. 2000).

In accordance with previous data that showed PED/PEA-15 as a phospholipase D interactor, I verified the association between the two proteins in a well characterized cellular system, the HEK293 human embryonic kidney cells stably overexpressing PED/PEA-15 (Y1). These cells have been subjected to western blot analysis to evaluate PED/PEA-15 and PLD1 protein levels, and untransfected 293 cells were used as control cells (293). PED/PEA-15 protein was significantly overexpressed in Y1 cells compared to control cells. As shown in figure 12 A, PLD1 levels were also higher in Y1 cells compared to 293 cells. This finding suggested that PED/PEA-15 overexpression was correlated with increased levels of PLD1.

It has been demonstrated that Protein kinase C (PKC)- $\alpha$  is constitutively activated in L6 skeletal muscle cells overexpressing PED/PEA-15 (Condorelli et al. 2001).

To further investigate this effect in HEK293 cells and to address the role of PKC $\alpha$  in PED/PEA-15 function, I evaluated the levels of activation of PKC $\alpha$  in 293 overexpressing PED/PEA-15. I observed that in Y1 cells the activation of PKC $\alpha$  was increased by three-fold compared to control cells (Figure 12 B).

These findings showed that also in HEK293 cells, PED/PEA-15 overexpression was associated with increased PLD1 levels and induction of PKC $\alpha$  activation.

To verify the interaction between PED/PEA-15 and PLD1, lysates from Y1 and 293 cells were precipitated with anti-PED/PEA-15 antibody and the immunoprecipitated proteins were analyzed by western blot with specific antibody against PLD1. The enhanced chemiluminescence (ECL) revealed three-fold increased levels of PLD1 associated to PED/PEA-15 in Y1 cells compared to 293 cells (Figure 12 B).

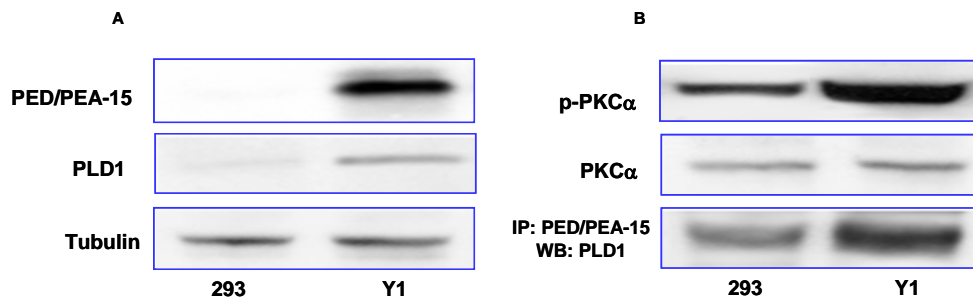


**Figure 12: Effect of PED/PEA-15 expression in 293 and 293Y1 cells.** Cellular lysates of control (293) and PED/PEA-15 (Y1) cells have been subjected to western blotting analysis to analyze PED/PEA-15, PLD1 and PKC $\alpha$  expression levels. The autoradiography shows an increased expression of PED/PEA-15 and PLD1 proteins in Y1 cells compared to 293 cells. Anti-Tubulin antibody has been used to normalize (A). PKC $\alpha$  hyperactivation has been observed also in Y1 cells compared with 293 cells (B). Co-immunoprecipitation experiments in these cells demonstrated that PED/PEA-15 binds phospholipase D1 at higher extent in Y1, compared to 293 cells (B).

In previous studies we have demonstrated that in differentiated L6 skeletal muscle cells and 3T3-L1 adipocytes, the increased expression of PED/PEA-15 blocks insulin-dependent translocation of GLUT4. These changes occurred with no detectable alterations in the total content of GLUT4, the major insulin-stimulated glucose transporter. Like glucose transport, PKC $\alpha$  and PKC $\beta$  are also constitutively activated and are not further stimutable by insulin in L6<sub>PED</sub>. PKC-zeta features no basal change but completely loses insulin sensitivity in L6<sub>PED</sub> (Condorelli et al. 2001). However, the impaired translocation of GLUT4 is due to the alteration of PKC signalling caused by PED/PEA-15/PLD1 interaction (Vigliotta et al. 2003; see below attached publications).

Indeed, by western blot analysis I demonstrated that PLD expression was three-fold higher also in L6 skeletal muscle cells stably overexpressing PED/PEA-15 (L6<sub>PED</sub>), as compared to controls (L6) (Figure 13 A).

Furthermore, as shown by co-immunoprecipitation experiments, PED/PEA-15/PLD1 interaction was more evident in L6<sub>PED</sub> cells than in L6 control cells (Figure 13 B). Thus, this binding stabilized PLD1, leading to enhanced phospholipase activity in the cells overexpressing PED/PEA-15. These changes are accompanied by increased diacylglycerol levels, a major activator of classical PKCs (Condorelli et al. 2001).

Consistently, PKC $\alpha$  phosphorylation was also increased in L6 cells.

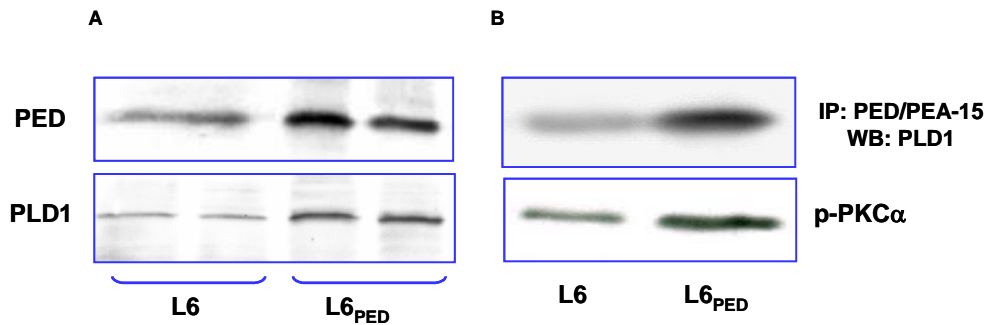


**Figure 13: PED/PEA-15 and PLD1 expression.** Cell lysates of L6 and L6 cells stably transfected with PED/PEA-15 cDNA have been subjected to western blotting analysis to analyze the expression levels of PED/PEA-15 and PLD1 proteins (A). An increase of both proteins was shown in L6<sub>PED</sub> cells to compared control cells and also an increase of PKC $\alpha$  activation was present in L6<sub>PED</sub>. Next, the co-immunoprecipitation experiment showed that PED/PEA-15/PLD1 interaction was higher in L6<sub>PED</sub> than L6 cells (B).

As described by Zhang et al. 2000 the binding of PED/PEA-15 to PLD1 protein induced an increase of phospholipase D cellular activity. To verify if the increased amount of PLD1 was paralleled by an increased activity, PLD1 activity was evaluated by measuring the levels of transphosphatidylbutanol generated by the transphosphatidylation reaction. Y1 and 293 cells have been treated with TPA (100 nM) for 30 minutes and then, subjected to lipid extraction as described in Materials and Methods. PLD1 activity has been measured evaluating the specific reaction of transphosphatidylation catalyzed by the enzyme using 1-butanol as a substrate. The chromatography showed that TPA stimulates PLD1 activity in 293 cells; in Y1 cells, there was an increase in both basal and TPA-stimulated PLD1 activity, compared to 293 cells (Figure 14 A). Similar results were also obtained in L6 cells. These results indicated that the overexpression of PED/PEA-15 causes an increase in the expression and activation of PLD1.

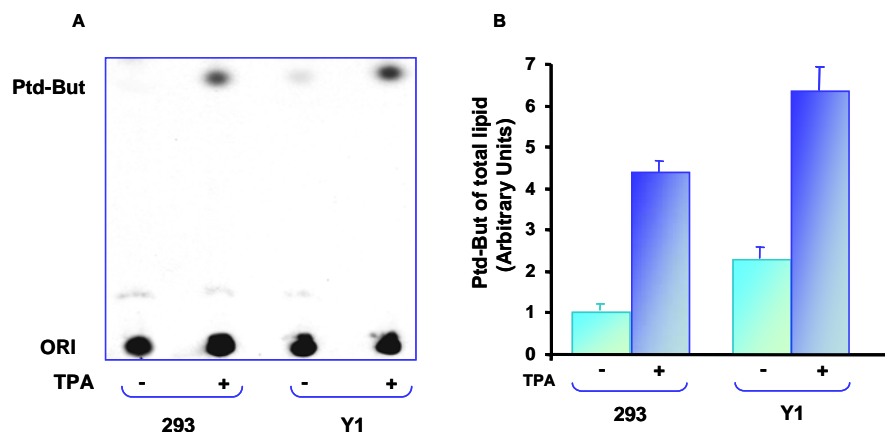


**Figure 14: PED/PEA-15 overexpression increases PLD1 activity.** PLD1 activity analyzed by measuring the transphosphatidyl-butanol levels was increased either in basal state or upon TPA (100 nM) stimulation in Y1, compared to 293 cells (A). Each experiment was determined in triplicate and this was a representative of three experiments. The autoradiograph shows a representative experiment. The bar graph represents the densitometric quantitation of the spots in three experiments in triplicate  $\pm$  SD (B).

### The role of PED/PEA-15 phosphorylation

Several reports indicate that PED/PEA-15 is phosphorylated at the level of Ser<sub>116</sub> by calcium–calmodulin kinase II (CaMKII) and PKB/Akt, facilitating further phosphorylation by protein kinase C (PKC) at Ser<sub>104</sub>→Gly. Thus, PED/PEA-15 is present in the cell in both unphosphorylated and phosphorylated form.

To clarify the role of the Ser<sub>104</sub> and Ser<sub>116</sub> phosphorylation on the association of PED/PEA-15 with PLD1, I transiently transfected the wild type form (Y1) or Ser<sub>104</sub>→Gly and Ser<sub>116</sub>→Gly mutants of PED/PEA-15 (generated in our laboratory as described in Trencia et al. 2003; see below attached publications) in 293 cells.

No significant differences in the activation of PKC $\alpha$  were observed both in PED<sub>S104</sub> and PED<sub>S116</sub> 293 cells, as compared with wild type cells (Figure 15). The co-immunoprecipitation experiments using anti-PLD1 antibody also showed that the mutation of both Ser<sub>104</sub> and Ser<sub>116</sub> did not significantly affect PED/PEA-15/PLD1 association.

These data demonstrated that the phosphorylation of PED/PEA-15 protein did not control the binding with phospholipase D1.

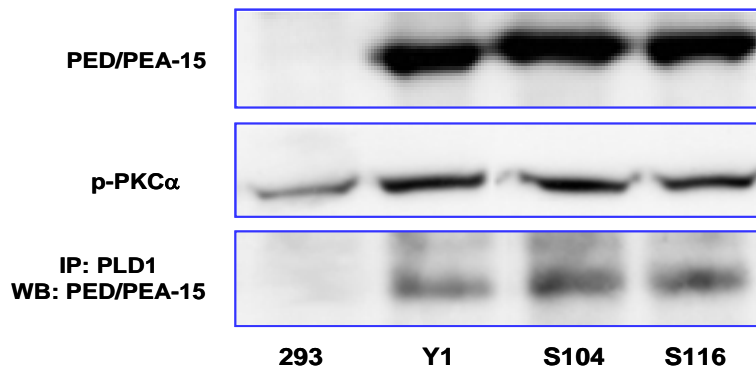


**Figure 15: PED/PEA-15 phosphorylation defective mutants and PLD1 function.** Lysates from 293 cells transfected with PED/PEA-15 (Y1) and Ser<sub>104</sub>→Gly (S104), Ser<sub>116</sub>→Gly (S116) mutants have been analyzed for PKC $\alpha$  activation levels and immunoprecipitated using anti-PLD1 antibody. The second panel shows that PKC $\alpha$  activity is up-regulated in all transfected cells. Co-immunoprecipitation experiments (lower panel) show that PED/PEA-15 and its S104, S116 mutants were equally capable to associate with PLD1.

### Generation of D4 fragment: its effects *in vitro*

A previous study (Condorelli et al. 2001) has demonstrated that the activation of PKC $\alpha$  prevented insulin induction of PKC $\zeta$  activity in L6 cells. The use of PKC $\zeta$  constitutively active mutants in these same cells rescued the activity of the kinase and the insulin effect on glucose uptake.

Thus, increased PED/PEA-15/PLD1 interaction caused insulin-resistance by dysregulating the PKC signaling system.

With this background, I wanted to prove the concept that, limiting this

interaction may improve insulin-sensitivity *in vitro* and *in vivo*. To this aim, I generated the minimum PLD1 fragment (D4) conserving the ability to bind PED/PEA-15 (Zhang et al. 2000). Following RT-PCR amplification of D4, DNA sequencing was performed to confirm the correct sequence.

Furthermore, the D4 fragment was inserted into the pcDNA3 vector in frame with the HA epitope. Indeed, the D4 fragment has been cloned between Hind III and Xba I sites. I transfected the construct pcDNA3-HA-D4 in 293 and in Y1 cells. Lysates obtained have been analyzed by Western blot with HA antibody to verify the expression of the fragment. The HA-tagged D4 fragment was expressed at comparable levels both in 293 and Y1 cells (Figure 16).

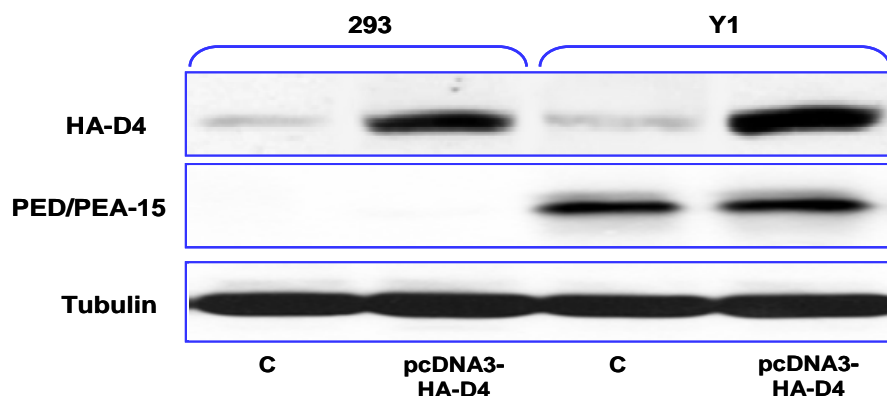


**Figure 16: Effect of D4 transfection.** D4 fragment has been transfected in 293 and Y1 cells and the presence of the construct (pcDNA3-HA-D4) has been analyzed using anti-HA antibody.

D4 cDNA was also cloned into a pEGFP vector. The GFP-D4 fusion protein, generated as described in Materials and Methods, has been transfected in 293 and Y1 cells. After 48 hours the cells were lysed and analyzed by western blot with anti-GFP antibody (Figure 17). A specific band was detected in the cells which have been transfected with the construct, indicating that the chimerical protein was expressed in both 293 and Y1 cells.

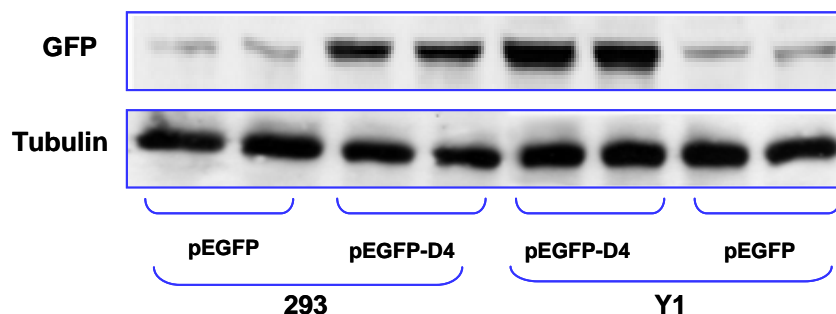


**Figure 17: Expression of pEGFP-D4.** The pEGFP-D4 construct has been transiently transfected in 293 and Y1 cells. The effect of this transfection has been detected with anti-GFP antibody.

Next, I performed co-immunoprecipitation experiments following transfection of pcDNA3-HA-D4 and pEGFP-D4 constructs, to verify the effect of D4 expression on PED/PEA-15 and PLD1 association.

In particular, lysates from 293, Y1 and Y1 transfected with pcDNA3-HA-D4 and pEGFP-D4 respectively, have been immunoprecipitated with PED/PEA-15 antibody and subjected to Western blot analysis, using PLD1 antibody (Figure 18). The expression of D4 was able to significantly reduce the PED/PEA-15/PLD1 interaction in Y1 transfected with either pcDNA3-HA-D4 or pEGFP-D4 constructs.

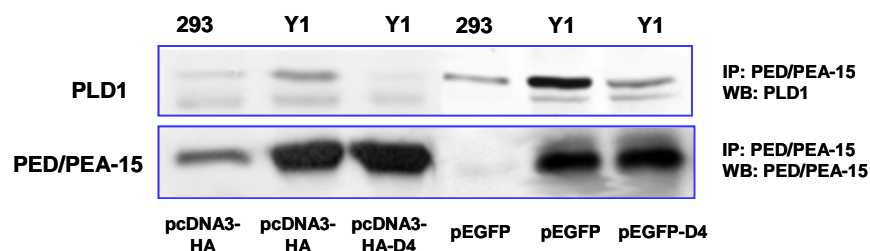


**Figure 18: Effect of D4 on the PED/PEA-15/PLD1 association.** Aliquots (300 µg) of cells transfected with pcDNA3-HA, pcDNA3-HA-D4, pEGFP and pEGFP-D4 have been immunoprecipitated with anti-PED/PEA-15 and probed with anti-PLD1 antibody. The D4 fragment significantly reduce the association between PED/PEA-15/PLD1 in Y1 cells compared to cells transfected with empty vectors.

Once confirmed that the expression of D4 fragment reduced the association of PED/PEA-15 with PLD1 in cells overexpressing PED/PEA-15, I evaluated the effects of D4 on basal and insulin-induced activation of the PKCs. Insulin activated PKC $\alpha$  in 293 cells, as shown by determination of the phosphorylated form of the protein with specific anti-phospho-PKC $\alpha$  antibody. By contrast, in Y1 cells PKC $\alpha$  was constitutively activated in basal condition and no further stimulated by insulin. In Y1 cells, the expression of D4 fragment reduced the basal activity of PKC $\alpha$  to levels comparable to 293 control cells. Moreover, the D4 construct was able to almost completely rescue the normal kinase activation of PKC  $\alpha$ , in response to insulin stimulation (Figure 19 A).

Insulin activated PKC $\zeta$  in 293 cells transfected with the empty pcDNA3-HA vector, while in Y1 cells, the overexpression of PED/PEA-15 prevented the insulin-stimulated activation of PKC $\zeta$ . In these cells, D4 expression rescued the normal activation of PKC $\zeta$  in response to insulin (Figure 19 B).

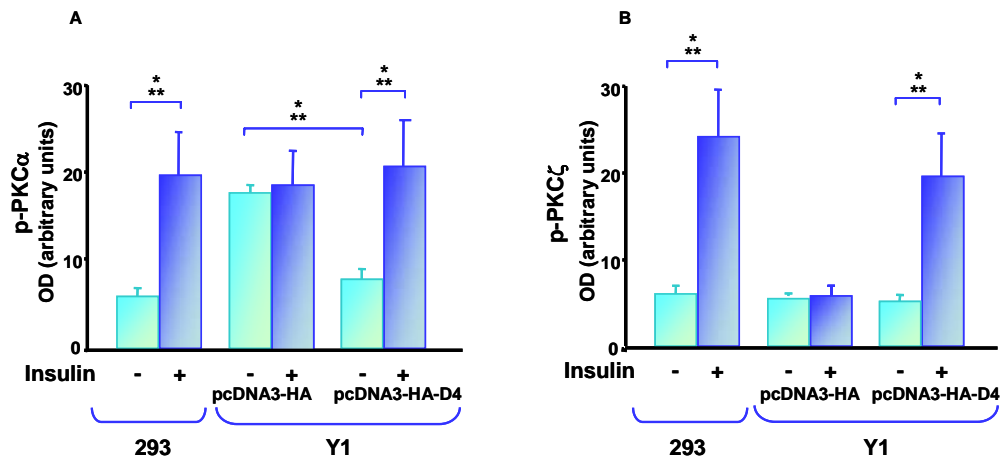


**Figure 19: Insulin-stimulates activation of PKCs upon D4 transfection.** 293 and Y1 cells have been stimulated with insulin (100 nM) to measure PKC $\alpha$  activation. Transfections have been analyzed with anti-HA antibody. Densitometric quantitation from western blotting analysis showed that in Y1 cells transfected with pcDNA3-HA, PKC $\alpha$  is constitutively activated and does not respond to insulin, compared to control cells (A). No significant change occurred in PKC $\zeta$  activation. In the same cells, the expression of pcDNA3-HA-D4 construct reduces PKC $\alpha$  activation and restores its responsiveness to insulin (A). The same is shown for PKC $\zeta$  (B). Bars represent the means  $\pm$  SD of triplicate determinations in four independent experiments. Asterisks denote statistically significant differences (\*\*\*,  $P < 0.001$ ).

Similar results were also obtained in Y1 cells transfected with pEGFP and pEGFP-D4 (not shown).

In conclusion, these findings indicated that the inhibition of PED/PEA-15 and PLD1 interaction rescues insulin action on PKC signaling pathways, supporting the hypothesis of a key role of phospholipase D1 in the negative effect of PED/PEA-15 on glucose transport.

### Generation of PED/PEA-15 derived peptides

In order to test PED/PEA-15 molecular determinants involved in PLD1 binding, peptides corresponding to aminoacids 1-53, 53-79 and 79-112 of PED/PEA-15 protein were generated (collaboration with the IBB-CNR). To analyze the entry of PED/PEA-15 peptides in our cellular system, 293 and Y1 cells were incubated with the fluorescein isothiocyanate-conjugated peptides (FITC) PED/PEA-15<sub>1-53</sub>, PED/PEA-15<sub>53-79</sub>, PED/PEA-15<sub>79-112</sub> peptides. Intracellular loading of the synthetic peptides was achieved by means of cationic lipid mixture. As revealed by fluorescence microscopy, FITC-PED<sub>79-112</sub> was efficiently transduced in both 293 and Y1 cells (~90%) (Figure 20).

Similar results were obtained with the other peptides (not shown).

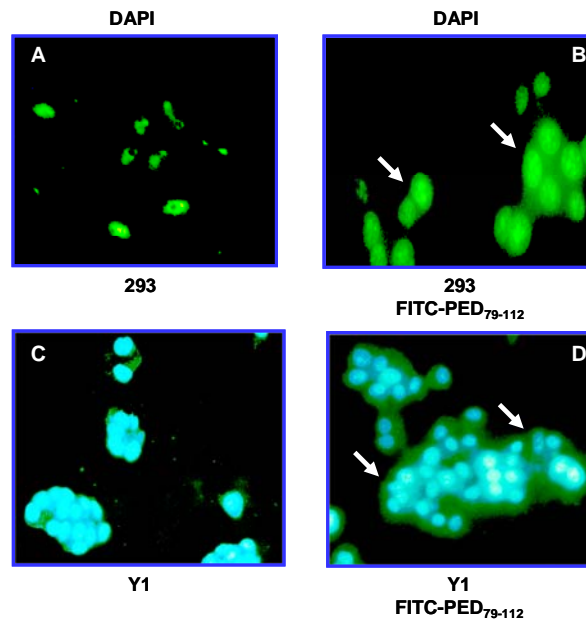


**Figure 20: PED/PEA-15<sub>79-112</sub> peptide location by fluorescence microscopy.** 293 and Y1 cells have been transiently transfected with FITC-PED/PEA-15<sub>79-112</sub> peptide and after 24 hours the cells have been fixed and visualized with fluorescence microscopy. In both cells (A-C panels) DAPI staining showed the presence of peptide compared with untransfected cells (B-D panels).

Next, I performed co-immunoprecipitation experiments in Y1 cells to evaluate the effect of these peptides on PED/PEA-15/PLD1 association. As shown in figure 21, only the peptide PED<sub>79-112</sub> was able to decrease PED/PEA-15/PLD1 association compared to control cells.

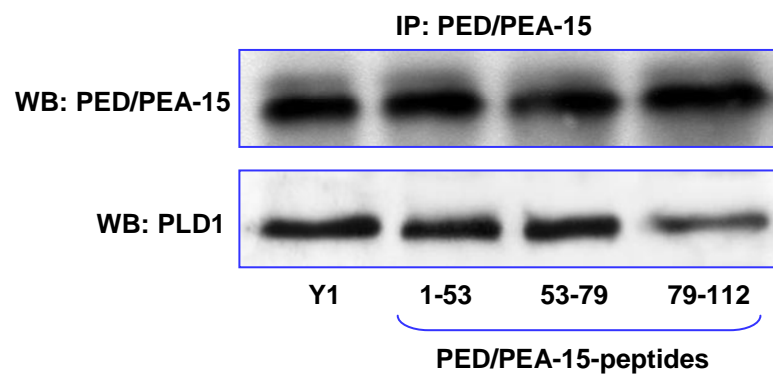


**Figure 21: Co-immunoprecipitation experiments with peptides.** Lysates (500 µg) from Y1 cells have been co-immunoprecipitated in presence of PED/PEA-15 peptides (1-53, 53-79, 79-112). The experiment showed a decrease in PLD1 protein levels in presence of PED/PEA-15<sub>79-112</sub> peptide.

To test the potential role of PED/PEA-15<sub>79-112</sub> peptide in the rescue of PKC signaling, 293 and Y1 cells were stimulated with insulin in the absence or in the presence of the transduced peptide and analyzed by western blotting with anti-phospho-PKC $\alpha$  antibody. The activation of PKC $\alpha$  in 293 cells was not significantly modified by FITC-PED/PEA-15<sub>79-112</sub> peptide. In the Y1 cells, however, the PED/PEA-15<sub>79-112</sub> peptide was able to reduce the PKC $\alpha$  activation and to partially rescue the response to insulin.

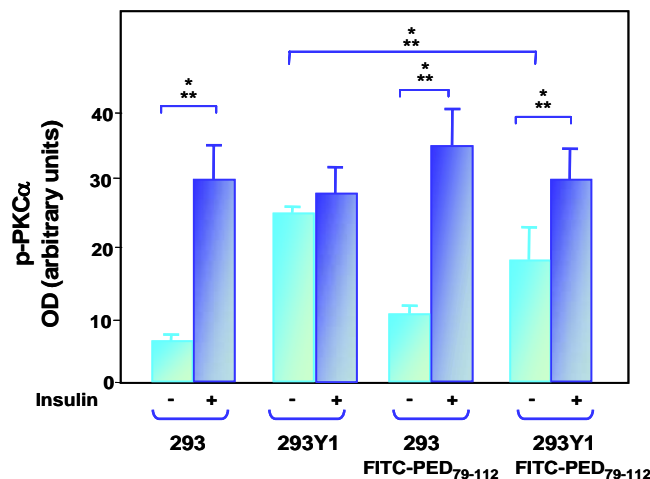


**Figure 22: Effect of PED/PEA-15<sub>79-112</sub> peptide on PKC $\alpha$  activation.** Lysates from 293 and Y1 cells loaded with FITC-PED/PEA-15<sub>79-112</sub> peptide and stimulated with insulin (100 nM for 30 minutes) have been analyzed using anti-phospho-PKC $\alpha$  antibody. PKC $\alpha$  activation was not modified in 293 cells loaded with FITC-PED/PEA-15<sub>79-112</sub> peptide compared to untransfected cells. In Y1 cells, FITC-PED/PEA-15<sub>79-112</sub> peptide decreased basal PKC $\alpha$  activation and significantly rescued the response to insulin compared to untransfected Y1 cells. The graph represents mean  $\pm$  SD of three different experiments in triplicate. Asterisks denote statistically significant differences (\*\*\*,  $P < 0,001$ ).

### The interaction between PED/PEA-15 and PLD1 *in vivo*

As described in Vigliotta et al. 2003 (see below attached publications), Ped/Pea-15 transgenic mice feature a two-fold increase of PLD1 protein levels in muscle and adipose tissues. To confirm that PED/PEA-15 was able to bind PLD1 also *in vivo*, I performed co-immunoprecipitation experiments in cellular extracts from brain and skeletal muscle tissues of transgenic and control mice. The brain tissue has been used as positive control because it is enriched of both proteins.

These experiments demonstrated that PED/PEA-15 binds PLD1 in skeletal muscle and in brain tissues. This association is further accompanied by increased PKC $\alpha$  activation in transgenics compared to controls (Figure 23).

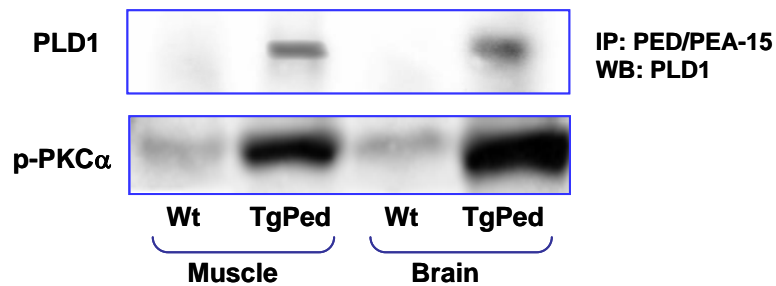


**Figure 23: PED/PEA-15/PLD1 interaction *in vivo*.** The lysates from muscle and brain tissues have been immunoprecipitated with anti-PED/PEA-15 antibody. The immunoprecipitated proteins have been subjected to 7% SDS-PAGE and immunoblotted with anti-PLD1 antibody. Data were representative results from three experiments and showed that the interaction between proteins was increased in lysates prepared from brain and muscle of transgenic mice (lanes 2-4) compared with their controls (lanes 1-3).

Based on these results, I performed a PLD assay *in vitro* using extracts from skeletal muscle of transgenic mice and their nontransgenic littermates. As revealed by thin-layer chromatography analysis, PLD1 activity from Ped/Pea-15 transgenic mice was increased two-fold versus control mice. Similar results were also obtained with brain extracts.

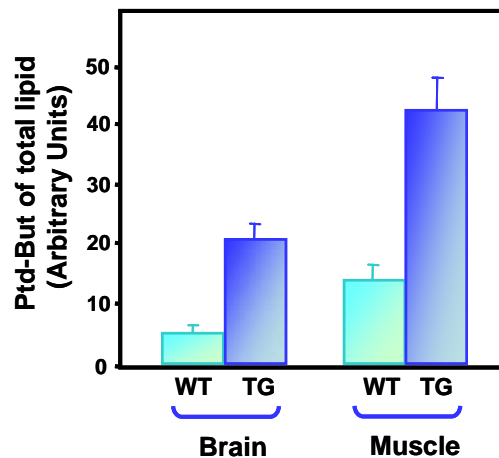


**Figure 24: PLD1 activity *in vivo*.** The lysates of brain and muscle tissues have been prepared and assayed for PLD1 activity in fasting condition. Results have been expressed as the mean  $\pm$  SD of the duplicate assays and each bar represents a preparation from a single mouse, with two determinations for each preparation. The level of PLD1 activity was up-regulated in the brains and muscles of transgenic mice (bars 3-4 and 7-8) compared with their controls (bars 1-2 and 5-6). Bars represent the mean  $\pm$  SD of the spots in three experiments in triplicate.

### ***In vitro* and *in vivo* modulation of adenovirus**

Recently, there has been considerable interest in developing adenoviruses as defective vectors to carry and express foreign genes for therapeutic purposes. One reason for this is that the adenovirus is a versatile system and its genome can be easily manipulated *in vitro* and *in vivo*.

Furthermore, in most recombinant vectors, the gene of interest is introduced by replacing E1 early region. The E1 deletion makes the viruses defective for replication and incapable of producing infectious viral particles in the target cells. Thus, I considered the hypothesis of generating an adenoviral construct bearing the D4 fragment, to block PED/PEA-15/PLD1 interaction both *in vitro* and *in vivo*. I performed several experiments to test the feasibility of the adenoviral systems, for this purpose.

To this aim, I used an adenovirus containing the Green Fluorescent Protein (AdGFP) and an adenovirus containing  $\beta$ -Galactosidase gene (Ad $\beta$ Gal) as adenoviral vectors, respectively, incorporated into the adenoviral backbone, that can allow direct observation of the infection efficiency.

First of all, I infected L6 cells with raising concentration of AdGFP (0, 100, 200, 400 pfu) for 24 hours. After incubation, the viral entry has been analyzed measuring the GFP fluorescence by flow cytometry. The results obtained showed that the infection with AdGFP was achieved in both cellular types and the increase of fluorescence was dose-dependent (Figure 25).

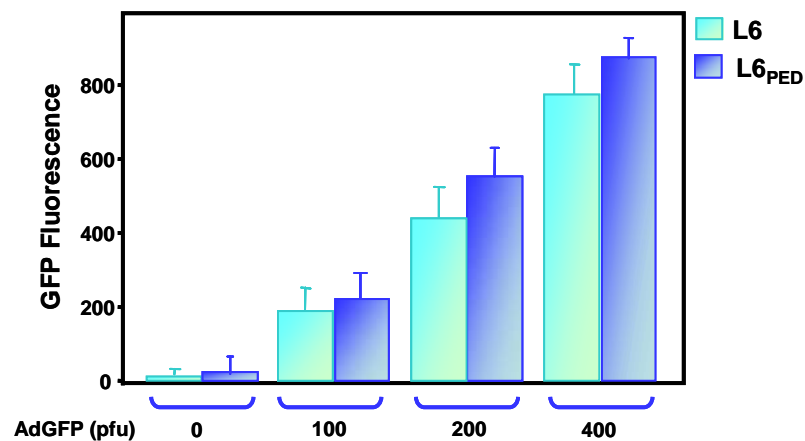


**Figure 25: AdGFP infection *in vitro*.** L6 and L6<sub>PED</sub> have been infected with AdGFP (0, 100, 200, 400 pfu for 24 hours) and analyzed by flow cytometry. The figure shows a dose-dependent increase in cellular fluorescence in both cell types. The bar graph represents mean  $\pm$  s d of three different experiments in triplicate.

In a second series of experiments, I used the Ad $\beta$ Gal adenovirus. The protocol of infection with this adenovirus was identical to the previous one, and I evaluated viral entry in individual intact cells with *in situ* X-Galactosidase staining. In infected cells,  $\beta$ -Galactosidase cleaves 5-bromo-4-chloro-3-indoyl- $\beta$ -galactopyranoside (X-Gal) to produce a blue stain. The viral entry has been determined by showing stained and unstained cells with a microscope in the total population. The blue cells, indeed, have been infected by Ad $\beta$ Gal as compared to control cells (Figure 26).

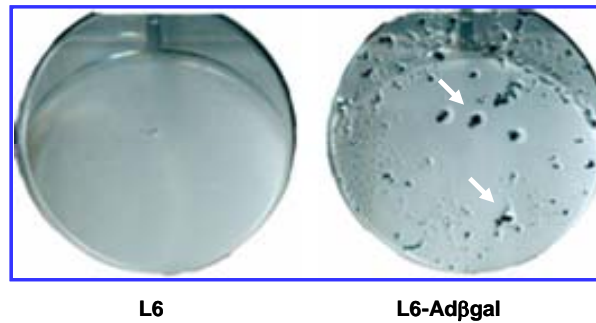


**Figure 26: X-Galactosidase staining *in vitro*.** X-Gal staining has been performed at 24 hours after infection with Ad $\beta$ gal (400 pfu). The positive cells (L6) were stained after infection and compared with uninfected cells. As shown in the figure X-Gal staining showed the viral entry.

This data indicated that L6 cells were significantly infected by both adenoviruses AdGFP and Ad $\beta$ Gal. Once obtained the results *in vitro*, I also performed the infection *in vivo*. In particular, I anesthetized six mice and then introduced the AdGFP ( $2 \times 10^7$  pfu in 200  $\mu$ l) by intramuscular direct (i.m.) injection in quadriceps and tibialis muscles of both mouse's paws. Subsequently, mice have been killed with 2,2,2-tribromoethanol overdose, the quadriceps and tibialis muscles have been quickly taken and kept in dry-ice. The infection has been prolonged for several times to evaluate the time-course of AdGFP expression. The injected tissues have been processed as described in Materials and Methods. Western blotting analysis demonstrated a time-dependent increase in GFP expression after injection in the quadriceps and tibialis muscles compared with non infected tissues (Figure 27). The GFP protein, indeed, was increased in the muscle after 4 hours, and started to decrease after 8-12 hours. This expression was completely switched off after 24-72 hours. These results were obtained in both Ped/Pea-15 transgenic mice and in their nontransgenic littermates (WT).

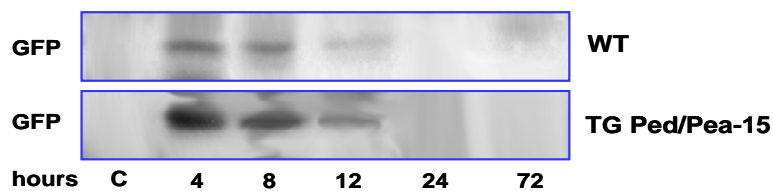


**Figure 27: AdGFP infection *in vivo*.** Western blotting analysis with anti-GFP antibody at different times after direct intramuscular injection of AdGFP ( $2 \times 10^7$  pfu in 200  $\mu$ l) in the right and left hind legs of three months-old wild type and transgenic mice.

Similar experiments were performed by using Ad $\beta$ Gal. After direct intramuscular injection, mice have been killed at different times (0, 4, 8, 12,

24, 72 hours) and muscles have been homogenized and  $\beta$ -Galactosidase activity has been evaluated in the lysates. As shown in figure 28, the infection was time-dependent compared with control muscle infected with the vehicle alone.

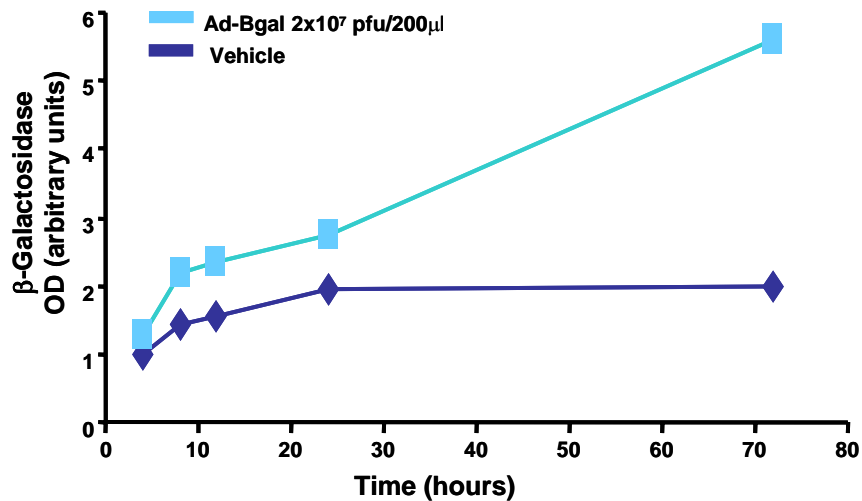


**Figure 28: Ad $\beta$ Gal infection *in vivo*.** The lysates of muscles from mice have been prepared and assayed for  $\beta$ -Galactosidase activity at different times as described in Materials and Methods. The graph represents mean  $\pm$  SD of three different experiments in triplicate.

The expression of the AdGFP and the Ad $\beta$ Gal adenoviruses demonstrated that infection with adenoviral constructs might represent a feasible strategy to express the gene of our interest both in cultured cells and *in vivo*.

### **Generation of an adenovirus containing D4 fragment**

Next, I cloned D4 cDNA in the polylinker of the pAdTrack-CMV vector to generate the AdTrack-CMV-D4 adenovirus. I selected candidate colonies by their resistance to kanamycin provided by the shuttle vector and obtained the DNA from them. Furthermore, I digested DNA using Hind III-Kpn I restriction enzymes to verify the presence of D4 fragment (Figure 29).

The plasmid DNA preparation containing the GFP-D4 construct has been linearized with a restriction endonuclease and transformed together with a supercoiled adenoviral vector (pAdEasy-E1) into E.coli strain BJ5183. Recombinants have been selected with kanamycin and screened by restriction endonuclease digestion.

The positive recombinant adenoviral construct has been linearized and

transfected in packaging cell lines (HEK293) to visualize the GFP reporter that was incorporated into the viral backbone. After 7-10 days viruses have been harvested and used directly for infection experiments either *in vitro* or *in vivo*.

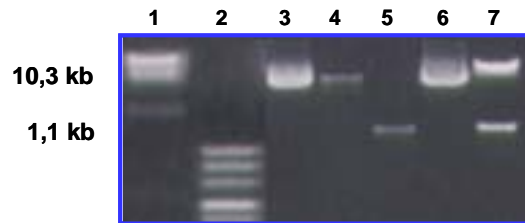


**Figure 29: Cloning D4 fragment in pAdTrack-CMV shuttle vector.** Numbers indicates:  $\lambda$ DNA-HindIII marker (1), pUC Mix marker (2), pAdTrack-CMV vector (3), pAdTrack-CMV digested Hind III - Kpn I (4), PCR-derived D4 fragment (5), pAdTrack-CMV-D4 construct (6), pAdTrack-CMV and D4 fragment digested Hind III - Kpn I (7).

To assess viral effect of AdTrack-CMV-D4 (Ad-D4) in the cells, L6 and L6<sub>PED</sub> were infected with 100 pfu of adenovirus and glucose uptake was measured upon insulin (100 nM) stimulation. The Figure 30 shows that the AdTrack-CMV-D4 infection rescued insulin-stimulated glucose uptake in L6 cells overexpressing PED/PEA-15 compared to their controls infected with AdGFP alone. By contrast, no difference was observed by infecting untransfected L6 cells.

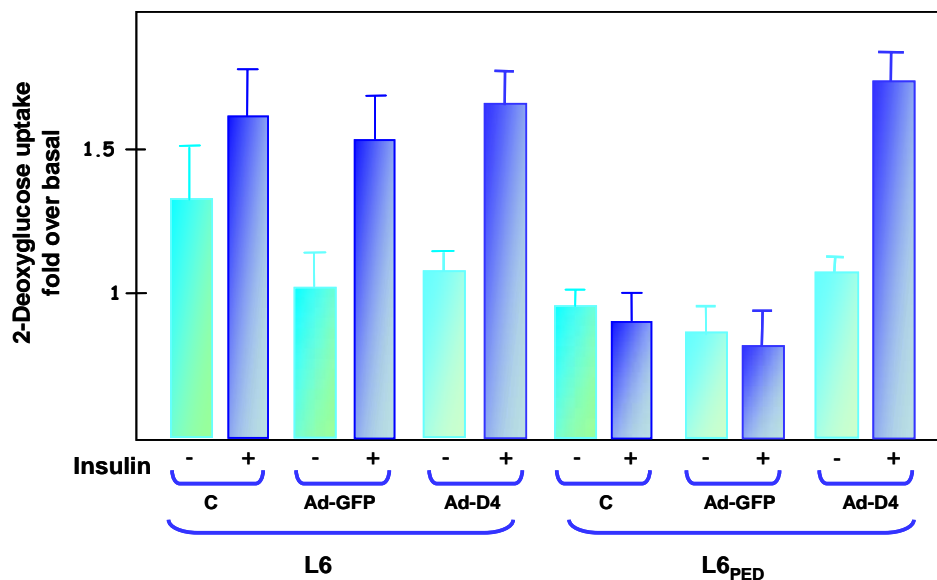


**Figure 30: Glucose uptake upon AdTrack-CMV-D4 infection.** L6 and L6<sub>PED</sub> cells were infected with pAdTrack-CMV-D4 adenovirus (100 pfu). Then, the cells were exposed to 100 nM insulin and assayed for 2-DG uptake. Infection completely rescued the low levels of basal glucose uptake of the L6<sub>PED</sub> cells and restored maximal levels of insulin-stimulated uptake. Bars represent mean  $\pm$  SD of three different experiments in triplicate.

## CONCLUSIONS

The generation of a cellular model overexpressing PED/PEA-15 protein has brought new insights in the study of the physiopathology of insulin-sensitivity.

The PED/PEA-15 overexpressing cells, indeed, feature an increase in stability and activity of PLD1, with subsequent activation of classical PKCs. The increase of PKC $\alpha$ , in turn, inhibits insulin-induced PKC $\zeta$  activation and impairs GLUT4 translocation to the plasma membrane and glucose-uptake.

Moreover, the Tg-*ped/pea-15* mice ubiquitously, feature insulin-resistance, accompanied by increased PLD1/PKC $\alpha$  signaling. The Tg-*ped/pea-15* mice, therefore, show a reduced glucose tolerance, which progress to overt diabetes under appropriate environmental conditions.

Based on these observations, I tested the possibility that limiting PED/PEA-15/PLD1 interaction may improve insulin-sensitivity *in vivo*, and ameliorate glucose tolerance.

Thus, the generation of a peptide able to block PED/PEA-15/PLD1 interaction may represent a therapeutic tool to ameliorate insulin-sensitivity caused by PED/PEA-15 overexpression.

Zhang et al. 2000, have previously identified in a yeast two-hybrid system a portion of phospholipase D1 interacting with PED/PEA-15 protein. This fragment, indeed, named D4 constitutes the minimal fragment of interaction between the two proteins.

Here, I show that the expression of D4 fragment in HEK293 and L6 cells decrease PED/PEA-15/PLD1 association, thereby reducing PKC $\alpha$  activation and restoring insulin-stimulated glucose uptake in cells overexpressing PED/PEA-15.

This suggests that reduction of PED/PEA-15 interaction with PLD1 represent a novel strategy to improve glucose tolerance in individuals with type 2 diabetes.

## ACKNOWLEDGEMENTS

I thank *Prof. Francesco Beguinot* to give me the opportunity to work in his laboratory, for all confidence shown in my ability, for support, supervision and passion that he always places in his work and in every initiative, rare gift...

I would like to thank *Prof. Giancarlo Vecchio* to let me attend this Doctorate program under his supervision.

I thank *Dr. Claudia Miele*, who taught me, suggested and helped during the development of experiments and elaboration of thesis with patient and critic mind. I'm grating for the assessment that she showed me and the enthusiasm for research transmitted, but also for friendship and hours spent in joyful atmosphere.

I thank *Prof. Pietro Formisano* for constant availability and courtesy towards me; his indications and his scientific approaches resulted particularly precious with which I constantly drove in the elaboration of this thesis.

I thank *Drs. Paola Ungaro, Luca Ulianich and Francesco Oriente* for precious advice and courtesy always shown towards me.

I want to express all my gratitude to *Drs. Flora Paturzo and Raffaele Teperino*, who significantly contributed to some discussed results in this thesis, for availability and affection to me and above all to have been close to my side day after day.

I lovely thank *Dr. Giuseppe Perruolo*, who I lived joys and sorrows and above all to have been always near me with support in my bad moments.

I would like to thank my friends of *Diablab laboratory*, everybody contributed in one way or another these years to become "betters". Thanks to them, I laughed during hours spent in the laboratory, I will never forget them.

Thank you also to *Drs. Chiara Romano, Gregory Alexander Raciti, Ferdinando Giacco and Annalisa Iardi*, who I often collaborated with and extremely helpful for me.

A proper thank to *Salvatore Sequino*, to give me the possibility to spend work time in friendship atmosphere, but above all to give me all the assistance that I need during my in vivo work.

## REFERENCES

- Araujo H, Danziger N, Cordier J, Glowinski J, Chneiweiss H. Characterization of PEA-15, a major substrate for protein kinase C in astrocytes. *J Biol Chem* 1993; 268(8):5911-20.
- Bandyopadhyay G, Standaert ML, Galloway L, Moscat J, Farese RV. Evidence for involvement of protein kinase C (PKC)- $\zeta$  and non-involvement of diacylglycerol-sensitive PKCs in insulin-stimulated glucose transport in L6 myotubes. *Endocrinology* 1997; 138:4721-4731.
- Brunet A, Bonni A, Zigmond MJ, Lin MZ, Juo P, Hu LS, Anderson MJ, Arden KC, Blenis J, Greenberg ME. Akt promotes cell survival by phosphorylating and inhibiting a Forkhead transcription factor. *Cell* 1999; 96(6):857-68.
- Cantley LC. The phosphoinositide 3-kinase pathway. *Science* 2002; 296(5573):1655-7.
- Cavenagh MM, Whitney JA, Carroll K, Zhang C, Boman AL, Rosenwald AG, Mellman I, Kahn RA. Intracellular distribution of Arf proteins in mammalian cells. Arf6 is uniquely localized to the plasma membrane. *J Biol Chem* 1996; 271(36):21767-74.
- Chang L, Chiang SH, Saltiel AR. Insulin signalling and the regulation of glucose transport. *Mol Med* 2004; 10(7-12):65-71.
- Chin JE, Dickens M, Tavare JM, Roth RA. Overexpression of protein kinase C isoenzymes alpha, beta I, gamma, and epsilon in cells overexpressing the insulin receptor. Effects on receptor phosphorylation and signaling. *J Biol Chem* 1993; 268(9):6338-47.
- Chong LD, Traynor-Kaplan A, Bokoch GM, Schwartz MA. The small GTP-binding protein Rho regulates a phosphatidylinositol 4-phosphate 5-kinase in mammalian cells. *Cell*. 1994; 79(3):507-13.
- Colley WC, Altshuller YM, Sue-Ling CK, Copeland NG, Gilbert DJ, Jenkins NA, Branch KD, Tsira SE, Bollag RJ, Bollag WB, Frohman MA. Cloning and expression analysis of murine phospholipase D1. *Biochem J* 1997; 326:745-53.
- Condorelli G, Trencia A, Vigliotta G, Perfetti A, Goglia U, Autori E, Cassese A, Musti A, Miele C, Santopietro S, Formisano P, Beguinot F. Multiple members of the mitogen-activated protein kinase family are necessary for PED/PEA-15 anti-apoptotic function. *J Biol Chem* 2002; 277:11013-18.
- Condorelli G, Vigliotta G, Cafieri A, Trencia A, Andalo P, Oriente F, Miele C, Caruso M, Formisano P, Beguinot F. PED/PEA-15: an anti-apoptotic molecule that regulates FAS/TNFR1-induced apoptosis. *Oncogene* 1999; 18(31):4409-15.

- Condorelli G, Vigliotta G, Iavarone C, Caruso M, Tocchetti CG, Andreozzi F, Cafieri A, Tecce MF, Formisano P, Beguinot L, Beguinot F. PED/PEA-15 gene controls glucose transport and is overexpressed in type 2 diabetes mellitus. *EMBO J* 1998; 17(14):3858-66.
- Condorelli G, Vigliotta G, Trencia A, Maitan MA, Caruso M, Miele C, Oriente F, Santopietro S, Formisano P, Beguinot F. Protein kinase C (PKC)-alpha activation inhibits PKC-zeta and mediates the action of PED/PEA-15 on glucose transport in the L6 skeletal muscle cells. *Diabetes* 2001; 50(6):1244-52.
- Cortright RN, Azevedo JL, Qian Zhou JR, Sinha M, Pories WJ, Itani SI, Dohm GL. Protein kinase C modulates insulin action in human skeletal muscle. *Am J Physiol Endocrinol Metab* 2000; 278:E553-E562.
- Crews CM, Alessandrini A, Erikson RL. The primary structure of MEK, a protein kinase that phosphorylates the ERK gene product. *Science* 1992; 258(5081):478-80.
- Cusi K, Maezono K, Osman A, Pendergrass M, Patti ME, Pratipanawatr T, DeFronzo RA, Kahn CR, Mandarino LJ. Insulin resistance differentially affects the PI 3-kinase-and MAP kinase-mediated signaling in human muscle. *J Clin Inv* 2000; 105 (3):311-20.
- Del Guerra S, Lupi R, Marselli L, Masini M, Bugliani M, Sbrana S, Torri S, Pollera M, Boggi U, Mosca F, Del Prato S, Marchetti P. Functional and molecular defects of pancreatic islets in human type 2 diabetes. *Diabetes* 2005; 54:727-35.
- Emoto M, Klarlund JK, Waters SB, Hu V, Buxton JM, Chawla A, Czech MP. Arole for phospholipase D in GLUT4 glucose transporter translocation. *J Biol Chem* 2000; 275(10):7144-51.
- Estelles A, Yokoyama M, Nothias F, Vincent JD, Glowinski J, Vernier P, Chneiweiss H. The major astrocytic phosphoprotein PEA-15 is encoded by two mRNAs conserved on their full length in mouse and human. *J Biol Chem* 1996; 271(25):14800-06.
- Exton JH. Phospholipase D-structure, regulation and function. *Rev Physiol Biochem Pharmacol* 2002; 144:1-94.
- Exton JH. Regulation of Phospholipase D. *FEBS Letters* 2002; 531: 58-61.
- Farese RV. Protein kinase C in insulin action, resistance and secretion. Austin 1994; TX:Landes.
- Farese RV, Sajan MP, Standaert ML. Atypical protein kinase C in insulin action and insulin resistance. *Biochem Soc Trans* 2005; 33:350-53.
- Flores-Riveros JR, McLenithan JC, Esaki O, Lane D. Insulin down-regulates expression of the insulin-responsive glucose transporter (GLUT4) gene: effects on transcription and mRNA turnover. *Proc Natl Acad Sci.* 1993; 90:512-16.

- Formisano P, Perruolo G, Libertini S, Santopietro S, Troncone G, Raciti GA, Oriente F, Portella G, Miele C, Beguinot F. Raised expression of the antiapoptotic protein ped/pea-15 increases susceptibility to chemically induced skin tumor development. *Oncogene* 2005; 24 (47): 7012-21.
- Formstecher E, Ramos JW, Fauquet M, Calderwood DA, Hsieh JC, Canton B, Nguyen XT, Barnier JV, Camonis J, Ginsberg MH, Chneiweiss H. PEA-15 mediates cytoplasmic sequestration of ERK MAP kinase. *Dev Cell* 2001; (2):239-50.
- Gillespie K.M. Type 1 diabetes: pathogenesis and prevention. *CMAJ* 2006; 175(2):165-70.
- Hao C, Beguinot F, Condorelli G, Trecia A, Van Meir EG, Yong VW, Parney IF, Roa WH, Petruk KC. Induction and intracellular regulation of tumor necrosis factor-related apoptosis-inducing ligand (TRAIL) mediated apoptosis in human malignant glioma cells. *Cancer Res* 2001; 61(3):1162-70.
- He TC, Zhou S, Da Costa LT, Yu J, Kinzler KW, Vogelstein B. A simplified system for generating recombinant adenoviruses. *Proc Natl Acad Sci* 1998; 95:2509-14.
- Hill JM, Vaidyanathan H, Ramos JW, Ginsberg MH, Werner MH. Recognition of ERK MAP kinase by PEA-15 reveals a common docking site within the death domain and death effector domain. *EMBO J* 2002; 21(23):6494-504.
- Jaken S. Protein kinase C isozymes and substrates. *Curr Opin in Cell Biol* 1996; 8(2):168-73.
- Jenkins GM, Frohman MA, Phospholipase D: a lipid centric review. *Cell Mol Life Sci* 2005; 62: 2305-2316.
- Jiang H, Luo JQ, Urano T, Frankel P, Lu Z, Foster DA, Feig LA. Involvement of Ral GTPase in v-Src-induced phospholipase D activation. *Nature* 1995; 378(6555):409-12.
- Katayama K, Kodaki T, Nagamachi Y, Yamashita S. Cloning differential regulation and tissue distribution of alternatively spliced isoforms of ADP-ribosylation-factor-dependent phospholipase D from rat liver. *Biochem J* 1998; 329: 647-652.
- Kessler A, Uphues I, Ouwens DM, Till M, Eckel J. Diversification of cardiac insulin signaling involves the p85 alpha/beta subunits of phosphatidylinositol 3-kinase. *Am J Physiol Endocrinol Metab* 2001; 280(1):E65-74.
- Kim J, Choi BH, Jang KL, Min DS. Phospholipase D activity is elevated in hepatitis C virus core protein-transformed NIH3T3 mouse fibroblast cells. *Experimental and Molecular Medicine* 2004; 36 (5):454-460.
- Klarlund JK, Guilherme A, Holik JJ, Virbasius JV, Chawla A, Czech MP. Signaling by phosphoinositide-3,4,5-trisphosphate through proteins containing pleckstrin and Sec7 homology domains. *Science* 1997; 275(5308):1927-30.

- Klip A, Tsakiridis T, Marette A, Ortiz PA. Regulation of expression of glucose transporters by glucose: a review of studies in vivo and in cell cultures. *Faseb Journal* 1994; 8:43-53.
- Kubes M, Cordier J, Glowinski J, Girault JA, Chneiweiss H. Endothelin induces a calcium-dependent phosphorylation of PEA-15 in intact astrocytes: identification of Ser104 and Ser116 phosphorylated, respectively, by protein kinase C and calcium/calmodulin kinase II in vitro. *J Neurochem* 1998; 71(3):1307-14.
- Le Roith D, Zick Y. Recent advances in our understanding of insulin action and insulin resistance. *Diabetes Care* 2001; 24(3):588-97.
- Lietzke SE, Bose S, Cronin T, Klarlund J, Chawla A, Czech MP, Lambright DG. Structural basis of 3-phosphoinositide recognition by pleckstrin homology domains. *Mol Cell* 2000; 6(2):385-94.
- Liscovitch M, Czarny M, Ciucci G, Tang X. Phospholipase D: molecular and cell biology of a novel family. *Biochem J* 2000; 345: 401-415.
- Malecki MT, Klupa T. Type 2 diabetes mellitus: from genes to disease. *Pharmacological Reports* 2005; 57:20-32.
- Mlinar B, Marc J, Janez A, Pfeifer M. Molecular mechanisms of insulin resistance and associated diseases. *Clin Chim Acta* 2007; 375(1-2):20-35.
- Newton AC. Regulation of protein kinase C. *Curr Opin in Cell Biol* 1997; 9:161-67.
- Paz K, Hemi R, LeRoith D, Karasik A, Elhanany E, Kanety H, Zick Y. A molecular basis for insulin-resistance. *J Biol Chem* 1997; 272(47):29911-18.
- Pessin JE, Saltiel AR. Signaling pathways in insulin action: molecular targets of insulin resistance. *J Clin Inv* 2000; 106 (2):165-69.
- Pirola L, Johnston A.M, Van Obberghen E, Modulation of insulin action. *Diabetologia* 2004; 47:170-184.
- Saltiel AR, Kahn CR. Insulin signalling and the regulation of glucose and lipid metabolism. *Nature* 2001; 414(6865):799-806.
- Samaras K, McElduff A, Twigg SM, Proietto J, Prins JB, Welborn TA, Zimmet P, Chisholm DJ, Campbell LV. Insulin levels in insulin resistance: phantom of the metabolic opera. *Med J Aust* 2006; 185(3):159-61.
- Sarri E, Pardo r, Fensome-Green A, Cockcroft S. Endogenous phospholipase D2 localizes to the plasma membrane of RBL-2H3 mast cells and can be distinguished from ADP ribosylation factor-stimulated phospholipase D1 activity by its specific sensitivity to oleic acid. *Biochem J* 2003; 369:319-29.
- Skolnik EY, Batzer A, Li N, Lee CH, Lowenstein E, Mohammadi M, Margolis B, Schlessinger J. The function of GRB2 in linking the insulin receptor to Ras signaling pathways. *Science* 1993; 260:1953-55.

- Stern MP. Strategies and prospects for finding insulin resistance genes. *J Clin Inv* 2000; 106 (3):323-27.
- Sung TC, Altshuller YM, Morris AJ, Frohman M.A, Molecular analysis of mammalian Phospholipase D2. *J Biol Chem* 1999; 274(1):494-502.
- Sung TC, Roper RL, Zhang Y, Rudge SA, Temel R, Hammond SM, Morris AJ, Moss B, Engebrecht JA, Frohman MA. Mutagenesis of phospholipase D defines a superfamily including a trans-Golgi viral protein required for poxvirus pathogenicity. *EMBO J* 1997; 16(15):4519-30.
- Trencia A, Fiory F, Maitan MA, Vito P, Barbagallo AP, Perfetti A, Miele C, Ungaro P, Oriente F, Cilenti L, Zervos AS, Formisano P, Beguinot F. Omi/HtrA2 promotes cell death by binding and degrading the anti-apoptotic protein ped/pea-15. *J Biol Chem* 2004; 279(45):46566-72.
- Trencia A, Perfetti A, Cassese A, Vigliotta G, Miele C, Oriente F, Santopietro S, Giacco F, Condorelli G, Formisano P, Beguinot F. Protein kinase B/Akt binds and phosphorylates PED/PEA-15, stabilizing its antiapoptotic action. *Mol Cell Biol* 2003; 23(13):4511-21.
- Tseng CH. The potential biological mechanisms of arsenic-induced diabetes mellitus. *Toxicology and Applied Pharmacology* 2004; 197:67-83.
- Valentino R, Lupoli GA, Raciti GA, Oriente F, Marinaro E, Della Valle E, Salomone M, Riccardi G, Vaccaio O, Donnarumma G, Sesti G, Hribal ML, Cardellini M, Miele C, Formisano P, Beguinot F. The PEA15 gene is overexpressed and related to insulin resistance in healthy first-degree relatives of patients with type 2 diabetes. *Diabetologia* 2006;
- Vanhaesebroeck B, Alessi DR. The PI3K-PDK1 connection: more than just a road to PKB. *Biochem J* 2000; 346:561-76.
- Vigliotta G, Miele C, Santopietro S, Portella G, Perfetti A, Maitan MA, Cassese A, Oriente F, Trencia A, Fiory F, Romano C, Tiveron C, Tatangelo L, Troncone G, Formisano P, Beguinot F. Overexpression of the ped/pea-15 gene causes diabetes by impairing glucose-stimulated insulin secretion in addition to insulin action. *Mol Cell Biol* 2004; 24 (11): 5005-5015.
- Watson RT, Pessin JE. Intracellular organization of insulin signalling and GLUT4 translocation. *Endoc Soc* 2006; 175-191.
- White MF. The IRS-signaling system: A network of docking proteins that mediate insulin action. *Mol and Cell Bioch* 1998; 182:3-11.
- Xie Z, Ho WT, Exton JH. Conserved amino acids at the C-terminus of rat phospholipase D1 are essential for enzymatic activity. *Eur J Biochem.* 2000; 267(24):7138-46.
- Zhang Y, Redina O, Altshuller YM, Yamazaki M, Ramos J, Chneiweiss H, Kanaho Y, Frohman MA. Regulation of expression of phospholipase D1 and

D2 by PEA-15, a novel protein that interacts with them. *J Biol Chem* 2000; 275(45):35224-32.

Zimmet P, Alberti KG, Shaw J. Global and societal implications of the diabetes epidemic. *Nature* 2001; 414:782-87.

## Multiple Members of the Mitogen-activated Protein Kinase Family Are Necessary for PED/PEA-15 Anti-apoptotic Function\*

Received for publication, November 15, 2001, and in revised form, January 8, 2002  
Published, JBC Papers in Press, January 14, 2002, DOI 10.1074/jbc.M110934200

Gerolama Condorelli‡§, Alessandra Trencia‡§, Giovanni Vigliotta‡¶, Anna Perfetti‡, Umberto Goglia‡, Angela Cassese‡, Anna Maria Musti‡||, Claudia Miele‡, Stefania Santopietro‡, Pietro Formisano‡, and Francesco Beguinot‡\*\*

From the ‡Dipartimento di Biologia e Patologia Cellulare e Molecolare & Centro di Endocrinologia ed Oncologia Sperimentale del Consiglio Nazionale delle Ricerche, Università di Napoli Federico II, Via S. Pansini, 5, 80131 Naples, and the ||Dipartimento Farmaco-Biologico, Università della Calabria, 87040 Rende, Italy

293 kidney embryonic cells feature very low levels of the anti-apoptotic protein PED. In these cells, expression of PED to levels comparable with those occurring in normal adult cells inhibits apoptosis induced by growth factor deprivation and by exposure to H<sub>2</sub>O<sub>2</sub> or anisomycin. In PED-expressing 293 cells (293<sub>PED</sub>), inhibition of apoptosis upon growth factor deprivation was paralleled by decreased phosphorylation of JNK1/2. In 293<sub>PED</sub> cells, decreased apoptosis induced by anisomycin and H<sub>2</sub>O<sub>2</sub> was also accompanied by block of JNK1/2 and p38 phosphorylations, respectively. Impaired activity of these stress kinases by PED correlated with inhibition of stress-induced Cdc-42, MKK4, and MKK6 activation. At variance with JNK1/2 and p38, PED expression increased basal and growth factor-stimulated Ras-Raf-1 co-precipitation and MAPK phosphorylation and activity. Treatment of 293<sub>PED</sub> cells with the MEK inhibitor PD98059 blocked ERK1/2 phosphorylations with no effect on inhibition of JNK1/2 and p38 activities. Complete rescue of JNK and p38 functions in 293<sub>PED</sub> cells by over-expressing JNK1 or p38, respectively, enabled only partial recovery of apoptotic response to growth factor deprivation and anisomycin. However, simultaneous rescue of JNK and p38 activities accompanied by block of ERK1/2 fully restored these responses. Thus, PED controls activity of the ERK, JNK, and p38 subfamilies of MAPKs. PED anti-apoptotic function in the 293 cells requires PED simultaneous activation of ERK1/2 and inhibition of the JNK/p38 signaling systems by PED.

PED is a 15-kDa protein with almost ubiquitous expression (1, 2). cDNA sequencing led to the identification of a canonical death effector domain (DED)<sup>1</sup> at PED N terminus (3, 4). More

recently, we and others (3, 5) demonstrated that the DED of PED binds the DED of both FAS-associated death domain (FADD) and caspase 8 (FLICE). Through this mechanism, PED inhibits FLICE activation by tumor necrosis factor- $\alpha$  and FasL, thereby blocking the apoptotic effects of these cytokines. It has subsequently been shown that PED potentiates phosphorylation of the ERKs through a Ras-dependent mechanism (6). PED also anchors the ERKs in the cytoplasm, preventing phosphorylation of their nuclear substrates and restraining cell proliferation (7). These findings suggest that PED may feature a broad function in control of cell survival. However, the molecular mechanisms involved in PED action have only partially been elucidated.

Mitogen-activated protein kinases (MAPKs) play a major role in mediating cellular responses to a variety of extracellular stimuli, including death and survival signals (8, 9). MAPKs include at least three main subgroups: the extracellular signal-regulated kinases (ERK1/2 or p42/44<sup>MAPK</sup>), the c-Jun N-terminal kinases (p46/54<sup>JNK</sup>), and p38<sup>MAPK</sup>. While structurally related, MAPK families undergo activation in response to extracellular stimuli through distinct upstream dual specificity kinases, thereby functioning in separate MAPK cascades (10, 11). The Raf/ERK kinase1/2/ERK1/2 cascade is stimulated by mitogenic and survival stimuli, largely through the Ras-Raf-1-dependent pathway (12, 13). At variance, p46/54<sup>JNK</sup> and p38<sup>MAPK</sup> are primarily activated by cellular stresses including oxidative agents, UV irradiation, hypoxia, proinflammatory cytokines, and anisomycin (14, 15). Exposure to these agents often results in cell apoptosis (16). Dual specificity kinases activating p46/54<sup>JNK</sup> are MAPK kinases 4 and 7 (MKK4 and MKK7), while MKK3 and MKK6 were proved to activate p38<sup>MAPK</sup>. MAPKs phosphorylate and activate a variety of cytoplasmic and nuclear substrates, including transcription factors.

Despite the dicotomy in the main action of ERKs and stress kinases, current evidence indicates that ERKs and p46/54<sup>JNK</sup>-p38<sup>MAPK</sup> cooperate in inducing cells to survive or to die. Activation of the stress kinase cascade, alone, may not be sufficient to induce apoptosis under all circumstances (17). Also, concomitant inactivation of survival signals appears to be necessary for enabling p46/54<sup>JNK</sup> and p38<sup>MAPK</sup> induction to cause cell death (17–21). It appears therefore that the balance between the ERK and the p46/54<sup>JNK</sup>-p38<sup>MAPK</sup> signaling systems is crit-

\* This work was supported in part by the European Community (Grant QLRT-1999-00674 (to F. B.)), grants from the Associazione Italiana per la Ricerca sul Cancro (AIRC) (to F. B. and P. F.), the Ministero dell'Università e della Ricerca Scientifica, the Consiglio Nazionale delle Ricerche Target Project on Biotechnology (to F. B.), by the Telethon-Italy (Grant 0896 to F.B.), and by Novartis Pharmaceuticals. The costs of publication of this article were defrayed in part by the payment of page charges. This article must therefore be hereby marked "advertisement" in accordance with 18 U.S.C. Section 1734 solely to indicate this fact.

§ These authors contributed equally to this work.

¶ Recipient of a fellowship of the Consiglio Nazionale delle Ricerche (CNR).

\*\* To whom all correspondence should be addressed: Dipartimento di Biologia e Patologia Cellulare e Molecolare, Università di Napoli Federico II, Via S. Pansini, 5, 80131 Naples, Italy. Tel.: 39-081-7463248; Fax: 39-081-7463235; E-mail: beguino@unina.it.

<sup>1</sup> The abbreviations used are: DED, death effector domain; GST,

glutathione S-transferase; ERK, extracellular signal-regulated kinase; MAPK, mitogen-activated protein kinase; JNK, c-Jun N-terminal kinase; HA, hemagglutinin; DMEM, Dulbecco's modified Eagle's medium; CNF1, cytotoxic necrotizing factor 1; CRIB, Cdc-42/Rac-interactive binding motif; PAK, p21-activated kinase.

ical for inducing the cell to die or survive. However, the molecular mechanisms responsible for tuning the ratio of activities in these cascades are largely elusive. For instance, there is little information on whether checkpoint proteins exist in the cell that foster survival signal transduction through the ERK pathway while inhibiting p46/54<sup>JNK</sup>-p38<sup>MAPK</sup> signaling or vice versa. Answering this question will greatly help in the understanding how the cells control their own survival.

In the present report we show that PED inhibits p46/54<sup>JNK</sup> and p38<sup>MAPK</sup> signaling and protects cells from stress-induced apoptosis. More importantly, we report that full PED anti-apoptotic action requires both ERK activation and inhibition of p46/54<sup>JNK</sup>-p38<sup>MAPK</sup> function, indicating that PED represents a major MAPK regulatory protein, which gathers antiapoptotic signals toward the cell machinery.

#### EXPERIMENTAL PROCEDURES

**Materials**—Media, sera, antibiotics for cell culture, and the LipofectAMINE reagent were from Invitrogen. Rabbit polyclonal antibodies toward ERK1/2, p38, and JNK/SAPK were purchased from Santa Cruz, Inc. (Santa Cruz, CA). All phosphokinase antibodies were from New England Biolabs Inc. (Beverly, MA), and PED antibodies have been described previously (2). The HA-tagged JNK-1 and GST-tagged MKK6 cDNA plasmids were generously donated by Dr. S. Gutkind (National Institutes of Health, Bethesda, MD) and the GST-CRIB cDNA by Dr. P. Di Fiore (Istituto Europeo di Oncologia, Milan, Italy). The c-Jun cDNA has been reported previously (22). SDS-PAGE reagents were purchased from Bio-Rad, and radiochemicals, Western blotting, and ECL reagents were from Amersham Biosciences. All other chemicals were from Sigma.

**Cell Culture and Transfection and Cell Death Assays**—The 293 human kidney embryonic cells were grown in DMEM supplemented with 10% fetal calf serum, 100 IU/ml penicillin, 100 IU/ml streptomycin, and 2% L-glutamine in a humidified CO<sub>2</sub> incubator. A pcDNA3 expression vector containing the Myc-tagged PED cDNA was generated by first amplifying PED wild-type cDNA with the following two primers: PED5' (5'-GGCCGGTACCGCCAGAGCGCGGGGAGTGTG-3') and 3'MycPEDB (5'-CGCGGATCCTCACAGATCCTTCTGAGATGAGTTTTTGTTCGGCCTTCTTCCGTGGGGAGCCAATTTGATGATCTCTT-3'), carrying the *Kpn*I and the *Bam*HI restriction sites, respectively. The amplification product was then cloned in the pcDNA3 plasmid and sequence verified using the T7Sequencing Kit by Amersham Biosciences. The construct was stably transfected in 293 cells using the lipofectamine method as in Ref. 2. Selection was accomplished using G418 at the effective dose of 0.8 mg/ml. Transient transfections of JNK-1, MKK6, and c-Jun cDNAs were accomplished by the LipofectAMINE method according to the manufacturer's instructions. Briefly, cells were cultured in p60 dishes up to 80% confluence and incubated for 24 h with 3 μg of cDNA and 15 μl of LipofectAMINE in serum-free DMEM. An equal volume of DMEM supplemented with 20% fetal calf serum was added for 5 h. The medium was then replaced with DMEM supplemented with 10% serum and cells further incubated for 24 additional hours before being assayed.

For detecting apoptosis, the cells were kept in the presence or the absence of serum or incubated with 50 μM anisomycin (18 h) or 500 nM H<sub>2</sub>O<sub>2</sub> (1 h) or 100 μM PD98059 (18 h), as indicated in the description of the individual experiments. Apoptosis was then assayed by DNA laddering detection according to Ref. 23 or quantitated using the Apoptosis ELISA Plus kit (Roche Diagnostics GmbH, Mannheim, Germany), according to the manufacturer's instructions.

**Western Blot Analysis**—For these assays, the cells were solubilized in lysis buffer (50 mM Hepes, pH 7.5, 150 mM NaCl, 4 mM EDTA, 10 mM Na<sub>4</sub>PO<sub>7</sub>, 2 mM Na<sub>3</sub>VO<sub>4</sub>, 100 mM NaF, 10% glycerol, 1% Triton, 1 mM phenylmethylsulfonyl fluoride, 100 μg/ml aprotinin, 1 mM leupeptin) for 30 min at 4 °C. Lysates were centrifuged at 5,000 × *g* for 15 min. Solubilized proteins were separated by SDS-PAGE and transferred on 0.45 μm Immobilon-P membranes (Millipore, Bedford, MA). Upon incubation with the primary and secondary antibodies, immunoreactive bands were detected by ECL according to the manufacturer's instructions.

**MAPK Activity and Cdc-42 GTP Loading**—MAPK activity was assayed *in vitro* as reported previously (24). Briefly, cells were solubilized in lysis buffer and lysates clarified by centrifugation at 5,000 × *g* for 20 min. Equal aliquots of the lysates (200 μg) were immunoprecipitated with MAPK antibodies, and phosphorylation reactions were initiated by

adding 2 μg of the myelin basic protein substrate, the phosphorylation mixture (20 mM Hepes, pH 7.2, 10 mM MgCl<sub>2</sub>, 10 mM MnCl<sub>2</sub>, 1 mM dithiothreitol, 5 mM ATP, 0.2 mM EGTA, 1 mM PKA inhibitor, final concentrations) and 10 μCi/reaction [<sup>32</sup>P]ATP. Phosphorylation reactions were prolonged for 30 min at 22 °C, stopped by rapid cooling on ice, and spotted on phosphocellulose disc papers. Discs were washed twice with 1% H<sub>3</sub>PO<sub>4</sub>, followed by additional washes in water, and the disc-bound radioactivity was quantified by liquid scintillation counting.

For estimating GTP loading of Cdc-42, cells were incubated in the presence or the absence of cytotoxic necrotizing factor 1 (CNF1) (30 ng/ml) for 6 h and solubilized in 1% Nonidet P-40, 25 mM Tris, pH 7.5, 5 mM MgCl<sub>2</sub>, 100 mM NaCl, 5% glycerol, 1 mM phenylmethylsulfonyl fluoride, 1 μg/ml leupeptin, and 2 mM Na<sub>3</sub>VO<sub>4</sub>. Protein lysates (1 μg) were then incubated for 20 min at 4 °C in the presence of 10 μg of agarose-bound GST CRIB in 2 volumes of binding buffer (0.5% Nonidet P-40, 25 mM Tris, pH 7.5, 30 mM MgCl<sub>2</sub>, 40 mM NaCl, 1 mM dithiothreitol). Complexes were washed four times with lysis buffer and then resuspended in Laemli buffer followed by boiling for 4 min and centrifugation at 25,000 × *g* for 3 min. Supernatants were analyzed by SDS-PAGE and blotting with Cdc-42 antibodies.

#### RESULTS

**Reduced Apoptosis in PED-overexpressing 293 Cells**—293 human embryonic kidney cells were stably transfected with a Myc-tagged PED cDNA. Several clones of PED-overexpressing cells were obtained and three of them, termed 293<sub>PEDC11</sub>, 293<sub>PEDC12</sub>, and 293<sub>PEDC13</sub>, were studied in detail. Immunoblotting with either Myc or PED antibodies indicated that the expression of PED in these transfected cells was increased by >100-fold compared with control cells, either those transfected with the resistance plasmid alone (293<sub>PC</sub>) or the 293 untransfected cells (293<sub>WT</sub>) (Fig. 1A). The 293<sub>WT</sub> cells feature very low levels of endogenous PED. On a per milligram protein bases, the levels of PED expression achieved in the transfectants were comparable with those in mouse brain and fat tissues (data not shown). Based on DNA laddering, serum deprivation of parental cells induced a time-dependent increase in DNA fragmentation (Fig. 1B). In these cells, fragmentation was well detectable upon 24 h of serum deprivation, further increasing upon 48 and 72 h. At variance, no DNA fragmentation was observed in PED-transfected cells up to 48 h after serum deprivation. In these cells, apoptosis became detectable only by 72 h. The same delay in the onset of DNA laddering in response to serum starvation was observed in the two other transfected clones (data not shown). To further investigate PED apoptosis-protective action, we compared the effects of the stress kinase activators anisomycin and hydrogen peroxide in 293<sub>PEDC11</sub> and control cells. As shown in Fig. 1C, treatment with anisomycin for 18 h increased apoptosis by >3-fold in parental 293<sub>WT</sub> and 293<sub>PC</sub> cells, same as 48-h serum deprivation. In these same cells, 1-h incubation with hydrogen peroxide induced a 5-fold increase in apoptosis. In 293<sub>PEDC11</sub> cells there was a >2-fold inhibition in the apoptotic responses to all of these agents, compared with the control cells (*p* < 0.001). Almost identical inhibition of apoptosis was observed in the other two clones of PED-overexpressing cells.

**JNK and p38 Function in PED-overexpressing 293 Cells**—In different cell types, the MAPK-related enzymes JNK and p38 play a major role in signaling apoptosis and undergo phosphorylation and activation in responses to growth factor withdrawal, anisomycin, and oxidative stress (19–21). In control 293 cells, anisomycin also induced a 10-fold increase in phosphorylation of the key activation sites of JNK (Thr<sup>183</sup> and Tyr<sup>185</sup>; Fig. 2A). Anisomycin-induced phosphorylation was reduced by 3-fold in PED-transfected compared with the control cells with no change in JNK expression levels. Similar to anisomycin, serum deprivation increased JNK phosphorylation in 293<sub>WT</sub> cells. This effect peaked at 10–16 h after serum starvation and was 2.5-fold less evident in the 293<sub>PEDC11</sub> cells (Fig. 2B). The decrease in JNK phosphorylation upon anisomycin treatment

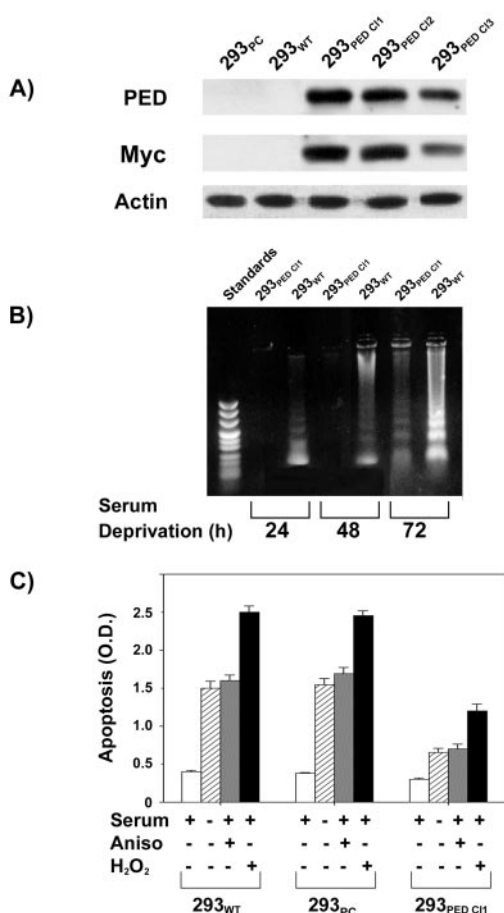


**FIG. 1. PED action on stress-induced apoptosis in 293 cells.** *A*, 293 human embryonic kidney cells were stably transfected with a Myc-tagged PED cDNA as indicated. PED-overexpressing cell clones (293<sub>PEDC11</sub>, 293<sub>PEDC12</sub>, 293<sub>PEDC13</sub>) and control cells (untransfected cells, 293<sub>WT</sub>; cells transfected with the empty plasmid, 293<sub>PC</sub>) were solubilized and immunoblotted with Myc, PED, or actin antibodies, as indicated. Blotted proteins were revealed by ECL and autoradiography. *B*, alternatively, the cells were incubated in the absence or the presence of 10% serum for the indicated times. Cytoplasmic DNA was extracted and analyzed by 1.2% agarose gel electrophoresis and ethidium bromide staining. Representative experiments are shown in *A* and *B*. *C*, the cells were incubated in the absence or the presence of 10% serum (48 h), 50  $\mu$ M anisomycin (18 h), or 500 nM H<sub>2</sub>O<sub>2</sub> (1 h), as indicated. Apoptosis was quantitated by the ELISA Plus detection kit as described under "Experimental Procedures." Bars represent the mean  $\pm$  S.D. of four independent experiments in duplicate.

or serum starvation was paralleled by a 2.5-fold decreased phosphorylation of the JNK substrate c-Jun in the PED-overexpressing compared with control cells (Fig. 2C). Based on Western blotting with specific phospho-p38 antibodies, hydrogen peroxide and serum deprivation treatments of control cells also increased phosphorylation of p38 key activation sites (Thr<sup>180</sup>, Thr<sup>182</sup>) by 6- and 2.5-fold, respectively (Fig. 3, *A* and *B*). Phosphorylation of p38 by hydrogen peroxide and serum deprivation were 2- and 4-fold inhibited in PED-transfected cells. Control experiments with the 293<sub>PEDC12</sub> and 293<sub>PEDC13</sub> cells revealed very similar results (data not shown).

In Chinese hamster ovary cells, PED overexpression induces ERK1/2 signaling through the Ras pathway (6). We therefore hypothesized that increased ERK1/2 activity may be responsible for inhibiting JNK and p38 function in 293 PED-transfected cells. As in PED-overexpressing Chinese hamster ovary cells, extracts from 293 PED-expressing cells featured a 2.5-fold increased Raf-1 co-precipitation with active Ras (Fig. 4A). In addition, the 293 PED-transfected cells showed a constitutive increase in ERK1/2 phosphorylation and activity (Fig. 4, *B* and

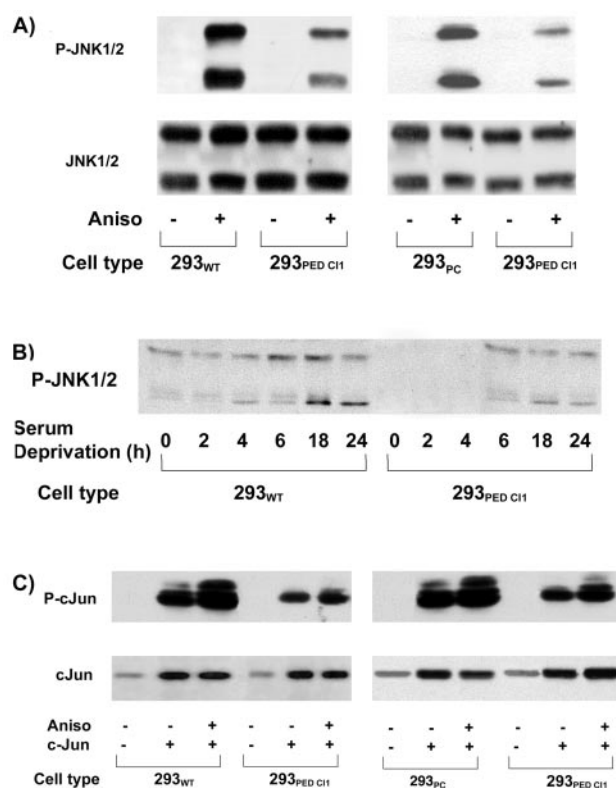


**FIG. 2. PED action on JNK activity in 293 cells.** *A*, 293<sub>PEDC11</sub> and control cells were incubated with 50  $\mu$ M anisomycin for 30 min. The cells were solubilized, and 50  $\mu$ g of cell proteins were blotted with phospho-JNK (pJNK1/2) or JNK (JNK1/2) antibodies. Filters were revealed by ECL according to the manufacturer's instructions. Alternatively (*B*), the cells were incubated in the presence or the absence of serum for the indicated times, solubilized, and blotted with pJNK1/2 antibodies as above. *C*, to test JNK activity, cells were first transfected with c-Jun cDNA as reported under "Experimental Procedures." The cells were then exposed to anisomycin for 30 min. Phospho-c-Jun was identified by Western blotting equal amounts of cell lysates with phospho-c-Jun antibodies. The autoradiographs shown are representative of four (*A*) and three (*B*) representative experiments.

*C*). Further increase in ERK phosphorylation and activity in response to serum were reduced in these cells, with no significant change in ERK1/2 expression.

In both the PED-transfected and the control cells, inhibition of the ERK upstream kinase MEK with PD98059 blocked basal and serum-stimulated ERK activities (Fig. 5A). Interestingly, however, PD98059 had no effect on the impaired activation of JNK by anisomycin in 293<sub>PEDC11</sub> cells (Fig. 5B). Similarly, PD98059 treatment did not allow any recovery of p38 phosphorylation by hydrogen peroxide in PED-expressing as compared with wild-type cells (Fig. 5C) and to cells transfected with the empty plasmid (not shown). Thus, ERK activation, alone, did not account for the inhibition of JNK and p38 functions in PED-overexpressing cells.

**Cdc-42 Signaling in PED-overexpressing 293 Cells**—JNK and p38 have been reported to be induced by the Cdc-42/PAK-1 signaling cascade in response to different stress-inducing agents (25). In 293 cells, CNF1 (26) increased the pull-down of the CRIB interaction domain of PAK-1 kinase with Cdc-42 by 4-fold (Fig. 6A). These effects did not occur in PED-expressing 293 cells, however. Phosphorylation of the key activation sites on PAK-1 downstream kinases MKK4 and MKK6 (Thr<sup>223</sup> and Ser<sup>189</sup>/Ser<sup>207</sup>, respectively) were also increased by 8- and 2.5-fold by anisomycin and hydrogen peroxide (Fig. 6B). As was the case for the CRIB-Cdc-42 interaction, these effects were abolished in the 293<sub>PEDC11</sub> cells, suggesting that PED may inhibit JNK and p38 activation by blocking signaling through the

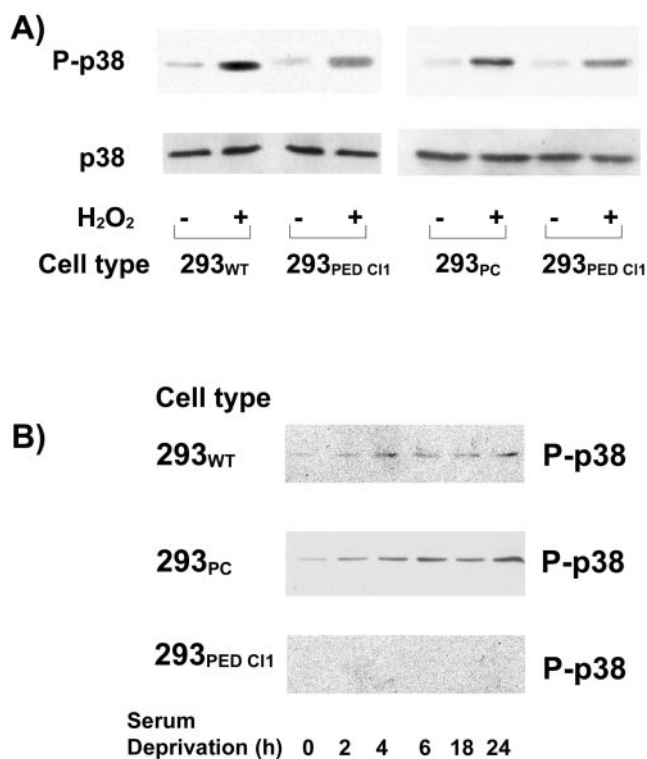


**FIG. 3. PED action on p38 phosphorylation.** A,  $293_{\text{PEDC1}}$  and control cells were exposed to 500 nM  $\text{H}_2\text{O}_2$  for 30 min. The cells were solubilized, and 50  $\mu\text{g}$  of cell proteins were blotted with phospho-p38 (*P-p38*) or with p38 antibodies as indicated. Alternatively (B), the cells were incubated in the presence or the absence of serum for the indicated times, and cell proteins were immunoblotted with P-p38 antibodies as outlined above. Filters were revealed by ECL and autoradiography. The autoradiographs shown are representative of four (A) and three (B) independent experiments.

Cdc-42/PAK-1 pathway at an upstream step. There were no changes in the expression levels of Cdc-42, MKK4, and MKK6 (Fig. 6, A and B) in PED-overexpressing compared with the control cells.

**ERK and JNK/p38 Function in PED Anti-apoptotic Effect**—To further investigate the hypothesis that abrogation of JNK and p38 activation is responsible for PED anti-apoptotic effect, we sought to force JNK and p38 function in PED-expressing 293 cells. We transfected the cells with the HA-tagged JNK-1, GST-tagged MKK6, or with both cDNAs. Western blot analysis with phospho-JNK and phospho-p38 antibodies revealed that these overexpressions activated JNK and p38 kinases to almost identical extents in  $293_{\text{PEDC1}}$  and in control cells (Fig. 7A), indicating that kinase overexpression succeeded in overcoming their inhibition by PED. Consistently, co-transfection of JNK-1 with the c-Jun substrate cDNA resulted in a 4-fold increase in c-Jun phosphorylation compared with the cells transfected with c-Jun alone, both in  $293_{\text{PEDC1}}$  and in control cells (Fig. 7B). In the control cells, overexpression of JNK-1 or MKK6 increased apoptosis in response to serum deprivation by 2.2-fold (Fig. 7C). Simultaneous overexpression of these two kinases showed no additive effect. In the PED-transfected cells, overexpression of JNK-1, MKK6, or both cDNAs caused a 70% increase in cell apoptosis, bypassing PED inhibition (difference with the  $293_{\text{WT}}$  cells significant at the  $p < 0.01$  level). Thus, despite full activation of JNK and p38 function in these cells, apoptosis remained significantly lower than that in the  $293_{\text{WT}}$  cells. This finding suggested that the inhibition of JNK and p38 by PED overexpression in 293 cells does not fully account for PED anti-apoptotic effect.

We therefore tested whether induction of ERK1/2 in PED-

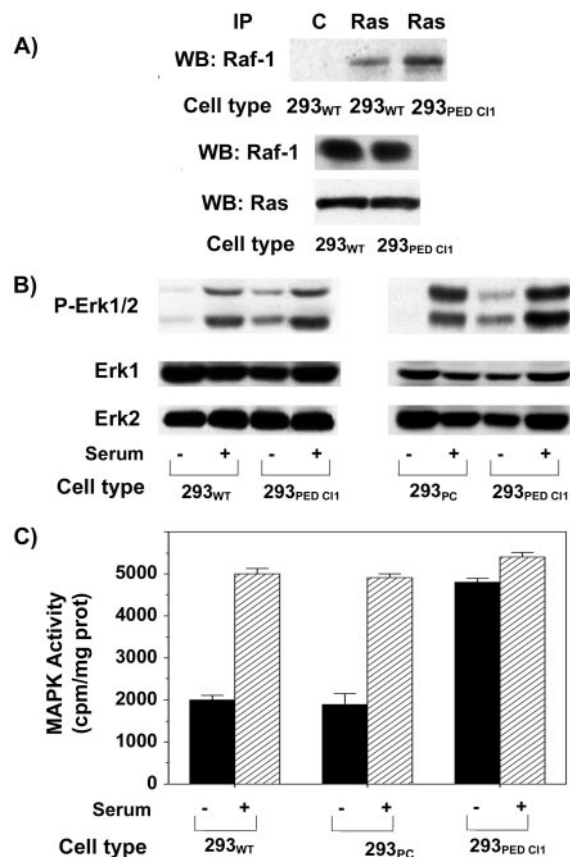


**FIG. 4. PED effect on Ras-Raf-1 co-precipitation and MAPK activation.** A,  $293_{\text{PEDC1}}$  and control cells were solubilized as described under "Experimental Procedures" and lysates (200  $\mu\text{g}$  of protein/sample) immunoprecipitated with either pan-Ras (*Ras*) or nonspecific IgG (C), as indicated. Precipitated proteins were Western blotted with Raf-1 antibodies (*Raf-1*) or Ras antibodies (*Ras*). B,  $293_{\text{PEDC1}}$  and control cells were exposed to 10% serum for 20 min as described under "Experimental Procedures." The cells were then solubilized and cell proteins (50  $\mu\text{g}$ ) blotted with phospho-ERK (*P-ERK1/2*) or ERK antibodies. Filters were revealed by ECL and autoradiography. The autoradiographs shown are representative of three (A) and four (B) independent experiments. C, cell lysates from control and serum-stimulated cells (200  $\mu\text{g}$  of protein) were precipitated with MAPK antibodies. Precipitates were assayed for MAPK activity using MBP as substrate as described under "Experimental Procedures." Bars represent the mean  $\pm$  S.D. from four duplicate experiments.

overexpressing cells may also contribute to protection from apoptosis, while not accounting for the inhibition of JNK and p38. To this end, we blocked ERK activity with the PD98059 inhibitor. Treatment of serum-deprived cells with PD98059, alone, caused no change in apoptosis, either in control or in PED-expressing cells. In control cells overexpressing JNK-1 and/or MKK6, however, PD98059 enhanced apoptotic response by 50%. Interestingly, in PED-transfected cells overexpressing JNK-1 and/or MKK6, PD98059 treatment increased apoptosis to levels identical to the control cells. Similar data were obtained when cell apoptosis was induced by actinomycin rather than serum depletion. Thus, PED protection from stress-induced apoptosis in 293 cells appeared to depend on the simultaneous induction of ERK activity and inhibition of JNK and p38 function.

#### DISCUSSION

We have recently identified PED as a DED-containing protein, which blocks FasL- and tumor necrosis factor- $\alpha$ -induced apoptosis through its DED. In the present report, we show that PED features a broader biological function, forwarding mutu-

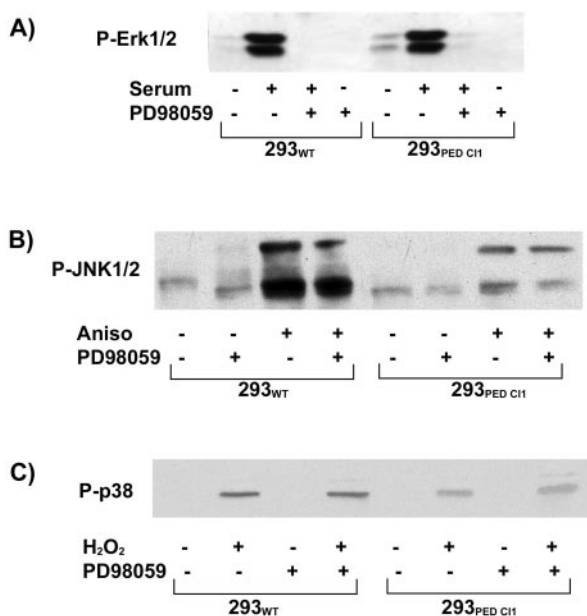


**FIG. 5. Effect of MAPK inhibition on JNK and p38 activation.** A,  $293_{\text{PEDC11}}$  and control cells were preincubated in serum-free medium for 18 h, exposed to  $50 \mu\text{M}$  PD98059 for further 45 min, and then to 10% serum for 10 min as indicated. Cells were solubilized, and lysates ( $50 \mu\text{g}$  of protein) were Western blotted with phospho-ERK antibodies (*P-ERK1/2*). B, the cells were preincubated in serum-free culture medium for 18 h in the presence or the absence of PD98059 and further incubated for 30 min with either  $50 \mu\text{M}$  anisomycin or  $500 \text{ nM}$   $\text{H}_2\text{O}_2$ , as indicated. Cells were then solubilized and cell protein ( $50 \mu\text{g}$ ) immunoblotted with either phospho-JNK (*P-JNK*) or phospho-p38 (*P-p38*) antibodies. Filters were revealed by ECL and autoradiography. The autoradiographs shown are representative of three (A and C) and four (B) independent experiments.

ally reinforcing survival and anti-apoptotic signals to the cell machinery through the ERK and the JNK-p38 pathways.

We found that PED overexpression in 293 kidney cells strongly inhibits apoptosis caused by serum deprivation, oxidative stress, and anisomycin treatment. Simultaneously, PED blocks phosphorylation and activation of JNK and p38 by these agents, indicating an important role of decreased signaling through the JNK-p38 system in PED protection from stress-induced apoptosis. Consistent with this mechanism, forced expression of JNK and p38 activities rescues the sensitivity to stress-induced apoptosis in PED-overexpressing 293 cells. In parallel with the block of stress-induced activation of JNK and p38, their upstream activating kinases MKK4 and MKK6 were also blocked in PED-overexpressing cells. In addition, in these cells, PED inhibits Cdc-42 co-precipitation with the crib interaction domain of PAK-1, suggesting that high levels of PED may inhibit Cdc-42 signaling. Collectively, these data indicate that PED may prevent induction of JNK and p38 stress kinases by acting at a very early step in their activation pathways. It is possible that PED binds PAK-1 and inhibits its interaction with Cdc-42. However, we could not detect co-precipitation of PED with PAK-1 (data not shown). Alternatively, PED may inhibit Cdc-42 activation, either by interacting with Cdc-42 or with a protein upstream Cdc-42 in the signaling cascade. Understanding the mechanism of PED activation of JNK and p38 stress kinases will require the identification of PED-binding proteins, which is presently in progress in our laboratory.

Studies by Ramos *et al.* (6) showed that, in Chinese hamster ovary cells, PED activates ERK1/2 in a Ras-dependent manner. ERK activation by PED also occurs in 293 cells, accompanied by that of early mechanisms in the Ras signaling cascade. Activation of the ERKs was not responsible for the inhibition of JNK and p38 function in cells expressing high levels of PED.

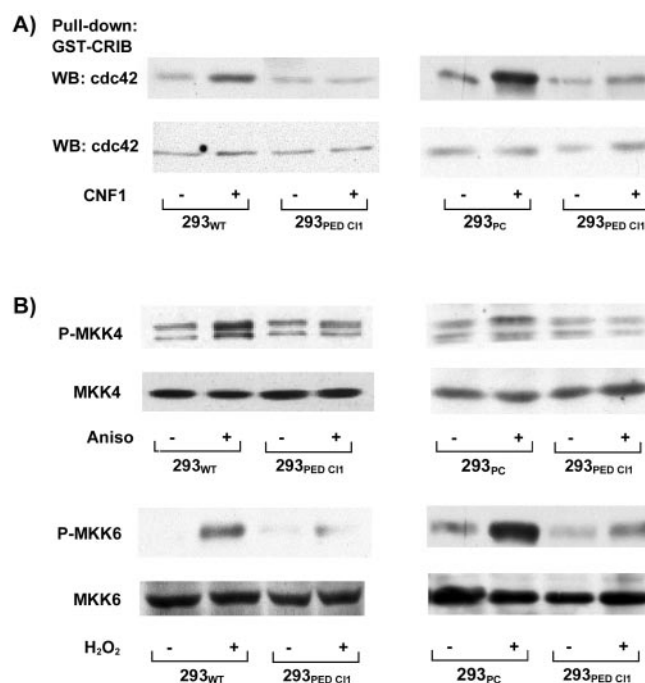


**FIG. 6. PED action on Cdc-42, MKK4, and MKK6 activation.** A,  $293_{\text{PEDC11}}$ , untransfected 293 cells ( $293_{\text{WT}}$ ), and cells transfected with the empty plasmid ( $293_{\text{PC}}$ ) were exposed to CNF1 ( $30 \text{ ng/ml}$ ) for 6 h as indicated. The cells were solubilized, and lysates ( $500 \mu\text{g}$  of cell protein) were incubated with  $10 \mu\text{g}$  of agarose-bound GST-CRIB. The complex was then analyzed by SDS-PAGE followed by Western blotting with Cdc-42 antibodies. B, the cells were exposed for 30 min to  $50 \mu\text{M}$  anisomycin or  $500 \text{ nM}$   $\text{H}_2\text{O}_2$ , as indicated. The cells were solubilized, and cell lysates ( $50 \mu\text{g}$  of protein) were blotted with phospho-MKK6 (*P-MKK6*), MKK6, phospho-MKK4 (*P-MKK4*), or MKK4 antibodies, as indicated. Filters were revealed by ECL and autoradiography. The autoradiographs shown are representative of four (A and B, left panels) and three (A and B, right panels) independent experiments.

Hence, block of ERK activity with the PD98059 inhibitor caused no change in JNK-p38 inactivation in the  $293_{\text{PED}}$  cells. PD98059 treatment does not affect apoptosis caused by serum deprivation either in wild-type 293 cells (expressing almost no endogenous PED) or in PED-overexpressing cells. Thus, ERK activity, alone, is unable to prevent stress-induced apoptosis in these cells. Rescue of JNK-p38 activities in PED-overexpressing 293 cells is not sufficient either, since it did not allow complete recovery of sensitivity to stress apoptosis. Interestingly, the full apoptotic effect of serum deprivation and anisomycin in PED-overexpressing 293 cells were restored by simultaneous block of ERK activation and reintegration of JNK-p38 function. This finding led us to propose that (i) in 293 cells, PED operates as a major survival protein, which simultaneously controls the major mitogen-activated protein kinases; and (ii) in these cells, stress-induced activation of apoptotic programs depends on the concomitant inhibition of ERK survival pathway and on activation of death signaling through the JNK-p38 routes.

Triggering of stress-activated kinases in concomitance with the inhibition of the ERK pathway has been observed in a number of cell systems undergoing programmed cell death (17–21). Activation of the stress kinase cascade may not always be sufficient to induce apoptosis in the cell (17). In fact, concomitant inactivation of survival signals has been proposed to be a prerequisite for the JNK-p38 kinases to induce cell death (17–21). Thus, the balance between the ERK and the JNK-p38 signaling systems seems critical for enabling the cell to die or survive. How the cells control this balance has been less extensively investigated. The pathways leading to activation of

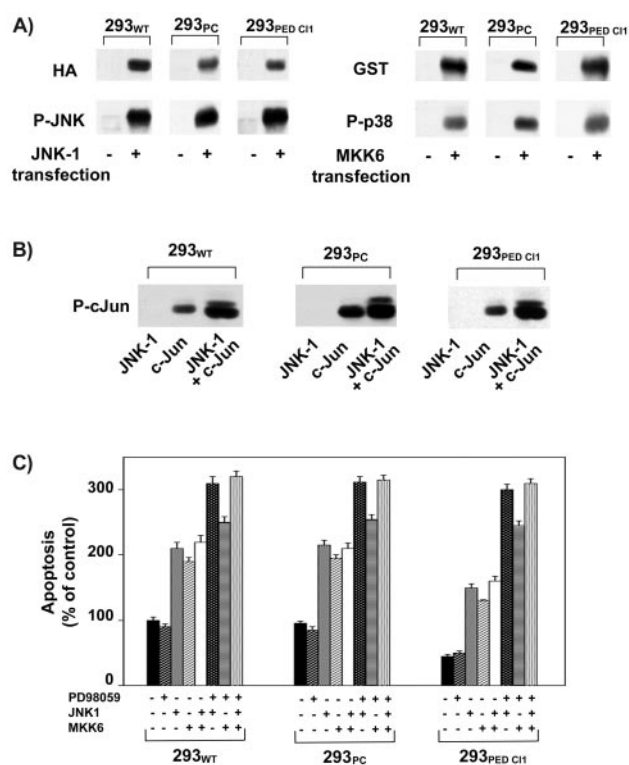


**FIG. 7. Effect of JNK-1 and MKK6 overexpression on apoptosis in 293<sub>PED</sub> cells.** A, 293<sub>PEDCH1</sub> and control cells were transiently transfected with HA-tagged c-JNK-1 and/or GST-tagged MKK6 cDNAs. For control, lysates from the transfected cells (100  $\mu$ g of protein) were separated by SDS-PAGE followed by blotting with HA, GST, phospho-JNK (P-JNK), or phospho-p38 (P-p38) antibodies, as indicated. B, to control the activity of the transfected JNK-1 cDNA, the cells were further transfected with HA-tagged c-JNK-1 and/or c-Jun cDNAs, as indicated and cell proteins blotted with phospho c-Jun antibodies (P-c-Jun). Filters were revealed by ECL and autoradiography. Representative autoradiographs are shown. C, the cells were subsequently exposed to 50  $\mu$ M PD98058 for 18 h, as indicated, and apoptosis was quantified by the ELISA plus apoptosis detection kit as described under "Experimental Procedures." Bars represent the mean  $\pm$  S.D. of four independent experiments in duplicate.

ERKs and of JNK-p38 consist of multiple signaling components, most of which are regulated by protein phosphorylation. Cross-talk may occur between these pathways and contribute to regulate ERK/JNK-p38 activity balance. Consistent with this possibility, simple inhibition of ERK basal activity in HeLa cells has been recently reported to be sufficient to trigger p38 activation in a caspase-dependent manner (27). It has also been proposed that ERK and JNK-p38 pathways may down-regulate each other by turning on the expression of phosphatases, which act on the other (28). In the present report, we show that increasing the PED expression level in cells simultaneously fosters ERK survival function and inhibits JNK-p38 apoptotic signaling in 293 cells. Thus, changing PED expression may represent a third mechanism for the cell to control the balance between ERK and JNK-p38 activities and to foster cell survival.

Most recently, PED has been shown to possess a nuclear export sequence (7). Through this sequence, PED was reported to restrict ERKs to the cytoplasm in cultured astrocytes (7). The cytoplasmic anchoring of ERKs does not affect phosphorylation of their cytosolic substrates, but inhibits ERK-dependent c-Fos transcription and cell proliferation. Inhibition of cell proliferation also occurs in 293 cells overexpressing PED (data not shown). Thus, PED is a multifunctional protein. Increasing its level may allow the cells to become quiescent and resistant to different kinds of apoptotic stimuli.

**Acknowledgments**—We are grateful to Dr. E. Consiglio for his continuous support during the course of this work. We also thank Dr. L. Beguinot (Dipartimento di Ricerca Biologica e Biotecnologica, H. S. Raffaele, Milan, Italy) for critical reading of the manuscript and Dr. D. Liguoro for technical help.

#### REFERENCES

- Araujo, H., Danziger, N., Cordier, J., Glowinski, J., and Chneiweiss, H. (1993) *J. Biol. Chem.* **268**, 5911–5920
- Condorelli, G., Vigliotta, G., Iavarone, C., Caruso, M., Tocchetti, C. G., Andreozzi, F., Tecce, M. F., Cafieri, A., Formisano, P., Beguinot, L., and Beguinot, F. (1998) *EMBO J.* **17**, 3858–3865
- Condorelli, G., Vigliotta, G., Cafieri, A., Trecia, A., Andalò, P., Oriente, F., Miele, C., Caruso, M., Formisano, P., and Beguinot, F. (1999) *Oncogene* **18**, 4409–4415
- Muzio, M., Chinnaiyan, A. M., Kischkel, F. C., O'Rourke, K., Shevchenko, A., Ni, J., Scaffidi, C., Bretz, J. D., Zhang, M., Gentz, R., Mann, M., Kramer, P. H., Peter, M., and Dixit, V. M. (1996) *Cell* **85**, 817–827
- Kitsberg, D., Formstecher, E., Fauquet, M., Kubes, M., Cordier, J., Canton, B., Pan, G., Rolli, M., Glowinski, J., and Chneiweiss, H. (1999) *J. Neurosci.* **19**, 8244–8251
- Ramos, J. W., Hughes, P. E., Renshaw, M. W., Schwartz, M. A., Formstecher, E., Chneiweiss, H., and Ginsberg, M. H. (2000) *Mol. Biol. Cell* **11**, 2863–2872
- Formstecher, E., Ramos, J. W., Fauquet, M., Calderwood, D. A., Hsieh, J., Canton, B., Nguyen, X., Barnier, J., Camonis, J., Ginsberg, M., and Chneiweiss, H. (2001) *Dev. Cell* **1**, 239–250
- Davis, R. J. (1993) *J. Biol. Chem.* **268**, 14553–14556
- Robinson, M. J., and Cobb, M. H. (1997) *Curr. Opin. Cell Biol.* **9**, 180–186
- Davis, R. J. (1994) *Trends Biochem. Sci.* **19**, 470–473
- Kyriakis, J., Banerjee, P., Nikolakaki, E., Dai, T., Rubie, E., Ahmad, M., Avruch, J., and Woodgett, J. (1994) *Nature* **369**, 156–160
- Ichijo, H. (1999) *Oncogene* **18**, 6087–6093
- L'Allemain, G. L., Her, J. H., Wu, J., Sturgil, T. W., and Weber, M. J. (1992) *Mol. Cell. Biol.* **12**, 2222–2229
- Ip, Y. T., and Davis, R. Y. (1998) *Curr. Opin. Cell Biol.* **10**, 205–219
- Ishikawa, Y., and Kitamura, M. (1999) *Biochem. Biophys. Res. Commun.* **264**, 696–701
- Cross, T. G., Scheel-Toellner, D., Henriquez, N. V., Deacon, E., Salmon, M., and Lord, J. M. (2000) *Exp. Cell Res.* **256**, 34–41
- Xia, Z., Dickens, M., Raingeaud, J., Davis, R. J., and Greenberg, M. (1995) *Science* **270**, 1326–1331
- Gupta, K., Kshirsagar, S., Li, W., Gui, L., Ramakrishnan, S., Gupta, P., Law, P. Y., and Hebbel, R. P. (1999) *Exp. Cell Res.* **247**, 495–504
- Shan, R., Price, J. O., Gaarde, W. A., Monia, B. P., Krantz, S. B., and Zhao, Z. J. (1999) *Blood* **12**, 4067–4076
- Berra, E., Diaz-Meco, M. T., and Moscat, J. (1998) *J. Biol. Chem.* **273**, 10792–10797
- Huang, Y., Hutter, D., Liu, Y., Wang, X., Sheikh, S. M., Chan, M. L., and Holbrook, N. J. (2000) *J. Biol. Chem.* **275**, 18234–18242
- Musti, A. M., Treier, M., and Bohmann, D. (1997) *Science* **275**, 400–402
- Donath, M. Y., Gross, D. J., Cerasi, E., and Kaiser, N. (1999) *Diabetes* **48**, 738–744
- Formisano, P., Oriente, F., Fiory, F., Caruso, M., Miele, C., Maitan, A., Andreozzi, F., Vigliotta, G., Condorelli, G., and Beguinot, F. (2000) *Mol. Cell. Biol.* **20**, 6323–6333
- Coso, O. A., Chiariello, M., Yu, J. C., Termoto, H., Crespo, P., Xu, N., Miki, T., and Gutkind, J. S. (1995) *Cell* **81**, 1137–1146
- Lerm, M., Selzer, J., Hoffmeyer, A., Rapp, U. R., Aktories, K., and Schmidt, G. (1999) *Infect. Immun.* **67**, 496–503
- Le Niculescu, H., Bonfoco, E., Kasuya, Y., Claret, F., Green, D. R., and Karin, M. (1999) *Mol. Cell. Biol.* **19**, 751–763
- Keyse, S. M. (2000) *Curr. Opin. Cell Biol.* **12**, 186–192

## Protein Kinase B/Akt Binds and Phosphorylates PED/PEA-15, Stabilizing Its Antiapoptotic Action

Alessandra Trencia, Anna Perfetti, Angela Cassese, Giovanni Vigliotta, Claudia Miele, Francesco Oriente, Stefania Santopietro, Ferdinando Giacco, Gerolama Condorelli, Pietro Formisano, and Francesco Beguinot\*

*Dipartimento di Biologia e Patologia Cellulare e Molecolare and Istituto di Endocrinologia ed Oncologia Sperimentale del C.N.R., Federico II University of Naples, Naples, Italy*

Received 8 November 2002/Returned for modification 6 January 2003/Accepted 8 April 2003

**The antiapoptotic protein PED/PEA-15 features an Akt phosphorylation motif upstream from Ser<sub>116</sub>. In vitro, recombinant PED/PEA-15 was phosphorylated by Akt with a stoichiometry close to 1. Based on Western blotting with specific phospho-Ser<sub>116</sub> PED/PEA-15 antibodies, Akt phosphorylation of PED/PEA-15 occurred mainly at Ser<sub>116</sub>. In addition, a mutant of PED/PEA-15 featuring the substitution of Ser<sub>116</sub>→Gly (PED<sub>S116→G</sub>) showed 10-fold-decreased phosphorylation by Akt. In intact 293 cells, Akt also induced phosphorylation of PED/PEA-15 at Ser<sub>116</sub>. Based on pull-down and coprecipitation assays, PED/PEA-15 specifically bound Akt, independently of Akt activity. Serum activation of Akt as well as BAD phosphorylation by Akt showed no difference in 293 cells transfected with PED/PEA-15 and in untransfected cells (which express no endogenous PED/PEA-15). However, the antiapoptotic action of PED/PEA-15 was almost twofold reduced in PED<sub>S116→G</sub> compared to that in PED/PEA-15<sub>WT</sub> cells. PED/PEA-15 stability closely paralleled Akt activation by serum in 293 cells. In these cells, the nonphosphorylatable PED<sub>S116→G</sub> mutant exhibited a degradation rate threefold greater than that observed with wild-type PED/PEA-15. In the U373MG glioma cells, blocking Akt also reduced PED/PEA-15 levels and induced sensitivity to tumor necrosis factor-related apoptosis-inducing ligand apoptosis. Thus, phosphorylation by Akt regulates the antiapoptotic function of PED/PEA-15 at least in part by controlling the stability of PED/PEA-15. In part, Akt survival signaling may be mediated by PED/PEA-15.**

PED/PEA-15 is a recently identified cytosolic protein featuring ubiquitous expression (8, 6). PED/PEA-15 has been shown to exert antiapoptotic action through distinct mechanisms. First, PED/PEA-15 inhibits formation of the death-inducing signaling complex (DISC) and caspase 3 activation by different apoptotic cytokines including FASL, tumor necrosis factor alpha, and tumor necrosis factor-related apoptosis-inducing ligand (TRAIL) (7, 16, 22). At least in part, this action is accomplished through the death-effector-domain of PED/PEA-15 upon PED/PEA-15 recruitment to the DISC (7, 16, 22). Secondly, PED/PEA-15 inhibits the induction of different stress-activated protein kinases (SAPKs) triggered by growth factor deprivation, hydrogen peroxide, and anisomycin (5). This action of PED/PEA-15 is exerted by the blocking of an upstream event in the SAPK activation cascade (5) and requires the interaction of PED with ERK1/2 (14, 17).

PED/PEA-15 is phosphorylated at Ser<sub>116</sub> by calcium-calmodulin kinase II (CaMKII) (2) facilitating further phosphorylation by protein kinase C (PKC) at Ser<sub>104</sub> (23). Thus, PED/PEA-15 is present in the cell in the unphosphorylated (N), singly phosphorylated (Pa), and doubly phosphorylated (Pb) forms. Previous studies have shown that only the Pb form of PED/PEA-15 can be recruited to the DISC and inhibit TRAIL apoptotic signaling (31). In addition, the antiapoptotic action

of PED/PEA-15 requires PKC activity (7, 16, 22), indicating that, in the cell, PED/PEA-15 function is regulated by phosphorylation. However, whether kinases different from PKC and CaMKII may trigger survival or antiapoptotic signals by regulating PED/PEA-15 function is currently unknown.

Akt/PKB is a serine/threonine kinase that plays a major role in transducing proliferative and survival signals intracellularly (15, 21, 25). Akt/PKB has been demonstrated to phosphorylate a number of proteins involved in apoptotic signaling cascades, including the BCL2 family member BAD (12), the protease caspase 9 (4), the Forkhead transcription factor FRLH (3), and p21<sup>Cip</sup><sup>WAF1</sup> (24). Phosphorylation of these proteins prevents apoptosis through several different mechanisms. For instance, unphosphorylated BAD induces cell death by forming heterodimers with BCL-X<sub>L</sub> and generating BAX homodimers (12). Upon activation of Akt/PKB, phosphorylated BAD promotes cell survival by binding the 14-3-3 protein, which prevents BAD association to BCL-X<sub>L</sub> (12). At variance, in the case of p21<sup>Cip</sup><sup>WAF1</sup>, phosphorylation by Akt/PKB results in increased stability, promoting cell survival (24).

The finding that PED/PEA-15 possesses a low-stringency Akt/PKB phosphorylation consensus led us to analyze the possibility that PED/PEA-15 may also represent a relevant Akt/PKB substrate and that PED/PEA-15 phosphorylation by this kinase may regulate the antiapoptotic function of PED/PEA-15. In the present work we demonstrate that Akt, in addition to CaMKII, phosphorylates PED at Ser<sub>116</sub> in vitro and in vivo, regulating PED/PEA-15 function on cellular apoptosis. In part, Akt survival signaling may be mediated by PED/PEA-15.

\* Corresponding author. Mailing address: Dipartimento di Biologia e Patologia Cellulare e Molecolare, Università di Napoli Federico II, Via S. Pansini, 5, 80131 Naples, Italy. Phone: 39 081 7463248. Fax: 39 081 7463235. E-mail: beguino@unina.it.

## MATERIALS AND METHODS

**Materials.** Media, sera, and antibiotics for cell culture and the Lipofectamine reagent were purchased from Invitrogen Ltd. (Paisley, United Kingdom). Rabbit polyclonal Akt antibodies were from Santa Cruz Biotechnology (Santa Cruz, Calif.), and phosphokinase antibodies were from New England Biolabs Inc. (Beverly, Mass.). PED/PEA-15 antibodies have been previously reported (6). The HA-Akt, HA-Akt<sub>mΔ4-129</sub>, and HA-Akt<sub>K179M</sub> plasmids were donated by G. L. Condorelli (La Sapienza University of Rome) and have been previously reported (13), while recombinant Akt (rAkt) was purchased from Upstate Biotechnology Inc. (Lake Placid, N.Y.). Antisera against phospho-Serine<sub>116</sub> PED/PEA-15 (pSer<sub>116</sub> PED Ab) were prepared in rabbits by PRIMM (Milan, Italy) by using the PED/PEA-15 KLH-conjugated phosphopeptide NH<sub>2</sub>-CKDIIRQP(Sp)EEEEIKLAP-COOH. The specificity of this antiserum is shown in Fig. 2 in the present paper. The S<sub>70</sub> (HIFEISRRPDL), S<sub>104</sub> (LTRIPSAKKYKD), and S<sub>116</sub> (IIRQPSEIHK) PED/PEA-15 dodecapeptides were also synthesized by PRIMM. Sodium dodecyl sulfate-polyacrylamide gel electrophoresis (SDS-PAGE) reagents were purchased from Bio-Rad (Richmond, Va.). Western blotting and ECL reagents and radiochemicals were from Amersham (Arlington Heights, Ill.). All other reagents were from Sigma (St. Louis, Mo.).

**Plasmid preparation, cell culture, and transfection and apoptosis assays.** The PED<sub>S116-G</sub> and PED<sub>S104-G</sub> mutant cDNAs were prepared by using a pcDNA3PED/PEA-15 cDNA and the site-directed mutagenesis kit by Stratagene (Heidelberg, Germany) according to the kit manufacturer's instructions. Sequences were confirmed by the Sanger method with the T7 sequencing kit (Pharmacia-LKB, Milan, Italy). Stable expression of the mutant cDNAs in 293 cells was achieved as reported in reference 5. The 293 cells expressing the wild-type PED/PEA-15 cDNA have been described in reference 16. The cells were cultured in Dulbecco's modified Eagle's medium (DMEM) supplemented with 10% fetal calf serum, 100 IU of penicillin/ml, 100 IU of streptomycin/ml, and 2% L-glutamine in a humidified CO<sub>2</sub> incubator as reported in reference 5. Transient transfection of wild-type or mutant Akt cDNAs in these cells was accomplished by using the Lipofectamine method according to the manufacturer's instructions. Briefly, the cells were cultured in 60-mm-diameter dishes and incubated for 24 h in serum-free DMEM supplemented with 3 μg of cDNA and 15 μl of Lipofectamine reagent. An equal volume of DMEM supplemented with 20% fetal calf serum was then added for 5 h, followed by replacement with DMEM supplemented with 10% serum for 24 h before the assays. The U373MG human glioma cells were generously provided by G. Hao (University of Alberta, Edmonton, Canada). These cells were cultured and transfected as described in reference 16.

Apoptosis was quantitated by using the Apoptosis ELISA Plus kit (Roche Diagnostics GmbH, Mannheim, Germany) according to the manufacturer's instructions.

**Western blot analysis, PED/PEA-15 phosphorylation, and determination of Akt activity.** For Western blotting, the cells were solubilized in lysis buffer (50 mM HEPES [pH 7.5], 150 mM NaCl, 4 mM EDTA, 10 mM Na<sub>2</sub>PO<sub>7</sub>, 2 mM Na<sub>2</sub>VO<sub>4</sub>, 100 mM NaF, 10% glycerol, 1% Triton X-100, 1 mM phenylmethylsulfonyl fluoride, 100 mg of aprotinin/ml, 1 mM leupeptin) for 60 min at 4°C. Cell lysates were clarified at 5,000 × g for 15 min. Solubilized proteins were then separated by SDS-PAGE and transferred onto 0.45-μm-pore-size Immobilon-P membranes (Millipore, Bedford, Mass.). Upon incubation with the primary and secondary antibodies, immunoreactive bands were detected by ECL according to the manufacturer's instructions.

For studying phosphorylation of PED/PEA-15 in intact cells, 293 cells were transiently transfected with the different Akt constructs as indicated. After 24 h, the cells were rinsed with 150 mM NaCl, incubated in phosphate- and serum-free culture medium for 16 h at 37°C, and then further incubated for 8 h in this same medium supplemented with 200 μCi of [<sup>32</sup>P]orthophosphate/ml. Insulin (final concentration, 100 nM) was then added, and the cells were rapidly rinsed with ice-cold saline followed by solubilization with 0.5 ml of lysis buffer per dish for 1 h at 4°C. Lysates were centrifuged at 5,000 × g for 20 min, and solubilized proteins were precipitated with PED/PEA-15 antibodies, separated by SDS-PAGE, and revealed by autoradiography. In these assays, insulin action on PED phosphorylation was dose dependent, with half-maximal effect at 3 nM and maximal effect at 100 nM.

Akt activity was assayed *in vitro* as previously reported (11). Briefly, 293 cells expressing either the wild-type or the mutant PED/PEA-15 cDNAs were solubilized in lysis buffer and lysates were clarified by centrifugation at 5,000 × g for 20 min. Two hundred micrograms of the lysates were immunoprecipitated with Myc antibodies. The precipitates (or 2 μg of recombinant PED) were incubated in a kinase reaction mixture containing 20 mM HEPES [pH 7.2], 10 mM MgCl<sub>2</sub>, 10 mM MnCl<sub>2</sub>, 1 mM dithiothreitol, 5 mM ATP, 0.2 mM EGTA, 1 mM protein

kinase inhibitor, 10 μCi of [γ-<sup>32</sup>P]ATP, and 0.4 μg of rAkt or Akt or CaMKII immunoprecipitates, as indicated. Alternatively, rAkt was incubated in the kinase reaction mixture in the presence of 1 mM concentration of the S<sub>70</sub>, S<sub>104</sub>, or S<sub>116</sub> PED/PEA-15 dodecapeptides. Phosphorylation reactions were prolonged for 10 min, stopped by cooling on ice, and spotted on phosphocellulose disk papers. Disks were washed with 1% H<sub>3</sub>PO<sub>4</sub>, and disk-bound radioactivity was quantified by liquid scintillation counting. Alternatively, phosphorylated proteins were separated by SDS-PAGE and analyzed by autoradiography. The stoichiometry of PED phosphorylation by Akt and CaMKII was determined by allowing the reactions to proceed for 1 h at 30°C in the presence of excess kinase to saturate the reaction mixture. The number of moles of phosphate transferred per mole of recombinant PED was calculated based on a [γ-<sup>32</sup>P]ATP standard curve.

**PED/PEA-15-Akt interaction.** To investigate the interaction of PED/PEA-15 with Akt, PED/PEA-15-glutathione *S*-transferase (GST) fusion protein was generated. To this end, wild-type PED/PEA-15 cDNA was amplified by using the following two sets of primers: PED/PEA-15 5' *Eco*RI (5'-CCGGAATTCATGGTTGAGTACGGGACCCTC-3') and PED/PEA-15 3' *Sal*I (5'-GTCGACTCAGGCCTTCTCGGTGGGGGACC-3'). PED/PEA-15 cDNA was then cloned in the pGEX 4T1 plasmid, and the sequence was confirmed by using the T7 sequencing kit. Lysates from Akt-transfected cells (500 μg) or 0.4 μg of recombinant Akt were incubated in the presence of 50 μl of Sepharose-bound GST-PED/PEA-15 (approximately 2 μg) for 2 h at 4°C. Beads were washed four times with TNT buffer (0.5% NP-40, 25 mM TRIS [pH 7.5], 30 mM MgCl<sub>2</sub>, 40 mM NaCl, 1 mM dithiothreitol) and then resuspended in Laemmli buffer followed by boiling for 4 min and centrifugation at 25,000 × g for 3 min. Supernatants were analyzed by SDS-PAGE and blotting with Akt antibodies.

## RESULTS

**In vitro phosphorylation of PED/PEA-15 by Akt.** PED/PEA-15 sequence analysis revealed the presence of a low-stringency Akt phosphorylation motif including the Ser<sub>116</sub> residue of PED/PEA-15 (Fig. 1A). To verify the hypothesis that PED/PEA-15 is an Akt substrate, we first expressed the hemagglutinin (HA)-tagged wild-type Akt (AktWT), the constitutively active HA-Akt<sub>mΔ4-129</sub> (AktD+), and the inactive HA-Akt<sub>K179M</sub> mutant cDNAs (AktD-) in 293 human embryonic kidney cells, because these cells express no detectable levels of endogenous PED/PEA-15. HA antibody-precipitated Akt from these cells was then tested for its ability to phosphorylate His-tagged recombinant PED/PEA-15 *in vitro*. SDS-PAGE analysis of the phosphorylation mixtures revealed that wild-type Akt induced PED/PEA-15 phosphorylation (Fig. 1B). The constitutively active Akt induced fourfold-greater phosphorylation of PED/PEA-15 than did wild-type Akt. In contrast, precipitated inactive Akt or HA precipitates from cells transfected with the empty vector (PC) did not. Blotting with PED/PEA-15 and HA antibodies revealed that these variations were not due to differences in the amounts of either PED/PEA-15 or Akt in the assays. In addition, blotting with specific antibodies toward the key Akt Serine activation site (serine<sub>473</sub>; P-Akt) showed that the different phosphorylation levels of PED/PEA-15 closely paralleled the Akt activation state in each assay. Endogenous Akt precipitated from 293 cells upon stimulation with 100 nM insulin also induced a fivefold increase in PED/PEA-15 phosphorylation over the level observed with unstimulated cells (Fig. 1C). Again, blotting with PED/PEA-15, Akt-1, and phospho-Akt antibodies indicated that the changes in PED/PEA-15 phosphorylation reflected differences in the activation state of Akt rather than different amounts of Akt or PED/PEA-15 in the assays. PED was indeed phosphorylated by Akt with a stoichiometry of 0.82 mol of phosphate/mol of recombinant PED, a value close to that observed in the case of CaMKII

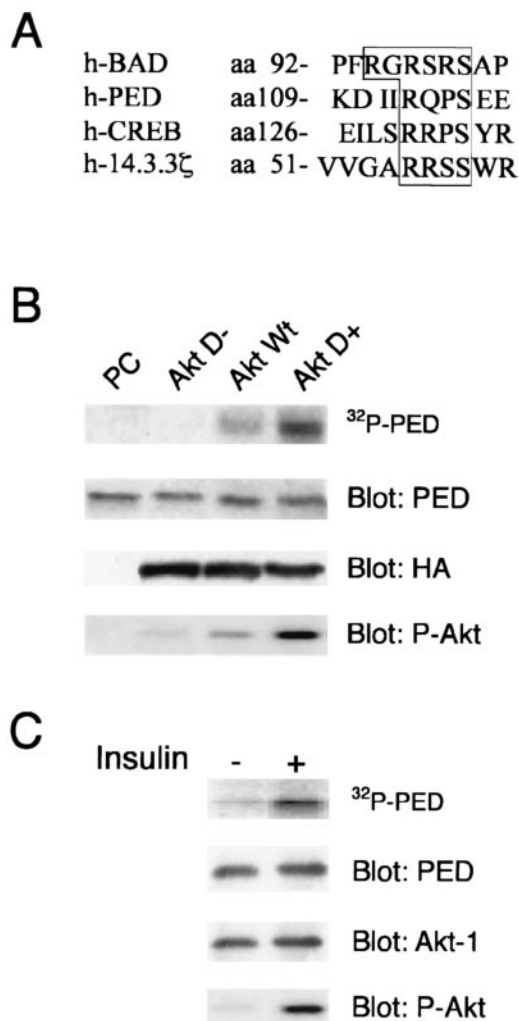


FIG. 1. In vitro phosphorylation of PED/PEA-15 by Akt (A) Partial amino acid sequence alignment of serine phosphorylation sites in Akt substrates. hBAD (29); hCREB (18, 30); h14.3.3.ζ (19, 27); hPED/PEA-15 (2). Sequences have been aligned to maximize the homology in the region upstream from the Ser<sub>116</sub> of PED/PEA-15. The single-letter amino acid code is used. (B) The HA-tagged wild-type Akt (Akt<sub>WT</sub>), constitutively active HA-Akt<sub>mΔ4-129</sub> (Akt<sub>D+</sub>), inactive HA-Akt<sub>K179M</sub> (Akt<sub>D-</sub>) mutant cDNAs, or the PcDNA3 empty vector (PC) was transfected in 293 cells. Cells maintained in the presence of 10% serum were solubilized, and cell lysates were precipitated with HA antibodies. Precipitated Akt was incubated with 2 μg of His-tagged recombinant PED/PEA-15 in the presence of 10 μCi of [ $\gamma$ -<sup>32</sup>P]ATP. The phosphorylation reaction was terminated with Laemmli buffer, and samples were subjected to SDS-PAGE and autoradiography. For control, the gels were also blotted with PED/PEA-15, HA, and Akt phosphoserine<sup>473</sup> antibodies (P-Akt), as indicated. (C) 293 cells were stimulated with 100 nM insulin for 10 min and solubilized as described in Materials and Methods, and lysates were immunoprecipitated with Akt1 antibodies. Precipitated Akt was incubated with recombinant PED/PEA-15, and PED/PEA-15 phosphorylation was assayed as described above. For control, the gels were blotted with PED/PEA-15, Akt-1, and P-Akt antibodies. The autoradiographs shown are representative of three (B) and four (C) independent experiments.

phosphorylation (0.87 mol of phosphate/mol of PED; the difference is not statistically significant).

#### Identification of PED/PEA-15 phosphorylation site by Akt.

To prove that the Ser<sub>116</sub> of PED/PEA-15 is phosphorylated by

Akt, we generated a cDNA mutant of PED/PEA-15 featuring the Ser<sub>116</sub>→Gly substitution. We then stably expressed the PED/PEA-15 Ser<sub>116</sub>→Gly cDNA and the wild-type PED/PEA-15 cDNA in 293 cells (293<sub>S116→G</sub> and 293<sub>PEDWT</sub> cells; three independent clones of cells expressing the mutant and four expressing the wild-type PED were selected and characterized in detail). For control, three independent clones of cells expressing a second mutant cDNA of PED/PEA-15, featuring the Ser<sub>104</sub>→Gly substitution, were also selected and used (PED<sub>S104→G</sub> cells; the Ser<sub>104</sub>→Gly mutation abolishes PED/PEA-15 phosphorylation by PKC [23]). Precipitates of these cells with PED/PEA-15 antibodies were phosphorylated by using HA precipitates from insulin-exposed cells expressing wild-type HA-Akt. In these assays, the Ser<sub>116</sub>→G mutant of PED/PEA-15 showed a fourfold-decreased phosphorylation by Akt compared to that of wild-type PED/PEA-15 (Fig. 2A). Phosphorylation of the Ser<sub>104</sub>→Gly mutant showed no significant difference from that of wild-type PED/PEA-15. In addition, blotting with antisera raised against a specific phosphoserine<sub>116</sub> PED/PEA-15 peptide showed a 15-fold-decreased phosphorylation of the Ser<sub>116</sub>→G compared to that of the Ser<sub>104</sub>→G PED mutant or the wild-type PED. Also, incubation of recombinant active Akt with same amounts of PED/PEA-15 precipitated from cells expressing either the wild-type or the S<sub>116</sub>→G mutant PED/PEA-15 cDNAs showed 10-fold-decreased phosphorylation of the PED/PEA-15 mutant compared to that of the wild-type (Fig. 2B). In this same assay, however, the active Akt phosphorylated the Ser<sub>104</sub>→Gly mutant of PED/PEA-15 at a level similar to that observed with wild-type PED/PEA-15. In vitro, the active Akt also phosphorylated twofold more effectively a synthetic dodecapeptide featuring the sequence of PED/PEA-15 surrounding Ser<sub>116</sub> (S<sub>116</sub> peptide) than a PED/PEA-15 dodecapeptide including Ser<sub>70</sub> (S<sub>70</sub> peptide; Fig. 2C). An additional PED/PEA-15 dodecapeptide including Ser<sub>104</sub> (S<sub>104</sub> peptide) was phosphorylated to a level similar to that of the S<sub>70</sub> peptide. Thus, in vitro, Akt phosphorylates PED/PEA-15 on Ser<sub>116</sub>.

**In vivo phosphorylation of PED by Akt.** We also examined the phosphorylation of PED/PEA-15 by Akt in intact 293<sub>PEDWT</sub> cells upon metabolic labeling with [<sup>32</sup>P]orthophosphate. Incubation of 293<sub>PEDWT</sub> cells with 100 nM insulin for 10 min stimulated PED/PEA-15 phosphorylation twofold above the basal level (Fig. 3A). Overexpression of similar levels of wild-type or active Akt cDNAs also increased phosphorylation of PED/PEA-15 1.8- and 3.2-fold, respectively. The same results were obtained with two further independent clones of 293<sub>PEDWT</sub> cells (not shown), indicating that, at least in part, insulin may induce PED/PEA-15 phosphorylation through Akt activation. Consistent with the role of Akt in insulin- and serum-stimulated phosphorylation of PED, preincubation of 293 cells with the phosphatidylinositol (PI) 3-kinase blockers Wortmannin or LY294002 inhibited insulin- as well as serum-stimulated phosphorylation of PED/PEA-15 by >70% (Fig. 3B). These decreases in phosphorylation of PED were accompanied by a decrease of similar size in phosphorylation of the key site of BAD by Akt.

Since Akt phosphorylates PED/PEA-15 at Ser<sub>116</sub> in vitro, we asked whether Ser<sub>116</sub> is also phosphorylated in intact cells. To answer this question, we compared PED/PEA-15 phosphorylation in the 293<sub>PEDWT</sub>, the 293<sub>S116→G</sub>, and the 293<sub>S104→G</sub>

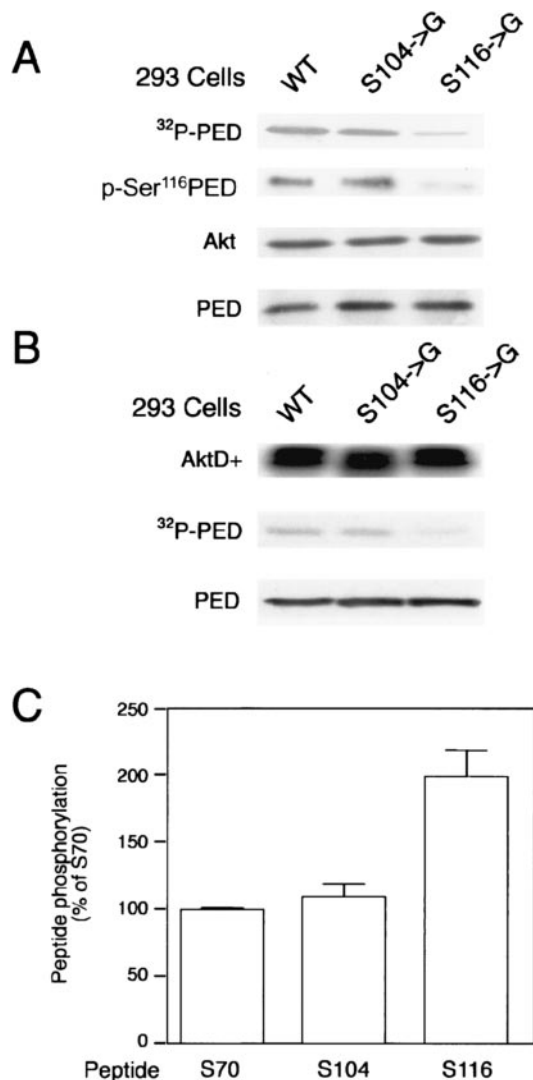


FIG. 2. Identification of the *in vitro* Akt phosphorylation site of PED/PEA-15. (A) 293 cells expressing the wild-type (WT), the Ser<sub>104</sub>→Gly or the Ser<sub>116</sub>→Gly PED/PEA-15 cDNAs were solubilized and precipitated with PED/PEA-15 antibodies. PED/PEA-15 precipitates were phosphorylated with Akt<sub>WT</sub> as outlined in the legend to Fig. 1, and samples were subjected to SDS-PAGE and autoradiography. For control, aliquots of the phosphorylation mixtures were also blotted with Akt, pSer<sub>116</sub> PED/PEA-15, or PED/PEA-15 antibodies as indicated. (B) Constitutively active Akt<sub>D+</sub> (recombinant; 0.5 μg) was incubated with PED/PEA-15 antibody precipitates from 293<sub>PEDWT</sub>, 293<sub>S104→G</sub>, and 293<sub>S116→G</sub> cells. Phosphorylation reactions were performed as outlined above, and samples were subjected to SDS-PAGE and autoradiography. To ensure equal amounts of Akt and PED/PEA-15 in each assay, aliquots of the samples were also blotted with Akt or PED/PEA-15 antibodies. The autoradiographs shown are representative of three (A) and four (B) independent experiments. (C) Synthetic dodecapeptides matching the sequence of PED/PEA-15 surrounding Ser<sub>70</sub>, Ser<sub>104</sub>, or Ser<sub>116</sub> (PEP70, PEP104, or PEP116, respectively) were incubated with recombinant Akt<sub>D+</sub> (0.5 μg). Phosphorylation reactions were initiated by addition of 10 μCi of [ $\gamma$ -<sup>32</sup>P]ATP and prolonged for 30 min. Peptide phosphorylation was then quantitated as described in Materials and Methods. Each bar represents the mean  $\pm$  standard deviation of five independent experiments. Based on *t* test analysis, the difference in phosphorylation of the PEP116 and those of the other peptides was significant at *P* values of <0.002.

cells upon expression of the constitutively active HA-Akt or insulin stimulation. As shown in Fig. 3C, PED/PEA-15 phosphorylation by active Akt was evident in the 293<sub>PEDWT</sub> and 293<sub>S104→G</sub> (3.2-fold increase) but not the 293<sub>S116→G</sub> cells. Insulin also increased PED/PEA-15 phosphorylation twofold and 40% in the 293<sub>PEDWT</sub> and the 293<sub>S104→G</sub> cells, respectively, but elicited only a slight 20% increase in the 293<sub>S116→G</sub> cells. In addition, Wortmannin preincubation of the cells almost completely inhibited insulin-stimulated phosphorylations of wild-type PED/PEA-15 and of the Ser<sub>104</sub>→Gly mutant but showed no effect on that of the Ser<sub>116</sub>→Gly mutant, indicating that the latter phosphorylation is independent of Akt. Blotting with phospho-Ser<sub>116</sub> PED antibodies revealed that wild-type PED underwent phosphorylation in cells transfected with wild-type Akt (upon insulin exposure) or with the active, but not the inactive, Akt (Fig. 3D). Importantly, insulin-induced phosphorylation of PED at Ser<sub>116</sub> was unaffected by cell preincubation with KN-93 and bisindolylmaleimide (BDM), which inhibit CaMKII and PKC, respectively. It appears therefore that Ser<sub>116</sub> represents the major Akt phosphorylation site of PED/PEA-15 in intact cells as well as *in vitro*.

**Action of Akt on PED function in 293 cells.** To further investigate the functional significance of Akt–PED/PEA-15 interaction, we first analyzed whether Akt directly binds PED/PEA-15. To this end, we incubated PED/PEA-15–GST fusion protein with either recombinant active Akt or lysates from cells expressing the constitutively active cDNA of Akt. Bound proteins were then pulled down and blotted with Akt antibodies. As shown in Fig. 4A, PED/PEA-15–GST bound both recombinant and transfected Akt. No Akt binding was evident upon incubation with GST alone. PED/PEA-15–GST did not bind to HA precipitates from cells expressing an HA–JNK-1 cDNA either, indicating specificity of the PED/PEA-15–Akt interaction (Fig. 4B). Based on overlay binding studies, PED/PEA-15 bound Akt and ERK1 with similar affinities (data not shown). Importantly, precipitation of 293<sub>PEDWT</sub> lysates with PED/PEA-15 antibodies followed by blotting with Akt antibodies, or vice versa, also revealed coprecipitation of PED/PEA-15 with Akt, indicating that Akt–PED/PEA-15 binding may occur in intact cells as well as *in vitro* (Fig. 4C). PED/PEA-15–GST incubation of extracts from cells expressing constitutively active, kinase-defective, and wild-type HA-Akt cDNAs followed by Akt blotting revealed that the mutant, the wild-type, and the endogenous Akt equally bound to PED/PEA-15 (Fig. 4D). Direct blotting of the cell extract with HA antibodies showed similar levels of transfected Akt in the cells. It appeared therefore that the formation of the PED/PEA-15–Akt complex is independent of Akt activity.

PED exerts a broad antiapoptotic action (5, 7, 16, 22). The finding that PED/PEA-15 binds and is phosphorylated by Akt led us to hypothesize that the antiapoptotic action of PED/PEA-15 may be contributed by activation of Akt signaling, or it may be regulated by phosphorylation by Akt, or both. To answer these questions, we compared the serum activation of Akt in the 293<sub>PEDWT</sub> cells with that in cells transfected with the empty plasmid (293<sub>PC</sub>). As shown in Fig. 5A, there was no difference between the phosphorylation levels of the key Akt serine activation sites in these two cell types. Also, BAD phosphorylation by Akt featured no difference in the 293<sub>PEDWT</sub> and the 293<sub>PC</sub> cells (Fig. 5B), indicating that Akt activity is not

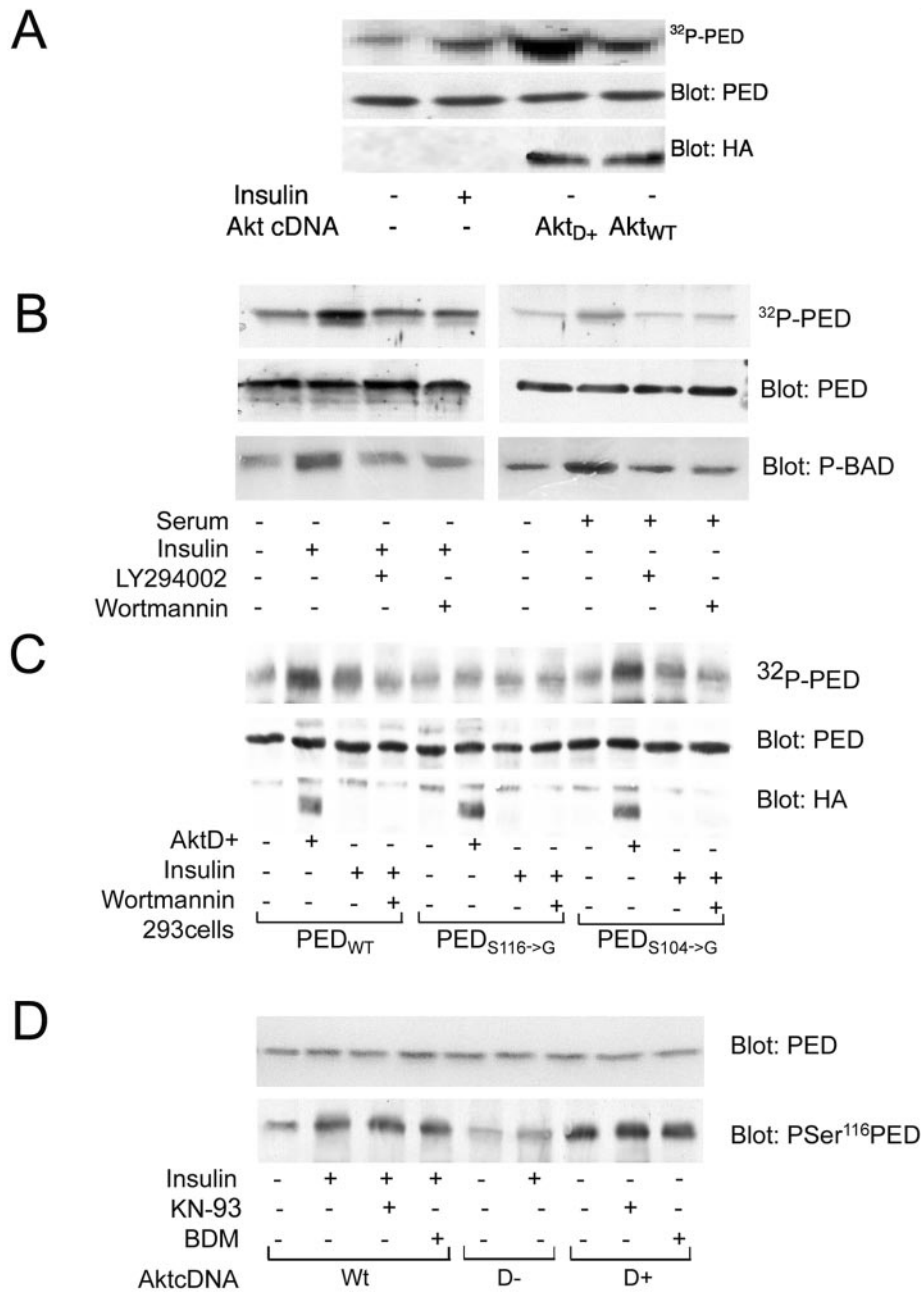


FIG. 3. PED/PEA-15 phosphorylation by Akt in intact cells. (A) The HA-tagged wild-type and constitutively active Akt (Akt<sub>WT</sub> and Akt<sub>D+</sub>, respectively) were transiently transfected in 293<sub>PEDWT</sub> cells. The cells were then labeled with [<sup>32</sup>P]orthophosphate and, when indicated, exposed to 100 nM insulin for 10 min. Cells were lysed and precipitated with PED/PEA-15 antibodies, and precipitated proteins were analyzed by SDS-PAGE and autoradiography. For control, aliquots of the samples were also blotted with PED/PEA-15 or HA antibodies. (B) 293<sub>PEDWT</sub> cells were labeled with [<sup>32</sup>P]orthophosphate, preincubated with 50 nM Wortmannin or 110 μM LY294002 for 30 min, and stimulated with either 100 nM insulin (left panel) or 10% serum (right panel) for a further 10 min. The cells were solubilized and immunoprecipitated with PED/PEA-15 antibodies, and precipitates were subjected to SDS-PAGE and autoradiography. For control, the gels were subsequently blotted with either PED/PEA-15 or phosphoBAD antibodies. (C) 293<sub>PEDWT</sub>, 293<sub>S116>G</sub>, and 293<sub>S104>G</sub> cells were transiently transfected with the active Akt<sub>D+</sub> cDNA (HA tagged) and labeled with [<sup>32</sup>P]orthophosphate. The cells were then incubated with 50 nM Wortmannin and further stimulated with insulin as indicated. Cell lysates were precipitated with PED/PEA-15 antibodies and analyzed by SDS-PAGE and autoradiography. For control, aliquots of the cell lysates were also blotted with PED/PEA-15 or HA antibodies. (D) 293<sub>PEDWT</sub> cells were transfected with the wild-type (WT), the constitutively active (D+) or inactive (D-) Akt, incubated with 50 μM KN-93 or 100 nM BDM, and then stimulated with 100 μM insulin as indicated. Cell lysates were blotted with pSer<sub>116</sub> PED/PEA-15 antibodies and, for control, reblotted with PED/PEA-15 antibodies. Filters were revealed by ECL and autoradiography. The autoradiographs shown are representative of three (A, B, and D) and four (C) independent experiments.

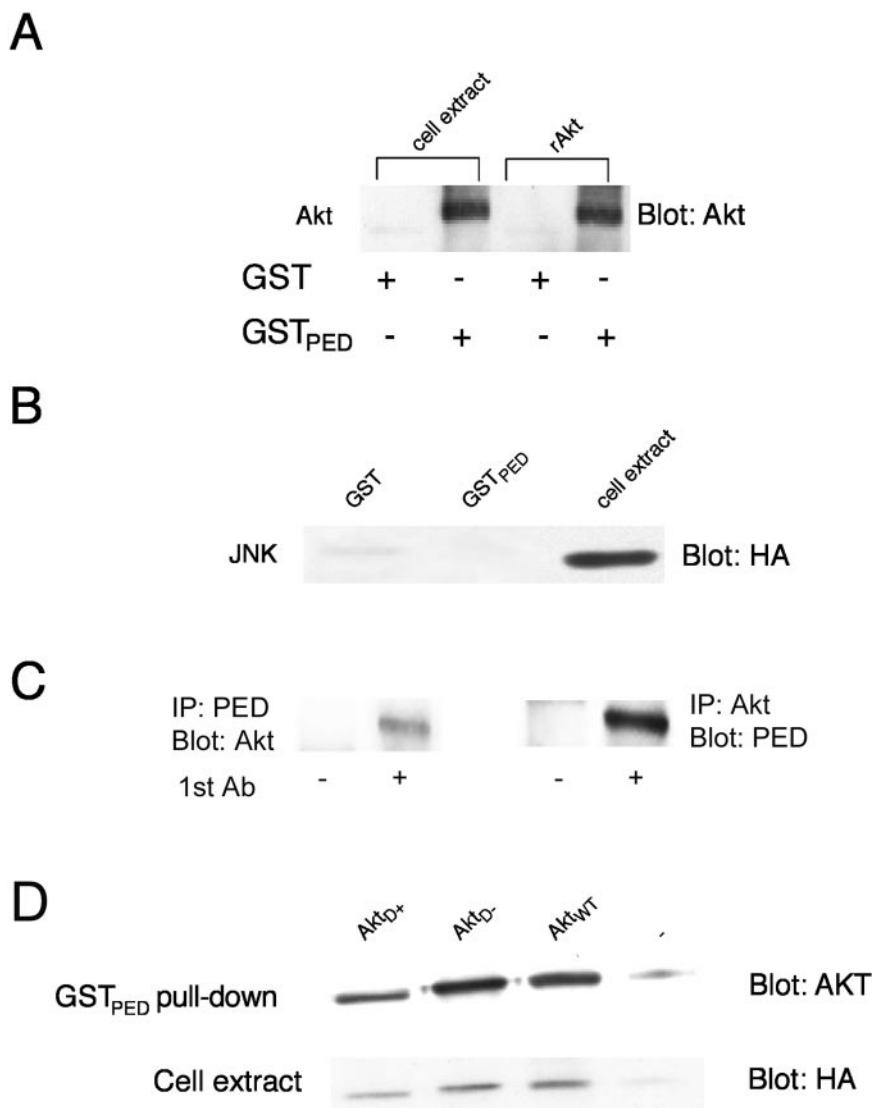


FIG. 4. In vitro interaction of PED/PEA-15 and Akt. (A) Lysates from  $293_{\text{PEDWT}}$  cells expressing the  $\text{Akt}_{\text{D}+}$  mutant (500  $\mu\text{g}$  of cell protein) and recombinant  $\text{Akt}_{\text{D}+}$  (rAkt; 0.4  $\mu\text{g}$ ) were incubated with agarose-bound GST-PED/PEA-15 or, for control, agarose-bound GST, as indicated. Pulled-down complexes were then analyzed by SDS-PAGE followed by Western blotting with Akt antibodies. Filters were revealed by ECL and autoradiography. (B) In parallel experiments,  $293_{\text{PEDWT}}$  cells were transiently transfected with HA-tagged JNK-1 cDNA. Cell lysates (500  $\mu\text{g}$  of protein) were incubated with agarose-bound GST-PED/PEA-15 or GST, as indicated, pulled-down, and analyzed by blotting with HA antibodies and autoradiography. (C)  $293_{\text{PEDWT}}$  cells were solubilized, and cell lysates were immunoprecipitated with either PED/PEA-15 or preimmune antisera followed by blotting with Akt antibodies (left panel). Alternatively, the lysates were precipitated with Akt or nonimmune antibodies followed by blotting with PED/PEA-15 antibodies. Filters were revealed by ECL and autoradiography. (D)  $293_{\text{PEDWT}}$  cells were transiently transfected with the HA-tagged active  $\text{Akt}_{\text{D}+}$ , inactive  $\text{Akt}_{\text{D}-}$ , or  $\text{Akt}_{\text{WT}}$  cDNAs as indicated. Cell lysates were analyzed by GST-PED/PEA-15 pull-down assays as outlined above. For control, aliquots of the cell extracts were also blotted with HA antibodies followed by ECL and autoradiography. The autoradiographs shown are representative of four (A) and three (B, C, and D) independent experiments.

affected by cellular levels of PED/PEA-15. We therefore investigated whether phosphorylation by Akt regulates the antiapoptotic function of PED/PEA-15. To this end, we compared the apoptosis induced by growth factor deprivation in untransfected 293 cells with the apoptosis induced in cells expressing comparable levels of wild-type or mutant PED/PEA-15. Consistent with previous findings (6), the expression of wild-type PED/PEA-15 resulted in a >2-fold decrease in apoptosis following serum deprivation compared to that observed for the 293 cells transfected with the empty vector ( $293_{\text{PC}}$  cells; Fig.

5C). But this protective effect was >60% less evident in cells expressing the nonphosphorylatable  $\text{S}_{116}\rightarrow\text{G}$  mutant of PED/PEA-15. In comparison, substitution of  $\text{Ser}_{104}\rightarrow\text{Gly}$  reduced PED/PEA-15 antiapoptotic function by only 35%. The levels of ERK activation by serum in cells expressing wild-type PED/PEA-15, in cells expressing mutant PED/PEA-15, and in untransfected 293 cells were not different (data not shown).

$293_{\text{PEDWT}}$  cells featured very low levels of apoptosis when maintained in the presence of serum. However, exposure of these cells to Wortmannin and BDM increased apoptosis nine-

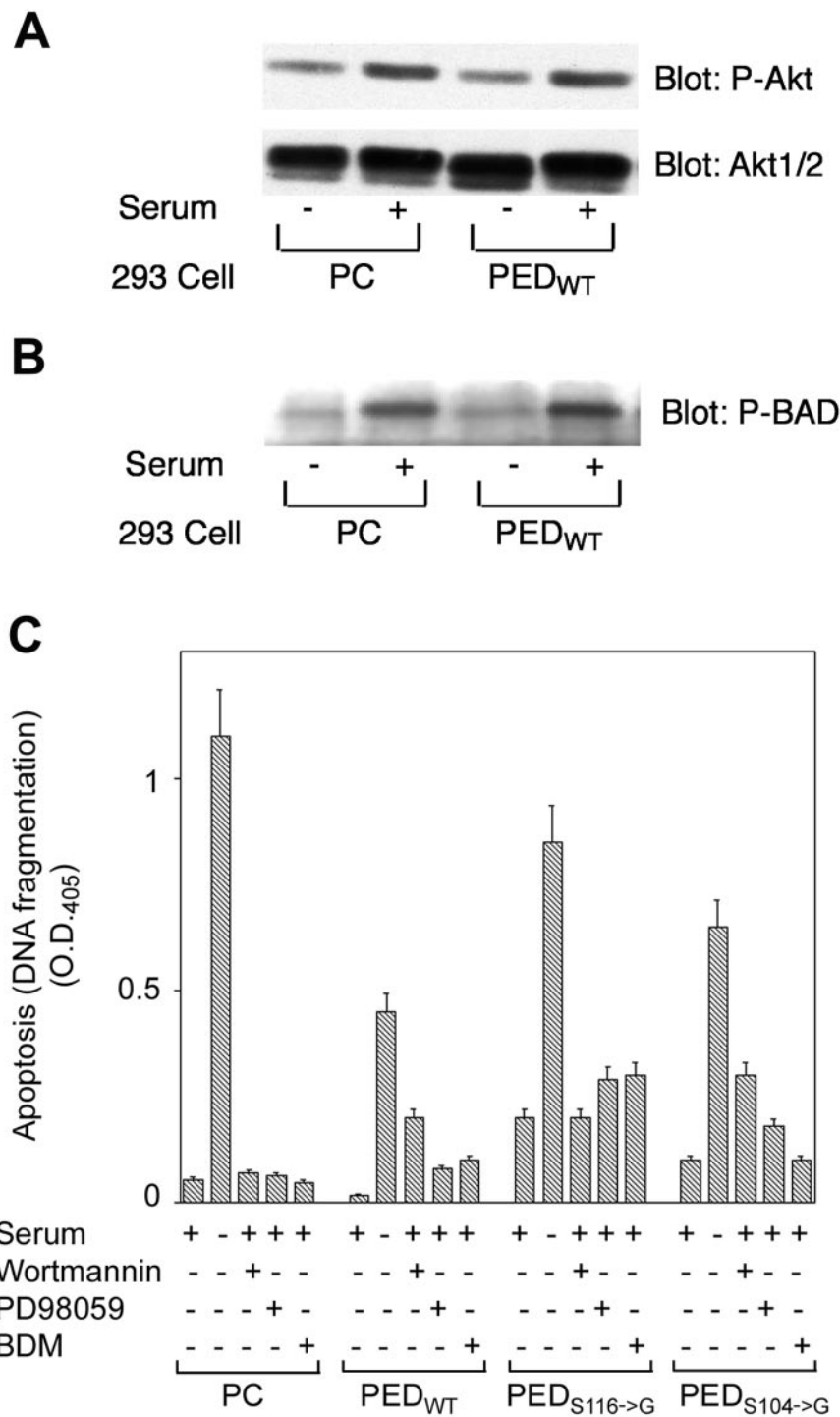


FIG. 5. Effects of phosphorylation by Akt on the antiapoptotic action of PED/PEA-15. (A) 293<sub>PEDWT</sub> and 293<sub>PC</sub> control cells were deprived of serum overnight, followed by 10% serum stimulation as indicated. The cells were solubilized, and cell lysates were subjected to SDS-PAGE followed by immunoblotting with Akt phosphoserine<sup>473</sup> antibodies (P-Akt). For control, aliquots of the lysates were also blotted with Akt1/2 antibodies. (B) Further aliquots of the cell lysates were blotted with phospho-BAD (P-BAD). Filters were revealed by ECL and autoradiography. The autoradiographs shown are representative of three (A) and four (B) independent experiments. (C) 293<sub>PC</sub>, 293<sub>PEDWT</sub>, 293<sub>S116->G</sub>, and 293<sub>S104->G</sub> cells were incubated in the presence or the absence of serum for 48 h. Cells were further incubated with 50 nM Wortmannin, 50 μM PD98059, or 100 nM BDM, as indicated. Apoptosis was quantitated by the ELISA Plus detection kit as described in Materials and Methods. Bars represent the means ± standard deviations from four duplicate experiments. Based on *t* test analysis, the difference in apoptosis following serum deprivation between the 293<sub>S116->G</sub> and 293<sub>PEDWT</sub> cells is significant at *P* values of <0.01. O.D.<sub>405</sub>, optical density at 405 nm.

and fivefold, respectively. According to previous observations in 293 cells (5), cell treatment with the MEK inhibitor PD98059 also induced an increase in apoptosis of almost fourfold. The effects of Wortmannin, PD98059, and BDM were more pronounced than in untransfected cells ( $P < 0.001$  by *t* test analysis), indicating an important role of PED/PEA-15 in their elicitation. The 293<sub>S116→G</sub> and 293<sub>S104→G</sub> cells exhibited, respectively, nine- and fivefold-higher basal rates of apoptosis compared to the 293<sub>PEDWT</sub> cells ( $P < 0.001$ ). Wortmannin had no further effect on apoptosis in the 293<sub>S116→G</sub> cells, whereas it increased the apoptosis in the 293<sub>S104→G</sub> cells threefold. In contrast, BDM slightly increased apoptosis in the 293<sub>S116→G</sub> cells (40%;  $P < 0.05$ ) but had no effect at all in those expressing the Ser<sub>104→G</sub> mutant. PD98059 increased apoptosis by 40% and twofold, respectively, in the 293<sub>S116→G</sub> and the 293<sub>S104→G</sub> cells. Thus, Akt as well as PKC phosphorylations exerted an important role in regulating PED function.

**Akt action on PED stability in 293 cells.** To elucidate the significance of phosphorylation by Akt for PED/PEA-15 function, we tested the possibility that Akt phosphorylation affects the half-life of PED/PEA-15 in the cells. We first compared the expression levels of wild-type PED/PEA-15 in cells maintained in the presence and in the absence of serum, when phosphorylation of the key Akt activation site is maximal and undetectable, respectively. As shown in Fig. 6A, PED/PEA-15 levels were fivefold higher in the cells exposed to serum than in the starved cells. Also, the effect of serum on the expression level of PED/PEA-15 was reduced threefold by Wortmannin, in parallel with the effect of serum on Akt phosphorylation. Very similar results were obtained in the presence of 100 nM insulin instead of serum (data not shown). More compelling, in the serum-starved cells, expression of the constitutively active Akt mutant resulted in PED/PEA-15 expression levels comparable to those measured in cells maintained in the presence of serum. In addition, both the effect of serum and that of the active Akt on PED/PEA-15 levels were absent in the 293<sub>S116→G</sub> cells, demonstrating the role of Akt phosphorylation in determining the intracellular levels of PED/PEA-15.

Next, we directly examined whether Akt phosphorylation may increase the stability of PED/PEA-15. We incubated 293<sub>PEDWT</sub> and 293<sub>S116→G</sub> cells with the protein synthesis inhibitor cycloheximide. We then compared the degradation rates of PED/PEA-15 in the two cell types. As shown in Fig. 6B, in the 293<sub>PEDWT</sub> cells, almost 50% of the initial levels of PED/PEA-15 were still present after 6 h of incubation with cycloheximide. The disappearance of PED/PEA-15 was much faster in the 293<sub>S116→G</sub> cells, since in these cells 50% of PED/PEA-15 levels became undetectable within only 1 h. Again, the difference in PED stability in the 293<sub>PEDWT</sub> and the 293<sub>S116→G</sub> cells was confirmed in two other clones of each cell line (data not shown). Earlier reports showed that PKC phosphorylation at Ser<sub>104</sub> depends on previous phosphorylation at Ser<sub>116</sub> (23). Thus, phosphoserine<sub>104</sub> might also contribute to PED stability. Accordingly, wild-type PED stability also decreased when PKC activity was blocked by BDM, although less evidently than with the Ser<sub>116→Gly</sub> mutant. Hence, upon treatment with BDM, 50% of the initial levels of wild-type PED were present after 3 h of incubation with cycloheximide. Consistent with the permissive role of Ser<sub>116</sub> phosphorylation on that of Ser<sub>104</sub> (23),

treatment with BDM caused only a slight further increase in the degradation rate of PED<sub>S116→G</sub>.

**Action of Akt on PED stability and function in human glioma cells.** To further address the significance of PED phosphorylation by Akt, we have blocked Akt activity in the U373MG human glioma cell line. These cells feature high levels of PED determining resistance to the apoptotic cytokine TRAIL (16, 31). Similar to what was observed with the 293 cells, in the U373MG glioma cells preincubation with either Wortmannin or LY294002 caused an 80% increase in apoptosis ( $P < 0.001$ ; Fig. 7). This induction of apoptosis was accompanied by a >3-fold decrease in PED phosphorylation at Ser<sub>116</sub> and in the cellular levels of PED (Fig. 7, top). Interestingly, both treatment with Wortmannin and treatment with LY294002 rescued sensitivity to TRAIL apoptosis. Wortmannin and LY294002 also reduced Akt activity as well as PED recruitment to TRAIL-induced DISC by >80% (data not shown), supporting the major role of this kinase in controlling the cellular function of PED in the glioma as well as in other cells.

## DISCUSSION

PED/PEA-15 is a recently identified protein featuring a broad antiapoptotic function (5, 7, 16, 22). PED/PEA-15 inhibits the apoptotic signal of FasL, tumor necrosis factor alpha, and TRAIL (7, 16, 22) and also blocks apoptosis following the activation of several SAPKs (6). Previous work in our own as well as in other laboratories has shown that phosphorylation by PKC plays an important role in enabling the antiapoptotic function of PED/PEA-15 (7, 16, 22). In the present paper we demonstrate that PED/PEA-15 phosphorylation by Akt also regulates PED/PEA-15 control of cell apoptosis.

We have shown that Akt phosphorylates PED/PEA-15 in vitro as well as in intact cells. PED/PEA-15 sequence analysis revealed a low-stringency Akt phosphorylation site, Ser<sub>116</sub>. Hence, in vitro, Akt phosphorylates the wild-type PED/PEA-15 but not a mutant PED/PEA-15 featuring the Ser<sub>116→Gly</sub> substitution. Akt also phosphorylates twofold more effectively a synthetic peptide featuring the sequence of PED/PEA-15 surrounding Ser<sub>116</sub> than two other equally sized PED/PEA-15 peptides including either Ser<sub>104</sub> or Ser<sub>70</sub>. In addition, active Akt does not phosphorylate the PED<sub>S116→G</sub> mutant when expressed in 293 cells, whereas it does phosphorylate wild-type PED/PEA-15. Finally, Western blotting studies with a specific phospho-Ser<sub>116</sub> PED/PEA-15 antiserum identified Ser<sub>116</sub> as the major Akt phosphorylation site of PED/PEA-15 in vivo and in vitro. Akt substrate serines are usually embedded in RRRXXS consensus sequences (1). In contrast, the 5-amino-acid region of PED/PEA-15 upstream from Ser<sub>116</sub> exhibits only a single Arg residue. The same structural feature has been reported for the Akt Ser substrates of CREB (10) and of the 14-3-3 $\zeta$  scaffold protein (27). In the case of PED/PEA-15, we showed that PED/PEA-15 directly binds to Akt. The binding is independent of Akt activity, as it effectively occurs to both constitutively active and inactive Akt mutants as well as to wild-type Akt. In addition, PED/PEA-15 binds Akt with an affinity similar to that exhibited for ERK1, a known PED/PEA-15 ligand (14, 17) (data not shown). It is possible, therefore,

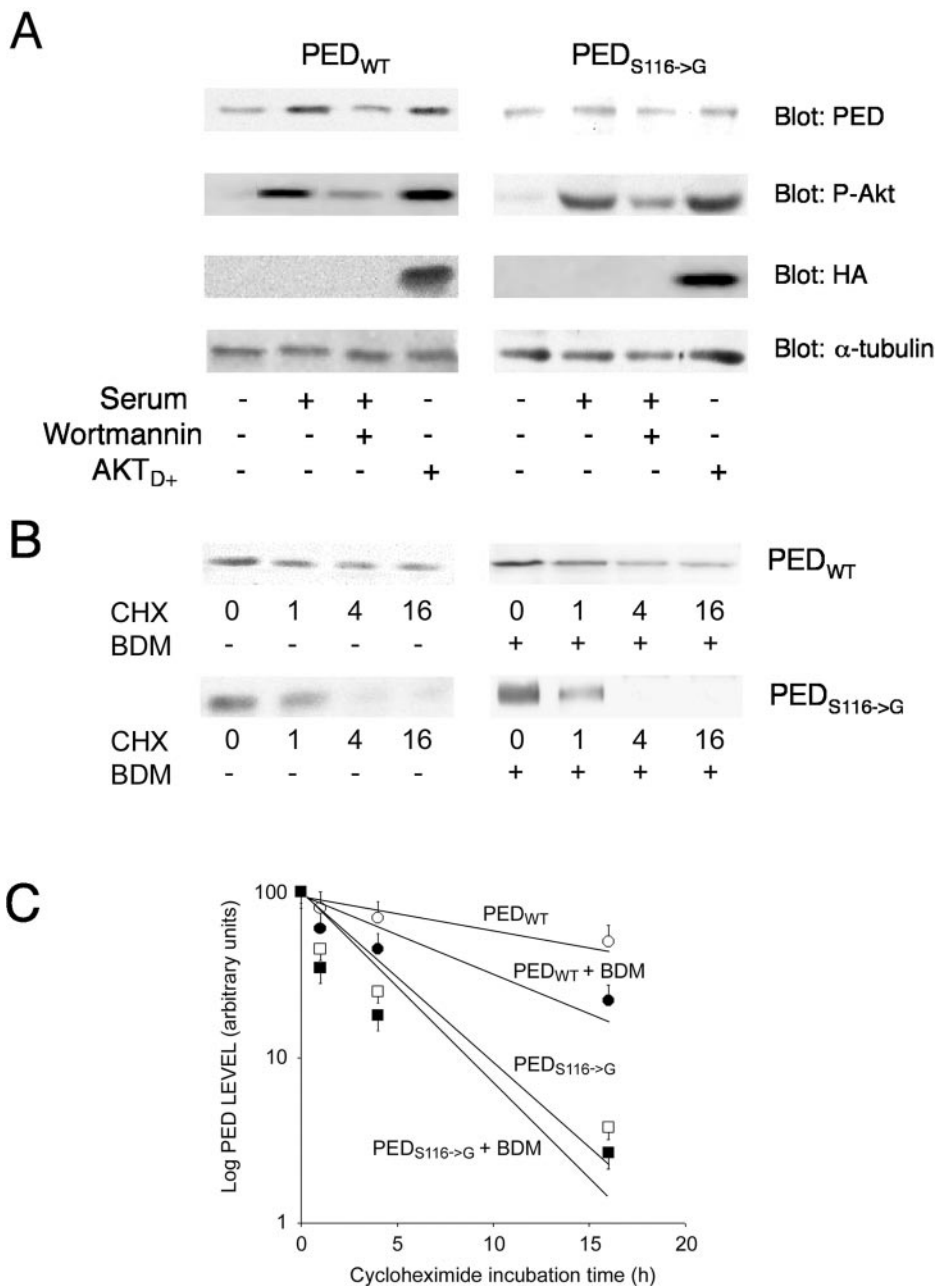


FIG. 6. Akt action on PED/PEA-15 stability in 293 cells. (A) 293<sub>PED<sub>WT</sub></sub> and 293<sub>PED<sub>S116-G</sub></sub> cells were transiently transfected with the active HA-Akt<sub>D+</sub> mutant as indicated. The cells were maintained in the absence or the presence of serum for 16 h. During the last 3 h of incubation, Wortmannin was added at a final concentration of 50 nM, as indicated. The cells were then solubilized and sequentially blotted with PED/PEA-15, P-Akt, HA, and α-tubulin antibodies. Filters were revealed by ECL and autoradiography. The autoradiograph shown is representative of three independent experiments. (B) Alternatively, 293<sub>PED<sub>WT</sub></sub> and 293<sub>PED<sub>S116-G</sub></sub> cells were deprived of serum for 14 h and then further incubated with 40 μg of cycloheximide/ml for the indicated times in the absence or the presence of 100 nM BDM. Cells were then solubilized, and 100 μg of cell proteins were subjected to SDS-PAGE followed by blotting with PED/PEA-15 antibodies, ECL, and autoradiography. (C) Autoradiographs were analyzed by laser densitometry. Each data point is the mean ± standard deviation of four independent experiments, one of which is shown in panel B.

that in the cell PED/PEA-15 recruits Akt and that this facilitates PED/PEA-15 phosphorylation by the kinase.

When expressed in 293 cells, the S<sub>116</sub>→G mutant PED/PEA-15 showed an almost twofold decrease in antiapoptotic function compared to wild-type PED/PEA-15. In 293 cells, PED inhibition of apoptosis requires PED activation of ERKs (5). However, reduced antiapoptotic function of the Ser<sub>116</sub>→G

mutant did not appear to depend on changes in its interaction with ERKs, as ERK activation levels were not different in cells expressing the mutant and in wild-type cells (data not shown). Interestingly, a pharmacological blocking of wild-type PED/PEA-15 phosphorylation at Ser<sub>116</sub> was accompanied by a significant increase in 293 cell apoptosis, even in the presence of serum. These findings suggest that, at least in the 293 cells,

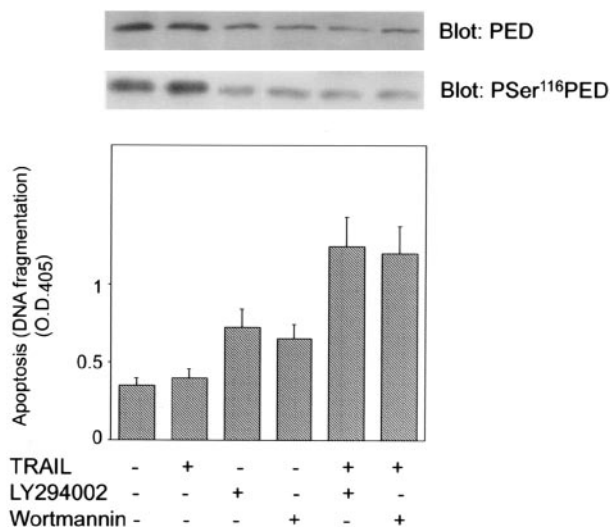


FIG. 7. Akt action on PED function in U373MG cells. U373MG cells were preincubated with 100  $\mu$ M LY294002 or 50 nM Wortmannin for 3 h and then exposed to 300 ng of TRAIL/ml, as indicated. Apoptosis was quantitated by evaluating the level of DNA fragmentation by using the ELISA Plus detection kit as described in Materials and Methods. Some of the cells were also solubilized and Western blotted with either PED/PEA-15 or pSer<sub>116</sub> PED/PEA-15 antibodies (top). Bars represent the means  $\pm$  standard deviations of duplicate determinations from three independent experiments.

PED may switch from an unphosphorylated proapoptotic form to a phosphorylated antiapoptotic form. Hence, expression of the Ser<sub>116</sub>→Gly mutant induces apoptosis, likely contributing to the reduced protection from apoptosis observed in 293PED<sub>S116→G</sub> compared to the 293<sub>PEDWT</sub> cells. Kubes et al. reported that endothelin-activated CaMKII also phosphorylates PED/PEA-15 at Ser<sub>116</sub> (23). Consistent with our findings, endothelin exerts antiapoptotic action in different cell types (9). It is unlikely that CaMKII serves as a downstream mediator of Akt action on PED/PEA-15 phosphorylation in the intact cell, as blocking of CaMKII does not inhibit Akt phosphorylation of PED/PEA-15 at Ser<sub>116</sub>. More likely, therefore, PED/PEA-15 represents a common target for multiple kinases transducing survival signals triggered by growth factors and cytokines, supporting an important role of PED/PEA-15 in the cellular regulation of apoptotic programs.

Earlier works indicated that PED/PEA-15 phosphorylation at Ser<sub>116</sub> facilitates subsequent phosphorylation by PKC at Ser<sub>104</sub>. In the present report, we show that the single substitution Ser<sub>104</sub>→G of PED/PEA-15 also reduced the antiapoptotic activity of PED/PEA-15, but only by 30%. These findings indicate that impaired phosphorylation at Ser<sub>104</sub> may account, in part, for reducing PED/PEA-15 antiapoptotic action when phosphorylation of Ser<sub>116</sub> is disabled. Consistent with this possibility, blocking of PKC only slightly increased apoptosis in 293<sub>S116→G</sub> cells.

Despite the relevance of phosphorylation at Ser<sub>116</sub>, other factors seemed to be involved in regulating PED/PEA-15 antiapoptotic function in 293 cells. Hence, apoptosis induced by serum starvation was less in cells expressing the S<sub>116</sub>→G mutant than in cells expressing no PED/PEA-15 at all. Akt regu-

lation of PED function is not unique to the 293 cells, however. In fact, we report that blocking of Akt in human glioma cells expressing high levels of PED/PEA-15 simultaneously decreases PED/PEA-15 phosphorylation at Ser<sub>116</sub> and rescues sensitivity to the apoptotic cytokine TRAIL.

Akt regulates a number of cellular functions including cell survival (25). Different substrates are phosphorylated by Akt and converted into survival proteins (3, 4, 12, 24). This function, in turn, is accomplished by regulating protein-protein interaction (12), by affecting protein localization (3) or protein stability (24). In the present work, we show that Akt phosphorylation increases the stability of PED/PEA-15 in the cell. Hence, PED/PEA-15 levels are low in cells subjected to serum starvation, when Akt activity is inhibited, and in cells subjected to pharmacological blocking of the PI 3-K/Akt pathway. PED/PEA-15 cellular levels increase upon expression of a constitutively active Akt mutant. In addition, we report that the S<sub>116</sub>→G PED/PEA-15 mutant features reduced stability compared to that of wild-type PED/PEA-15. At variance with wild-type PED/PEA-15, the S<sub>116</sub>→G mutant is unaffected by Akt. Thus, at least in part, Akt regulates PED protein stability and antiapoptotic function by phosphorylating PED/PEA-15 at Ser<sub>116</sub>. PED/PEA-15 degradation is blocked by treatment of the cells with the proteasome inhibitor lactacystin, suggesting that PED/PEA-15 intracellular levels are regulated by the ubiquitin pathway (data not shown). Whether this hypothesis holds and whether PED/PEA-15 ubiquitination is, in turn, inhibited by Akt phosphorylation is currently being investigated in our laboratory.

The PED/PEA-15 gene is amplified in human breast cancer (20) as well as in other tumors and PED/PEA-15 overexpression may have a role in skin carcinogenesis (S. Santopietro and J. Portella, personal communication). Akt is also upregulated in a number of human cancers (26, 28, 29). In this work, we demonstrated that PED/PEA-15 is a substrate for Akt and obtained evidence that Akt phosphorylation and stabilization of PED/PEA-15 is a previously unrecognized mechanism involved in Akt survival signaling. Simultaneous increases in PED/PEA-15 cellular levels and Akt activity might function cooperatively in tumorigenesis and/or tumor progression in humans.

#### ACKNOWLEDGMENTS

This work was supported in part by the European Community (grant QLRT-1999-00674 to F.B. [EUDG program]), grants from the Associazione Italiana per la Ricerca sul Cancro (AIRC) to F.B. and P.F., and the Ministero dell'Università e della Ricerca Scientifica. The financial support of Telethon—Italy is gratefully acknowledged.

Alessandra Trencia and Anna Perfetti contributed equally to this work.

#### REFERENCES

1. Alessi, D. R., F. B. Caudwell, M. Andjelkovic, B. A. Hemmings, and P. Cohen. 1996. Molecular basis for the substrate specificity of protein kinase B; comparison with MAPKAP kinase-1 and p70 S6 kinase. *FEBS Lett.* **399**: 333–338.
2. Araujo, H., N. Danzinger, J. Cordier, J. Glowinski, and H. Chneiweiss. 1993. Characterization of PEA-15, a major substrate for protein kinase C in astrocytes. *J. Biol. Chem.* **268**:5911–5920.
3. Brunet, A., A. Bonni, M. J. Zigmond, M. Z. Lin, P. Juo, L. S. Hu, M. J. Anderson, K. C. Arden, J. Blenis, and M. E. Greenberg. 1999. Akt promotes cell survival by phosphorylating and inhibiting a Forkhead transcription factor. *Cell* **96**:857–868.
4. Cardone, M. H., N. Roy, H. R. Stennicke, G. S. Salvesen, T. F. Franke, E.

- Stanbridge, S. Frisch, and J. C. Reed. 1998. Regulation of cell death protease caspase-9 by phosphorylation. *Science* **282**:1318–1321.
5. Condorelli, G., A. Trencia, G. Vigliotta, A. Perfetti, U. Goglia, E. Autori, A. Cassese, A. Musti, C. Miele, S. Santopietro, P. Formisano, and F. Beguinot. 2002. Multiple members of the mitogen-activated protein kinase family are necessary for PED/PEA-15 anti-apoptotic function. *J. Biol. Chem.* **277**:11013–11018.
  6. Condorelli, G., G. Vigliotta, C. Iavarone, M. Caruso, C. G. Tocchetti, F. Andreozzi, M. F. Tecce, A. Cafieri, P. Formisano, L. Beguinot, and F. Beguinot. 1998. PED/PEA-15 gene controls glucose transport and is overexpressed in type 2 diabetes mellitus. *EMBO J.* **17**:3858–3865.
  7. Condorelli, G., G. Vigliotta, C. Iavarone, A. Trencia, P. Andalò, F. Oriente, C. Miele, M. Caruso, P. Formisano, and F. Beguinot. 1999. PED/PEA-15: an anti-apoptotic molecule that regulates FAS/TNFR1-induced apoptosis. *Oncogene* **18**:4409–4415.
  8. Danzinger, N., M. Yokohama, T. Jay, J. Cordier, J. Glowinski, and H. Chneiweiss. 1995. Cellular expression, developmental regulation, and phylogenetic conservation of PEA-15, the astrocytic major phosphoprotein and protein kinase C substrate. *J. Neurochem.* **64**:1016–1025.
  9. Del Bufalo, D., V. Di Castro, A. Biroccio, M. Varmi, D. Salani, L. Rosano, D. Triscioglio, F. Spinella, and A. Bagnato. 2002. Endothelin-1 protects ovarian carcinoma cells against paclitaxel-induced apoptosis: requirement for Akt activation. *Mol. Pharmacol.* **61**:524–532.
  10. Du, K., and M. Montminy. 1998. CREB is a regulatory target for the protein kinase Akt/PKB. *J. Biol. Chem.* **273**:32377–32379.
  11. Dudek, H., S. R. Datta, T. F. Franke, M. Brinbaum, R. Yao, G. M. Cooper, R. A. Segal, D. R. Kaplan, and M. E. Greenberg. 1997. Regulation of neuronal survival by the serine-threonine protein kinase Akt. *Science* **275**:661–665.
  12. Dudek, H., S. R. Datta, X. Tao, S. Masters, H. Fu, Y. Gotoh, and M. E. Greenberg. 1997. Akt phosphorylation of BAD couples survival signals to the cell-intrinsic death machinery. *Cell* **91**:231–241.
  13. Eves, E. M., W. Xiong, A. Bellacosa, S. G. Kennedy, P. N. Tschlis, M. R. Rosner, and N. Hay. 1998. Akt, a target of phosphatidylinositol 3-kinase, inhibits apoptosis in a differentiating neuronal cell line. *Mol. Cell. Biol.* **18**:2143–2152.
  14. Formstecher, E., J. W. Ramos, M. Fauquet, D. A. Calderwood, J. C. Hsieh, B. Canton, X. T. Nguyen, J. V. Barnier, J. Camonis, M. H. Ginsberg, and H. Chneiweiss. 2001. PEA-15 mediates cytoplasmic sequestration of ERK MAP kinase. *Dev. Cell* **1**:239–250.
  15. Franke, T. F., D. R. Kaplan, L. C. Cantly, and A. Tokar. 1997. Direct regulation of the Akt proto-oncogene product by phosphatidylinositol-3,4-bisphosphate. *Science* **275**:665–668.
  16. Hao, C., F. Beguinot, G. Condorelli, A. Trencia, H. T. Chen, E. G. Van Meir, V. W. Yong, I. F. Parney, W. H. Roa, and K. C. Petruk. 2001. Induction and intracellular regulation of tumor necrosis factor-related apoptosis-inducing ligand (TRAIL) mediated apoptosis in human malignant glioma cells. *Cancer Res.* **61**:1–9.
  17. Hill, J. M., H. Vaidyanathan, J. W. Ramos, M. H. Ginsberg, and M. H. Werner. 2002. Recognition of ERK MAP kinase by PEA-15 reveals a common docking site within the death domain and death effector domain. *EMBO J.* **21**:6494–6504.
  18. Hoeffler, J. P., T. E. Meyer, Y. Yun, J. L. Jameson, and J. F. Habener. 1988. Cyclic AMP-responsive DNA-binding protein: structure based on a cloned placental cDNA. *Science* **242**:1430–1433.
  19. Honda, R., Y. Ohba, and H. Yasuda. 1997. 14-3-3 zeta protein binds to the carboxyl half of mouse wee1 kinase. *Biochem. Biophys. Res. Commun.* **230**:262–265.
  20. Hwang, S., W. Kuo, J. F. Cochran, R. C. Gurman, T. Tsukamoto, G. Bandyopadhyay, K. Mambo, and C. C. Collins. 1997. Assignment of HMAT1, the human homolog of the murine mammary transforming gene (MAT1) associated with tumorigenesis, to 1q21.1, a region frequently gained in human breast cancers. *Genomics* **42**:540–542.
  21. Khwaja, A., S. Rodriguez-Viciana Wennstrom, P. H. Warne, and J. Downward. 1997. Matrix adhesion and Ras transformation both activate a phosphoinositide 3-OH kinase and protein kinase B/Akt cellular survival pathway. *EMBO J.* **16**:2783–2793.
  22. Kitsberg, D., E. Formstecher, M. Fauquet, M. Kubes, J. Cordier, B. Canton, G. Pan, M. Rolli, J. Glowinski, and H. Chneiweiss. 1999. Knock-out of the neural death effector domain protein PEA-15 demonstrates that its expression protects astrocytes from TNFalpha-induced apoptosis. *J. Neurosci.* **19**:8244–8251.
  23. Kubes, M., J. Cordier, J. Glowinski, J. A. Girault, and H. Chneiweiss. 1998. Endothelin induces a calcium-dependent phosphorylation of PEA-15 in intact astrocytes: identification of Ser104 and Ser116 phosphorylated, respectively, by protein kinase C and calcium/calmodulin kinase II in vitro. *J. Neurochem.* **71**:1303–1314.
  24. Li, Y., D. Dowbenko, and L. A. Lasky. 2002. AKT/PKB phosphorylation of p21Cip/WAF1 enhances protein stability of p21Cip/WAF1 and promotes cell survival. *J. Biol. Chem.* **277**:11352–11361.
  25. Marte, B. M., and J. Downward. 1997. PKB/Akt: connecting phosphoinositide 3-kinase to cell survival and beyond. *Trends Biochem. Sci.* **22**:355–358.
  26. Nicholson, K. M., and N. G. Anderson. 2002. The protein kinase B/Akt signalling pathway in human malignancy. *Cell Signal.* **14**:381–395.
  27. Powell, D. W., M. J. Rane, Q. Chen, S. Singh, and K. R. McLeish. 2002. Identification of 14-3-3zeta as a protein kinase B/Akt substrate. *J. Biol. Chem.* **277**:21639–21642.
  28. Testa, J. R., and A. Bellacosa. 2001. AKT plays a central role in tumorigenesis. *Proc. Natl. Acad. Sci. USA* **98**:10983–10985.
  29. Vivano, I., and C. L. Sawyers. 2002. The phosphatidylinositol 3-kinase AKT pathway in human cancer. *Nat. Rev. Cancer* **2**:489–502.
  30. Wang, H. G., U. R. Rapp, and J. C. Reed. 1996. Bcl-2 targets the protein kinase Raf-1 to mitochondria. *Cell* **87**:629–638.
  31. Xiao, C., B. F. Yang, N. Asadi, F. Beguinot, and C. Hao. 2002. Tumor necrosis factor-related apoptosis-inducing ligand-induced death-inducing signaling complex and its modulation by c-FLIP and PED/PEA-15 in glioma cells. *J. Biol. Chem.* **277**:25020–25025.

## Overexpression of the *ped/pea-15* Gene Causes Diabetes by Impairing Glucose-Stimulated Insulin Secretion in Addition to Insulin Action

Giovanni Vigliotta,<sup>1,2†‡</sup> Claudia Miele,<sup>1,2†</sup> Stefania Santopietro,<sup>1,2</sup> Giuseppe Portella,<sup>1,2</sup>  
Anna Perfetti,<sup>1,2</sup> Maria Alessandra Maitan,<sup>1,2</sup> Angela Cassese,<sup>1,2</sup> Francesco Oriente,<sup>1,2</sup>  
Alessandra Trencia,<sup>1,2</sup> Francesca Fiory,<sup>1,2</sup> Chiara Romano,<sup>1,2</sup> Cecilia Tiveron,<sup>3</sup>  
Laura Tatangelo,<sup>3</sup> Giancarlo Troncone,<sup>4</sup> Pietro Formisano,<sup>1,2</sup>  
and Francesco Beguinot<sup>1,2\*</sup>

*Dipartimento di Biologia e Patologia Cellulare e Molecolare*<sup>1</sup> and *Dipartimento di Scienze Biomorfologiche e Funzionali*,<sup>4</sup>  
*Federico II University of Naples, and Istituto di Endocrinologia ed Oncologia Sperimentale del CNR*,<sup>2</sup> *Naples, and*  
*Transgenic Mouse Service Center, Istituto Regina Elena, Rome*,<sup>3</sup> *Italy*

Received 14 November 2003/Returned for modification 24 January 2004/Accepted 7 March 2004

**Overexpression of the *ped/pea-15* gene is a common feature of type 2 diabetes. In the present work, we show that transgenic mice ubiquitously overexpressing *ped/pea-15* exhibited mildly elevated random-fed blood glucose levels and decreased glucose tolerance. Treatment with a 60% fat diet led *ped/pea-15* transgenic mice to develop diabetes. Consistent with insulin resistance in these mice, insulin administration reduced glucose levels by only 35% after 45 min, compared to 70% in control mice. In vivo, insulin-stimulated glucose uptake was decreased by almost 50% in fat and muscle tissues of the *ped/pea-15* transgenic mice, accompanied by protein kinase C $\alpha$  activation and block of insulin induction of protein kinase C $\zeta$ . These changes persisted in isolated adipocytes from the transgenic mice and were rescued by the protein kinase C inhibitor bisindolylmaleimide. In addition to insulin resistance, *ped/pea-15* transgenic mice showed a 70% reduction in insulin response to glucose loading. Stable overexpression of *ped/pea-15* in the glucose-responsive MIN6 beta-cell line also caused protein kinase C $\alpha$  activation and a marked decline in glucose-stimulated insulin secretion. Antisense block of endogenous *ped/pea-15* increased glucose sensitivity by 2.5-fold in these cells. Thus, in vivo, overexpression of *ped/pea-15* may lead to diabetes by impairing insulin secretion in addition to insulin action.**

Type 2 diabetes is a genetically determined disorder, affecting over 150 million people worldwide (35). The pathogenesis of type 2 diabetes is characterized both by insulin resistance in muscle, fat, and liver and by impaired insulin secretion (10, 16). Whether a single genetic defect may simultaneously cause impaired insulin action and secretion in common forms of human diabetes and by what mechanism are unknown.

PED/PEA-15 is a ubiquitously expressed multifunctional protein. It controls mitogenic signaling by binding extracellular signal-regulated kinases and anchoring them to the cytoplasm (14). PED/PEA-15 also inhibits several apoptotic pathways through a number of different mechanisms and plays an important role in tumor development and sensitivity to antineoplastic agents (5, 6, 11, 15, 30, 34). Recently, PED/PEA-15 was reported to bind to and increase the cellular stability of phospholipase D, enhancing its activity in the cell (8, 35). In addition, we showed that overexpression of the *ped/pea-15* gene is a common defect in type 2 diabetes (7). Overexpression of PED/PEA-15 protein impairs insulin-stimulated GLUT4 translocation and glucose transport in cultured muscle and adipose cells, suggesting that *ped/pea-15* overexpression may contribute to insulin resistance in type 2 diabetics (7).

Other studies have demonstrated that *ped/pea-15*-induced resistance to insulin action on glucose disposal is accompanied by activation of the classical protein kinase C (PKC) isoform PKC $\alpha$  (8). In turn, the induction of PKC $\alpha$  by *ped/pea-15* overexpression prevents subsequent activation of atypical PKC $\zeta/\lambda$  by insulin (8). Rescue of PKC $\zeta/\lambda$  function in *ped/pea-15*-overexpressing cells restores glucose transport to its normal sensitivity to insulin. Thus, in cultured muscle and adipose cells, *ped/pea-15* generates resistance to insulin action on glucose disposal by impairing normal regulation of PKC $\zeta/\lambda$  function by PKC $\alpha$ . Accumulating evidence now indicates that the atypical PKCs  $\zeta$  and  $\lambda$  are major downstream effectors activating the glucose transport machinery in response to insulin in both skeletal muscle and adipose tissues (12). Activation of atypical PKCs by insulin is defective in humans with type 2 diabetes as well as in animal models of type 2 diabetes (12, 17, 18). It therefore appears that atypical PKCs are key molecules in the pathogenesis of type 2 diabetes and may represent important drug targets as well.

Defective insulin secretion in response to secretagogues also plays an important role in the pathogenesis of type 2 diabetes (24). At least in part, this further abnormality appears to be genetically determined (2, 33). However, metabolic abnormalities determined by insulin resistance also contribute to beta-cell failure in type 2 diabetes (2, 24, 33). In the present report, we show that overexpression of *ped/pea-15* to levels similar to those found in many type 2 diabetics may lead to diabetes in transgenic mice. This defect is accompanied by defective insulin action on glucose transport and, additionally, by impaired

\* Corresponding author. Mailing address: Dipartimento di Biologia e Patologia Cellulare e Molecolare, Università di Napoli Federico II, Via Sergio Pansini, 5, Naples 80131, Italy. Phone: 39081 7463248. Fax: 39081 7463235. E-mail: beguino@unina.it.

† G.V. and C.M. contributed equally to this work.

‡ Present address: Dipartimento di Scienze e Tecnologie Biologiche ed Ambientali, University of Lecce, Lecce, Italy.

glucose-stimulated insulin secretion. Thus, overexpression of the *ped/pea-15* gene may cause diabetes by impairing beta-cell function in addition to insulin sensitivity.

## MATERIALS AND METHODS

**Generation of *ped/pea-15* transgenic mice.** *ped/pea-15* cDNA (7) was cloned in the BamHI sites of plasmid pBap2, containing the human beta-actin promoter. To generate transgenic mice, the 5.2-kb ClaI fragment was excised, purified by agarose gel electrophoresis, and injected into pronuclei of C57BL/6J × DBA/2J mouse embryos. Three F<sub>0</sub> founders were identified by Southern blot analysis of genomic DNA by probing with the PstI fragment of the human β-actin promoter.

To establish transgenic lines, founder mice were mated with BDF1 mice. Heterozygous transgenic mice were subsequently identified by Southern blotting with either the ClaI fragment or the PCR amplification product of the fragment obtained with primers 5'-CGCGATCCATGCTGAGTACGGGACCCTC-3' and 5'-GGCCTTCTTCGGTGGGGGAGCCAATTTGATGATCTCTCTCCTC A-3'; by Northern blotting with the ClaI fragment; and by Western blotting with polyclonal rabbit antibodies against PED/PEA-15 protein (7). Three lines (L1, L61, and L30) overexpressing PED/PEA-15 protein were established. Animals were kept in a 12-h dark-light cycle and fed standard or chow with a 60 kcal% fat content (Research Diets formulae D12328 and D12331, respectively; Research Diets, Inc., New Brunswick, N.J.) ad libitum. All procedures described below were approved by the Institutional Animal Care and Utilization Committee.

**Phenotypic analysis.** Blood glucose levels were measured with glucometers (Accu-check; Boehringer Mannheim), plasma insulin was measured by enzyme immunoassays (ultrasensitive mouse insulin enzyme-linked immunosorbent assay; Mercordia AB, Uppsala, Sweden), fasting plasma free fatty acids were measured with the Wako NEFA C kit (Wako, Richmond, Va.), and triglycerides were measured with the Infinity triglyceride reagent (Sigma, St. Louis, Mo.).

**Insulin tolerance tests.** Random-fed mice were subjected to intraperitoneal injection with insulin (0.75 mU g of body weight<sup>-1</sup>). Venous blood was subsequently drawn by tail clipping at 0, 15, 30, 45, 60, 90, and 120 min after insulin injection to determine blood glucose levels.

**Glucose tolerance tests and insulin secretion.** Mice were fasted overnight and then injected with glucose (2 g kg of body weight<sup>-1</sup>) intraperitoneally. Venous blood glucose was drawn by tail clipping at 0, 15, 30, 45, 60, 90, and 120 min without re-clipping of the tails. We also measured plasma insulin concentrations at 2, 5, 15, and 30 min.

**In vivo tissue glucose transport during glucose tolerance tests.** 2-Deoxy-D-[1,2-<sup>3</sup>H]glucose (Amersham) was mixed with 20% glucose and then injected intraperitoneally (2 mg kg of body weight<sup>-1</sup>; 10 μCi/mouse) into weight-matched mice. Blood samples were obtained from the tail veins at 0, 15, 30, 45, 60, 90, and 120 min, and glucose concentrations were determined. The glucose specific activity was determined as described before (37). At 120 min, mice were killed and tissues were snap frozen in liquid nitrogen. To determine tissue accumulation of 2-deoxyglucose-6-phosphate, 100 to 500 mg of tissue was homogenized in 2 ml of distilled water, and 1.6 ml of the homogenate was transferred to 1.6 ml of 7% ice-cold perchloric acid. The sample was centrifuged to remove precipitated protein, and 2.5 ml of the supernatant was neutralized for 30 min with 625 μl of 2.2 M KHCO<sub>3</sub>. The precipitate was removed by centrifugation, and the supernatant was divided into 800-μl aliquots. One aliquot was used to determine total <sup>3</sup>H radioactivity, and another was passed through an AG 1-X8 anion exchange resin column (Bio-Rad, Hercules, Calif.) to remove labeled 2-deoxyglucose-phosphate. The column was washed with 3 ml of distilled water, and the radioactivity in the eluted volume was measured in a scintillation counter. The difference between total and eluted <sup>3</sup>H radioactivity represents accumulated 2-deoxy-D-[1,2-<sup>3</sup>H]glucose-6-phosphate. The protein pellet was digested for 20 min at 55°C with 1 N KOH, and the protein concentration was determined by the Bradford assay (Bio-Rad, Hercules, Calif.). To calculate 2-deoxyglucose uptake, the radioactivity was divided by the integrated glucose specific activity area under the curve and the sample protein content.

**Tissue collection and immunoblotting.** Tissue samples (tibialis and soleus muscles and subcutaneous and perigonadal adipose tissues) were collected rapidly after mice were sacrificed by pentobarbitone overdose. Tissues were snap frozen in liquid nitrogen and stored at -80°C for subsequent Western blotting, biochemical assays of PKC activity, and diacylglycerol levels. Tissue samples were homogenized in a Polytron (Brinkman Instruments, Westbury, N.Y.) in 100 mg of buffer A per ml according to the method of Qu et al. (26). After centrifugation at 3,000 × g, the supernatant was centrifuged at 200,000 × g for 90 min to pellet the crude membrane and cytosolic fractions. Further purifications to obtain the plasma membrane fractions were achieved as described by Uphues et al. (32).

Ouabain-sensitive Na<sup>+</sup>/K<sup>+</sup> ATPase was used as a marker enzyme for plasma membranes, and activity was determined as described by Russ et al. (29).

Membranes recovered from the 0.72 M sucrose layer were 12-fold enriched in the activity of the Na<sup>+</sup>/K<sup>+</sup> ATPase and considered to represent the plasma membrane fraction. Preparation of total tissue lysates was achieved by homogenization in TAT buffer (4). Total homogenates and plasma membrane fractions were subjected to sodium dodecyl sulfate-polyacrylamide gel electrophoresis (SDS-PAGE) with 10% gels, as described by Laemmli (21). Proteins separated on the gels were electroblotted onto nitrocellulose filters as described before (8) and probed with antibodies to GLUT4, PKC (Santa Cruz Biotech Inc., Santa Cruz, Calif.), PLD (BioSource International, Camarillo, Calif.) phospho-Akt (Ser473) (Cell Signaling Technology, Inc., Beverly, Mass.), or Akt (Upstate Biotechnology, Lake Placid, N.Y.).

**Determination of PKC and phosphatidylinositol 3-kinase activities.** For determination of PKCα activity, tissues and cells were homogenized in TAT buffer, followed by immunoprecipitation with specific PKCα antibodies. PKC activity in the immunoprecipitates was then assayed as described by Condorelli et al. (8). Alternatively, for assaying phosphatidylinositol 3-kinase, tissue homogenates were precipitated with phosphotyrosine antibodies coupled to protein A-Sepharose, and phosphatidylinositol 3-kinase activity in the immunoprecipitates was determined as described by Filippa et al. (13).

**Lipid extraction and diacylglycerol measurement.** Muscle and adipose tissues and cells were powdered under liquid nitrogen and then extracted in 1:2 (vol/vol) chloroform-methanol as described by Turinsky et al. (31). *sn*-1,2 Diacylglycerol was determined with the diacylglycerol kinase assay of Preiss et al. (25). [ $\gamma$ -<sup>32</sup>P]phosphatidic acid was separated by thin-layer chromatography on Silica Gel-60 plates (Merck) as described previously (31). The plates were developed in chloroform-methanol-acetic acid (65:15:5, vol/vol/vol), and the positions of the spots corresponding to [ $\gamma$ -<sup>32</sup>P]phosphatidic acid were determined by autoradiography. Radioactivity in the spots was determined by liquid scintillation counting.

**Cell culture procedures and transfection.** MIN6 cells were cultured in Dulbecco's modified Eagle's medium (Life Technologies, Karlsruhe, Germany) containing 25 mM glucose, 50 μM 2-mercaptoethanol, and 10% fetal calf serum (Biochrom, Hamburg, Germany) at 37°C in a 5% CO<sub>2</sub> atmosphere (23). For insulin secretion experiments, cells were seeded into 96-well plates at a density of 3 × 10<sup>4</sup> cells per well. Three days after plating, the cells were washed with Earle's balanced salt solution containing 0.1% bovine serum albumin (Sigma). After starvation for 1 h in the same salt solution, the cells were incubated with either 0.1 or 16.7 mM glucose, as indicated, for 1 additional hour. The cell supernatant was filtered through Multiscreen MAVN filter plates (Millipore, Eschborn, Germany) and stored at -20°C until the insulin determination was performed.

*ped/pea-15* antisense (5'-TGACGCCTCCGGAGCTGAGA-3') and scrambled (5'-GGCAATTTTCGAGCGGCACGC-3') oligonucleotides were synthesized by PRIMM (Milan, Italy). The *ped/pea-15* expression vector has been reported (7). Transfection of *ped/pea-15* cDNA and antisense DNAs was performed as described previously (15).

Adipocytes were isolated from epididymal fat pads by collagenase digestion, as described previously (28). The number of adipocytes isolated was adjusted to 10<sup>6</sup> cells/ml of suspension, and 2-deoxyglucose uptake was measured as described previously (6).

**Immunohistochemical analysis.** Pancreas from transgenic and control animals were fixed in 4% paraformaldehyde-0.1 M sodium phosphate buffer at 4°C overnight and placed in 30% sucrose at 4°C overnight. After being embedded in Tissue-Tek OTC compound and frozen at -20°C, tissue sections were prepared. Immunohistochemical analysis was carried out with the H38 rabbit insulin antibody (Santa Cruz Biotechnology, Inc.; 1:200 dilution), the N-17 goat glucagon antibody (Santa Cruz Biotechnology, Inc.; 1:200 dilution), or PED/PEA-15 antiserum (7) (1:20,000 dilution). Incubation with the primary antibody was followed by incubation with biotinylated anti-rabbit or anti-goat immunoglobulin G and peroxidase-labeled streptavidin. Analysis of serial consecutive islet sections stained with either insulin or the PED/PEA-15 antibodies was used to confirm *ped/pea-15* expression in insulin-immunopositive beta cells.

**Statistical procedures.** Data were analyzed with Statview software (Abacus-concepts) by one-factor analysis of variance. *P* values of less than 0.05 were considered statistically significant. The total area under the curve for glucose response during the insulin tolerance test was calculated by the trapezoidal method.

## RESULTS

**Generation of transgenic mice overexpressing *ped/pea-15*.** To investigate the relevance of *ped/pea-15* overexpression to

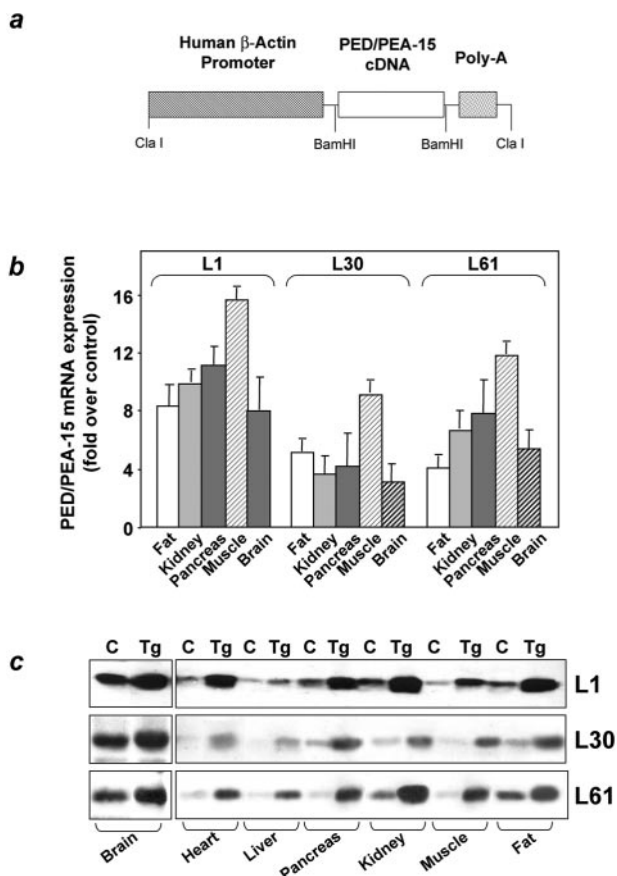


FIG. 1. Generation of *ped/pea-15* transgenic mice. a. Subcloning of the *ped/pea-15* cDNA in the BamHI sites of plasmid pBap2 containing the  $\beta$ -actin promoter. Tissues from *ped/pea-15* transgenic mice (Tg) and their nontransgenic littermates (C) were collected as described under Materials and Methods and subjected to Northern (b) or Western (c) blotting. Northern blots (25  $\mu$ g of RNA/lane) were probed with *ped/pea-15* cDNA as reported (6). Loading of the same amount of RNA in each lane was ensured by further blotting for  $\beta$ -actin. Quantitation of the blots was performed by densitometric analysis. Data are plotted as increase of *ped/pea-15* mRNA expression in transgenic versus control mice. Bars represent the means  $\pm$  standard deviation of comparisons in five transgenic and five nontransgenic animals. For Western blotting, tissues from control and transgenic mice (L1, L30, and L6 lines) were solubilized, and lysates (100  $\mu$ g of protein/lane) were blotted with PED/PEA-15 antiserum (6), followed by chemiluminescence and autoradiography. Three representative experiments are shown.

glucose tolerance, we used the  $\beta$ -actin promoter to generate transgenic mice overexpressing human *ped/pea-15* (*hped/pea-15*) ubiquitously, as *ped/pea-15* overexpression frequently occurs in type 2 diabetes (7) (Fig. 1a). Three lines of mice (L1, L61, and L30) were established in which *ped/pea-15* RNA as well as *ped/pea-15* protein featured a 5 to 20-fold increased expression in fat, in skeletal and in cardiac muscles, three major targets of insulin action (Fig. 1b and c). Transgenic mice were fertile and generated viable offspring showing no significant growth alterations compared to control mice or other apparent abnormalities. L1 *ped/pea-15* transgenic mice also exhibited normal fasting glucose levels (Fig. 2a). However, random-fed blood glucose levels were mildly elevated in the

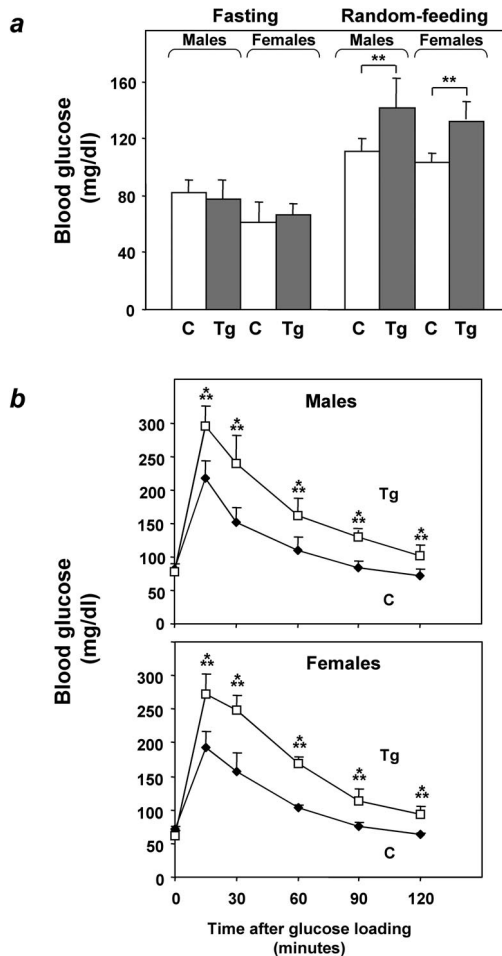


FIG. 2. Glucose tolerance in *ped/pea-15* transgenic mice. (a) *ped/pea-15* transgenic mice (Tg) and their nontransgenic littermates (C) were either fasted for 12 h or fed ad libitum (random feeding). Blood glucose levels were then determined as described under Materials and Methods. Bars represent the mean  $\pm$  standard deviation of determinations in at least 10 mice in each group. The differences in fasting glucose levels between transgenic and control mice were not statistically significant. Alternatively (b), whole-blood glucose was determined at 0 to 120 min after intraperitoneal glucose injection (2 mg  $\text{kg}^{-1}$ ) of age-matched male (top panel) and female (bottom panel) transgenic and control mice after overnight fasting. Values are expressed as mean  $\pm$  standard deviation for at least 12 mice in each group. Asterisks denote statistically significant differences (\*\*,  $P < 0.01$ ; \*\*\*,  $P < 0.001$ ).

transgenic ( $145 \pm 40$  and  $138 \pm 28$  mg/dl in male and female mice, respectively) versus the nontransgenic littermates ( $115 \pm 37$  and  $103 \pm 18$  mg/dl in males and females, respectively). The difference between transgenic and control mice was significant ( $P < 0.01$ ). In addition, glucose loading (2 mg  $\text{kg}^{-1}$ ) rendered the transgenic mice significantly hyperglycemic for the following 120 min. (Fig. 2b and c), indicating decreased glucose tolerance in *ped/pea-15* transgenic mice. Almost identical abnormalities were observed in L61 and L30 transgenic mice (data not shown). As shown in Fig. 2, gender had no effect on the impairment in glucose tolerance caused by overexpression of *ped/pea-15*. Aging (3 to 12 months) also determined no

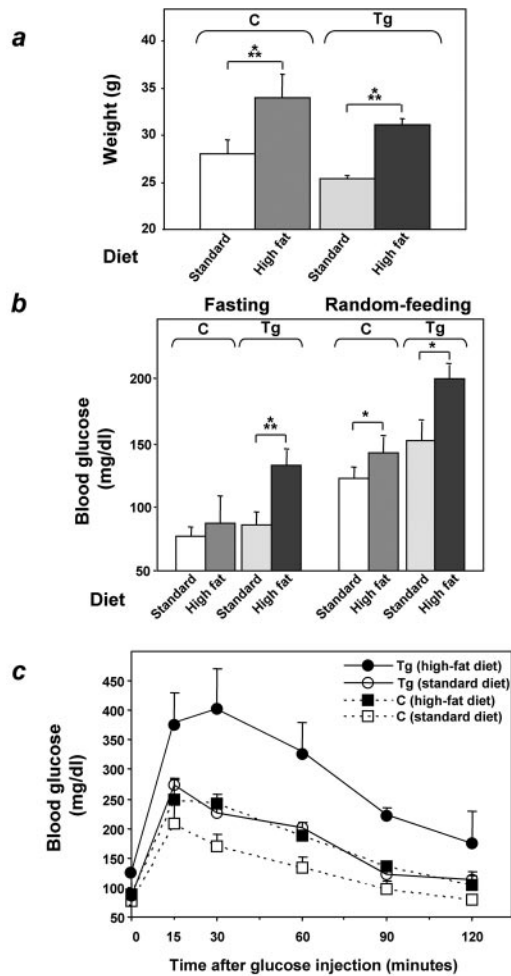


FIG. 3. Effect of high-fat feeding on glucose tolerance in *ped/pea-15* transgenic mice. Three-month-old female transgenic (Tg) and control (C; nontransgenic littermates) mice were fed either standard (10% fat) or 60% fat diets for 10 weeks. Animals were then weighed (a), and blood glucose levels were determined (b) after overnight fasting and in random-fed animals. Bars represent the mean  $\pm$  standard deviation of values from at least 10 mice in each group. The differences in fasting blood glucose levels in control mice treated with standard or high-fat diets were not statistically significant. Asterisks denote statistically significant differences (\*,  $P < 0.05$ ; \*\*\*,  $P < 0.001$ ). Alternatively (c), glucose tolerance was compared in weight-matched female transgenic and control animals (at least 10 animals/group) subjected to the two different diets, as outlined in the legend to Fig. 2. Differences in blood glucose levels after high-fat diet treatment were significant at  $P < 0.001$  (transgenic mice) and  $P < 0.06$  (control mice).

significant changes in *ped/pea-15*-induced decreases in glucose tolerance (data not shown).

Feeding L1 *ped/pea-15* transgenic mice and their nontransgenic littermates a 60% fat diet for 10 weeks led to a 25% increased body weight compared to the standard 10% fat diet ( $P < 0.001$ ; Fig. 3a). This increase in body weight caused only slight elevations of both fasting and random-fed blood glucose levels in nontransgenic animals (Fig. 3b). Glucose levels during tolerance tests were only moderately increased in nontransgenic mice after high-fat diet feeding (Fig. 3c). In *ped/pea-15* transgenic mice, increased body weight was accompanied by a

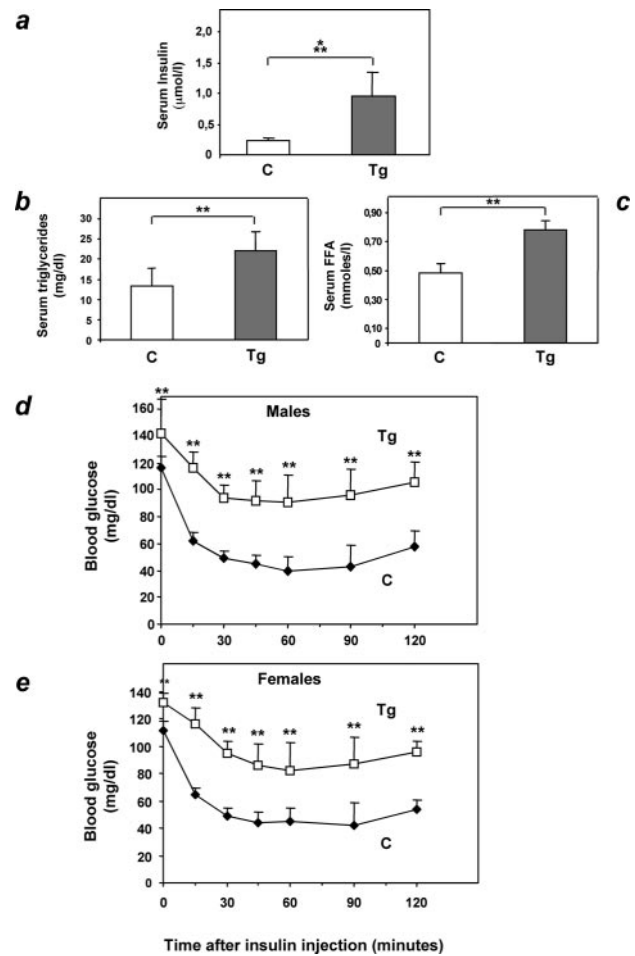


FIG. 4. Insulin sensitivity in *ped/pea-15* transgenic mice. Three-month old female *ped/pea-15* transgenic mice and age-matched nontransgenic littermates (16 per group) were fasted for 12 h, followed by determination of insulin (a), triglycerides (b), and free fatty acid (c) levels in plasma as described under Materials and Methods. Bars represent the mean  $\pm$  standard deviation of duplicate determinations in each animal. Differences between transgenic and control mice were significant at  $P < 0.001$  (serum insulin) and  $P < 0.01$  (serum free fatty acids and triglycerides). Alternatively, random-fed male (d) or female (e) mice ( $n = 12/\text{group}$ ) were injected intraperitoneally with insulin ( $0.75 \text{ mU g}^{-1}$ ), followed by determinations of blood glucose levels at the indicated times. Values are expressed as mean  $\pm$  standard deviation of duplicate determinations in each animal. Asterisks denote statistically significant differences ( $P < 0.01$ ).

significant elevation in both fasting and random-fed blood glucose levels ( $138 \pm 20$  and  $204 \pm 38$ , respectively, versus  $68 \pm 32$  and  $124 \pm 40$ , respectively, in control mice;  $P < 0.001$ ). Moreover, as shown by glucose loading, the high-fat diet further and severely deteriorated glucose tolerance in the *ped/pea-15* transgenic mice, indicating that, in vivo, overexpression of *ped/pea-15* in conjunction with environmental modifiers may lead to diabetes. Gender had no significant effect on these diet-induced abnormalities in *ped/pea-15* transgenic mice (data not shown).

**Effect of *ped/pea-15* overexpression on insulin sensitivity.** Female L1 *ped/pea-15* transgenic mice featured a 10-fold increase in fasting insulin levels compared to control animals

(Fig. 4a;  $P < 0.001$ ). Fasting nonesterified free fatty acid and triglyceride blood concentrations in *ped/pea-15* transgenic mice were also increased by 47 and 65%, respectively, suggesting the presence of insulin resistance in these animals (Fig. 4b and c;  $P < 0.01$ ). Almost identical differences were present in male mice (data not shown). To address the effect of *ped/pea-15* overexpression on insulin sensitivity, we performed insulin tolerance tests. In control animals, intraperitoneal injection of insulin ( $0.125 \text{ mU g}^{-1}$ ) caused a severe and sustained drop in random-fed blood glucose levels (Fig. 4d and e). This decrease achieved a maximum (70%;  $P < 0.001$ ) after 45 min and was maintained for a further 45 min. At variance, insulin reduced glucose levels by only 40% after 45 min in *ped/pea-15* transgenic mice, whether male or female. This smaller reduction was followed by a progressive rescue of the initial blood glucose concentration over the next 45 min. The same differences were observed in transgenic mice of the L30 and L61 lines and in control animals (data not shown).

In cultured cells, *ped/pea-15* overexpression causes resistance to insulin action on glucose uptake (7). We therefore asked whether *ped/pea-15* overexpression also impairs insulin stimulation of the glucose transport machinery in vivo. We compared glucose uptake in perigonadal and subcutaneous fat and in the tibialis and soleus muscles in L1 *ped/pea-15* transgenic and in control mice. A 50% decrease in glucose uptake was observed in perigonadal and subcutaneous fat (Fig. 5a; the difference from control animals significant at the  $P < 0.001$  and  $P < 0.01$  levels, respectively). Also, glucose uptake in the tibialis and soleus muscles from transgenic animals was decreased by 43 and 37%, respectively, compared to the nontransgenic mice (Fig. 5b;  $P < 0.05$ ). Glucose uptake was similarly reduced in both female and male transgenic mice (data not shown). Thus, insulin resistance in peripheral tissues might provide an important contribution to the impaired glucose tolerance of *ped/pea-15* transgenic mice. In parallel with the decreased glucose uptake, GLUT4 membrane translocation in response to insulin and feeding was also significantly decreased in tibialis muscles and perigonadal adipose tissues from *ped/pea-15* transgenic mice (Fig. 5c). This abnormality was accompanied by no significant change in the total GLUT4 levels in transgenic muscle or adipose tissues.

**PKC signaling in *ped/pea-15* transgenic mice.** To address the molecular mechanism responsible for these abnormalities, we measured PKC $\alpha$  activity in immunoprecipitates from lysates of transgenic and control tissues. PKC $\alpha$  activity was constitutively increased in adipose tissue from fasted transgenic mice (Fig. 6a). In addition, there was little further activation in the random-fed state in these animals, even upon insulin injection. At variance with the *ped/pea-15* transgenic mice, PKC $\alpha$  activity increased by twofold in the fed state in the nontransgenic mice. In addition, in these mice, insulin further increased PKC $\alpha$  activity up to 2.5-fold above fasting levels.

The differences in PKC $\alpha$  activity between transgenic and control mice were accompanied by parallel changes in phosphorylation of the Ser<sub>657</sub> PKC $\alpha$  key activation site, with no change in the total levels of PKC $\alpha$  in the tissues (Fig. 6b). In the control mice, transition from the fasted to the fed state was also accompanied by fourfold-increased phosphorylation of the Thr<sub>410</sub> key activation site of PKC $\zeta/\lambda$  ( $P < 0.001$ ), indicating PKC $\zeta/\lambda$  activation. A similar induction of PKC $\zeta/\lambda$  was ob-

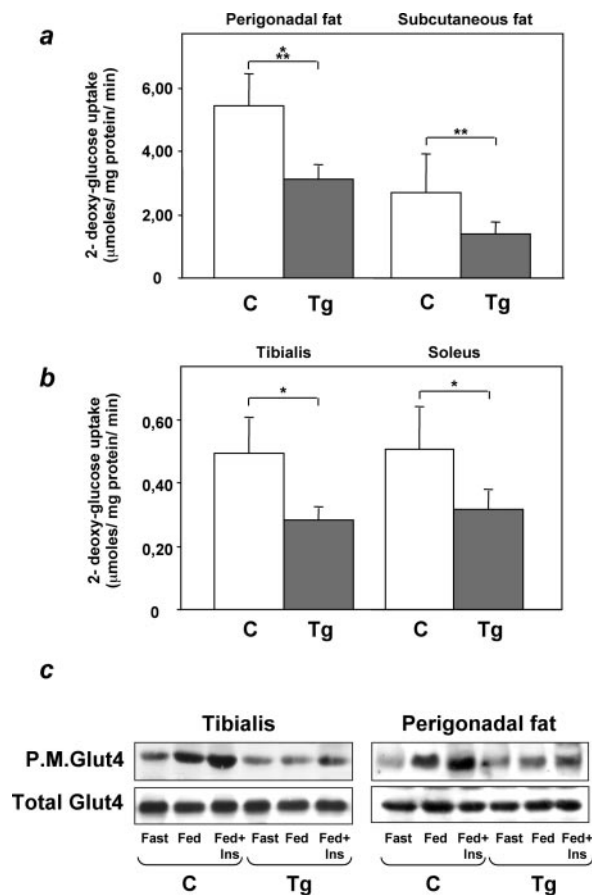


FIG. 5. Glucose transport in *ped/pea-15* transgenic mice. (a) Weight-matched female transgenic (Tg;  $n = 6$ ) and control (C;  $n = 6$ ) mice were subjected to intraperitoneal injection of D-[1,2- $^3\text{H}$ ]glucose ( $2 \text{ g kg of body weight}^{-1}$ ;  $10 \mu\text{Ci/mouse}$ ) and insulin ( $0.75 \text{ mU g of body weight}^{-1}$ ) and killed, and tissues were snap-frozen in liquid nitrogen. D-[1,2- $^3\text{H}$ ]glucose-6-phosphate accumulated in muscle and fat tissues was quantitated as described under Materials and Methods. Bars represent mean values  $\pm$  standard deviations. Differences between control and transgenic animals were significant at  $P < 0.05$  (tibialis and soleus muscles),  $P < 0.01$  (subcutaneous fat), and  $P < 0.001$  (perigonadal fat). (b) Alternatively, tissues from insulin-injected animals were frozen in liquid nitrogen and harvested for plasma membrane preparation as described under Materials and Methods. Total homogenates and plasma membrane lysates were then analyzed by Western blotting with GLUT4 antibodies. Blots were revealed by enhanced chemiluminescence and autoradiography. The autoradiographs shown are representative of four independent experiments.

served after administration of insulin to those animals (data not shown). The effect of feeding was decreased by 50% ( $P < 0.05$ ) and 80% ( $P < 0.01$ ) in muscle and adipose tissues, respectively, from the *ped/pea-15* transgenic mice. Again, the decrease in PKC $\zeta/\lambda$  activation was accompanied by no significant change in the total PKC $\zeta/\lambda$  levels in the tissues. The same changes in PKC $\alpha$  and  $\zeta/\lambda$  were observed in male and female *ped/pea-15* transgenic mice (data not shown).

PEP/PEA-15 is a phospholipase D interactor and increases phospholipase D cellular activity by enhancing its expression level (34). We therefore compared the levels of the phospholipase D product diacylglycerol in extracts from transgenic and control tissues, as diacylglycerol is a major PKC $\alpha$  activator. As

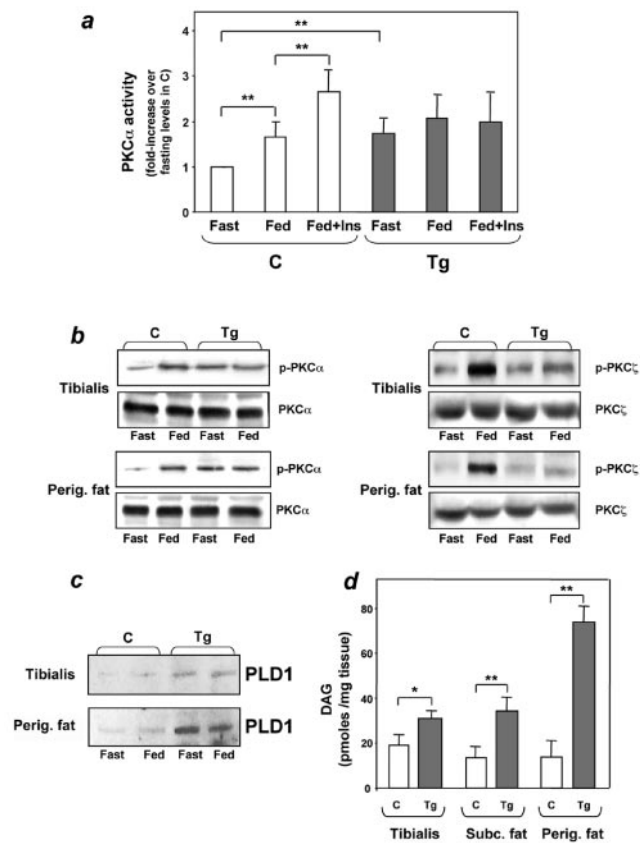


FIG. 6. PKC $\alpha$  activation in *ped/pea-15* transgenic mice. (a) Weight-matched female mice were fasted overnight or fed ad libitum, followed by intraperitoneal insulin injection ( $0.75 \text{ mU g}^{-1}$  body weight), as indicated. The animals were killed, and perigonadal fat tissue was collected, homogenized, and immunoprecipitated with PKC $\alpha$  antibodies. PKC activity was assayed in the immunoprecipitates as outlined under Materials and Methods. Bars represent the mean  $\pm$  standard deviation of data from at least seven mice per group. Asterisks denote statistically significant differences ( $P < 0.01$ ). Alternatively, fat or muscle tissues were solubilized, and lysates were Western blotted with phospho-PKC (P-PKC), PKC (panel b), or phospholipase D 1 (PLD1) antibodies (panel c). Bands were revealed by enhanced chemiluminescence and autoradiography. The autoradiographs shown are representative of four (PKC $\alpha$  and phospholipase D 1) and three (PKC $\zeta$ ) independent experiments. (d) For determining diacylglycerol levels, tissues were extracted in chloroform-methanol, and lipid extracts were assayed by adding diacylglycerol kinase and [ $\gamma$ - $^{32}\text{P}$ ]ATP as described under Materials and Methods. [ $^{32}\text{P}$ ]phosphatidic acid was separated by thin-layer chromatography and quantitated by liquid scintillation counting. Bars represent the mean  $\pm$  standard deviation of data from at least six mice per group. Asterisks denote statistically significant differences (\* $P < 0.05$ , \*\* $P < 0.01$ ).

revealed by thin-layer chromatography analysis, there diacylglycerol levels in subcutaneous and perigonadal adipose tissues from the *ped/pea-15* transgenic mice were increased  $>2$ -fold (Fig. 6d;  $P < 0.01$ ). In tibialis muscles from *ped/pea-15* transgenic mice, diacylglycerol levels were also increased by 60% ( $P < 0.05$ ) over that in the nontransgenic mice. Thus, diacylglycerol levels in fat and skeletal muscle tissues correlated with PED/PEA-15-induced PKC $\alpha$  activity in these tissues. PLD1 expression was also two- and fivefold higher in muscle and adipose tissues, respectively, from transgenic versus control

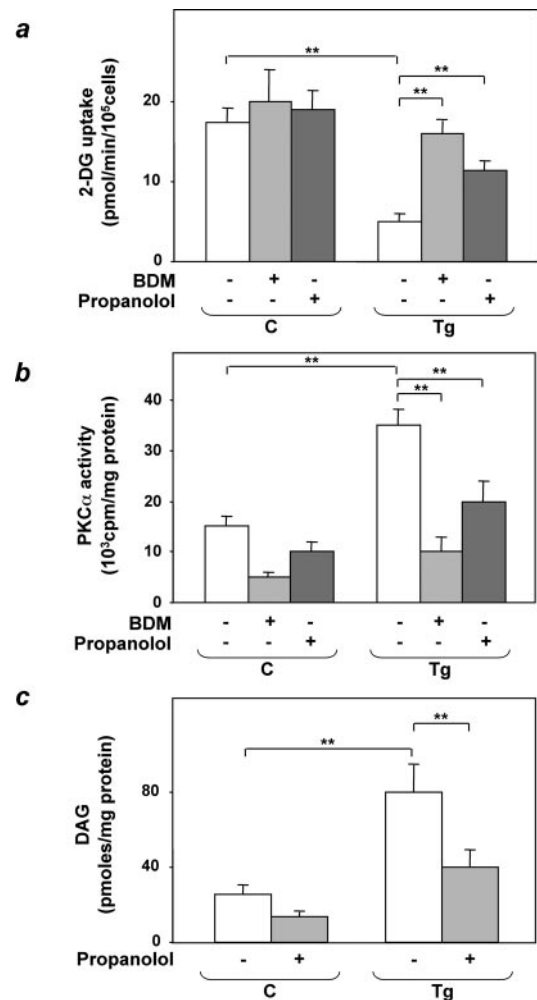


FIG. 7. Bisindolylmaleimide and propranolol effects on 2-deoxyglucose uptake in epididymal fat adipocytes from *ped/pea-15* transgenic mice. Adipocytes from transgenic (Tg) and control (C) mice were incubated with 100 nM bisindolylmaleimide (BDM) or 150  $\mu\text{M}$  propranolol for 30 min, as indicated; 100 nM insulin (final concentration) was then added, and the cells were assayed for 2-deoxyglucose uptake (a). Lysates of adipocytes from transgenic and control mice were immunoprecipitated with PKC $\alpha$  antibodies, followed by determination of PKC activity (b), as described under Materials and Methods. Alternatively, the cells were extracted and diacylglycerol (DAG) levels were determined as described under Materials and Methods (c). Bars represent the means  $\pm$  standard deviation of duplicate determinations in four (2-deoxyglucose uptake), three (PKC $\alpha$  activity), and five (diacylglycerol levels) independent experiments with fat pads from five transgenic and five control mice. Asterisks denote statistically significant differences (\*\*,  $P < 0.001$ ).

mice (Fig. 6c;  $P < 0.001$ ). This additional finding suggested that increased phospholipase activity is at least one of the mechanisms determining the high diacylglycerol levels in the tissues of the transgenic mice.

The significance of these findings to the impaired insulin-stimulated glucose uptake in tissues from *ped/pea-15* transgenic mice was addressed further in adipocytes isolated from the animals. Consistent with the fat tissue, isolated adipocytes from the transgenic mice showed an almost fivefold decrease in insulin-induced glucose uptake compared to control cells ( $P <$

0.01; Fig. 7a). Bisindolylmaleimide incubation reduced PKC $\alpha$  activity by fourfold in both wild-type and transgenic mouse adipocytes ( $P < 0.01$ ; Fig. 7b). Simultaneously, bisindolylmaleimide almost completely rescued insulin-stimulated glucose uptake in transgenic mouse adipocytes (Fig. 7a). Preincubation with the phospholipase D inhibitor propanolol also caused a >50% reduction in diacylglycerol and PKC $\alpha$  activity in adipocytes from transgenic as well as control mice. As with bisindolylmaleimide, these changes were accompanied by a significant recovery of insulin-stimulated glucose uptake, indicating an important role of the phospholipase D/PKC $\alpha$  pathway in alteration of glucose uptake by *ped/pea-15*.

Activation of the phosphatidylinositol 3-kinase/Akt/protein kinase B (PKB) pathway is a major event leading to stimulation of GLUT4 translocation by insulin. However, insulin injection caused a twofold activation of phosphatidylinositol 3-kinase in skeletal muscles from both transgenic and control mice (Fig. 8a). Based on immunoblotting with specific phospho-Ser<sub>473</sub> Akt antibodies, Akt/PKB activity was also normally induced by insulin in transgenic muscles (Fig. 8b), with no gender-related difference (data not shown). It therefore appeared that dysregulation of PKC signaling is a major mechanism responsible for *ped/pea-15*-induced resistance to insulin action in glucose uptake, independently of the phosphatidylinositol 3-kinase/Akt/PKB pathway. The mechanism of *ped/pea-15* inhibition of insulin-stimulated glucose uptake is shown schematically in Fig. 8c.

**Glucose-regulated insulin secretion in *ped/pea-15* transgenic mice.** Based on insulin tolerance tests, *ped/pea-15* transgenic mice developed only a further 20% increase in insulin resistance after the high-fat diet (Fig. 9a; difference from animals fed the standard diet was significant at the  $P < 0.05$  level). In comparison, nontransgenic mice underwent a 60% reduction in their sensitivity to insulin ( $P < 0.01$ ), and became as insulin resistant as their transgenic littermates (difference from transgenic mice not significant). Nevertheless, nontransgenic mice showed little change in glucose tolerance after the high-fat diet, while *ped/pea-15* transgenic mice developed diabetes (Fig. 3c). We therefore hypothesized that resistance to insulin action alone is not sufficient to cause the alteration in glucose tolerance of the *ped/pea-15* transgenic mice.

To address this possibility, we first analyzed the expression of *ped/pea-15* in beta cells of the transgenic mice. Staining of pancreas sections with specific PED/PEA-15 antibodies revealed a significant increase in the immunoreactivity of the islet cores, where beta cells are localized, in L1 transgenic compared to control mice (Fig. 9b). At variance, both insulin and glucagon immunoreactivities were comparable in *ped/pea-15* transgenic mice and controls. We next compared insulin secretion following a glucose load in L1 *ped/pea-15* transgenic mice and in their nontransgenic littermates. In control mice, a five- to sixfold increase in insulin secretion was observed 2 min after intraperitoneal glucose injection, and the levels remained higher than baseline values for up to 30 min, indicating a second-phase response (Fig. 9c). Based on insulin area under the curve quantitation, the acute first-phase insulin secretory response to glucose was reduced by almost 70% in transgenic mice ( $P < 0.001$ ). The second-phase response was also significantly impaired in *ped/pea-15* transgenic mice compared to control mice ( $P < 0.01$ ). Almost identical decreases in early

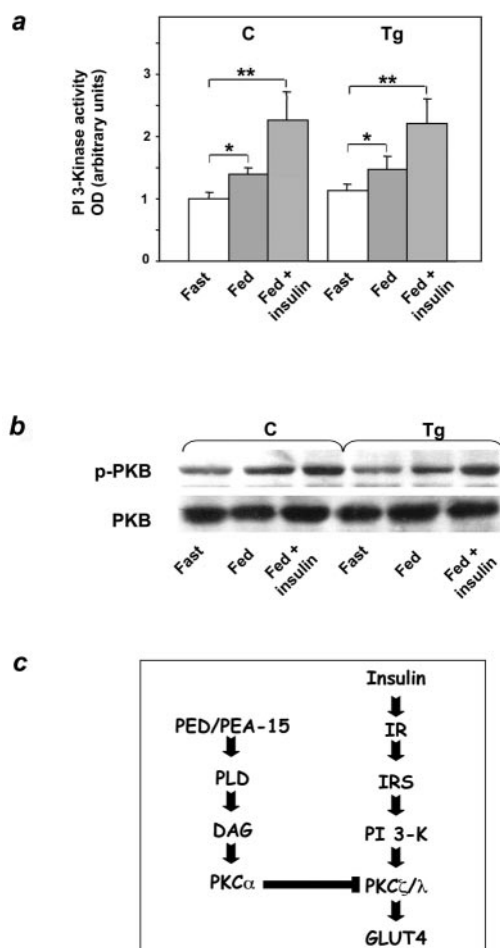


FIG. 8. Activation of phosphatidylinositol 3-kinase and Akt in *ped/pea-15* transgenic mice. (a) Weight-matched female mice were fasted overnight or fed ad libitum, followed by intraperitoneal insulin injection ( $0.75 \text{ mU g of body weight}^{-1}$ ), as indicated. Animals were sacrificed, and the tibialis muscles were collected, homogenized, and assayed for phosphatidylinositol (PI) 3-kinase activity as described under Materials and Methods. Bars represent the mean  $\pm$  standard deviation of data from five mice per group. The difference in insulin-induced PKB in transgenic versus control mice was not statistically significant. (b) Alternatively, tissue lysates were Western blotted with either PKB or phospho-PKB antibodies. Filters were revealed by enhanced chemiluminescence and autoradiography. The autoradiographs shown are representative of four independent experiments. (c) Proposed mechanism of PED action on insulin-stimulated glucose transport (details in the text). Asterisks denote statistically significant differences (\*,  $P < 0.05$ ; \*\*,  $P < 0.01$ ).

and late insulin responses were observed in both male and female transgenic mice. Again, defective insulin secretion was also observed with the L30 and L61 mouse lines (data not shown).

To test the further hypothesis that overexpression of *ped/pea-15* is sufficient to impair hyperglycemia-induced insulin secretion, we generated MIN6 beta-cell lines stably overexpressing *ped/pea-15* by 3- to 10-fold above endogenous levels (Fig. 10a). We then compared insulin secretion in these cells and in cells expressing only endogenous *ped/pea-15*. MIN6 control cells responded with a fivefold induction in insulin

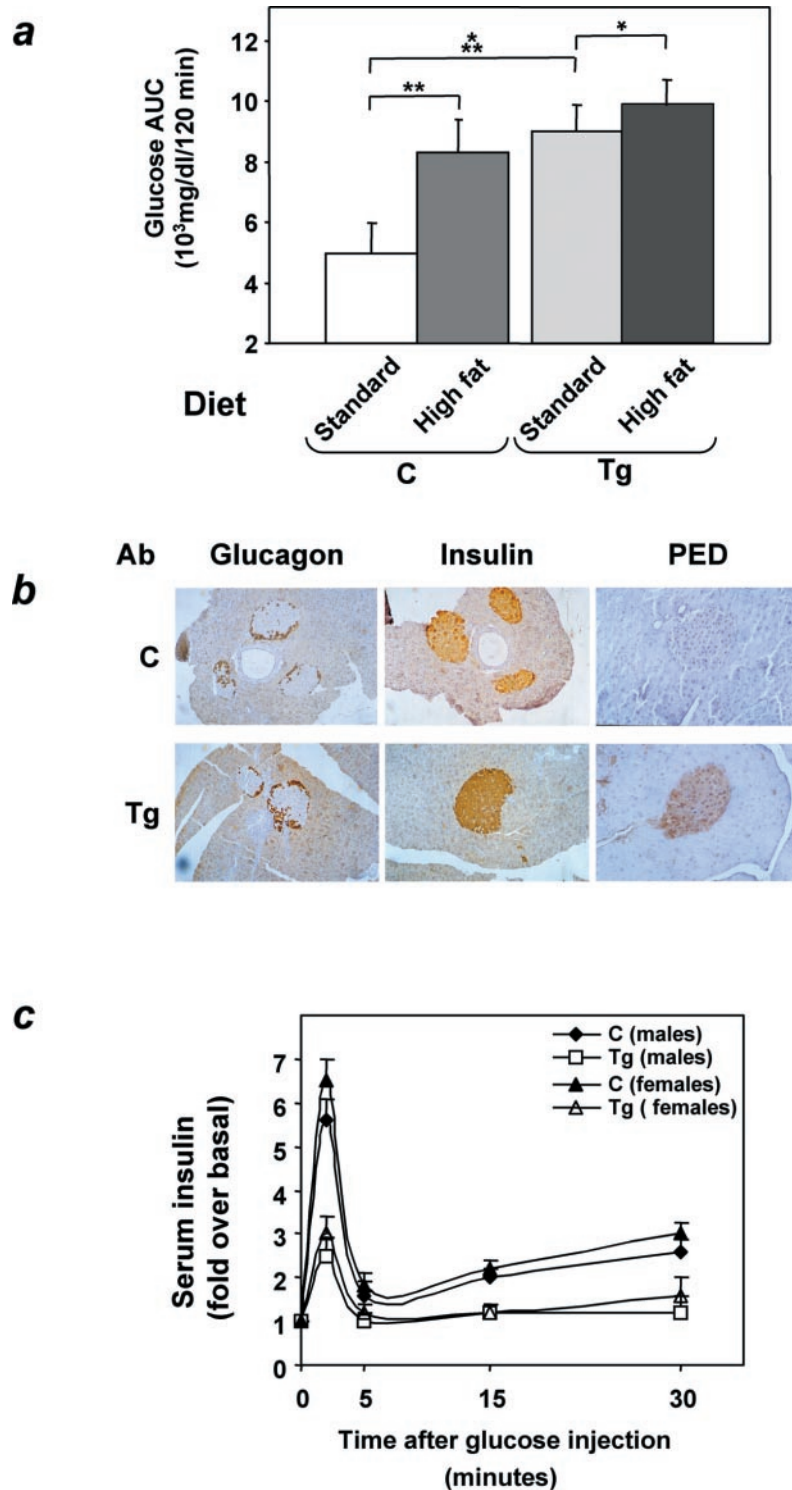


FIG. 9. Insulin secretion in *ped/pea-15* transgenic mice. (a) Transgenic (Tg) and control (C) female mice were fed either a 10% fat standard or a 60% high-fat diet for 10 weeks. Weight-matched animals were then subjected to intraperitoneal insulin tolerance tests as outlined in the legend to Fig. 4. The effect of the high-fat diet on insulin tolerance is expressed as total areas under the curve (glucose AUC). Bars represent the mean  $\pm$  standard deviation of data from seven mice per group. Asterisks denote statistically significant differences versus mice maintained on the standard diet (\*,  $P < 0.05$ ; \*\*,  $P < 0.01$ ; \*\*\*,  $P < 0.001$ ). (b) Overexpression of *ped/pea-15* in pancreas from *ped/pea-15* transgenic mice. Pancreas from *ped/pea-15* male transgenic mice (Tg) and their nontransgenic littermates (C) were fixed and embedded in Tissue-Tek OTC, and sections were prepared as described under Materials and Methods. Immunohistochemical analysis of the islets was carried out with PED/PEA-15, insulin, and glucagon antibodies as indicated. Anti-rabbit or anti-goat immunoglobulin G was used as the second antibody. Immunoreactivity was revealed by peroxidase-labeled streptavidin. The microphotographs shown are representative of images obtained from eight transgenic (four male and four female) and seven nontransgenic mice (three male and four female). (c) Weight-matched transgenic and control mice were subjected to intraperitoneal glucose loading as outlined in the legend to Fig. 2, followed by determination of plasma insulin levels at the indicated times. Data points represent the mean  $\pm$  standard deviation of determinations in 14 transgenic (seven female and seven male) and 16 control mice (eight female and eight male). Differences between control and transgenic mice were statistically significant, as indicated in the text.

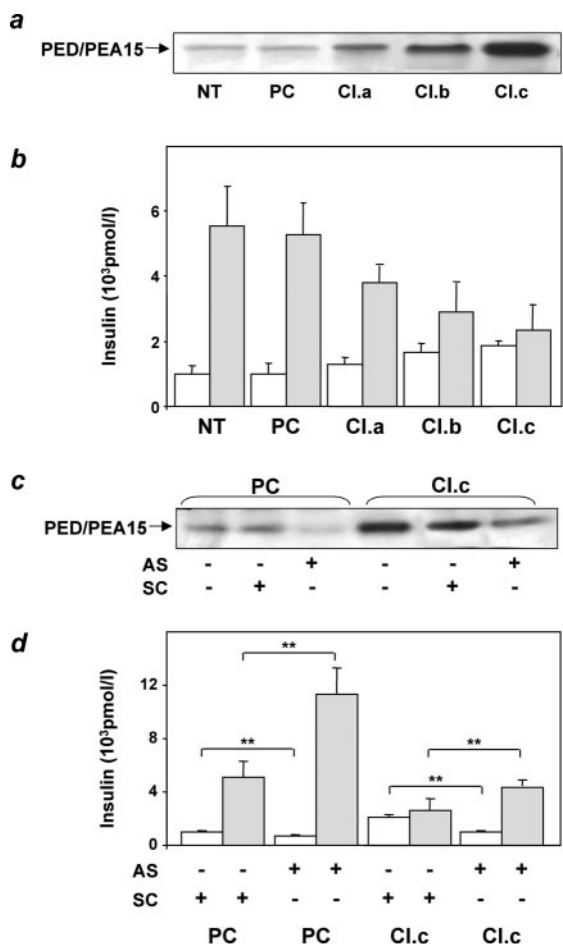


FIG. 10. Insulin secretion in *ped/pea-15*-overexpressing MIN6 cells. (a) MIN6 beta cells were stably transfected with *ped/pea-15* cDNA. Several clones overexpressing *ped/pea-15* by 3-, 5-, and 10-fold were selected. Three clones were further characterized (termed clones a, b, and c). (b) Transfected cell clones, untransfected cells (NT), and cells transfected with the empty plasmid (PC) were stimulated with either 0.1 mM glucose (open bars) or 16.7 mM glucose (dashed bars), and insulin was assayed in the culture medium as described in the text. Bars represent values  $\pm$  standard deviation of triplicate measurements in five independent experiments. The differences between *ped/pea-15*-overexpressing (all clones) and control cells (whether untransfected or transfected with the empty plasmid) were significant at  $P < 0.01$  (basal secretion) and  $P < 0.001$  (glucose-induced secretion). (c) Alternatively, control cells transfected with the empty plasmid (PC) or clone c (Cl.c) cells were transfected either with *ped/pea-15* antisense (AS) or with scrambled (SC) oligonucleotides. (d) Glucose-stimulated insulin secretion was assayed as outlined above. Bars represent values  $\pm$  standard deviation of triplicate measurements in four independent experiments. Basal insulin secretion differences in the antisense versus scrambled oligonucleotide-treated cells were significant at  $P < 0.001$  (empty plasmid-transfected cells) and  $P < 0.01$  (clone c cells). Glucose-stimulated secretion differences in the antisense versus scrambled oligonucleotide-treated cells were also significant at the  $P < 0.001$  (empty plasmid-transfected cells) and  $P < 0.01$  levels (clone c cells).

secretion when subjected to physiological increases in the glucose concentration in the medium (Fig. 10b). In these same cells, the overexpression of *ped/pea-15* increased basal insulin secretion (30 to 80%,  $P < 0.01$ ) and reduced that induced by glucose by 50 to 90% ( $P < 0.001$ ). These changes closely

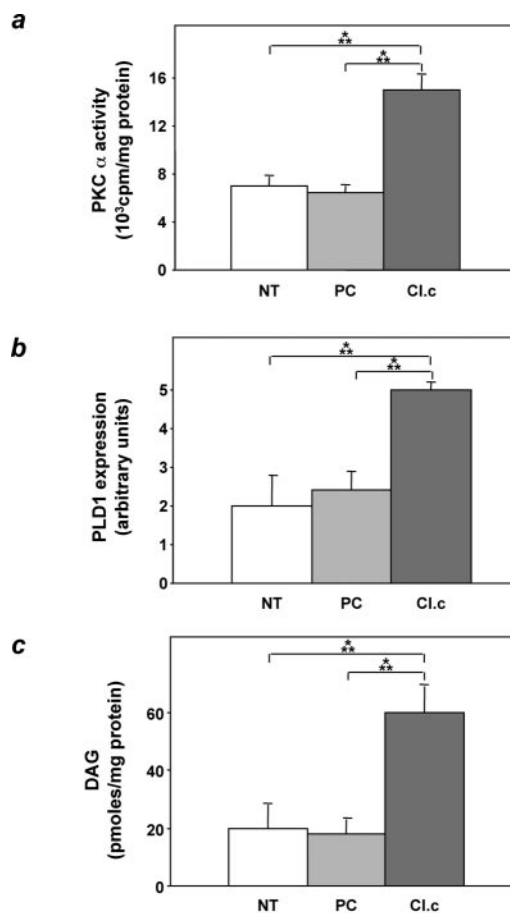


FIG. 11. PKC $\alpha$  activity, phospholipase D1 expression, and diacylglycerol levels in *ped/pea-15*-overexpressing MIN6 cells. MIN6 beta cells stably transfected with *ped/pea-15* cDNA (clone c) or the empty vector (empty plasmid-transfected cells [PC]) and untransfected cells (NT) were assayed for PKC $\alpha$  activity (a), phospholipase D1 (PLD1) expression (b), and diacylglycerol (DAG) (c) levels as outlined in the legend to Fig. 6. Western-blotted phospholipase D1 bands were revealed by enhanced chemiluminescence and autoradiography and quantitated by laser densitometry. Bars represent the means  $\pm$  standard deviation of four (PKC $\alpha$  and phospholipase D1), and five (diacylglycerol) independent determinations. Based on *t* test analysis, the differences between *ped/pea-15*-overexpressing and control cells were significant at the  $P < 0.001$  level.

correlated with the expression levels of *ped/pea-15* achieved in the cells. Treatment with a specific antisense oligonucleotide effectively blocked *ped/pea-15* expression and almost completely rescued the abnormal insulin secretion in the *ped/pea-15* overexpressors (Fig. 10c and d). More importantly, antisense transfection of cells expressing only the endogenous *ped/pea-15* enhanced glucose-induced insulin secretion by >2-fold, indicating that this gene has a physiological role in controlling beta-cell secretion in response to glucose.

As in other cell types, overexpression of *ped/pea-15* in MIN6 cells also caused a twofold activation of PKC $\alpha$  (Fig. 11a,  $P < 0.001$ ). Moreover, phospholipase D 1 and diacylglycerol levels in *ped/pea-15* overexpressing MIN6 cells were increased compared to those in control cells by 2.5- and 3-fold, respectively (Fig. 11b and c,  $P < 0.001$ ). Thus, activation of the phospho-

lipase D/PKC pathway also occurs in beta cells overexpressing *ped/pea-15*.

## DISCUSSION

Analysis of the gene expression profile revealed increased expression of the *ped/pea-15* gene in skeletal muscle and adipose tissues from individuals with type 2 diabetes (7). More recently, 5- to 20-fold overexpression of *ped/pea-15* has been demonstrated to occur in almost 30% of the type 2 diabetics in a large Italian cohort, indicating that increased expression of the *ped/pea-15* gene is a common abnormality in this form of diabetes (R. Valentino and F. Beguinot, unpublished data). In other studies, we reported that overexpression of *ped/pea-15* in cultured skeletal muscle cells and adipocytes impairs insulin action on glucose transport and cell surface recruitment of GLUT4 (7, 8). However, whether the *ped/pea-15* defect alone impairs glucose tolerance in vivo remains unknown.

In the present work, we report that transgenic mice overexpressing *ped/pea-15* to levels comparable to those occurring in human type 2 diabetes exhibit mildly elevated random-fed blood glucose levels and become hyperglycemic after glucose loading, indicating that increased expression of this gene is sufficient to impair glucose tolerance. Moreover, *ped/pea-15* transgenic mice become diabetic when body weight increases through administration of high-fat diets. This additional finding suggests an important interaction of environmental modifiers with *ped/pea-15* gene function, leading to a further derangement in glucose tolerance. Based on the insulin tolerance tests, *ped/pea-15* transgenic mice are much more insulin resistant than their nontransgenic littermates. The transgenic mice were consistently markedly hyperinsulinemic in the basal state and exhibited increased free fatty acid levels in blood. The transgenic mice also show reduced insulin response to a glucose challenge, indicating that the overexpression of *ped/pea-15* impairs insulin secretion in addition to insulin action. In addition, we found that, when fed high-fat diets, these animals become as insulin resistant as their nontransgenic littermates. Nevertheless, *ped/pea-15* transgenic mice develop random hyperglycemia while control animals remain euglycemic. It therefore appears that both decreased glucose-stimulated insulin secretion and impaired insulin action contribute to the abnormal glucose tolerance determined by *ped/pea-15* gene overexpression.

Decreased insulin sensitivity in *ped/pea-15* transgenic mice might have been determined by the increased free fatty acids (1, 3, 27). However, it is unlikely that higher free fatty acid levels in *ped/pea-15* transgenic mice could completely account for insulin resistance, as *ped/pea-15* overexpression also impairs insulin action on glucose uptake in cultured cells (7, 8). Previous studies in yeasts as well as in eukaryotic cells showed that *ped/pea-15* gene encodes a phospholipase D interactor (35). Importantly, in cultured cells, binding to PED/PEA-15 protein stabilizes the phospholipase, leading to enhanced phospholipase activity (35). In L6 skeletal muscle cells stably overexpressing *ped/pea-15*, inhibition of phospholipase D activity rescues insulin action on glucose transport (our unpublished observations), underlining the importance of proper phospholipase D function for normal insulin sensitivity of the insulin-regulated glucose transport system. In addition, our

previous work has shown that L6 cells overexpressing *ped/pea-15* feature constitutive activation of the classical PKC isoform PKC $\alpha$  (8). Activation of PKC $\alpha$  by *ped/pea-15*, in turn, determines almost complete loss of PKC $\zeta/\lambda$  sensitivity to insulin and of insulin action on glucose transport in these cells (8).

We now show that muscle and fat tissues from *ped/pea-15* transgenic mice also feature reduced insulin action on glucose transport and PKC $\zeta/\lambda$  activation and, simultaneously, increased PKC $\alpha$  activity and phospholipase D levels. Transgenic tissues also exhibit increased levels of diacylglycerol, a major activator of PKC $\alpha$ . The same abnormalities persist in epididymal fat pad adipocytes from *ped/pea-15* transgenic mice. In these cells, as in L6 muscle cells overexpressing *ped/pea-15* (8), pharmacological block of PKC $\alpha$  or phospholipase D activities rescues insulin-stimulated glucose transport. Thus, the overexpression of *ped/pea-15* in tissues from the transgenic mice seems to determine insulin resistance in glucose disposal by inhibiting PKC $\zeta/\lambda$  function through the induction of PKC $\alpha$  (Fig. 7). Consistent with this mechanism, Leitges et al. have recently shown that elimination of the PKC $\alpha$  gene by homologous recombination enhances insulin signaling and action on glucose transport in mice (22).

Insulin-induced activation of atypical PKCs is markedly impaired in tissues of type 2 diabetic individuals as well as in those from animal models of type 2 diabetes (12, 17, 18, 19). This abnormality has been proposed to account for the decreased insulin-stimulated glucose disposal observed during hyperinsulinemic-euglycemic clamps in type 2 diabetic humans and monkeys (12). The defective activation of atypical PKCs in skeletal muscle from type 2 diabetic individuals was also shown to be independent of PKC protein levels and accompanied by normal activation of phosphatidylinositol 3-kinase and Akt by insulin (12, 19, 20). Based on those studies, however, the mechanism responsible remains unclear. The finding that *ped/pea-15* gene overexpression impairs glucose disposal in major insulin target tissues by inhibiting insulin activation of PKC $\zeta/\lambda$  indicates that, at least in part, the impaired glucose utilization in type 2 diabetics can be accounted for by increased levels of *ped/pea-15*. In fact overexpression of *ped/pea-15* was found to represent a common abnormality in type 2 diabetes (7), and this defect does not determine changes in phosphatidylinositol 3-kinase or Akt activation by insulin in either cultured skeletal muscle cells (7, 8) or muscle tissue from *ped/pea-15* transgenic mice.

The abnormal beta-cell function in *ped/pea-15* transgenic mice might have been caused by the metabolic consequences of insulin resistance. More likely, *ped/pea-15* overexpression directly impairs beta-cell function. In fact, we have shown that *ped/pea-15* overexpression in cultured beta cells causes a two-fold increase in basal insulin secretion and inhibits that induced by glucose. Thus, beta-cell overexpression may contribute to the basal hyperinsulinemia found in *ped/pea-15* transgenic mice while rendering them unable to compensate for hyperglycemia by further increasing plasma insulin levels. Similar to other tissues from the transgenic mice, overexpression of *ped/pea-15* in cultured beta cells led to activation of the phospholipase D/PKC $\alpha$  pathway. At variance with insulin-regulated glucose transport, however, PKC $\alpha$  inhibition allowed only partial reversal of the insulin secretion defect in *ped/pea-15*-overexpressing beta cells (data not shown). Thus, abnormal

PKC $\alpha$  signaling might contribute to the secretion abnormalities in these cells. Whether different mechanisms play a major role and the identity of these mechanisms remain to be defined and are presently under investigation in our laboratory.

The control of glucose-regulated insulin secretion appears to represent a physiological function of *ped/pea-15* in beta cells. Hence, transfection of a specific antisense oligonucleotide into MIN6 cells expressing only endogenous *ped/pea-15* enhanced glucose-induced insulin secretion by almost threefold. This additional finding identifies *ped/pea-15* as a novel gene controlling insulin secretion in addition to insulin action. Under appropriate environmental conditions, *ped/pea-15* overexpression leads to diabetes by impairing both of these functions and may contribute to genetic susceptibility to type 2 diabetes in humans.

#### ACKNOWLEDGMENTS

This work was supported in part by the European Community (grant QLRT-1999-00674 to F.B., EUDG program), grants from the Associazione Italiana per la Ricerca sul Cancro (to F.B. and P.F.) and the Ministero dell'Università e della Ricerca Scientifica (PRIN to F.B. and P.F. and FIRB RBNE0155LB). The financial support of Telethon Italy is gratefully acknowledged (grants E.0896 to F.B. and C.40 to C.T.). M.A. Maitan and F. Fiory are recipients of fellowships from the Federazione Italiana per la Ricerca sul Cancro.

The technical help of Maria Russo and Salvatore Sequino is also acknowledged.

#### REFERENCES

- Arner, P. 2002. Insulin resistance in type 2 diabetes: role of fatty acids. *Diabetes Metab. Res. Rev.* **18**(Suppl. 2):S5–S9.
- Bell, G. I., and K. S. Polonsky. 2001. Diabetes mellitus and genetically programmed defects in beta-cell function. *Nature* **414**:788–791.
- Boden, G., and G. I. Shulman. 2002. Free fatty acids in obesity and type 2 diabetes: defining their role in the development of insulin resistance and beta-cell dysfunction. *Eur. J. Clin. Invest.* **32**(Suppl. 3):14–23.
- Caruso, M., C. Miele, A. Oliva, G. Condorelli, F. Oriente, G. Riccardi, B. Capaldo, F. Fiory, D. Accili, P. Formisano, and F. Beguinot. 2000. The IR1152 mutant insulin receptor selectively impairs insulin action in skeletal muscle but not in liver. *Diabetes* **49**:1194–1202.
- Condorelli, G., A. Trencia, G. Vigliotta, A. Perfetti, U. Goglia, A. Cassese, A. M. Musti, C. Miele, S. Santopietro, P. Formisano, and F. Beguinot. 2002. Multiple members of the mitogen-activated protein kinase family are necessary for PED/PEA-15 anti-apoptotic function. *J. Biol. Chem.* **277**:11013–11018.
- Condorelli, G., G. Vigliotta, A. Cafieri, A. Trencia, P. Andalo, F. Oriente, C. Miele, M. Caruso, P. Formisano, and F. Beguinot. 1999. PED/PEA-15: an anti-apoptotic molecule that regulates FAS/TNFR1-induced apoptosis. *Oncogene* **18**:4409–4415.
- Condorelli, G., G. Vigliotta, C. Iavarone, M. Caruso, C. G. Tocchetti, F. Andreozzi, A. Cafieri, M. F. Tecce, P. Formisano, L. Beguinot, and F. Beguinot. 1998. PED/PEA-15 gene controls glucose transport and is overexpressed in type 2 diabetes mellitus. *EMBO J.* **17**:3858–3866.
- Condorelli, G., G. Vigliotta, A. Trencia, M. A. Maitan, M. Caruso, C. Miele, F. Oriente, S. Santopietro, P. Formisano, and F. Beguinot. 2001. Protein kinase C (PKC)-alpha activation inhibits PKC-zeta and mediates the action of PED/PEA-15 on glucose transport in the L6 skeletal muscle cells. *Diabetes* **50**:1244–1252.
- Czech, M. P. 1980. Insulin action and the regulation of hexose transport. *Diabetes* **39**:399–409.
- DeFronzo, R. A. 1995. Pathogenesis of type 2 diabetes: metabolic and molecular implications for identifying diabetes genes. *Diabetes Rev.* **5**:177–269.
- Estelles, A., C. A. Charlton, and H. M. Blau. 1999. The phosphoprotein PEA-15 inhibits Fas- but increases TNF-R1-mediated caspase-8 activity and apoptosis. *Dev. Biol.* **216**:16–28.
- Farese, R. V. 2002. Function and dysfunction of aPKC isoforms for glucose transport in insulin-sensitive and insulin-resistant states. *Am. J. Physiol. Endocrinol. Metab.* **283**:E1–E11.
- Filippa, N., C. L. Sable, C. Filloux, B. Hemmings, and E. Van Obberghen. 1999. Mechanism of protein kinase B activation by cyclic AMP-dependent protein kinase. *Mol. Cell. Biol.* **19**:4989–5000.
- Formstecher, E., J. W. Ramos, M. Fauquet, D. A. Calderwood, J. C. Hsieh, B. Canton, X. T. Nguyen, J. V. Barnier, J. Camonis, M. H. Ginsberg, and H. Chneiweiss. 2001. PEA-15 mediates cytoplasmic sequestration of ERK MAP kinase. *Dev. Cell* **1**:239–250.
- Hao, C., F. Beguinot, G. Condorelli, A. Trencia, E. G. Van Meir, V. W. Yong, I. F. Parney, W. H. Roa, and K. C. Petruk. 2001. Induction and intracellular regulation of tumor necrosis factor-related apoptosis-inducing ligand (TRAIL) mediated apoptosis in human malignant glioma cells. *Cancer Res.* **61**:1162–1170.
- Kahn, C. R. 1994. Insulin action, diabetogenes, and the cause of type II diabetes. *Diabetes* **43**:1066–1084.
- Kanoh, Y., G. Bandyopadhyay, M. P. Sajan, M. L. Standaert, and R. V. Farese. 2000. Thiazolidinedione treatment enhances insulin effects on protein kinase C- $\zeta/\lambda$  activation and glucose transport in adipocytes of nondiabetic and Goto-Kakizaki type II diabetic rats. *J. Biol. Chem.* **275**:16690–16696.
- Kanoh, Y., G. Bandyopadhyay, M. P. Sajan, M. L. Standaert, and R. V. Farese. 2001. Rosiglitazone, insulin treatment, and fasting correct defective activation of protein kinase C- $\zeta/\lambda$  by insulin in vastus lateralis muscles and adipocytes of diabetic rats. *Endocrinology* **142**:1595–1605.
- Kim, Y. B., K. Kotani, T. P. Ciaraldi, R. V. Farese, R. R. Henry, and B. B. Kahn. 2001. Insulin-stimulated PKC $\zeta/\lambda$  activity is impaired in muscles of insulin resistant subjects. *Diabetes* **250**(Suppl. 2):A62.
- Kim, Y. B., S. E. Nikoulina, T. P. Ciaraldi, R. R. Henry, and B. B. Kahn. 1999. Normal insulin-dependent activation of Akt/protein kinase B, with diminished activation of phosphoinositide 3-kinase in muscle in type 2 diabetes. *J. Clin. Invest.* **104**:733–741.
- Laemmli, U. K. 1970. Cleavage of structural proteins during the assembly of the head of bacteriophage T4. *Nature* **227**:680–685.
- Leitges, M., M. Plomann, M. L. Standaert, G. Bandyopadhyay, M. P. Sajan, Y. Kanoh, and R. V. Farese. 2002. Knockout of PKC $\alpha$  enhances insulin signaling through PI3K. *Mol. Endocrinol.* **16**:847–858.
- Miyazaki, J., K. Araki, E. Yamato, H. Ikegami, T. Asano, Y. Shibasaki, Y. Oka, and K. Yamamura. 1990. Establishment of a pancreatic beta cell line that retains glucose-inducible insulin secretion: special reference to expression of glucose transporter isoforms. *Endocrinology* **127**:126–132.
- Pinget, M., and S. Boullu-Sanchis. 2002. Physiological basis of insulin secretion abnormalities. *Diabetes Metab.* **28**(Suppl. 6):S7–S13.
- Preis, J. E., C. R. Loomis, R. M. Bell, and J. E. Nidel. 1987. Quantitative measurement of sn-1,2-diacylglycerols. *Methods Enzymol.* **141**:294–299.
- Qu, X., J. P. Seale, and R. Donnelly. 1999. Tissue and isoform-selective activation of protein kinase C in insulin-resistant obese Zucker rats—effects of feeding. *J. Endocrinol.* **162**:207–214.
- Reaven, G. M. 1988. Role of insulin resistance in human diabetes. *Diabetes* **37**:1595–1607.
- Rodbell, M. 1964. Metabolism of isolated fat cells. *J. Biol. Chem.* **239**:173–181.
- Russ, M., A. Wichelhaus, I. Uphues, T. Kolter, and J. Eckel. 1994. Photoaffinity labelling of cardiac membrane GTP-binding proteins in response to insulin. *Eur. J. Biochem.* **219**:325–330.
- Trencia, A., A. Perfetti, A. Cassese, G. Vigliotta, C. Miele, F. Oriente, S. Santopietro, F. Giacco, G. Condorelli, P. Formisano, and F. Beguinot. 2003. Protein kinase B/Akt binds and phosphorylates PED/PEA-15, stabilizing its antiapoptotic action. *Mol. Cell. Biol.* **23**:4511–4521.
- Turinsky, J., B. P. Bayly, and D. M. O'Sullivan. 1990. 1,2-Diacylglycerol and ceramide levels in rat skeletal muscle and liver in vivo. *J. Biol. Chem.* **265**:7933–7938.
- Uphues, I., T. Kolter, B. Goud, and J. Eckel. 1995. Failure of insulin-regulated recruitment of the glucose transporter GLUT4 in cardiac muscle of obese Zucker rats is associated with alterations of small-molecular-mass GTP-binding proteins. *Biochem. J.* **311**:161–166.
- White, M. F. 2002. IRS proteins and the common path to diabetes. *Am. J. Physiol. Endocrinol. Metab.* **283**:E413–E422.
- Xiao, C., B. F. Yang, N. Asadi, F. Beguinot, and C. Hao. 2002. Tumor necrosis factor-related apoptosis-inducing ligand-induced death-inducing signaling complex and its modulation by c-FLIP and PED/PEA-15 in glioma cells. *J. Biol. Chem.* **277**:25020–25025.
- Zhang, Y., O. Redina, Y. M. Altshuler, M. Yamazaki, J. Ramos, H. Chneiweiss, Y. Kanaho, and M. A. Frohman. 2000. Regulation of expression of phospholipase D1 and D2 by PEA-15, a novel protein that interacts with them. *J. Biol. Chem.* **275**:35224–35232.
- Zimmet, P., K. G. Alberti, and J. Shaw. 2001. Global and societal implications of the diabetes epidemic. *Nature* **414**:782–787.
- Zisman, A., O. D. Peroni, E. D. Abel, M. D. Michael, F. Mauvais-Jarvis, B. B. Lowell, J. F. Wojtaszewski, M. F. Hirshman, A. Virkamaki, L. J. Goodyear, C. R. Kahn, and B. B. Kahn. 2000. Targeted disruption of the glucose transporter 4 selectively in muscle causes insulin resistance and glucose intolerance. *Nat. Med.* **6**:924–928.

# PED/PEA-15 Regulates Glucose-Induced Insulin Secretion by Restraining Potassium Channel Expression in Pancreatic $\beta$ -Cells

Claudia Miele,<sup>1</sup> Gregory Alexander Raciti,<sup>1</sup> Angela Cassese,<sup>1</sup> Chiara Romano,<sup>1</sup> Ferdinando Giacco,<sup>1</sup> Francesco Oriente,<sup>1</sup> Flora Paturzo,<sup>1</sup> Francesco Andreozzi,<sup>2</sup> Assunta Zabatta,<sup>3</sup> Giancarlo Troncone,<sup>3</sup> Fatima Bosch,<sup>4</sup> Anna Pujol,<sup>4</sup> Hervé Chneiweiss,<sup>5</sup> Pietro Formisano,<sup>1</sup> and Francesco Beguinot<sup>1</sup>

The phosphoprotein enriched in diabetes/phosphoprotein enriched in astrocytes (*ped/pea-15*) gene is overexpressed in human diabetes and causes this abnormality in mice. Transgenic mice with  $\beta$ -cell-specific overexpression of *ped/pea-15* ( $\beta$ -tg) exhibited decreased glucose tolerance but were not insulin resistant. However, they showed impaired insulin response to hyperglycemia. Islets from the  $\beta$ -tg also exhibited little response to glucose. mRNAs encoding the *Sur1* and *Kir6.2* potassium channel subunits and their upstream regulator *Foxa2* were specifically reduced in these islets. Overexpression of PED/PEA-15 inhibited the induction of the atypical protein kinase C (PKC)- $\zeta$  by glucose in mouse islets and in  $\beta$ -cells of the MIN-6 and INS-1 lines. Rescue of PKC- $\zeta$  activity elicited recovery of the expression of the *Sur1*, *Kir6.2*, and *Foxa2* genes and of glucose-induced insulin secretion in PED/PEA-15-overexpressing  $\beta$ -cells. Islets from *ped/pea-15*-null mice exhibited a twofold increased activation of PKC- $\zeta$  by glucose; increased abundance of the *Sur1*, *Kir6.2*, and *Foxa2* mRNAs; and enhanced glucose effect on insulin secretion. In conclusion, PED/PEA-15 is an endogenous regulator of glucose-induced insulin secretion, which restrains potassium channel expression in pancreatic  $\beta$ -cells. Overexpression of PED/PEA-15 dysregulates  $\beta$ -cell function and is sufficient to impair glucose tolerance in mice. *Diabetes* 56: 622–633, 2007

From the <sup>1</sup>Department of Cellular and Molecular Biology and Pathology and Institute of Experimental Endocrinology and Oncology—CNR, “Federico II” University of Naples, Naples, Italy; the <sup>2</sup>Department of Clinical and Experimental Medicine, University of Catanzaro “Magna Graecia,” Catanzaro, Italy; the <sup>3</sup>Department of Biomorphological and Functional Sciences, “Federico II” University of Naples, Naples, Italy; the <sup>4</sup>Center for Animal Biotechnology and Gene Therapy and Department of Biochemistry and Molecular Biology, School of Veterinary Medicine, Autonomous University of Barcelona, Barcelona, Spain; and <sup>5</sup>INSERM U752, University Paris 5 René Descartes, Paris, France.

Address correspondence and reprint requests to Dr. Francesco Beguinot, Department of Cellular and Molecular Biology and Pathology, “Federico II” University of Naples, via Sergio Pansini, 5, Naples 80131, Italy. E-mail: beguinot@unina.it.

Received for publication 7 September 2006 and accepted in revised form 6 November 2006.

C.M. and G.A.R. contributed equally to this work.

2-DG, 2-[1-<sup>3</sup>H]deoxy-D-glucose; PED/PEA-15, phosphoprotein enriched in diabetes/phosphoprotein enriched in astrocytes; PKC, protein kinase C; RIA, radioimmunoassay.

DOI: 10.2337/db06-1260

© 2007 by the American Diabetes Association.

The costs of publication of this article were defrayed in part by the payment of page charges. This article must therefore be hereby marked “advertisement” in accordance with 18 U.S.C. Section 1734 solely to indicate this fact.

Type 2 diabetes is a genetically determined disorder for which the pathogenesis is characterized by development of impaired secretagogue-regulated insulin secretion and insulin resistance (1,2). Metabolic abnormalities caused by insulin resistance contribute to  $\beta$ -cell dysfunction in type 2 diabetes (3–5). Deranged  $\beta$ -cell function is also determined by genetic factors, but their identity remains elusive (3,5).

Phosphoprotein enriched in diabetes/phosphoprotein enriched in astrocytes (PED/PEA-15) was originally identified as a major astrocyte phosphoprotein (6,7) and found to be widely expressed in different tissues (8) and highly conserved among mammals (7). It is a highly regulated protein (6,9,10) whose gene maps on human chromosome 1q21-22 (8). Several studies in cultured cells and rodent tissues have revealed that PED/PEA-15 is a cytosolic scaffold protein, as it regulates multiple cellular functions by binding to distinct components of major intracellular transduction pathways (10–14). These include extracellular signal-related kinase-1/2, Akt, and ribosomal protein S6kinase2. PED/PEA-15 is a death effector domain-containing protein (15). In part through this interaction domain, it inhibits a number of molecules conveying apoptotic signals to the nucleus (10–12). PED/PEA-15 also binds to and increases the stability of phospholipase D, enhancing its activity and controlling important mechanisms in cell metabolism (14).

Gene profile studies evidenced that *ped/pea-15* is commonly overexpressed in individuals with type 2 diabetes (8,16). In cultured muscle and adipose cells and in peripheral tissues from transgenic mice, high levels of PED/PEA-15 impair insulin-stimulated GLUT4 translocation and glucose transport, suggesting that PED/PEA-15 overexpression may contribute to insulin resistance in type 2 diabetes (13,17). Indeed, more recent studies revealed that in offspring of type 2 diabetic subjects, PED/PEA-15 levels negatively correlate to insulin sensitivity (16). Other studies have demonstrated that PED/PEA-15-induced resistance to insulin action on glucose disposal is accompanied by phospholipase D-dependent activation of the classical protein kinase C (PKC) isoform PKC- $\alpha$  (13). In turn, the induction of PKC- $\alpha$  by PED/PEA-15 prevents subsequent activation of the atypical PKC- $\zeta$  by insulin (13,17). Rescue of PKC- $\zeta$  activity in cells overexpressing PED/PEA-15 restores normal sensitivity to insulin of the glucose transport machinery (17). Thus, in muscle and adipose cells,

PED/PEA-15 generates resistance to insulin action on glucose disposal by impairing normal regulation of PKC- $\zeta$  (17). Characterization of transgenic mice overexpressing PED/PEA-15 ubiquitously evidenced that, in addition to generating insulin resistance and altered glucose tolerance, high levels of PED/PEA-15 impair glucose-regulated insulin secretion (13). Whether this effect is directly caused by the action of PED/PEA-15 in the  $\beta$ -cell and through which mechanism was not conclusively established in these studies. Whether PED/PEA-15-determined  $\beta$ -cell abnormalities are sufficient to impair glucose tolerance in these mice is also unknown.

## RESEARCH DESIGN AND METHODS

**Generation of transgenic mice.** The *rip-1/ped/pea-15* chimeric gene was obtained by introducing a 2.3-Kb *EcoRI* fragment containing the entire human *ped/pea-15* cDNA at the *EcoRI* site in a pB5-RIP- $\beta$ -globin expression vector (kindly provided by Prof. D. Accili, Columbia University, NY). This chimeric gene was microinjected into fertilized C57BL6/SJL mouse eggs. The general procedures used for microinjection and animal selection have been previously described (18). Six F<sub>0</sub> founders were identified by PCR as in reference 13. Mice were fed ad libitum with a standard diet (Research Diets formulas D12328; Research Diets, New Brunswick, NJ) and kept under a 12-h light/12-h dark cycle. Tissue samples were collected rapidly after mice were killed by pentobarbitone overdose. Tissues were snap frozen in liquid nitrogen and stored at  $-80^{\circ}\text{C}$ . All procedures described below were approved by the institutional animal care and utilization committee. Blood glucose levels were measured with glucometers (A. Menarini Diagnostics, Florence, Italy); insulin was measured by radioimmunoassay (RIA) with rat insulin as standard (Insulin Rat RIA kit; Linco Research, St. Louis, MO). Fasting plasma free fatty acids were measured with the Wako NEFA C kit (Wako Chemicals, Richmond, VA), and triglycerides were measured with the Infinity triglyceride reagent (Sigma-Aldrich, St. Louis, MO).

**Determination of glucose and insulin tolerance and assessment of insulin secretion and glucose utilization.** Glucose tolerance tests, insulin tolerance tests, and insulin secretion were measured as previously described (19,20). For analyzing glucose utilization by skeletal muscle, an intravenous injection of 1  $\mu\text{Ci}$  of the nonmetabolizable glucose analog 2-[1-<sup>3</sup>H]deoxy-D-glucose (2-DG) (Amersham Pharmacia Biotech, Piscataway, NJ) and an intraperitoneal injection of insulin (0.75 mU/g body wt) were administered to random fed mice. The specific blood 2-DG clearance was determined with 25- $\mu\text{l}$  blood samples (tail vein) obtained 1, 15, and 30 min after injection as previously reported (21). Skeletal muscles were removed 30 min after the injections. Glucose utilization index was determined by measuring the accumulation of radiolabeled compound (22). The amount of 2-DG-6 phosphate per milligram of protein was then divided by the integral of the concentration ratio of 2-DG to the measured unlabeled glucose. Glucose utilization indexes were expressed as picomoles per milligram of protein per minute.

**Immunohistochemistry and morphometric analysis.** Generation of PED/PEA-15 antibody has been previously reported (8). Immunohistochemical detection of PED/PEA-15, insulin, and glucagon in pancreases from control and transgenic mice were analyzed as described (13). Analysis of serial consecutive islet sections stained with either insulin or PED/PEA-15 antibodies was used to confirm PED/PEA-15 expression in insulin-immunopositive  $\beta$ -cells. Sections were also stained with hematoxylin and eosin. For morphometry, pancreases were obtained from 6-month-old control and transgenic mice, and immunohistochemical detection of insulin was performed in three sections (2–3  $\mu\text{m}$ ) separated by 200  $\mu\text{m}$  as in reference 18.

**Islet isolation, ex vivo insulin secretion assessment, and estimation of pancreatic insulin content.** Islets were isolated from 6-month-old mice by collagenase digestion and subsequent centrifugation on a Histopaque (Sigma-Aldrich) gradient as in reference 23. A total of 20 islets were manually selected and preincubated in Dulbecco's modified Eagle's medium (Life Technologies) at  $37^{\circ}\text{C}$  in a 5% CO<sub>2</sub> atmosphere for 24 h. Islets were then further incubated in Krebs-Ringer buffer (120 mmol/l NaCl, 1.2 mmol/l MgSO<sub>4</sub>, 5 mmol/l KCl, 10 mmol/l NaHCO<sub>3</sub>, 1.3 mmol/l CaCl<sub>2</sub>, and 1.2 mmol/l KH<sub>2</sub>PO<sub>4</sub>) for 30 min and then stimulated at  $37^{\circ}\text{C}$  with various concentrations of either glucose for 1 h, KCl for 30 min, or glyburide (Sigma-Aldrich) for 1 h. Islets were subsequently collected by centrifugation and supernatants assayed for insulin content by RIA. For measuring total pancreatic insulin content, pancreases were solubilized in acid-ethanol solution (75% ethanol, 1.5% HCl) overnight at  $4^{\circ}\text{C}$  and centrifuged for 15 min at 800g. Insulin was measured in the supernatants by RIA.

**Cell culture procedures and transfection.** MIN-6 cells were cultured in Dulbecco's modified Eagle's medium containing 25 mmol/l glucose, 50  $\mu\text{mol/l}$

2-mercaptoethanol, and 10% FCS (Biochrom) at  $37^{\circ}\text{C}$  in a 5% CO<sub>2</sub> atmosphere (24). INS-1 cells were cultured in RPMI-1640 medium (Life Technologies) containing 11 mmol/l glucose, 50  $\mu\text{mol/l}$  2-mercaptoethanol, and 10% fetal bovine serum (Biochrom) at  $37^{\circ}\text{C}$  in a 5% CO<sub>2</sub> atmosphere (25). Stable transfection of the *ped/pea-15* cDNA was performed with the lipofectamine method (13) according to the manufacturer's instructions. Transient transfection of the PKC- $\zeta$  cDNA was also performed with the lipofectamine method. By using PCAGGS- $\beta$ -Gal as a reporter, transfection efficiency was between 65 and 85%, staining with the chromogenic substrate 5-bromo-4-chloro-3-indolyl b-D-galactopyranoside.

**Northern blot and real-time RT-PCR analysis.** Total cellular RNA was isolated from pancreatic islets and tissue samples by using the RNeasy kit (Qiagen Sciences) according to the manufacturer's instructions. Northern blot analysis was performed as in reference 18. For real-time RT-PCR analysis, 1  $\mu\text{g}$  islet or cell RNA was reverse transcribed using Superscript II Reverse Transcriptase (Invitrogen, Carlsbad, CA). PCR were analyzed using SYBR Green mix (Invitrogen). Reactions were performed using Platinum SYBR Green qPCR Super-UDG using an iCycler IQ multicolor Real Time PCR Detection System (Biorad, Hercules, CA). All reactions were performed in triplicate, and  $\beta$ -actin was used as an internal standard. Primer sequences used were as follows: PED/PEA-15 forward 5'-TTCCCGCTGTTCCCTTAGG-3', PED/PEA-15 reverse 5'-TCTGGCTATCCGCATCC-3'; Kir6.2 forward 5'-TC CACCAGGTAGACATCCC-3', inwardly rectifying K<sup>+</sup> channel 6.2 (Kir6.2) reverse 5'-TAGGAGCCAGGTCGTAGAG-3'; sulfonylurea receptor 1 (SUR1) forward 5'-GCATCAACTTGTCTGGTG-3', SUR1 reverse 5'-ACTGTCTCTT GTCATCC-3'; forkhead box A2 (Foxa2) forward 5'-CACCTGAGTCCGAGTCTG 3', Foxa2 reverse 5'-CGAGTTCATGTTGGCGTAG-3'; glucose transporter 2 (Glut2) forward 5'-ACAGTACACCAGCATAC-3', Glut2 reverse 5'-ACCCA CCAAAGAATGAGG3'; glucokinase (GK) forward 5'-GCTGTACGAAAAGAT CATTGG-3', GK reverse 5'-TCCCGTGAACAGAAGATTC-3'; hexokinase (HK)1 forward 5'-ACGACACCCAGAGAATC-3', HK1 reverse 5'-AGTCTC CGAGGCATTACAGC-3'; HK2 forward 5'-CTCAGACACCACAGGCTAC-3', HK2 reverse 5'-TTCACACTGTTGGTCACTAAGG-3'; and  $\beta$ -actin forward 5'-GCGTGACATCAAAGAGAAG-3',  $\beta$ -actin reverse 5'-ACTGTGTTGGCATA GAGG-3'.

**Western blot analysis and PKC assay.** Tissues homogenates and cell lysates were separated by SDS-PAGE and analyzed by Western blot as previously described (13,17,26). Membranes were probed with antibodies to PED/PEA-15 (8), PKC- $\zeta$  (Santa Cruz Biotechnology, Santa Cruz, CA), or tubulin (Santa Cruz Biotechnology). For analyzing atypical PKC activity, cells were incubated with Krebs-Ringer buffer for 30 min and then incubated with either 2.8 or 16.7 mmol/l glucose containing medium for 1 h at  $37^{\circ}\text{C}$  in a 5% CO<sub>2</sub> atmosphere. Cells were solubilized in lysis buffer (25 mmol/l Tris-HCl, pH 7.4, 0.5 mmol/l EDTA, 0.5 mmol/l EGTA, 0.05% Triton X-100, 10 mmol/l  $\beta$ -mercaptoethanol, 1  $\mu\text{g/ml}$  leupeptin, and 1  $\mu\text{g/ml}$  aprotinin) for 1 h at  $4^{\circ}\text{C}$ . Lysates were precipitated with a PKC- $\zeta$  antibody (17), and PKC activity was assayed using the SignATECT PKC assay system (Promega, Madison, WI) according to the manufacturer's instructions. Determination of PKC activity using the Ac-MBP (4–14) or the pseudosubstrate region of PKC- $\epsilon$  (specific for atypical PKC) provided consistent results.

**Statistical procedures.** Data were analyzed with Statview software (Abacus Concepts) by one-factor ANOVA. *P* values  $<0.05$  were considered statistically significant. The total area under the curve for glucose response during the insulin tolerance test was calculated by the trapezoidal method (13).

## RESULTS

To investigate the relevance of PED/PEA-15-induced  $\beta$ -cell dysfunction to glucose tolerance, we used the insulin promoter to generate transgenic mice featuring selective overexpression of PED/PEA-15 in the  $\beta$ -cells ( $\beta$ -tg; Fig. 1A). Three lines of  $\beta$ -tg mice (L5, L8, and L9) were established in which *ped/pea-15* mRNA as well as PED/PEA-15 protein showed a 10- to 20-fold increased expression in the  $\beta$ -cells but unchanged expression in other tissues (Fig. 1B and C). Transgenic mice were fertile and generated viable offsprings showing no significant growth alterations compared with their nontransgenic littermates (controls) or other apparent abnormalities. L8 *ped/pea-15* transgenic mice, both male and female, exhibited slightly reduced fasting blood glucose levels compared with control mice (males  $84 \pm 6$  vs.  $91 \pm 7$  mg/dl; females  $82 \pm 8$  vs.  $92 \pm 6$  mg/dl; significant at  $P < 0.05$ ). Similarly reduced fasting blood glucose levels were mea-

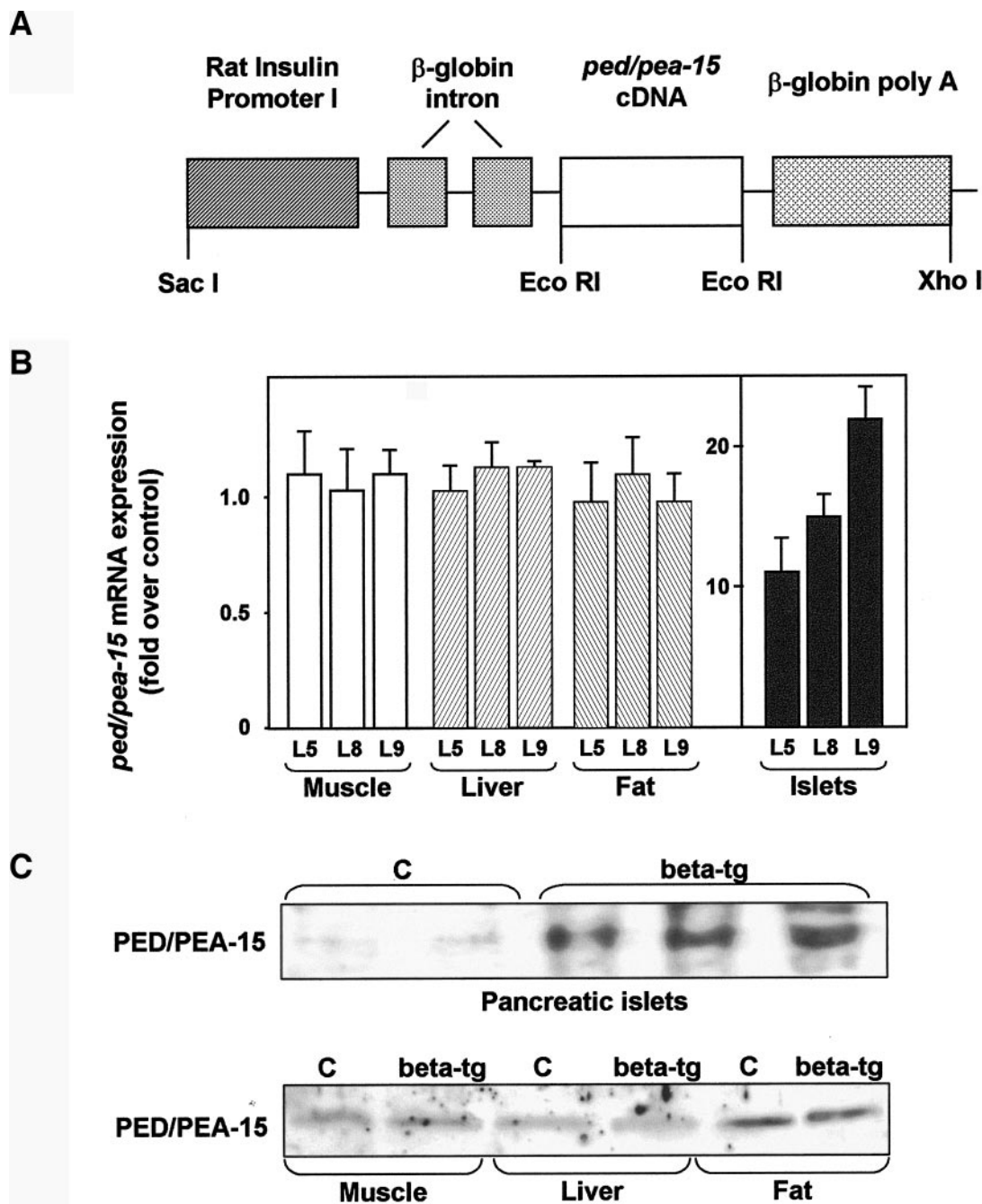


**FIG. 1.** Generation of  $\beta$ -tg (beta-tg) mice. **A:** Subcloning of the *ped/pea-15* cDNA in the pB5-RIP- $\beta$ -globin expression vector. Tissues are from three lines of  $\beta$ -tg mice (L5, L8, and L9) and from their nontransgenic littermates (C) and were subjected to Northern (**B**) or Western (**C**) blotting. Northern blots (30  $\mu$ g RNA/lane) were probed with *ped/pea-15* cDNA. Loading of the same amount of RNA in each lane was ensured by further blotting the filters for  $\beta$ -actin. Quantitation was performed by densitometric analysis. Data are plotted as increase of *ped/pea-15* mRNA expression in transgenic versus control mice. Each bar represents the means  $\pm$  SD of determinations in five transgenic and five nontransgenic animals. For Western blotting, tissue lysates (100  $\mu$ g proteins/lane) were blotted with the PED/PEA-15 antiserum. The autoradiographs shown are representative of five (*top*) and six (*bottom*) independent experiments.

sured in the other transgenic lines (data not shown). However, glucose loading (2 g/kg) rendered the  $\beta$ -tg mice significantly more hyperglycemic during the following 120 min compared with control mice (Fig. 2A and B). Very similar abnormalities were observed in the L5 and L9 lines (data not shown), indicating that  $\beta$ -cell overexpression of PED/PEA-15 is sufficient to impair glucose tolerance in mice. As shown in Fig. 2, sex had no effect on the impairment in glucose tolerance caused by  $\beta$ -cell overexpression of PED/PEA-15. Aging (3–14 months) also deter-

mined no significant changes in PED/PEA-15-induced decreases in glucose tolerance (data not shown).

L8  $\beta$ -tg mice featured no significant differences in fasting nonesterified free fatty acid and triglyceride blood concentrations compared with their controls (free fatty acids  $0.82 \pm 0.03$  vs.  $0.78 \pm 0.05$  mmol/l; triglycerides  $115 \pm 7$  vs.  $111 \pm 8$  mg/dl). However, fasting insulin levels were 80% increased in the transgenics ( $0.31 \pm 0.07$  vs.  $0.17 \pm 0.03$ ;  $P < 0.001$ ). The same results were obtained in the L5 and the L9 lines, with no sex- or age-related variation (data not

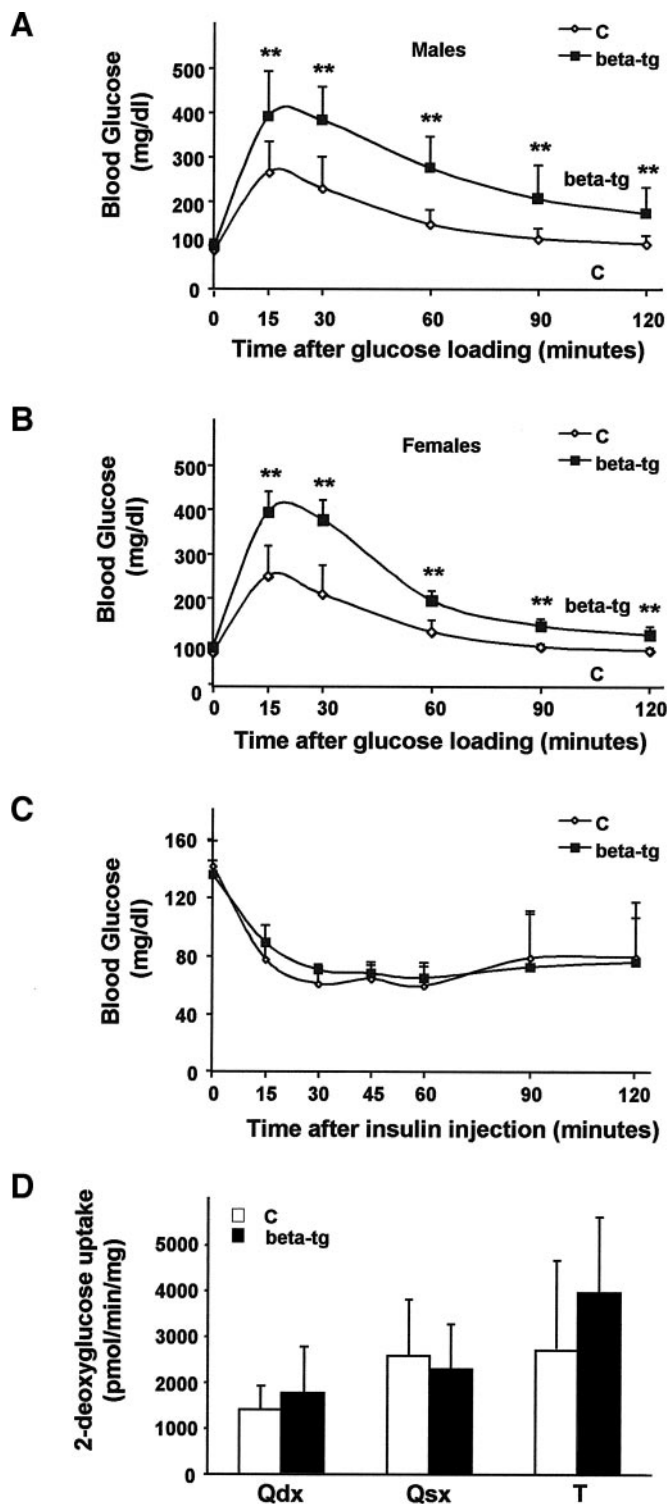


**FIG. 2.** Glucose tolerance, insulin sensitivity, and glucose transport in  $\beta$ -tg mice. Three-month-old  $\beta$ -tg male (A) and female (B) mice and their nontransgenic littermates (C) were fasted for 16 h and subjected to intraperitoneal glucose loading (2 g/kg body wt). Blood glucose levels were determined before and at the indicated times following the load. Values are expressed as means  $\pm$  SD of determinations in at least 12 (A) and 15 (B) mice per group. \*Statistically significant differences ( $*P < 0.05$ ;  $**P < 0.01$ ). C: Three-month-old random, fed  $\beta$ -tg mice and their nontransgenic littermates (C) ( $n = 12$ /group; 6 males and 6 females) were injected intraperitoneally with insulin (0.75 mU/g body wt), followed by determinations of blood glucose levels at the indicated times. Values are expressed as means  $\pm$  SD. D: Weight-matched, random, fed  $\beta$ -tg mice and their nontransgenic littermates were subjected to intravenous injection of 1  $\mu$ Ci of 2-DG and intraperitoneal injection of insulin. Tibialis (T) and right (dx)

shown). To verify whether  $\beta$ -cell overexpression of PED/PEA-15 is accompanied by reduced insulin sensitivity, we performed insulin tolerance tests. Intraperitoneal injection of insulin (0.75 mU/g) evoked comparable hypoglycemic responses in both  $\beta$ -tg and control mice (Fig. 2C) with no significant difference in glucose areas under the curve in all of the transgenic lines (C  $9,180 \pm 1,900$  mg/dl per 120 min; L5  $8,898 \pm 1,800$  mg/dl per 120 min; L8  $8,805 \pm 1,600$  mg/dl per 120 min; L9  $9,121 \pm 1,600$  mg/dl per 120 min). Furthermore, insulin-dependent glucose uptake in quadriceps and tibialis muscles from  $\beta$ -tg and control mice exhibited no difference (Fig. 2D).

We then investigated how glucose tolerance is reduced in the  $\beta$ -tg and analyzed their islets by immunohistochemistry and morphometry. Islets from  $\beta$ -tg mice immunostained with PED/PEA-15 antibody significantly more intensely than those from control mice (Fig. 3A). Importantly, islets from the  $\beta$ -tg mice were larger and showed a more elongated and irregular shape but feature normal distribution of  $\alpha$ - and  $\beta$ -cells compared with control islets (Fig. 3B). Also, quantitative morphometry revealed two-fold increased islet and  $\beta$ -cell mass per unit of total pancreatic area in the  $\beta$ -tg mice ( $P < 0.01$ ) with no significant difference in their pancreas weight (Table 1).

In control mice, a sevenfold increase in insulin secretion was observed 3 min after intraperitoneal glucose injection, and the levels remained higher than baseline values for up to 30 min, indicating second-phase response (Fig. 3C). Based on the area under the curve, the acute first-phase insulin secretory response to glucose was reduced by more than threefold in  $\beta$ -tg mice ( $P < 0.001$ ). The second-phase response was also significantly impaired in the  $\beta$ -tg compared with control mice ( $P < 0.001$ ). Again, almost identical decreases in early and late insulin responses were observed in both male and female  $\beta$ -tg mice and in all of the lines produced (data not shown). Thus, in vivo, isolated  $\beta$ -cell overexpression of PED/PEA-15 increases fasting insulinemia but impairs further insulin secretion response to hyperglycemia.

Similar as in intact mice,  $\beta$ -tg mouse islets also exhibited a twofold increased insulin release when incubated in medium containing 2.8 mmol/l glucose (Fig. 4A;  $P < 0.001$ ). Raising glucose concentration did not further increase the insulin release by these islets, while enhancing that from control mice by 3.9-fold ( $P < 0.001$ ). Similarly, islets from transgenic mice ubiquitously expressing PED/PEA-15 (13) showed 2.4-fold increased insulin release when exposed to 2.8 mmol/l glucose ( $P < 0.001$ ) and no further release upon exposure to 16.7 mmol/l glucose (Fig. 4B). At variance with glucose, exposure to the membrane depolarising agent potassium chloride (33 mmol/l) caused a comparable release of insulin by the  $\beta$ -tg and the control islets, suggesting an effect of PED/PEA-15 on earlier events of  $\beta$ -cell response to glucose. Total insulin content in pancreases was 25% increased in  $\beta$ -tg mice ( $2.9 \pm 0.4$  ng/mg in  $\beta$ -tg vs.  $2.3 \pm 0.2$  ng/mg in control mice;  $P < 0.05$ ).

To gain further insight into the mechanisms leading to dysfunction of  $\beta$ -cells overexpressing PED/PEA-15, we have profiled the expression of several genes relevant to the glucose sensory apparatus by real-time RT-PCR analysis of total RNA isolated from islets of  $\beta$ -tg mice (Fig. 4C).

and left (sx) quadriceps (Q) muscles were removed 30 min after and snap frozen in liquid nitrogen. 2-DG accumulated in muscle tissues was quantitated as described in RESEARCH DESIGN AND METHODS. Bars represent mean values  $\pm$  SD of determinations in at least seven mice/group.

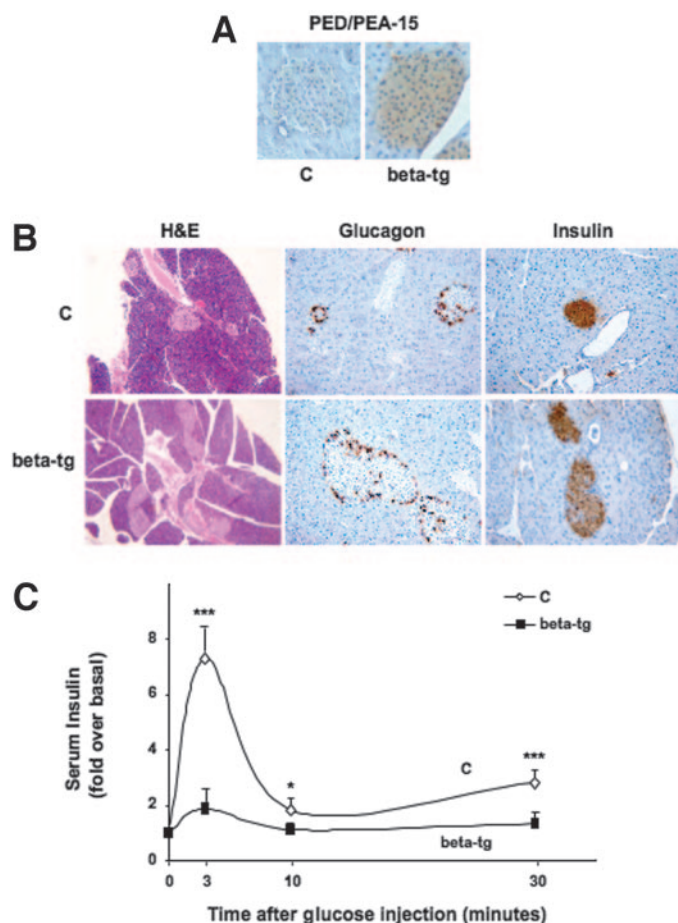


**FIG. 3.** Immunohistochemical analysis and insulin secretion in  $\beta$ -tg mice. **A** and **B**: Pancreases from  $\beta$ -tg and control (C) 6-month-old mice were fixed and embedded in Tissue-Tek OTC, and sections were prepared as described in RESEARCH DESIGN AND METHODS. Sections were stained with hematoxylin and eosin (H&E). Immunohistochemical analysis of the islets was carried out using PED/PEA-15 (**A**) or insulin or glucagon (**B**) antibodies, as indicated. Anti-goat or anti-rabbit immunoglobulin G was used as the second antibody. Immunoreactivity was revealed by peroxidase-labeled streptavidin. The microphotographs shown (H&E 200 $\times$ ; glucagon and insulin 400 $\times$ ) are representative of images obtained from eight transgenic (male/female = 1) and eight nontransgenic (male/female = 1) mice. Note that  $\beta$ -tg mice show an increased number of enlarged islets. **C**:  $\beta$ -Tg and control mice (C) were fasted overnight and then injected with glucose (3 g/kg body wt) intraperitoneally. Serum insulin concentrations were measured at the indicated times by RIA. Data points represent the means  $\pm$  SD of determinations in 10  $\beta$ -tg and 12 control mice. \*Statistically significant differences (\* $P < 0.05$ ; \*\*\* $P < 0.001$ ).

The amounts of mRNAs for the *Sur1* subunit of the ATP-sensitive  $K^+$  channel was significantly reduced by 30% in these islets compared with those in control mice ( $P < 0.001$ ). Consistently, islets from both the  $\beta$ -tg and the transgenic mice featuring ubiquitous overexpression of PED/PEA-15 exhibited no secretory response to the  $K^+$  channel locking agent glyburide (Fig. 4D). RNAs encoding the *Kir6.2* potassium channel subunit and the *Sur1/Kir6.2* upstream regulator *Foxa2* were also reduced, respectively, by 30 and 35% in the islets from the *ped/pea-15*  $\beta$ -cell-specific transgenics ( $P < 0.01$ ). Decreased expression of *Sur1*, *Kir6.2*, and *Foxa2* mRNAs was confirmed by Northern blot analysis (Fig. 4E). At variance, the abundance of *glucokinase*, *HK1*, *HK2*, and *GLUT2* mRNAs did not differ between transgenic and control mice (Fig. 4C and E).

A  $\sim$ 35% decrease in the abundance of the *Sur1*, *Kir6.2*, and *Foxa2* mRNAs has also been observed in the glucose-

**TABLE 1**  
Morphometric analysis of  $\beta$ -tg pancreas

	Control	$\beta$ -Tg
% islet area/pancreatic area	0.52 $\pm$ 0.06	1.04 $\pm$ 0.11**
% $\beta$ -cells/islet	76.87 $\pm$ 4.66	81.33 $\pm$ 2.08*
% $\alpha$ -cells/islet	17.23 $\pm$ 1.92	14.54 $\pm$ 1.85 NS
% other cells/islet	5.90 $\pm$ 0.71	4.13 $\pm$ 0.41 NS
Pancreas weight (mg)	182 $\pm$ 16	188 $\pm$ 12 NS
Islet cell mass (mg)	0.95 $\pm$ 0.08	1.96 $\pm$ 0.06**
$\beta$ -Cell mass (mg)	0.73 $\pm$ 0.05	1.59 $\pm$ 0.06**

Data are means  $\pm$  SD in six  $\beta$ -tg and six control (nontransgenic littermates) mice. Mice were analyzed as described in RESEARCH DESIGN AND METHODS. \* and \*\* denote statistically significant differences, respectively, at the  $P < 0.05$  and 0.01 levels.

responsive MIN-6 and INS-1  $\beta$ -cell lines upon transfection with *ped/pea-15* cDNA (Min-6<sub>ped/pea-15</sub>, INS-1<sub>ped/pea-15</sub>; Fig. 5A;  $P < 0.001$ ). As in the mouse islets, these changes were accompanied by a significantly greater release of insulin when in low-glucose medium (2.8 mmol/l glucose) with no further insulin secretion upon exposure to 16.7 mmol/l glucose (Fig. 5B;  $P < 0.001$ ). This raise in glucose concentration caused a 2.5- and 4-fold enhancement in insulin secretion, respectively, by the untransfected INS-1 and MIN-6 cells, however. In both the mouse islets and the cultured  $\beta$ -cell lines, the effect of glucose on insulin release was paralleled by a twofold increase in immunoprecipitated PKC- $\zeta$  activity, with no measurable change in its expression (Fig. 5C). Interestingly, however, the effect of glucose was almost completely abolished in cells overexpressing PED/PEA-15 whether the MIN-6 or the  $\beta$ -tg mouse islets. Similar data were obtained in the INS-1 cells (data not shown), further suggesting an important role of atypical PKCs in regulating genes of the insulin secretion pathway. To further analyze this issue, we forced the expression of PKC- $\zeta$  in the MIN-6<sub>ped/pea-15</sub> and the INS-1<sub>ped/pea-15</sub> cells. The overexpression largely rescued PKC- $\zeta$  activity in the precipitates from glucose-exposed MIN-6<sub>ped/pea-15</sub> cells (Fig. 6A). Importantly, this rescue was accompanied by recovery of the *Sur1*, *Kir6.2*, and *Foxa2* gene expression (Fig. 6B). In part, the changes in insulin release caused by PED/PEA-15 were also reverted, determining recovery of glucose-induced insulin secretion (Fig. 6C). The same results were obtained using the INS-1 cells (data not shown), indicating that the changes in atypical PKC function caused by PED/PEA-15 overexpression represent upstream abnormalities impairing the function of multiple genes involved in regulating insulin secretion by the  $\beta$ -cell.

To further address this issue, we used islets from *ped/pea-15*-null mice. These animals have been previously characterized and reported (27) and feature no PED/PEA-15 expression in  $\beta$ -cells (Fig. 7A). Importantly, islets from these animals evidenced a twofold increased PKC- $\zeta$  activation following glucose exposure, as compared with islets from control mice ( $P < 0.01$ ; Fig. 7B). In parallel with this enhanced response, islets from the *ped/pea-15*-null mice exhibited a significant twofold increase in sensitivity to glucose and glyburide effect on insulin secretion compared with control islets, with unchanged response to potassium chloride ( $P < 0.001$ ; Fig. 7C). Abundance of the *Sur1*, *Kir6.2*, and *Foxa2* mRNAs was also increased by 45% in these islets ( $P < 0.001$ ; Fig. 7D), indicating that these genes represent major effectors through which PED/PEA-15 physiologically controls insulin secretion.

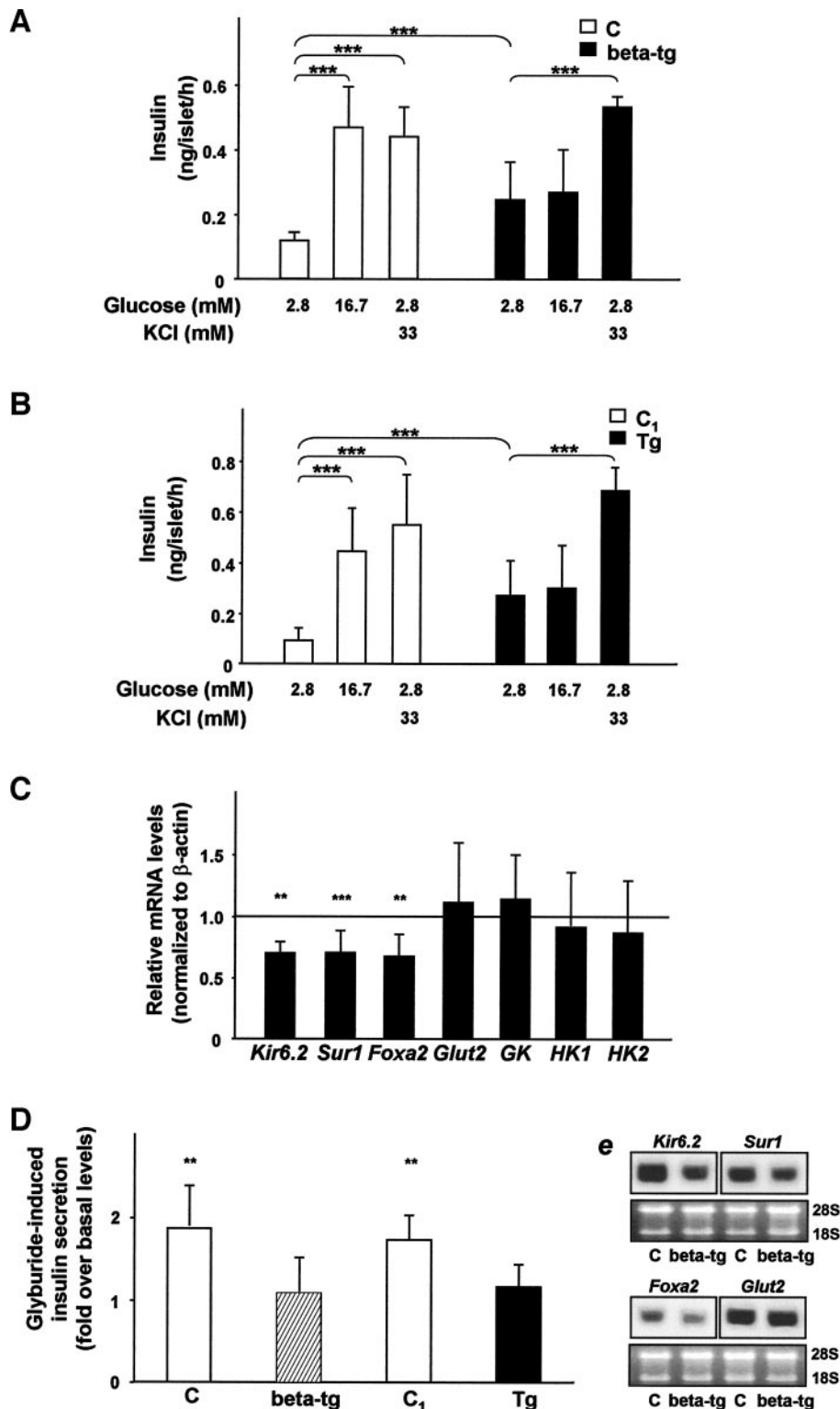


FIG. 4. Insulin secretion and gene expression profile in isolated islets from PED/PEA-15-overexpressing mice. Islets were isolated from 6-month-old mice, either from the  $\beta$ -tg and their nontransgenic littermates (C, open bars) (A) or from transgenic mice ubiquitously overexpressing PED/PEA-15 (33) and their nontransgenic littermates (C<sub>1</sub>, open bars) (B). Insulin release was determined upon exposure to the indicated concentrations of glucose or potassium chloride as described in RESEARCH DESIGN AND METHODS. Bars represent the means  $\pm$  SD of determinations in 12 (A) and 11 (B) independent experiments in duplicate. C: The abundance of mRNAs for the indicated proteins was determined by real-time RT-PCR analysis of total RNA isolated from islets of  $\beta$ -tg mice and their nontransgenic littermates using  $\beta$ -actin as internal standard. The mRNA levels in  $\beta$ -tg islets are relative to those in control animals (C). Each bar represents the mean  $\pm$  SD of four independent experiments in each of whom reactions were performed in triplicate using the pooled total RNAs from six mice/genotype. D: Islets were isolated from 6-month-old  $\beta$ -tg and ubiquitously PED/PEA-15-overexpressing transgenic mice and their nontransgenic littermates (respectively, C and C<sub>1</sub>). Insulin release was determined after exposure to 10  $\mu$ mol/l glyburide for 60 min, as described in RESEARCH DESIGN AND METHODS. Bars represent the means  $\pm$  SD of data from four independent experiments, each with at least three mice/group. \*Statistically significant differences (\*\* $P$  < 0.01; \*\*\* $P$  < 0.001). E: Total RNA isolated from  $\beta$ -tg and control (C) islets was analyzed by agarose-formaldehyde electrophoresis and hybridized to the indicated cDNA probes. 28S and 18S ribosomal RNA is shown as a loading control.

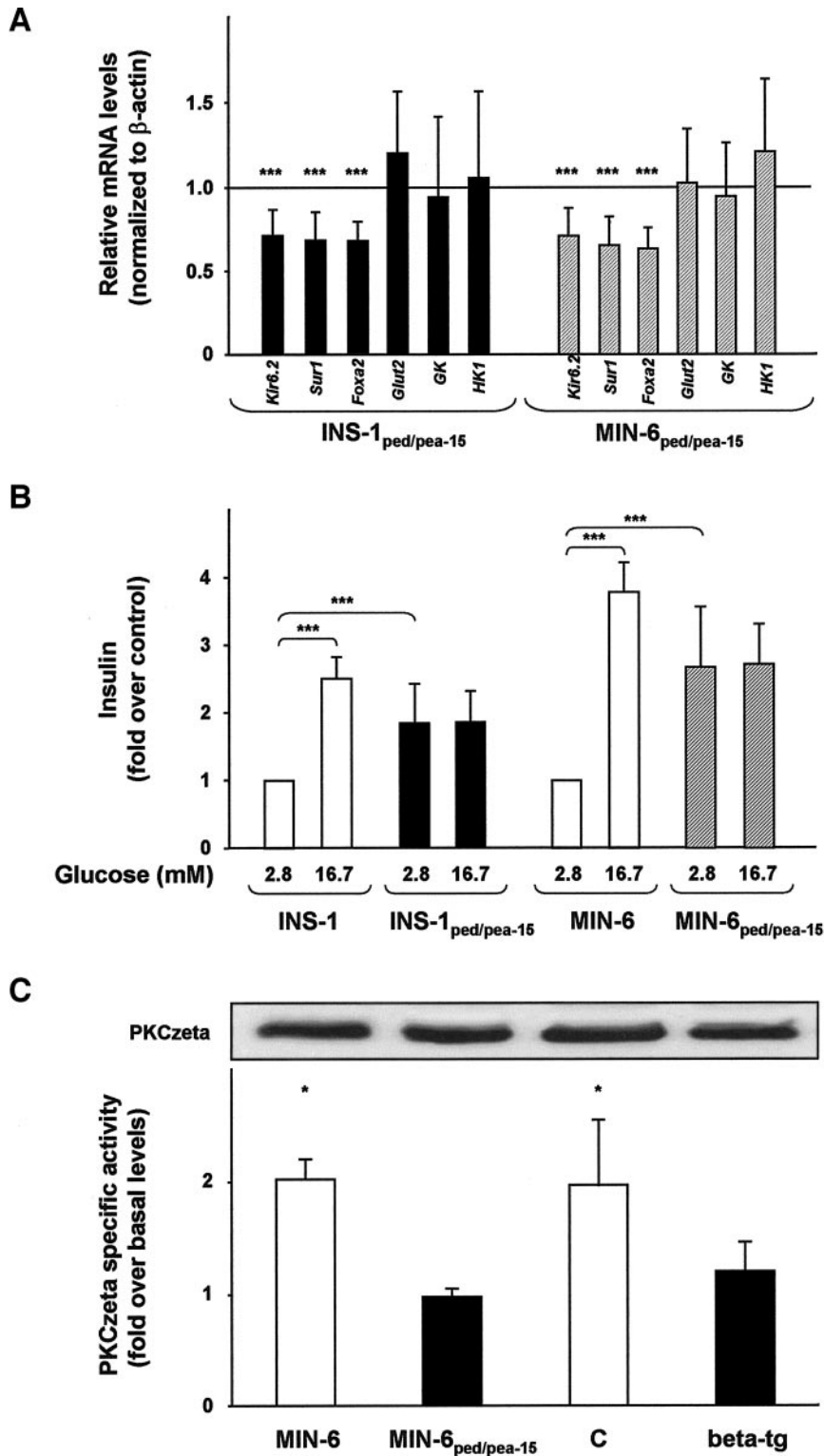
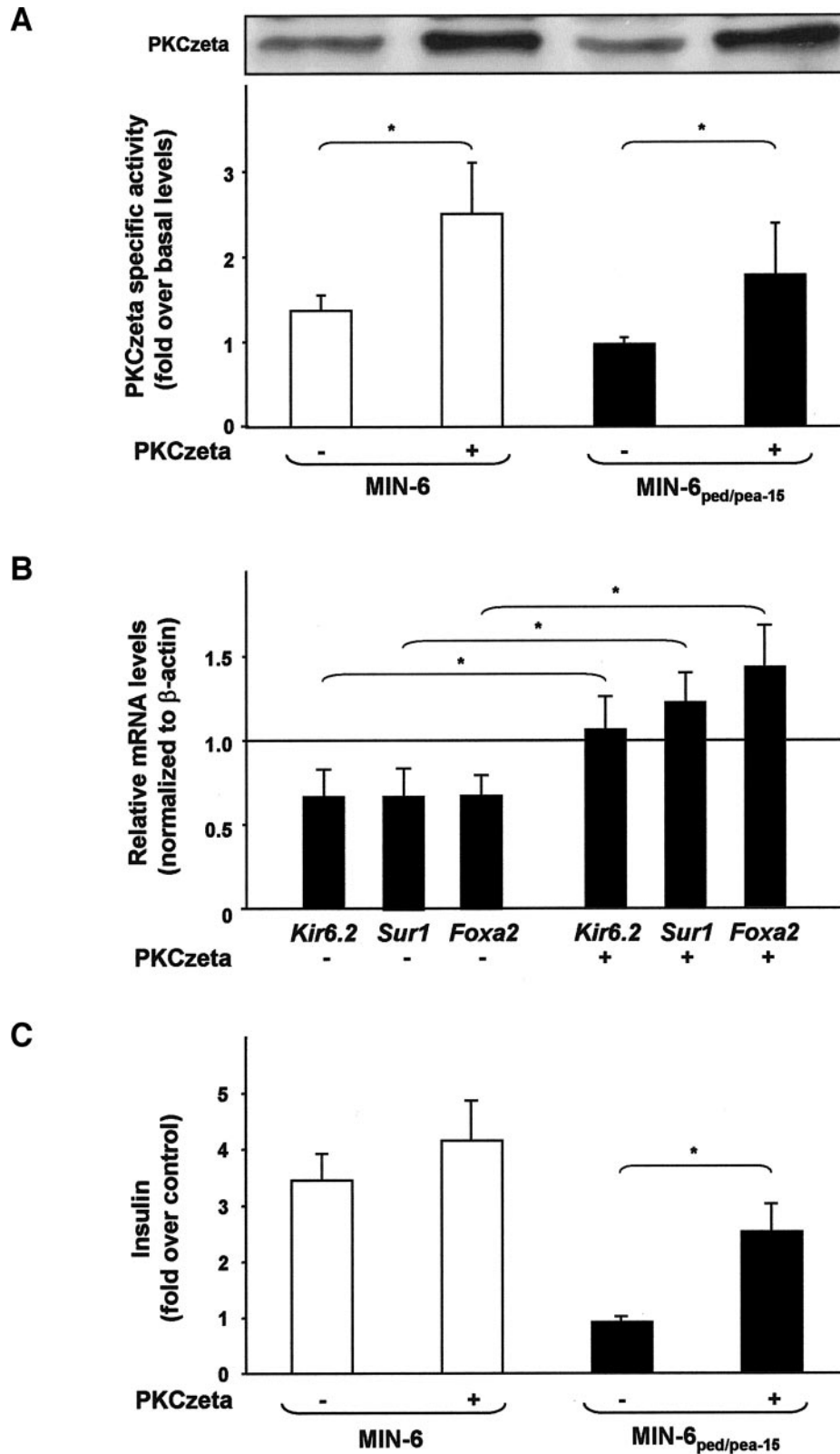
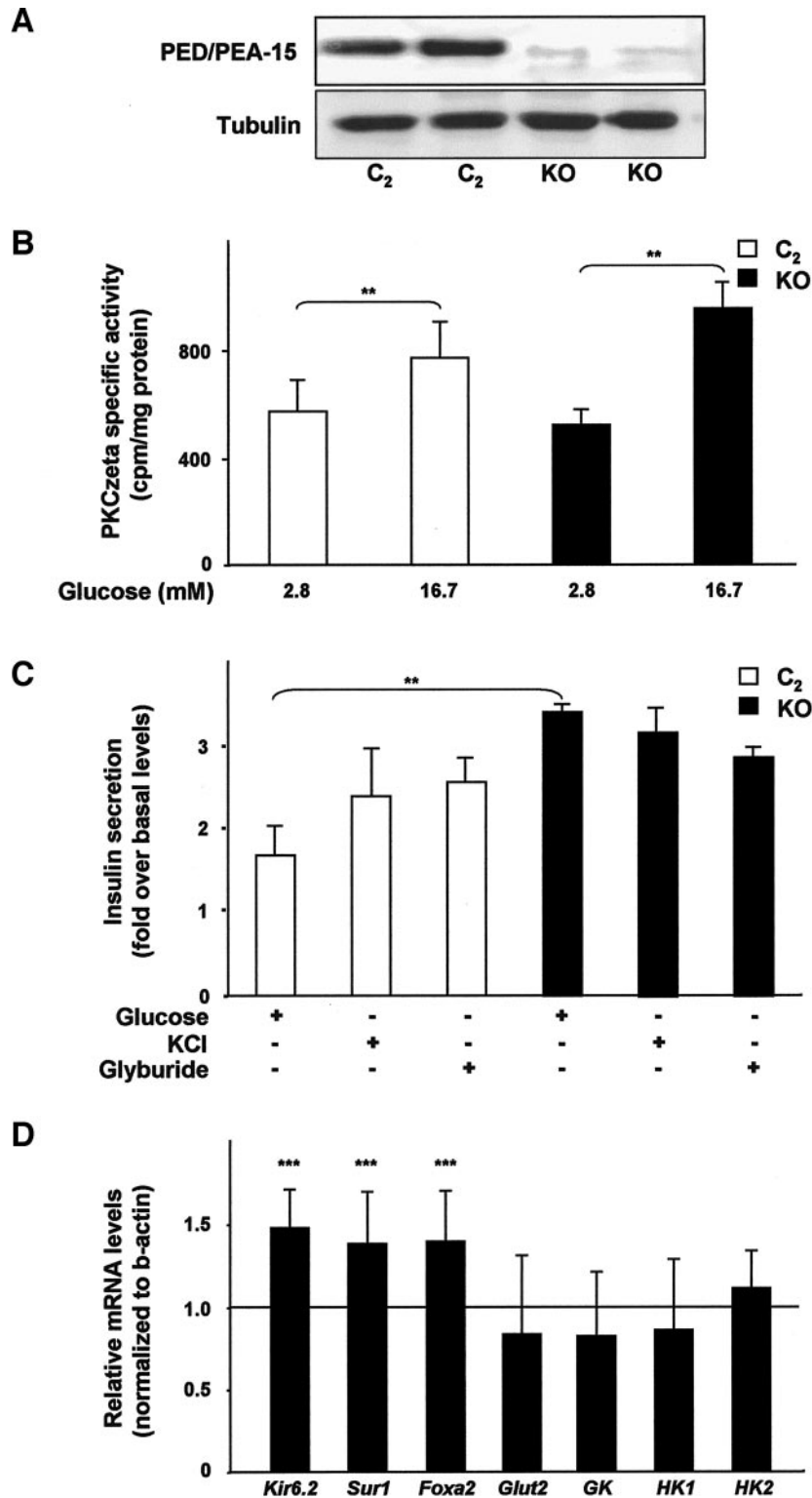


FIG. 5. Gene expression profile, glucose-stimulated insulin secretion and PKC- $\zeta$  activity in  $\beta$ -cell lines overexpressing PED/PEA-15. **A:** The abundance of mRNAs for the indicated proteins was determined by real-time RT-PCR analysis of total RNA isolated from INS-1 and MIN-6 wild-type cells and from the same cells stably transfected with a *ped/pea-15* cDNA (INS-1<sub>ped/pea-15</sub> and MIN-6<sub>ped/pea-15</sub>). Bars represent the mRNA levels in the transfected cells and are relative to those in wild-type (control) cells. Data are expressed as means  $\pm$  SD of triplicate reactions for total RNAs from each cell type in five independent experiments. **B:** Insulin release was assayed by RIA in the culture medium of the wild-type and the *ped/pea-15*-transfected  $\beta$ -cells upon 60 min incubation with the indicated glucose concentrations. Bars represent mean values  $\pm$  SD from six independent experiments each in duplicate. **C:** Islet from  $\beta$ -tg and control mice (*right*) and wild-type MIN-6 cells and those stably expressing the *ped/pea-15* cDNA (MIN-6<sub>ped/pea-15</sub>; *left*) were exposed to 16.7 mmol/l glucose for 60 min and then solubilized. A total of 100  $\mu$ g proteins were then precipitated with PKC- $\zeta$  antibody, and PKC activity was assayed as described in RESEARCH DESIGN AND METHODS. PKC activity is expressed as fold increase over basal activity (measured in the presence of 2.8 mmol/l glucose). Bars represent the mean  $\pm$  SD of data from four independent experiments. For control, aliquots of the cell lysates were normalized for protein and directly blotted with PKC- $\zeta$  antibodies. Blots were revealed by enhanced chemiluminescence and autoradiography. The blot shown in the inset is representative of those in the other three experiments. \*Statistically significant differences (\* $P$  < 0.05; \*\*\* $P$  < 0.001).



**FIG. 6.** Rescue of PKC- $\zeta$  activity, gene expression profile, and glucose-stimulated insulin secretion in MIN<sub>ped/pea-15</sub> cells. **A:** MIN-6 and MIN-6<sub>ped/pea-15</sub> cells were transiently transfected with a PKC- $\zeta$  cDNA, solubilized, and lysates immunoprecipitated with a PKC- $\zeta$  antibody. PKC activity was assayed in the immunoprecipitates. For control, aliquots of the lysates were blotted with the PKC- $\zeta$  antibody (*inset*). Bars represent the means  $\pm$  SD of five independent experiments in duplicate. The autoradiograph shown in the inset is representative of blots from the five experiments. **B:** The abundance of mRNAs for the indicated proteins was determined by real-time RT-PCR analysis of total RNA isolated from MIN-6 and MIN-6<sub>ped/pea-15</sub> cells. Bars represent the mRNA levels in the MIN-6<sub>ped/pea-15</sub> cells and are relative to those in the untransfected cells (MIN-6). Data are expressed as means  $\pm$  SD of triplicate reactions for total RNAs from each cell type in four independent experiments. **C:** The MIN-6 cells, either those transiently transfected with the PKC- $\zeta$  cDNA and the untransfected cells, were exposed to 16.7 mmol/l glucose for 60 min, and insulin release in the culture medium was assayed by RIA as described in RESEARCH DESIGN AND METHODS. Bars represent the means  $\pm$  SD of duplicate determinations in three independent experiments. \*Statistically significant differences ( $*P < 0.05$ ).



**FIG. 7.** PKC- $\zeta$  activity, insulin secretion, and gene expression profile in isolated islets from *ped/pea-15*-null mice. **B:** Islets were isolated from 6-month-old *ped/pea-15*-null mice (KO) and, for control, from their unmodified littermates (C<sub>2</sub>). The islets were exposed to glucose as indicated, solubilized, and precipitated with PKC- $\zeta$  antibodies. PKC activity was assayed in the immunoprecipitates as described in RESEARCH DESIGN AND METHODS. PKC activity is expressed as fold increase over basal activity (measured in the presence of 2.8 mmol/l glucose). Bars represent the means  $\pm$  SD of four independent experiments, each in which two mice/group were used. Aliquots of the lysates were blotted with PED/PEA-15 antibodies (A). For control, filters were probed with tubulin antibodies. The autoradiographs shown are representative of the blots performed in each of the four experiments. **C:** Islets from knockout and control mice were exposed to glucose, potassium chloride, or glyburide as indicated, and insulin was assayed in the culture medium by RIA. Insulin release is expressed as fold increase in medium insulin concentration over the basal (measured with cells exposed to 2.8 mmol/l glucose alone). Bars represent mean values  $\pm$  SD of data with islets from at least six mice in each group. **D:** The abundance of mRNAs for the indicated proteins was determined by real-time RT-PCR analysis of total RNA isolated from islets of *ped/pea-15*-null mice and their unmodified littermates, using  $\beta$ -actin as internal standard. The mRNA levels in knockout islets are relative to those in islets from the unmodified littermates. Each bar represents the mean  $\pm$  SD of four independent experiments, each in which reactions were performed in triplicate using the pooled total RNAs from six mice/genotype. \*Statistically significant differences (\*\* $P < 0.01$ ; \*\*\* $P < 0.001$ ).

## DISCUSSION

In the present study, we generated transgenic mice overexpressing PED/PEA-15 selectively in  $\beta$ -cells ( $\beta$ -tg mice). We found that PED/PEA-15 overexpression determines islet hyperplasia with a specific increase in  $\beta$ -cell mass. This may result from a direct effect on  $\beta$ -cell survival as PED/PEA-15 exerts a broad antiapoptotic action in a number of different cell types (10,15,27–30), including  $\beta$ -cells (C.M., unpublished observation). Increased  $\beta$ -cell mass is consistent with the increased fasting serum insulin levels detected in the  $\beta$ -tg mice. Indeed, these mice do not feature resistance to insulin action. They do show grossly impaired glucose tolerance and reduced insulin secretion in response to hyperglycemia, however. This latter defect is comparable with that occurring in mice with ubiquitous overexpression (13), leading us to conclude that  $\beta$ -cell overexpression of PED/PEA-15 is sufficient to impair glucose tolerance in mice. Previous studies in isolated cells and in vivo evidenced that chronic insulin resistance may impair  $\beta$ -cell function, ultimately reducing glucose response (2). Secondary impairment of  $\beta$ -cell function may also occur in the transgenic mice overexpressing PED/PEA-15 ubiquitously. However, the findings in the present study evidence that impaired response to glucose is a direct consequence of PED/PEA-15 overexpression in the  $\beta$ -cells. Consistently, islets from  $\beta$ -tg mice persistently show similarly impaired glucose response in culture as well as in the intact animal. Also, the expression of *ped/pea-15* cDNA in different  $\beta$ -cell lines inhibits insulin release following increased glucose concentration in the culture medium.

The defective insulin secretion induced by  $\beta$ -cell overexpression of PED/PEA-15 affected both the early and the late phases of insulin response to glucose, raising the possibility that the overexpression of PED/PEA-15 impairs the glucose-sensing machinery. Earlier reports evidenced that the KIR6.2 and SUR1 potassium channel subunits couple glucose metabolism to the electrical activity of  $\beta$ -cell membrane and insulin secretion by setting the resting membrane potential below the activation threshold for voltage-gated  $\text{Ca}^{2+}$  channels (31). We found that the membrane depolarizing agent potassium chloride causes a similar release of insulin by both transgenic and control mouse islets, indicating that the site of PED/PEA-15 action on glucose-induced secretion is upstream the membrane depolarization step. Indeed,  $\beta$ -cell expression profiling revealed that mRNA abundance of both the *Kir6.2* and the *Sur1* transcripts are significantly depressed by the overexpression of *ped/pea-15*. PED/PEA-15 action on the *Kir6.2* and *Sur1* genes represents a specific abnormality, as other genes encoding key components of the glucose-sensitive insulin secretion machinery were unaffected by PED/PEA-15. The latter include *GLUT2*, *HK1*, and *HK2*. Consistent with the functional consequence of this defect, glyburide showed impaired action on insulin secretion in PED/PEA-15-overexpressing islets.

Previous studies in mice evidenced that ablation of either the *Sur1* or the *Kir6.2* genes results in a phenotype reminiscent of that characterizing the  $\beta$ -tg mice (32–34). Indeed, both the *Sur1*<sup>-/-</sup> and the *Kir6.2*<sup>-/-</sup> mice feature blunted insulin secretion response to sulfanylureas. The defective insulin response to the sulfanylurea glyburide seems even more pronounced in the  $\beta$ -tg mice as, in these animals, <30% decrease in *Sur1* and *Kir6.2* gene expression blocks glyburide action. The simultaneous impair-

ment in *Sur1* and *Kir6.2* gene function may result in an additive effect on glyburide action in the  $\beta$ -tg mice. Similar to the  $\beta$ -tg, fasted *Sur1*<sup>-/-</sup> mice are more hyperinsulinemic than control animals due to persistent activation of voltage-gated calcium channels (33,34). These mice are also significantly more hypoglycemic than controls when fasted. Furthermore, both the *Sur1*<sup>-/-</sup> and the *Kir6.2*<sup>-/-</sup> mice feature impaired glucose tolerance and glucose-induced first- and second-phase insulin secretion. Thus, at least in part, the loss of potassium channels caused by  $\beta$ -cell overexpression of PED/PEA-15 may account for the abnormalities in basal and glucose-stimulated insulin secretion and in glucose tolerance observed in the  $\beta$ -tg mice.

Recent evidence in skeletal muscle and fat indicated that high cellular levels of PED/PEA-15 impair the function of the atypical PKC isoform PKC- $\zeta$  through a phospholipase D-mediated mechanism (13,17). Interestingly, the activity of PKC- $\zeta$  is also decreased in islets from the  $\beta$ -tg transgenics compared with those from control mice. PKC- $\zeta$  overexpression in  $\beta$ -cells transfected with a *ped/pea-15* cDNA simultaneously rescues glucose-induced insulin secretion and the expression of the *Sur1* and *Kir6.2* genes. These data evidence that PKC- $\zeta$  activation is sufficient to upregulate these genes, while not proving that the loss of PKC- $\zeta$  accompanying PED/PEA-15 overexpression causes *Sur1* and *Kir6.2* downregulation. Another atypical PKC isoform, PKC- $\lambda$ , has recently been shown to play a major role in regulating glucose-induced insulin secretion by modulating the expression of a number of pancreatic  $\beta$ -cell genes (35). However, the latter report did not exclude that, as we now show, the activation of PKC- $\zeta$  may also upregulate *Sur1* and *Kir6.2* gene function. Indeed, while clearly distinct and involved in a number of specialized mechanisms, PKC- $\zeta$  and - $\lambda$  also feature structural similarities and many common functions (36). Downregulation of PKC- $\zeta$  and/or - $\lambda$  may cause impaired glucose-induced insulin response in  $\beta$ -tg mouse islets by reducing *Sur1* and *Kir6.2* gene expression.

Atypical PKCs have been reported to control the function of a number of transcription factors (37,38). Very recent data by Hashimoto et al. (35) evidenced that in PKC- $\lambda$ -null mice, the abundance of pancreatic  $\beta$ -cells, the expression of the *Foxa2* mRNA in addition to that of *Sur1* and *Kir6.2*, is significantly reduced. In addition, in pancreatic  $\beta$ -cells, the expression of the *Sur1* and *Kir6.2* genes is dependent on *Foxa2* activity (25,39,40). Similar to the PKC $\lambda$ <sup>-/-</sup> mice, we now report that *Foxa2* mRNA abundance is also reduced in islets from  $\beta$ -tg transgenics. Thus, the impaired activity of PKC- $\zeta$  in  $\beta$ -cells overexpressing PED/PEA-15 may also prevent normal potassium channel generation and glucose-regulated secretion of insulin by depressing *Foxa2* expression. Supporting this conclusion, we evidenced that forcing the expression of PKC- $\zeta$  in PED/PEA-15-overexpressing  $\beta$ -cells rescued *Foxa2* levels, in addition to those of *Kir6.2* and *SUR1*, and glucose-induced insulin secretion. Importantly, islets from *ped/pea-15*-null mice feature upregulated PKC- $\zeta$  function. The enhanced PKC- $\zeta$  activity is accompanied by specific increases in the abundance of *Kir6.2*, *Sur1*, and *Foxa2* mRNAs and augmented insulin secretion in response to glucose. Thus, *Foxa2*-mediated control of glucose sensitivity represents a physiological function of PED/PEA-15 in the  $\beta$ -cell. Dysregulation of this mechanism may be relevant for type 2 diabetes in humans as well.

## ACKNOWLEDGMENTS

This work was supported, in part, by the European Community's FP6 EUGENE2 (LSHM-CT-2004-512013) grants from the European Foundation for the Study of Diabetes to F.B., the Associazione Italiana per la Ricerca sul Cancro (AIRC) to F.B. and P.F., and the Ministero dell'Università e della Ricerca Scientifica (PRIN to F.B. and P.F. and FIRB RBNE0155LB to F.B.) and a grant from Association pour la Recherche contre le Cancer (no. 3500 to H.C.). The financial support of Telethon-Italy is gratefully acknowledged.

The technical help of Salvatore Sequino is also acknowledged.

## REFERENCES

- De Fronzo RA: Pathogenesis of type 2 diabetes: metabolic and molecular implications for identifying diabetes genes. *Diabetes Rev* 5:177-269, 1995
- Kahn CR: Insulin action, diabetogenesis, and the cause of type II diabetes. *Diabetes* 43:1066-1084, 1994
- Bell GI, Polonsky KS: Diabetes mellitus and genetically programmed defects in beta-cell function. *Nature* 414:788-791, 2001
- Pinget M, Boullu-Sanchis S: Physiological basis of insulin secretion abnormalities. *Diabetes Metab* 28 (Suppl. 6):4S21-4S32, 2002
- White MF: IRS proteins and the common path to diabetes. *Am J Physiol Endocrinol Metab* 283:E413-E422, 2002
- Araujo H, Danziger N, Cordier J, Glowinski J, Chneiweiss H: Characterization of PEA-15, a major substrate for protein kinase C in astrocytes. *J Biol Chem* 268:5911-5920, 1993
- Danziger N, Yokoyama M, Jay T, Cordier J, Glowinski J, Chneiweiss H: Cellular expression, developmental regulation, and phylogenetic conservation of PEA-15, the astrocytic major phosphoprotein and protein kinase C substrate. *J Neurochem* 64:1016-1025, 1995
- Condorelli G, Vigliotta G, Iavarone C, Caruso M, Tocchetti CG, Andreozzi F, Cafieri A, Tecce MF, Formisano P, Beguinot L, Beguinot F: PED/PEA-15 gene controls glucose transport and is overexpressed in type 2 diabetes mellitus. *EMBO J* 17:3858-3866, 1998
- Kubes M, Cordier J, Glowinski J, Girault JA, Chneiweiss H: Endothelin induces a calcium-dependent phosphorylation of PEA-15 in intact astrocytes: identification of Ser104 and Ser116 phosphorylated, respectively, by protein kinase C and calcium/calmodulin kinase II in vitro. *J Neurochem* 71:1307-1314, 1998
- Trencia A, Perfetti A, Cassese A, Vigliotta G, Miele C, Oriente F, Santopietro S, Giacco F, Condorelli G, Formisano P, Beguinot F: Protein kinase B/Akt binds and phosphorylates PED/PEA-15, stabilizing its antiapoptotic action. *Mol Cell Biol* 23:4511-4521, 2003
- Formstecher E, Ramos JW, Fauquet M, Calderwood DA, Hsieh JC, Canton B, Nguyen XT, Barnier JV, Camonis J, Ginsberg MH, Chneiweiss H: PEA-15 mediates cytoplasmic sequestration of ERK MAP kinase. *Dev Cell* 1:239-250, 2001
- Vaidyanathan H, Ramos JW: RSK2 activity is regulated by its interaction with PEA-15. *J Biol Chem* 278:32367-32372, 2003
- Vigliotta G, Miele C, Santopietro S, Portella G, Perfetti A, Maitan MA, Cassese A, Oriente F, Trencia A, Fiory F, Romano C, Tiveron C, Tatangelo L, Troncone G, Formisano P, Beguinot F: Overexpression of the ped/pea-15 gene causes diabetes by impairing glucose-stimulated insulin secretion in addition to insulin action. *Mol Cell Biol* 24:5005-5015, 2004
- Zhang Y, Redina O, Altschuller YM, Yamazaki M, Ramos J, Chneiweiss H, Kanaho Y, Frohman MA: Regulation of expression of phospholipase D1 and D2 by PEA-15, a novel protein that interacts with them. *J Biol Chem* 275:35224-35232, 2000
- Condorelli G, Vigliotta G, Cafieri A, Trencia A, Andalo P, Oriente F, Miele C, Caruso M, Formisano P, Beguinot F: PED/PEA-15: an anti-apoptotic molecule that regulates FAS/TNFR1-induced apoptosis. *Oncogene* 18:4409-4415, 1999
- Valentino R, Lupoli GA, Raciti GA, Oriente F, Farinero E, Della Valle E, Salomone M, Riccardi G, Vaccaro O, Donnarumma G, Sesti G, Hribal ML, Cardellini M, Miele C, Formisano P, Beguinot F: In healthy first-degree relatives of type 2 diabetics, ped/pea-15 gene is overexpressed and related to insulin resistance. *Diabetologia* 49:3058-3066, 2006
- Condorelli G, Vigliotta G, Trencia A, Maitan MA, Caruso M, Miele C, Oriente F, Santopietro S, Formisano P, Beguinot F: Protein kinase C (PKC)- $\alpha$  activation inhibits PKC- $\zeta$  and mediates the action of PED/PEA-15 on glucose transport in the L6 skeletal muscle cells. *Diabetes* 50:1244-1252, 2001
- Devedjian JC, George M, Casellas A, Pujol A, Visa J, Pelegrin M, Gros L, Bosch F: Transgenic mice overexpressing insulin-like growth factor-II in beta cells develop type 2 diabetes. *J Clin Invest* 105:731-740, 2000
- Kulkarni RN, Bruning JC, Winnay JN, Postic C, Magnuson MA, Kahn CR: Tissue-specific knockout of the insulin receptor in pancreatic beta cells creates an insulin secretory defect similar to that in type 2 diabetes. *Cell* 96:329-339, 1999
- Bruning JC, Michael MD, Winnay JN, Hayashi T, Horsch D, Accili D, Goodyear LJ, Kahn CR: A muscle-specific insulin receptor knockout exhibits features of the metabolic syndrome of NIDDM without altering glucose tolerance. *Mol Cell* 2:559-569, 1998
- Somogyi M: Determination of blood sugar. *J Biol Chem* 160:69-73, 1945
- Ferre P, Leturque A, Burnol AF, Penicaud L, Girard J: A method to quantify glucose utilization in vivo in skeletal muscle and white adipose tissue of the anaesthetized rat. *Biochem J* 228:103-110, 1985
- Kitamura T, Kido Y, Nef S, Merenmies J, Parada LF, Accili D: Preserved pancreatic beta-cell development and function in mice lacking the insulin receptor-related receptor. *Mol Cell Biol* 21:5624-5630, 2001
- Miyazaki J, Araki K, Yamato E, Ikegami H, Asano T, Shibasaki Y, Oka Y, Yamamura K: Establishment of a pancreatic beta cell line that retains glucose-inducible insulin secretion: special reference to expression of glucose transporter isoforms. *Endocrinology* 127:126-132, 1990
- Wang H, Gauthier BR, Hagenfeldt-Johansson KA, Iezzi M, Wollheim CB: Foxa2 (HNF3beta) controls multiple genes implicated in metabolism-secretion coupling of glucose-induced insulin release. *J Biol Chem* 277:17564-17570, 2002
- Laemmli UK: Cleavage of structural proteins during the assembly of the head of bacteriophage T4. *Nature* 227:680-685, 1970
- Kitsberg D, Formstecher E, Fauquet M, Kubes M, Cordier J, Canton B, Pan G, Rolli M, Glowinski J, Chneiweiss H: Knock-out of the neural death effector domain protein PEA-15 demonstrates that its expression protects astrocytes from TNFalpha-induced apoptosis. *J Neurosci* 19:8244-8251, 1999
- Condorelli G, Trencia A, Vigliotta G, Perfetti A, Goglia U, Cassese A, Musti AM, Miele C, Santopietro S, Formisano P, Beguinot F: Multiple members of the mitogen-activated protein kinase family are necessary for PED/PEA-15 anti-apoptotic function. *J Biol Chem* 277:11013-11018, 2002
- Hao C, Beguinot F, Condorelli G, Trencia A, Van Meir EG, Yong VW, Parney IF, Roa WH, Petruk KC: Induction and intracellular regulation of tumor necrosis factor-related apoptosis-inducing ligand (TRAIL) mediated apoptosis in human malignant glioma cells. *Cancer Res* 61:1162-1170, 2001
- Xiao C, Yang BF, Asadi N, Beguinot F, Hao C: Tumor necrosis factor-related apoptosis-inducing ligand-induced death-inducing signaling complex and its modulation by c-FLIP and PED/PEA-15 in glioma cells. *J Biol Chem* 277:25020-25025, 2002
- Cook DL, Taborsky GJ: In *Ellenberg and Rifkin's Diabetes Mellitus*. 5th ed. Porte D, Sherwin RS, Eds. Stamford, CT, Appleton & Lange, 1997, p. 49-73
- Miki T, Nagashima K, Tashiro F, Kotake K, Yoshitomi H, Tamamoto A, Gono T, Iwanaga T, Miyazaki J, Seino S: Defective insulin secretion and enhanced insulin action in KATP channel-deficient mice. *Proc Natl Acad Sci U S A* 95:10402-10406, 1998
- Nequin M, Szollosi A, Aguilar-Bryan L, Bryan J, Henquin JC: Both triggering and amplifying pathways contribute to fuel-induced insulin secretion in the absence of sulfonylurea receptor-1 in pancreatic beta-cells. *J Biol Chem* 279:32316-32324, 2004
- Seghers V, Nakazaki M, DeMayo F, Aguilar-Bryan L, Bryan J: Sur1 knockout mice: a model for K(ATP) channel-independent regulation of insulin secretion. *J Biol Chem* 275:9270-9277, 2000
- Hashimoto N, Kido Y, Uchida T, Matsuda T, Suzuki K, Inoue H, Matsumoto M, Ogawa W, Maeda S, Fujihara H, Ueta Y, Uchiyama Y, Akimoto K, Ohno S, Noda T, Kasuga M: PKClambda regulates glucose-induced insulin secretion through modulation of gene expression in pancreatic beta cells. *J Clin Invest* 115:138-145, 2005
- Bandyopadhyay G, Standaert ML, Kikkawa U, Ono Y, Moscat J, Farese RV: Effects of transiently expressed atypical (zeta, lambda), conventional (alpha, beta) and novel (delta, epsilon) protein kinase C isoforms on insulin-stimulated translocation of epitope-tagged GLUT4 glucose transporters in rat adipocytes: specific interchangeable effects of protein kinases C-zeta and C-lambda. *Biochem J* 337:461-470, 1999
- Furukawa N, Shirotani T, Araki E, Kaneko K, Todaka M, Matsumoto K, Tsuruzoe K, Motoshima H, Yoshizato K, Kishikawa H, Shichiri M: Possible involvement of atypical protein kinase C (PKC) in glucose-sensitive expression of the human insulin gene: DNA-binding activity and transcriptional activity of pancreatic and duodenal homeobox gene-1 (PDX-1) are enhanced via calphostin C-sensitive but phorbol 12-myristate 13-acetate (PMA) and Go 6976-insensitive pathway. *Endocr J* 46:43-58, 1999

38. Matsumoto M, Ogawa W, Akimoto K, Inoue H, Miyake K, Furukawa K, Hayashi Y, Iguchi H, Matsuki Y, Hiramatsu R, Shimano H, Yamada N, Ohno S, Kasuga M, Noda T: PKC $\lambda$  in liver mediates insulin-induced SREBP-1c expression and determines both hepatic lipid content and overall insulin sensitivity. *J Clin Invest* 112:935–944, 2003
39. Lee CS, Sund NJ, Vatamaniuk MZ, Matschinsky FM, Stoffers DA, Kaestner KH: Foxa2 controls Pdx1 gene expression in pancreatic  $\beta$ -cells in vivo. *Diabetes* 51:2546–2551, 2002
40. Sund NJ, Vatamaniuk MZ, Casey M, Ang SL, Magnuson MA, Stoffers DA, Matschinsky FM, Kaestner KH: Tissue-specific deletion of *Foxa2* in pancreatic  $\beta$ -cells results in hyperinsulinemic hypoglycemia. *Genes Dev* 15:1706–1715, 2001